P501
521c

LIBRARY
Code: 40441
Issue: 0102
DEPT. of AGRICULTURE

BIOCHIMICA *et* BIOPHYSICA ACTA

INTERNATIONAL MONTHLY OF BIOCHEMISTRY AND BIOPHYSICS
REVUE MENSUELLE INTERNATIONALE DE BIOCHIMIE ET BIOPHYSIQUE
INTERNATIONALE MONATSSCHRIFT FÜR BIOCHEMIE UND BIOPHYSIK

EDITORIAL BOARD

W. T. Astbury (Leeds), J. Brachet (Brussels), A. Braunstein (Moscow), E. Chargaff (New York), C. F. Cori (St. Louis), Cl. Fromageot (Paris), K. Linderstrøm-Lang (Copenhagen), H. H. Weber (Heidelberg), H. G. K. Westenbrink (Utrecht), R. Wurmser (Paris), R. W. G Wyckoff (Bethesda)

ADVISORY BOARD

J. D. Bernal (London), T. Caspersson (Stockholm), C. R. Harington (London), A. J. Kluyver (Delft), H. A. Krebs (Sheffield), A. von Muralt (Bern), A. J. Oparin (Moscow), J. Roche (Paris), M. Sreenivasaya (Bangalore), D. L. Talmud (Moscow), A. Tiselius (Upsala), Hsien Wu (Peiping)

ELSEVIER PUBLISHING COMPANY

AMSTERDAM LONDON HOUSTON NEW YORK

Biochim. Biophys. Acta, Vol. 16 No. 1 (1955), p. 1 — 170, January 1955

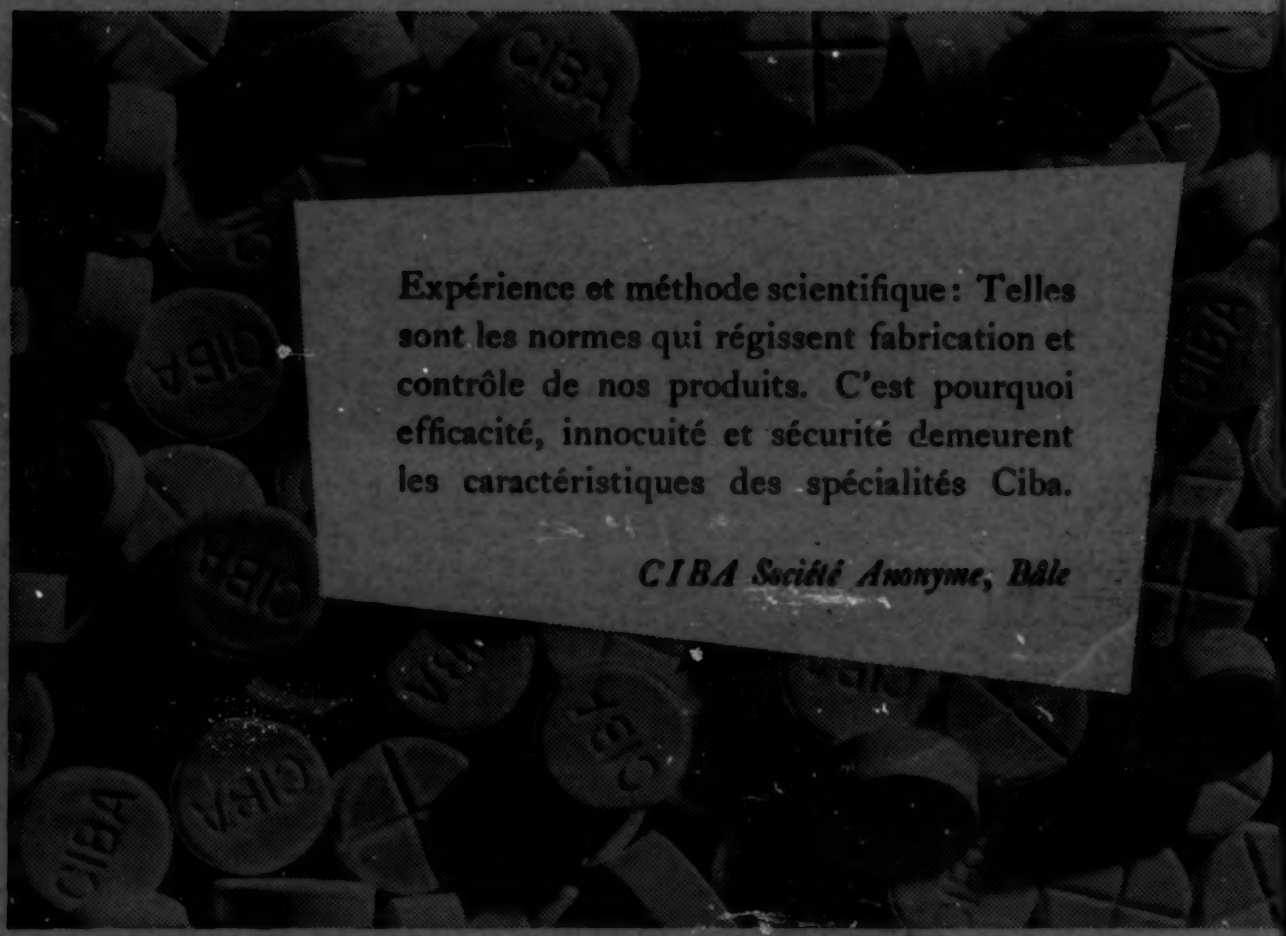
Expérience et méthode scientifique: Telles sont les normes qui régissent fabrication et contrôle de nos produits. C'est pourquoi efficacité, innocuité et sécurité demeurent les caractéristiques des spécialités Ciba.
CIBA Société Anonyme, Bâle

MANUSCRIPTS of papers or "Short Communications and Preliminary Notes" for prompt publication should be sent to one of the following Editors:

Professor W. T. ASTBURY, Department of Biomolecular Structure, The University, Leeds 2 (England)

Professor J. BRACHET, Laboratoire de Morphologie animale, Université Libre de Bruxelles, 1850 Chaussée de Wavre, Auderghem-Bruxelles (Belgique)

Professor E. CHARGAFF, Columbia University, College of Physicians and Surgeons, Cell Chemistry Laboratory, 630 West 168th Street, New York 32, N.Y. (U.S.A.)

Professor C. F. CORI, School of Medicine, Washington University, St. Louis, Mo. (U.S.A.)

Professor C. FROMAGEOT, Laboratoire de Chimie biologique, Faculté des Sciences, 96 Boulevard Raspail, Paris VI (France)

Professor K. LINDERSTRØM-LANG, Carlsberg Laboratorium, Kemisk Afdeling, 10 Gl. Carlsbergvej, København-Valby (Danmark)

Professor Dr. H. H. WEBER, Max-Planck-Institut für Physiologie, Jahnstrasse 29, Heidelberg (Deutschland)

Professor H. G. K. WESTENBRINK, Laboratorium voor Physiologische Chemie, Vondellaan 24a, Utrecht (Holland)

Professor R. WURMSER, Laboratoire de Biologie physico-chimique, 13 rue Pierre Curie, Paris V (France)

Dr. R. W. G. WYCKOFF, Laboratory of Physical Biology, National Institutes of Health, Bethesda 14, Md. (U.S.A.)

Subscription price per Volume, comprising 4 monthly issues of approximately 150 pages: $ 12.— (90 s) or equivalent value in other currencies.

All rights reserved

ELSEVIER PUBLISHING CO., AMSTERDAM
Printed in The Netherlands by
DRUKKERIJ MEIJER WORMERVEER AND AMSTERDAM

AN INVESTIGATION OF THE STRUCTURE OF SILK FIBROIN*

by

RICHARD E. MARSH, ROBERT B. COREY AND LINUS PAULING

*Gates and Crellin Laboratories of Chemistry***, California Institute of Technology, Pasadena, Calif. (U.S.A.)*

I. INTRODUCTION

Of all the fibrous proteins, silk fibroin might appear to be most suitable for a determination of structure by the methods of X-ray diffraction analysis. It is the simplest of the fibrous proteins in that it contains a preponderance of small amino-acid residues. Chemical analyses now account for 98% of its constituent residues; of these, glycine, the simplest of the amino acids, comprises about 44% and glycine, alanine, and serine, the three simplest, 82%. Its amino-acid composition, as given in the compilation of TRISTRAM[1], is shown in Table I. The X-ray diffraction pattern of silk fibroin indicates a highly ordered structure in comparison with most other fibrous proteins. Since the first observations of HERZOG AND JANCKE[2] in 1920, many attempts have been made to explain the X-ray diffraction patterns of fibroin in terms of groupings of polypeptide chains arranged approximately parallel to the fiber axis. All of these attempts have been qualitative rather than quantitative: proposed units of structure have been derived from the X-ray fiber diagram and suggestions have been made regarding the probable arrangement of extended polypeptide chains within the units, but none of these structures has been precisely formulated and hence the validity of none of them has been tested by comparison of observed and calculated intensities of the X-ray reflections.

In the present X-ray investigation of silk fibroin advantage has been taken of current knowledge of the dimensions and configurations of polypeptide chains in proteins[3] to assign definite positions to the C, N, and O atoms of the chain. From their positional coordinates the contributions of these atoms to the intensities of the X-ray reflections have been calculated. The critical discussion of the structure is therefore based upon the quantitative agreement between the observed and calculated X-ray diffraction patterns as well as upon other physical and chemical evidence.

The first attempt to derive the structure of silk fibroin from its X-ray diffraction pattern was made by BRILL[4] in 1923. He assigned indices to about 20 spots in the fiber diagram in terms of an orthogonal unit with identity distances of 7.0 A along the fiber axis and 9.3 and 10.4 A perpendicular to it. He concluded that silk fibroin consisted of at least two proteins, one of which was crystalline, and that the crystalline component was composed of equimolar quantities of glycine and alanine. For the composition of this

* This work was supported in part by Contract No. Nonr-220(05) between the California Institute of Technology and the Office of Naval Research.

** Contribution No. 1936.

References p. 33/34.

168075

TABLE I

AMINO-ACID COMPOSITION OF SILK FIBROIN (TRISTRAM[1])

Amino acid	*Moles/10^5 g protein*	*Residue %*
Glycine	581.0	44.7
Alanine	334.0	25.7
Serine	154.3	11.9
Tyrosine	70.7	5.4
Valine	30.8	2.4
Aspartic acid	20.75	1.6
Phenylalanine	20.4	1.6
Glutamic acid	14.7	1.1
Threonine	13.45	1.0
Isoleucine	8.40	0.6
Leucine	6.95	0.5
Proline	6.43	0.5
Arginine	6.33	0.5
Lysine	4.66	0.4
Histidine	2.32	0.2
Total	1275.2	98.1

crystalline component he suggested polymerization products of glycylalanine or alanylglycine and pointed out that the unit cell would contain one glycylalanyl portion of each of four chains. In a discussion based on BRILL's data, MEYER AND MARK[5] presented more definitely some possible arrangements of four polypeptide chains of alternating glycine and alanine residues. They suggested that the peptide chains were strongly attracted to one another by forces between the CO and NH groups of adjacent chains, and also that there might be occasional replacement of glycyl or alanyl by other amino-acid residues.

Double orientation of the silk fiber by rolling was first reported by HERZOG AND JANCKE[6] in 1929. Photographs of rolled silkworm gut showed marked differences in the relative intensities of the equatorial and layer-line reflections depending on whether the X-ray beam were perpendicular or parallel to the plane of rolling. This effect was further investigated by KRATKY[7]. He prepared his oriented specimens by moistening the freshly extracted silk gland with dilute acetic acid and then immediately deforming the contents of the gland by stretching and rolling it. He reported equatorial reflections corresponding to the following values of interplanar spacings: 9.4, 4.62, 4.26, and 3.04 A. Of these reflections, the first, second, and fourth are diffuse and arise from planes which are approximately parallel to the plane of the rolled sheet; the third is sharp and its plane apparently makes an angle of between 55° and 90° with the sheet. A few spots on the first layer line appeared to be related to diffuse and sharp spots on the equator. These observations on oriented specimens completely invalidated BRILL's earlier assignment of axes. KRATKY called attention to the possible implications of the broad, diffuse reflections, all apparently occurring from planes with a particular orientation—either the crystallite was very flat, or, more likely, the repetition in one direction was not exact. He pointed out that if the latter implication is true, it has especial significance with reference to the suggestions made by MEYER AND MARK[5] regarding the chemical constitution of silk, namely, the possibility of the occasional replacement of residues of alanine and glycine by residues of other amino acids.

References p. 33/34.

In a more extensive investigation, KRATKY AND KURIYAMA[8] reported that *Bombyx mori* and tussah silk gave similar but not identical X-ray patterns, and that four other silks gave patterns which resembled one another but were not closely related to that of *Bombyx mori*. Possible unit cells for *Bombyx mori* silk fibroin were derived from the diffraction patterns by selecting sets of three interplanar equatorial vectors corresponding to three reciprocal lattice vectors mutually related as the sides of a triangle. In their paper they concluded that the plane of the sharp equatorial reflection (4.26 A) must make an angle of between 60° and 75° with the plane of the rolled sheet. Of ten possible unit cells, four were eliminated because the densities calculated for them on the assumption of a molecular weight of 128 for each of four chains (alanylglycyl) failed to agree with the expected density of silk, 1.3 to 1.5 g/cm^3. No further selections were made among the six remaining unit cells. HUGGINS[9] has shown that of these six only two permit the polypeptide chains to be arranged in ways which are not in conflict with the X-ray data.

TROGUS AND HESS[10] compared the X-ray patterns, chemical analyses, and other properties of several varieties of silk. From measurements of their excellent X-ray patterns they obtained numerical data which were more accurate than those previously published; furthermore, the patterns of tussah silk, spider silk, and others differed somewhat from that of *Bombyx mori*. No attempt was made to derive new unit cells or to propose new structures for the crystalline constituent of fibroin. TROGUS and HESS suggested that silk may contain more than one crystalline component, one of which is common to all silks, and also an amorphous component.

In a paper published in 1943[11], BRILL suggested for silk fibroin a unit of structure having the dimensions $a = 9.65$ A, $b = 10.40$ A, $c = 6.95$ A (fiber axis), $\gamma = 62.4°$, and containing four alanylglycyl residues. Neighboring chains, arranged approximately in the *ac* plane, run in opposite directions and are held together by hydrogen bonds between CO and NH groups; methyl groups extend in the general direction of *b*, and probably require some rotation of adjacent chains in order to give satisfactory packing. No atomic parameters were assigned. BRILL emphasized the necessity for an adequate discussion of the X-ray intensities before this proposed structure could be considered to be other than hypothetical.

In discussing the composition of the crystalline component of fibroin BRILL raised the question which has bothered investigators from the beginning, namely, whether tyrosine can be included in the unit of structure, or must be relegated to a non-crystalline component. Unlike KRATKY, he preferred to explain the diffuseness of the reflections from planes making small angles with the *ac* plane as arising from the probable small dimensions of the micelle in directions roughly perpendicular to this plane, rather than from a randomness of intermolecular spacing due to the inclusion of side chains other than methyl. He concluded quite definitely that the benzene nucleus of a tyrosine residue requires so much room that tyrosine cannot be present in the crystalline portion of fibroin. In 1941 MEYER, FULD AND KLEMM[12] had reported that coupling of silk with diazobenzenesulfonic acid caused no change in the X-ray diagram, from which they concluded that tyrosine and presumably all amino-acid residues other than glycine, alanine and serine are present in silk in a noncrystalline component. Recently, similar conclusions were drawn by DRUCKER AND SMITH[13, 14]: tryptic digestion of "renatured" silk dissolved in cupriethylenediamine solution produced a precipitate which they reported to be a polypeptide of molecular weight 7000 consisting of glycine, alanine,

References p. 33/34.

and serine. On the other hand, FRIEDRICH-FREKSA, KRATKY AND SEKORA[15] had reported that silk in which most of the tyrosine residues were iodinated gave three new, very faint meridional reflections that could be correlated with a period of 70 A, suggesting that in the crystalline component of fibroin every twentieth residue is tyrosine. ZAHN, KRATKY AND SEKORA[16] reported in 1951 that nitration of silk in a manner which transformed the tyrosine into 3-nitrotyrosine and 3,5-dinitrotyrosine resulted in the introduction into the X-ray pattern of the first-order meridional reflection (6.95 A) and also two additional layer lines corresponding to spacings of 10.4 and 20.9 A. ZAHN[17] explained these results by assuming that the tyrosine residues occur at specific positions on the outer surface of the crystallites or between them. The conclusions drawn from experimental observations are thus conflicting, so that the presence or absence of tyrosine in crystalline portions of silk fibroin is as yet not satisfactorily established.

II. EXPERIMENTAL

The investigation into the structure of silk fibroin was begun at this Institute in 1940 by Dr. MAX ROGERS. Dr. ROGERS prepared a large number of samples of silkworm gut (*Bombyx mori*) many of which were doubly oriented by stretching and rolling in the manner described by previous workers[6,7,8]. Dr. ROGERS photographed these samples in a cylindrical vacuum camera with 3-cm radius using Kα radiation from both copper and cobalt targets. More recently, we have rephotographed many of the same samples in a cylindrical camera with 10-cm radius using Ni-filtered Cu Kα radiation. In this camera an atmosphere of helium was used in order to eliminate fogging of the film by air scattering. Photographs were taken with the X-ray beam perpendicular to the fiber axis and both parallel and perpendicular to the plane of rolling of the doubly-oriented samples. Typical photographs are reproduced in Figs. 1 and 2. The double orientation of these samples was also recorded on Weissenberg photographs taken with the X-ray beam perpendicular to the fiber axis.

Accurate values for the relative intensities and interplanar spacings of the equatorial reflections from silk fibroin were obtained by the use of an X-ray spectrometer. For the purpose seven strands of commercial silkworm gut were arranged in a cylindrical bundle about 1.5 mm in diameter which was bathed in a beam of crystal-monochromatized Cu Kα radiation. The equatorial spectrum was recorded by means of a Geiger counter, measurements being made at intervals of 10 minutes of arc. The intensity of the scattered radiation at each position of the counter was taken to be proportional to the counting rate—the reciprocal of the time required to accumulate 10,000 counts. The scattering curve for the equatorial spectrum, reproduced in Fig. 3, was obtained by plotting counting rate as a function of the scattering angle 2θ. The background scattering, estimated empirically as indicated in Fig. 3, was subtracted from the total scattering and the corrected counting rates thus obtained were used to derive the positions and the intensities of the diffraction maxima.

The positions of the centers of the four maxima 1, 4, 5, and 8 (Table II) were obtained by the following procedure. The assumption was made that the corrected counting rates in the vicinity of a diffraction maximum can be fitted to a Gaussian curve $R_x = R_0 \exp(-Ax^2 - Bx)$, in which R_0 is the counting rate at some arbitrary origin $x = 0$ near, but not necessarily coincident with, the center of the maximum, and R_x is the counting rate at the distance x, measured in degrees, from this origin. The center of the maximum

References p. 33/34.

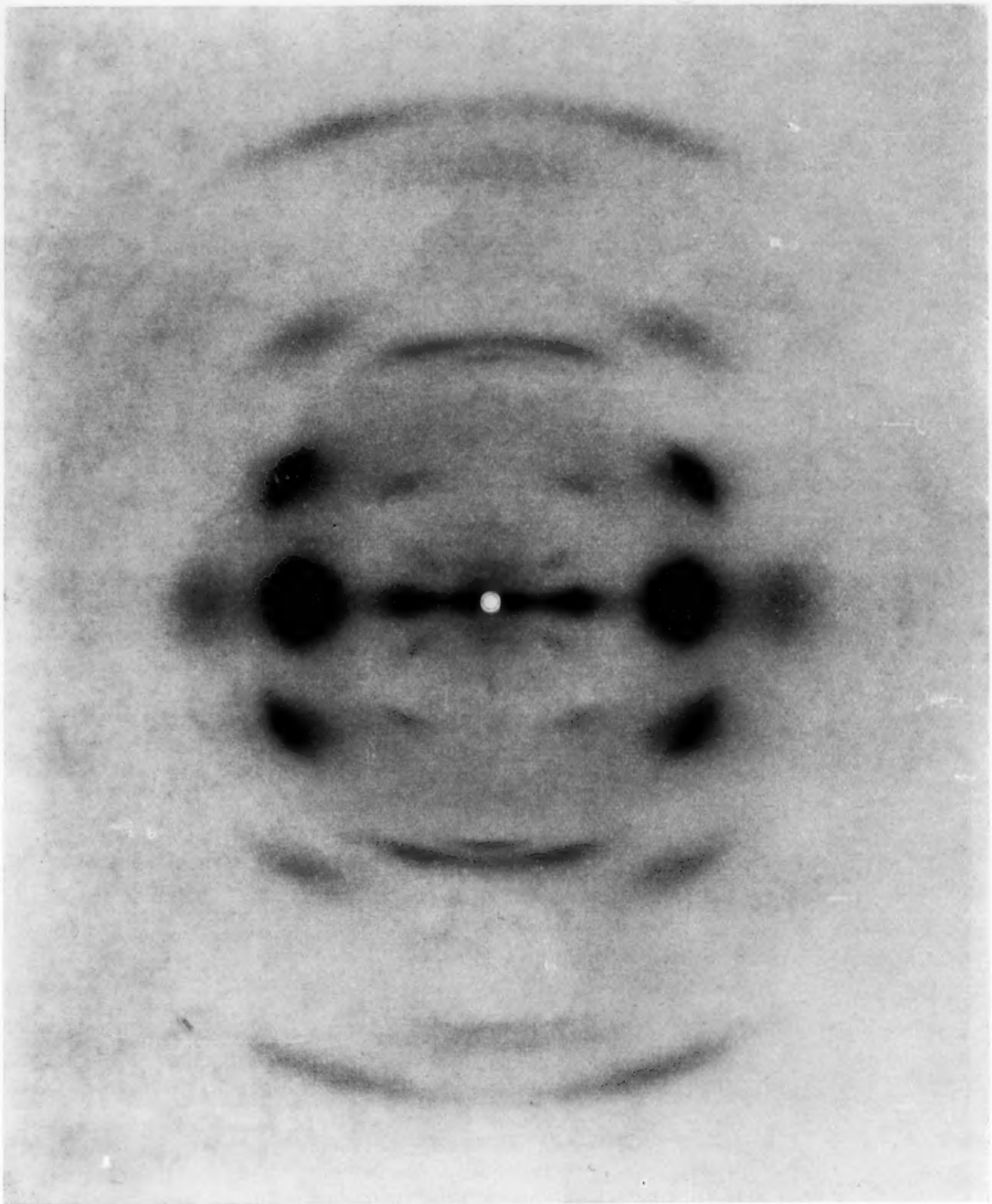

Fig. 1. X-ray diffraction pattern for silk fibroin.

is then given by $x_0 = -B/2A$, best values of A, B, and R_0 being determined from solution of the normal equations of a least-squares treatment*. In order to test the validity of the assumption that the observed counting rates representing individual maxima

* See, for example, *The Calculus of Observations* by E. T. WHITTAKER AND G. ROBINSON, London, 1937, Chapt. IX.

References p. 33/34.

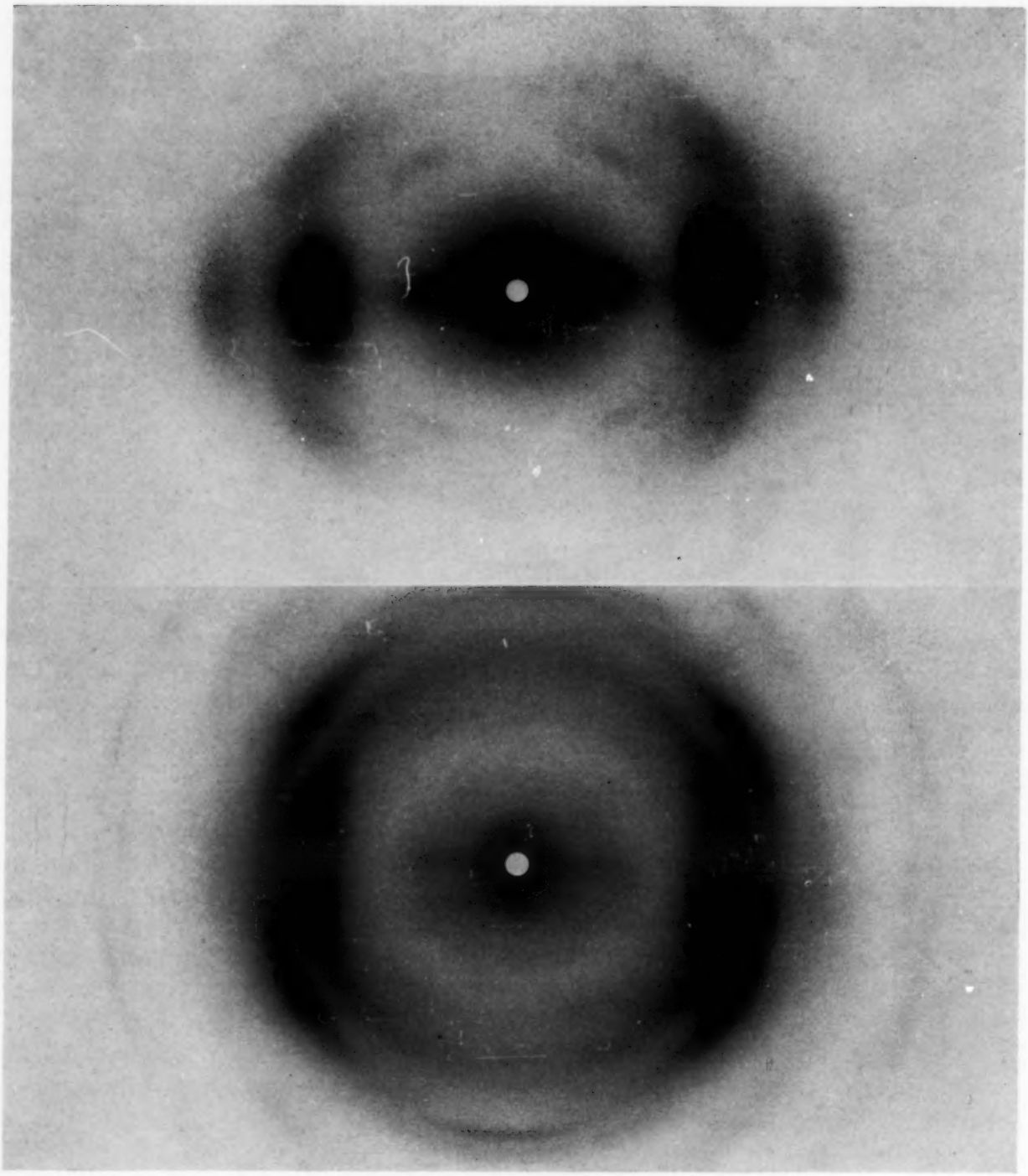

Fig. 2. X-ray photographs of doubly-oriented fibroin.
(above) X-ray beam parallel to plane of rolling.
(below) X-ray beam perpendicular to plane of rolling.

could be closely fitted to a Gaussian curve, values of R_x were calculated from these values of A, B, and R_0; for each of the four maxima, agreement with the observed values was found to be within the limits of error imposed by the statistics of the observed counting rates.

In our spectrometric measurements the two maxima 2 and 3, representing spacings of 4.7 and 4.2 A, could not be satisfactorily resolved. We were unable to obtain spectrometric data from the doubly-oriented specimens of silk fibroin; therefore, the positions

References p. 33/34.

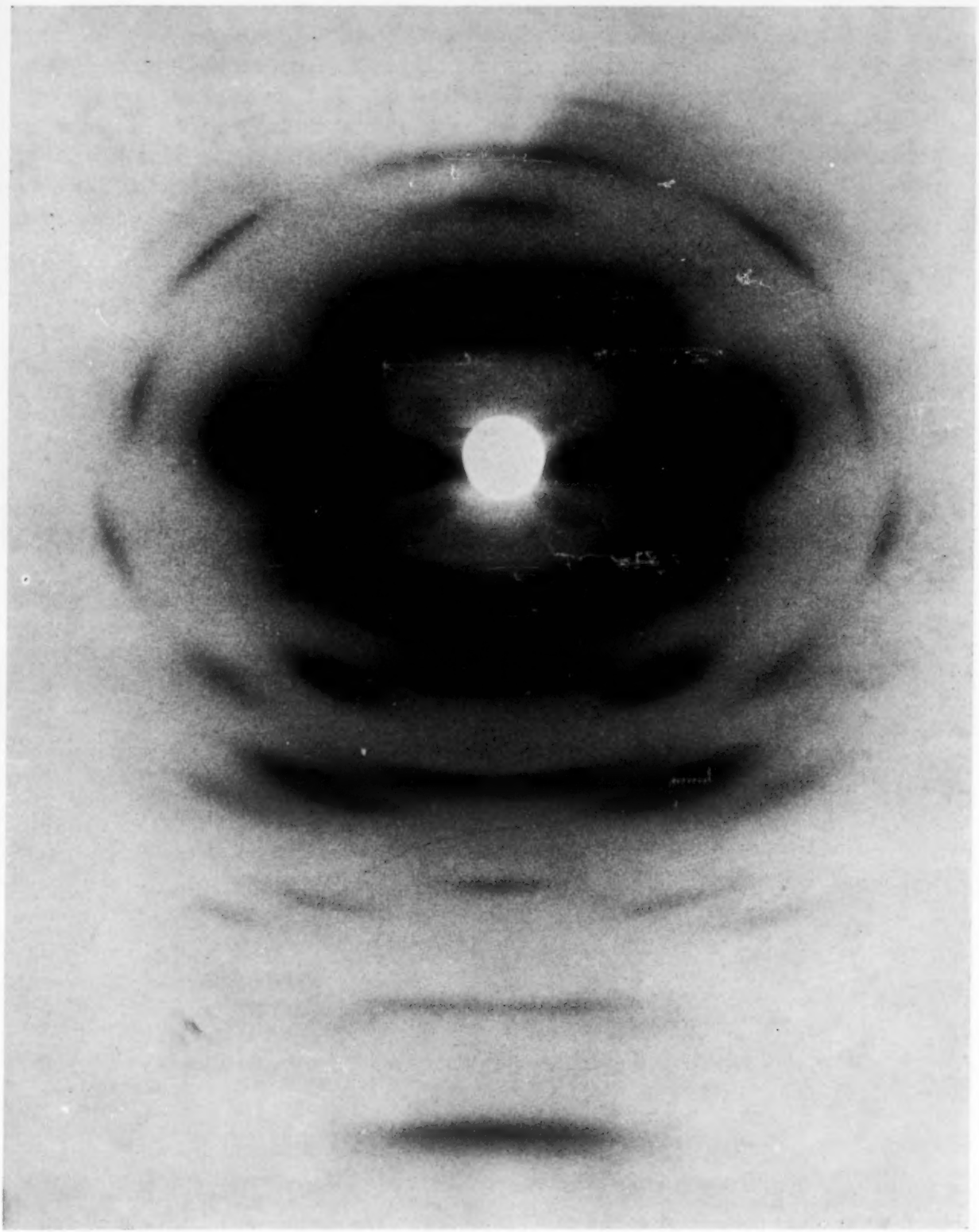

Fig. 4. Photograph of stretched silkworm gut taken in 3-cm radius camera with fiber axis horizontal and making an angle of 60° with the X-ray beam.

of these maxima were derived from measurements of photographs of doubly-oriented specimens taken in the 10-cm radius camera.

Final values for the spacings of the equatorial reflections are given in column 2

References p. 33/34.

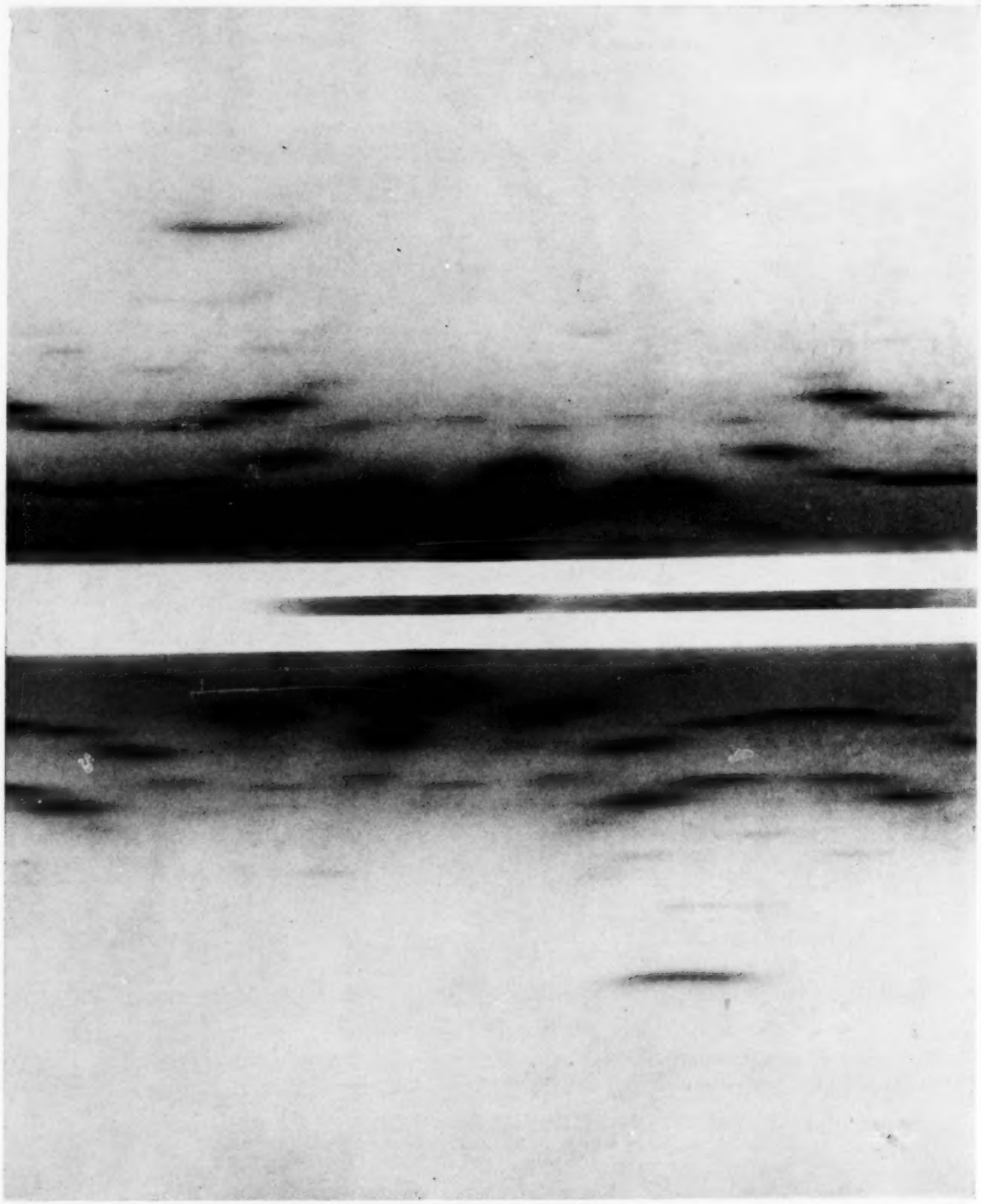

Fig. 5. Weissenberg photograph of stretched silkworm gut. The sample was rotated around an axis perpendicular to the fiber axis.

of Table II. The uncertainties given in the table are estimated limits of error (three times the standard deviations). For reflections 1, 4, 5, and 8, the limits of error as calculated from the residuals of the least-squares treatment were increased by approximately 50% to allow for small systematic errors in the experimental procedure. The limits of error for reflections 2 and 3 were estimated from the deviations of values

References p. 33/34.

obtained from measurements made on several photographs; reflections 6, 7, 9, and 10 were observed only on long exposures and no uncertainties for them are reported. For comparison, the spacing values reported by KRATKY AND KURIYAMA[8] are listed in column 4. The agreement with our values is satisfactory with the exception of reflection 1; the value of 9.28 A reported by KRATKY AND KURIYAMA for this reflection differs from our value of 9.7 A by an amount considerably greater than the limit of error of our determination.

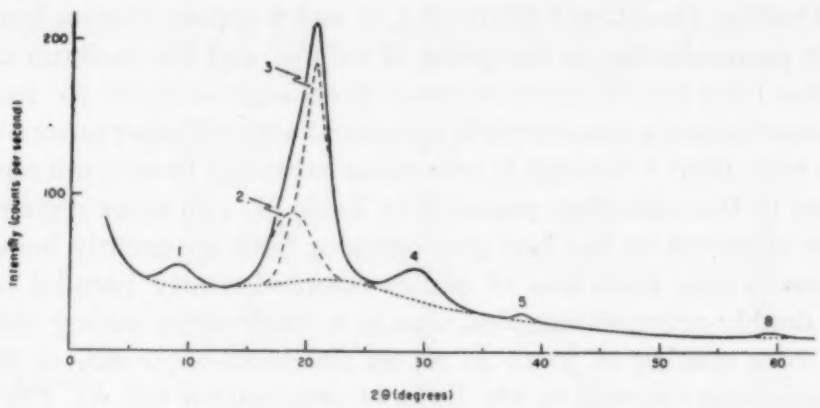

Fig. 3. Equatorial spectrum of silk fibroin obtained from spectrometric measurements.

TABLE II

EQUATORIAL REFLECTIONS FROM SILK FIBROIN

	This investigation		KRATKY AND KURIYAMA[8]			
(1)	*(2)*	*(3)*	*(4)*	*(5)*	*(6)**	*(7)*
No.	*Spacing (A)*	*Relative intensity*	*Spacing (A)*	*Relative intensity*	*Appearance*	*Orient.**
1	9.70 ± 0.25	90	9.28	S	Broad	∥
2	4.70 ± 0.20	450	4.59	S	Broad	∥
3	4.25 ± 0.15	900	4.33	V S	Med. Sharp	*ca.* 70°
4	3.05 ± 0.02	180	3.07	M	Broad	∥
5	2.35 ± 0.01	20	2.38	W	Sharp	⊥
6	2.10 ± 0.05	< 5 VW				
7	1.80 ± 0.05	< 5 VVW			Broad	∥
8	1.56 ± 0.01	18			Sharp	⊥
9	1.20 ± 0.05	< 5 VW			Sharp	⊥
10	0.95 (?)	< 5 VVW				

* Orientation of diffraction planes relative to the plane of rolling of the doubly oriented samples.

The relative intensities listed in column 3, Table II, were obtained from graphical integration of the spectrometric curve after correction for background scattering. On this curve, which is reproduced in Fig. 3, reflections 2 and 3 are represented by a single maximum, and it was necessary to separate this maximum empirically into its two components before performing the graphical integration. For this reason it is probable that the intensities reported for reflections 2 and 3 are less reliable than those reported for the other reflections. The reported intensities are not corrected for absorption, or for Lorentz or polarization factors. In general, the agreement with the qualitative estimates of intensity reported by KRATKY AND KURIYAMA (column 5) is satisfactory; again, the only serious discrepancy is in reflection 1, which we have observed to be considerably

References p. 33/34.

weaker than reported by KRATKY AND KURIYAMA. All of the photographs prepared in these Laboratories, as well as the spectrometric data, have indicated that reflection 1 is much weaker than reflection 2.

The relative sharpness or diffuseness of each equatorial reflection is indicated in column 6; the apparent orientation of the corresponding diffraction plane relative to the plane of rolling of the doubly-oriented sample is indicated in column 7. The diffuse reflections 1, 2, 4, and 7 apparently arise from sets of planes oriented very nearly parallel to the plane of rolling, the sharp reflections 5, 8, and 9 appear to arise from sets of planes oriented nearly perpendicular to the plane of rolling, and the medium sharp reflection 3 appears to arise from sets of planes oriented at an angle of about 70° from the plane of rolling. These observations are in complete agreement with the observations of KRATKY AND KURIYAMA for reflections 1 through 5; reflections 6 through 10 were not reported by them.

In addition to the reflections reported in Table II, two other regions of significant darkening were observed on our best photographs, both apparently being due to equatorial reflections arising from sets of planes oriented nearly parallel to the plane of rolling of the doubly-oriented samples. One is a moderately strong diffuse reflection corresponding to a spacing of 30 to 40 A; on the small-angle side of this reflection a continuous blackening extends to the limit of observation (78 A). The other appears to be a diffuse reflection of low intensity with a spacing of about 15 A; on poorer photographs this reflection merges with the stronger 9.7 A reflection.

The spacing along the fiber axis was determined from the layer-line separations on photographs of stretched silk-worm gut taken in cylindrical cameras with 3-cm and 10-cm radius. In addition, a photograph (Fig. 4) was taken in the 3-cm radius camera with the fiber tilted at an angle of 60° with the X-ray beam in order to obtain reflections of high order along the fiber axis, especially the strong sixth order. The value 6.97 $\pm$ 0.03 A was derived from measurements of these photographs; it is in close agreement with the value 6.94 A reported by BAMFORD *et al.*[18]. In long exposures made with stretched commercial silkworm gut two intermediate layer lines were observed corresponding to the first and second orders of a 21-A identity distance along the fiber axis. These two weak layer lines were also observed by KRATKY and co-workers[16,19] on photographs of nitrated and of alkalized silk.

Non-equatorial reflections were recorded on photographs taken in the two cylindrical cameras, in a flat-film camera with the sample-to-film distance equal to 10 cm, and in a Weissenberg camera (5.73 cm diameter). Measurements of the photographs taken in the 10-cm radius cylindrical camera and in the flat-film camera were used to compute the horizontal components, d_{hol}, of the interplanar spacings for reflections occurring on the first three layer lines, together with rough visual estimations of the relative intensities. For comparison, the spacing and intensity data of KRATKY AND KURIYAMA are also included. The higher layer lines were recorded on a photograph taken in a 3-cm radius cylindrical camera with the fiber axis of the sample perpendicular to the axis of the camera and making an angle of 60° with the direction of the X-ray beam (Fig. 4). The complete X-ray diffraction pattern was also recorded on a Weissenberg photograph taken with the sample (stretched but not rolled) rotated around an axis perpendicular to its fiber direction (Fig. 5).

Values of d_{hol}, together with some estimated probable errors, are listed in Table III; rough visual estimations of the relative intensities are also listed. For comparison the spacing and intensity data of KRATKY AND KURIYAMA[8] are included.

References p. 33/34.

TABLE III

SPACING AND INTENSITY DATA FOR NON-EQUATORIAL REFLECTIONS

	This investigation		KRATKY AND KURIYAMA	
	d_{hol} (Å)	*Int.*	d_{hol}	*Int.*
1st Layer	9.6 ± 0.4	W	9.6	W
	4.7 ± 0.2	W	4.73	M
	4.2 ± 0.1	S	4.24	S
	3.0 ± 0.1	VW		
	2.35 ± 0.03	M	2.38	W
	2.12 ± 0.03	W		
	1.8	VVW		
	0.95 (?)	VW		
2nd Layer	∞	VS	∞	M
	9.6 ± 0.8	MS	10.4	M
	5.1 ± 0.5 / 4.4 ± 0.4	MS	4.59	M
	3.0 ± 0.3	M	3.13	W
	2.3 ± 0.1	W		
3rd Layer	9	MS	8.9	W
	7	VW		
	4.1 ± 0.7	S	4.5	S
	3.0 ± 0.5	W		
	2.3	VW		
	1.85	VW		
	1.54	MW		
	1.32	MW		
	1.17	VW		
4th Layer	∞	MW		
	5	MW		
	3	W		
5th Layer	9	MW		
	5	W		
6th Layer	∞ / 9	S		

The effect of double orientation of the sample is less apparent on the layer-line reflections than on the equatorial reflections. Nevertheless, as can be seen in Fig. 2, the effect is great enough in some cases to permit a direct correlation of certain layer-line reflections with equatorial reflections having the same values of d_{hol}.

III. DERIVATION OF THE STRUCTURE

1. *The pleated-sheet configurations*

All previous attempts to derive an acceptable structure for silk fibroin were made before the fundamental dimensions of the polypeptide chain had been established and before specific configurations of these chains had been systematically investigated and precisely described. The method consisted in deriving probable unit cells from the X-ray fiber diagrams and proposing possible arrangements of polypeptide chains within these unit cells which were in rough qualitative agreement with the general features of the

References p. 33/34.

diffraction patterns. No atomic coordinates were assigned from which the intensities of X-ray reflections could be calculated.

Recent X-ray analyses of crystals of amino acids, simple peptides, and related substances have provided precise data from which the interatomic distances and bond angles in polypeptide chains have now been derived[3]. These X-ray studies have also established two structural principles of fundamental importance in arriving at the most probable configurations of polypeptide chains in fibrous and globular proteins: (1) the coplanarity of the atoms comprising the amide group, 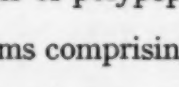 , and (2) the formation of close to the maximum possible number of N—H···O=C hydrogen bonds. The application of these structural principles and the use of accurate values for interatomic distances and bond angles led to the discovery and the exact description of several possible configurations of the polypeptide chain.

Of these possible configurations, the first to be discovered was the α-helix[20, 21, 22]. This configuration has been shown experimentally to be a principal structural constituent of many fibrous and globular proteins and synthetic polypeptides[23]. Another configuration of great interest was discovered in the course of a systematic survey[24] in which the arrangement of the amide groups was restricted to certain orientations around the C—C and C—N single bonds. The most significant feature of this configuration is the orientation of the >C=O and >N—H groups. The >C=O and >N—H groups of successive residues protrude from opposite sides of the helix; their orientation, nearly perpendicular to the axis of the helix, is particularly favorable to the formation of lateral C=O···H—N hydrogen bonds between adjacent helixes. A succession of helixes bonded together in this manner can build up two sheet structures, the parallel-chain and the antiparallel-chain pleated sheets, corresponding to a parallel or antiparallel arrangement of adjacent helixes. These two structures were originally formulated on the basis of specific, presumably favored orientations around the C—C and C—N single bonds[24]; subsequently[25] they were revised so as to make all N—H···O hydrogen bonds linear. Although this revision involved departure from the previous orientations around the single bonds, the new structures were considered to be probably more stable. The fiber-axis identity distance calculated for the new parallel-chain pleated sheet is 6.50 A and that for the antiparallel-chain pleated sheet is 7.00 A. The lateral displacement between equivalent chains (adjacent chains) in the parallel-chain pleated sheet is 4.85 A; between equivalent chains (alternate chains) of the antiparallel-chain pleated sheet this distance is 9.50 A. These dimensions gave rise to the suggestion[24] that the β-keratin proteins, for which the fiber-axis identity distance is about 6.6 A, probably have a structure based upon the parallel-chain pleated sheet, and that silk fibroin, for which the observed fiber-axis identity distance is 7.0 A, probably has a structure based upon the antiparallel-chain pleated sheet. A drawing of the antiparallel-chain pleated sheet is reproduced in Fig. 6.

Several features of the X-ray data give confirmation to the choice of an antiparallel-chain pleated sheet as the basic structural component of silk fibroin. The fact that silk fibroin may be doubly oriented by a rolling process indicates that a sheet, rather than an individual helix, forms the basis for the structure. The agreement between the calculated fiber-axis identity distance (7.0 A) and that obtained experimentally (6.97 A) has already been mentioned. The spacing of the C, O, and N atoms at an approximately uniform interval along the fiber axis might be expected to give rise to a sixth-order

References p. 33/34.

meridional reflection corresponding to a spacing of 1.17 A for the antiparallel-chain structure and 1.08 A for the parallel-chain structure; a strong 1.16-A meridional reflection is indeed observed. The three sharp equatorial reflections—the only reflections shown by the photographs of doubly-oriented specimens to arise from planes perpendicular to the plane of rolling—correspond approximately to fourth, sixth, and eighth orders of a 9.4-A spacing; the spacing of alternate (equivalent) chains calculated for the antiparallel-chain pleated sheet is 9.5 A. We have accordingly assumed that in silk fibroin the polypeptide chains are arranged in the form of antiparallel-chain pleated sheets and that the plane of rolling of the doubly-oriented samples is the plane of the pleated sheet.

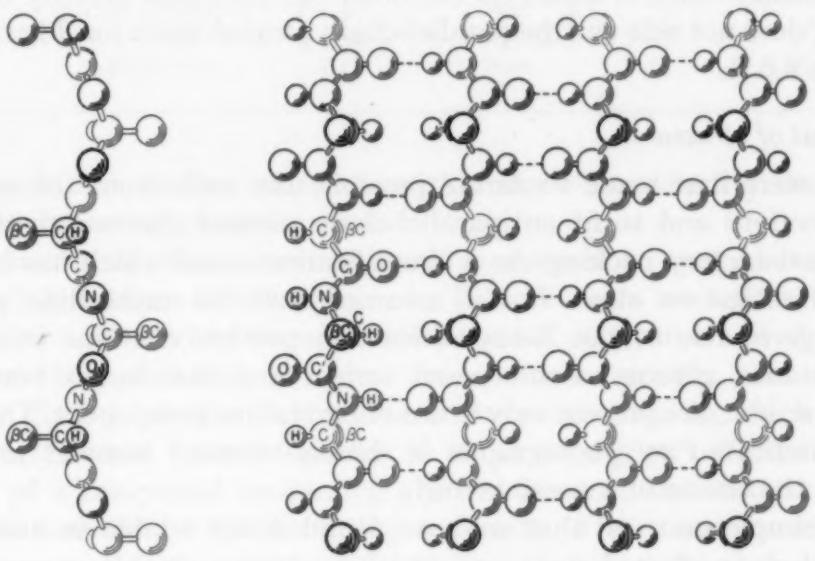

Fig. 6. A drawing of the antiparallel-chain pleated sheet.

The reasons for choosing the antiparallel-chain in preference to the parallel-chain pleated sheet should perhaps be clarified by additional brief discussion. It is evident that the observed reflections corresponding to the fourth, sixth, and eighth orders of a 9.4-A spacing between alternate chains of an antiparallel-chain pleated sheet could as readily be interpreted as second, third, and fourth orders of a 4.7-A spacing between adjacent chains of a parallel-chain sheet. On what, then, does the choice depend? The fundamental basis is our confidence in the reliability of the dimensions of the polypeptide chain in proteins as determined from precise X-ray analyses of crystals of amino acids, peptides, and related compounds[3], and of the observed lengths and directional characteristics of N—H···O hydrogen bonds as determined in the same analyses. The experimental evidence indicates that stable structures of peptides and other compounds related to proteins involve the formation of close to the maximum number of N—H···O hydrogen bonds, and that generally these bonds are approximately 2.8 A long and close to linear, that is, the N—H···O angle is generally close to 180°. Indeed it was the convincing nature of this experimental evidence which led to the conclusion that in the formation of stable pleated sheets from parallel and antiparallel assemblies of polypeptide chains the approximate linearity of the N—H···O hydrogen bond is of primary importance[25]. Polypeptide chains incorporating dimensions based on the best experimental data and extended so as to correspond to the observed 6.97-A fiber-axis identity

References p. 33/34.

distance of silk fibroin assume a configuration such that the C=O and N—H bonds are oriented almost exactly perpendicular to the fiber axis. Separated by 4.7 A and arranged in the antiparallel sense, these chains can form linear N— H···O hydrogen bonds 2.76 A in length and build up antiparallel-chain pleated sheets of dimensions compatible with the data from silk fibroin. Arranged in the parallel sense, on the other hand, these chains can, at best, form hydrogen bonds which are 2.97 A long and which depart from linearity by 20°. There seems to be little reason to doubt that antiparallel-chain pleated sheets involving short, linear hydrogen bonds would be significantly more stable than parallel-chain sheets involving longer and distorted hydrogen bonds. Accordingly the antiparallel-chain pleated sheet has been chosen as the structural basis for silk fibroin.

This argument, which is based on the observed fiber-axis identity distance 6.97 A for silk fibroin, does not rule out the parallel-chain pleated sheet for β-keratin, for which this distance is 6.6 A.

2. A pseudo unit of structure

Attempts were first made to derive possible unit cells from the spacings of the equatorial reflections and to fit antiparallel-chain pleated sheets into these unit cells so as to give satisfactory packing. As a simplification—one which has been attractive to previous investigators also—it was assumed that the crystalline portion of silk fibroin which gives rise to the X-ray diffraction pattern contains only the smallest amino-acid residues, glycine, alanine, and serine, and that larger residues, such as tyrosine, leucine, etc., are present only in a non-crystalline component. The orientational requirements indicated by photographs of doubly-oriented samples imposed further restrictions on the choice of a possible unit.

The only simple unit cell that we have found which is able to accommodate the the antiparallel-chain pleated sheet and which is also reasonably compatible with the positions and orientations of the equatorial reflections is an orthogonal one with dimensions $a_0 = 9.40$ A, $b_0 = 6.97$ A, $c_0 = 9.20$ A. The b axis of this unit cell is in the direction of the fiber axis; the a and c axes lie in the basal plane perpendicular to the fiber axis and are parallel and perpendicular, respectively, to the plane of rolling of the doubly-oriented samples. On the basis of this unit cell the equatorial reflections may be indexed as shown in Table IV. Reflections apparently arising from sets of planes oriented approximately perpendicular to the plane of rolling would be expected to be axial reflections of the type $h00$; the reflections arising from planes oriented parallel to the plane of rolling would be expected to be reflections of the type $00l$. The 4.25-A reflection apparently arises from sets of planes oriented at an angle of about 70° from the plane of rolling; this angle is consistent with crystallographic planes of the forms $\{201\}$ and $\{20\bar{1}\}$. The only discrepancy between the observed and calculated interplanar spacings is in the values 9.7 A reported and 9.20 A calculated for reflection No. 1; this discrepancy will be discussed in Part 3 of this section.

If one assumes that antiparallel-chain pleated sheets are arranged parallel to the plane of rolling of the doubly-oriented samples, then the a and b axes of the proposed unit cell must lie in the plane of the pleated sheet. The b axis is parallel to the axis of the polypeptide chains; its identity distance represents the distance occupied by two residues along each chain. The a axis is parallel to the lateral hydrogen bonds within the sheets; its identity distance represents the distance between alternate polypeptide chains within the sheets. Thus, four amino-acid residues of a pleated sheet can be fitted

References p. 33/34.

TABLE IV

INDICES OF EQUATORIAL REFLECTIONS BASED ON PSEUDO UNIT CELL

No.	Interplanar spacing		hol	Orientation	Intensity
	Observed (A)	Calculated (A)			
1	9.70 ± 0.25	9.20	001	∥	90
2	4.70 ± 0.20	4.60	002	∥	450
3	4.25 ± 0.15	4.19	201, 20$\bar{1}$	*ca.* 70°	900
4	3.05 ± 0.02	3.07	003	∥	180
5	2.35 ± 0.01	2.35	400	⊥	20
6	2.10 ± 0.05	2.09	402, 40$\bar{2}$		< 5
7	1.80 ± 0.05	1.84	005	∥	< 5
8	1.56 ± 0.01	1.57	600	⊥	18
		1.54	601, 60$\bar{1}$		
9	1.20 ± 0.05	1.18	800	⊥	< 5

into this unit cell; the number of sheets within the *c*-axis identity distance may be derived from the following considerations.

As stated previously, this pseudo unit cell is assumed to contain only the glycine, alanine, and serine residues in silk fibroin. In Table V there are listed the densities of these three amino acids and of some simple peptides of glycine and alanine. From a consideration of these densities, it seems reasonable to predict that a polypeptide containing only glycine, alanine, and serine in the proportions in which they occur in silk (about 3:2:1) would have a density of about 1.45 g/cm^3. Similarly the average residue weight of a compound containing glycine, alanine, and serine residues in the proportions 3:2:1 would be 67. Assuming a density of 1.45 and an average residue weight of 67, the number of residues within the pseudo unit cell is calculated to be 7.9. Thus, since four residues of each pleated sheet are contained within the pseudo unit, these calculations indicate that there are two pleated sheets per cell.

TABLE V

DENSITIES OF CRYSTALS OF SELECTED AMINO ACIDS AND PEPTIDES

Compound	Density (g/cm^3)	Reference
glycine	1.607	26
D,L-alanine	1.40	27
D,L-serine	1.537	28
α-triglycine	1.57	29
D,L-alanylglycine	1.429	30
glycyl-D,L-alanine	1.425	30
D,D-dialanine	1.280	31
L,L,L-trialanine	1.333	31

Information concerning the spacing of pleated sheets in the direction of the *c* axis can be obtained from the intensities of the equatorial reflections representing orders of (001). Four reflections of this type are observed, but the intensity of 005 was too low for spectrometric measurement. Relative values of F^2 for the reflections 001, 002, and 003 were obtained by correcting the observed intensities for Lorentz and polarization factors.

References p. 33/34.

These values of F^2 can be used for the computation of a one-dimensional Patterson function.

$$P(w) = \sum_l F^2_{00l} \cos 2\pi lw$$

A plot of this function is shown in Fig. 7.

Besides the peak at the origin, the only features of this function are the two related maxima at about 3.7 and 5.5 A from the origin. This Patterson projection can be interpreted as indicating that in the structure of silk fibroin the distances between adjacent pleated sheets are alternately 3.7 A and 5.5 A. The details of the packing of the pleated sheets in accordance with this interpretation may be derived from the following structural considerations.

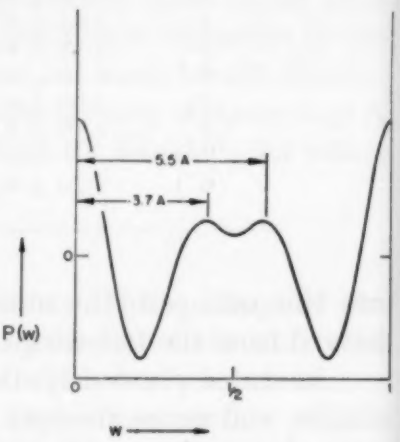

Fig. 7. The Patterson function $P(w)$ calculated from the intensities of the first three orders of (001). The vertical scale is arbitrary.

A feature of the pleated-sheet structures is that the bonds between the α-carbon atoms in the main polypeptide chains and the adjoining β-carbon atoms of the side chains are oriented approximately perpendicular to the plane of the sheet. As a consequence, the way in which adjacent sheets are packed together is determined almost entirely by the sizes and shapes of the side chains of the component amino-acid residues. Pleated sheets containing only glycine residues, in which β-carbon atoms are replaced by hydrogen atoms, would be expected to pack together much more closely than would pleated sheets consisting of alanine or of larger amino-acid residues. Indeed, construction of accurate scale models[32] of antiparallel-chain pleated sheets shows that two sheets consisting solely of glycine residues may pack together at a distance of about 3.5 A, whereas sheets containing only alanine or serine residues may pack together efficiently at a distance of about 5.7 A; larger amino-acid residues require larger packing distances.

An additional feature of the pleated-sheet structures is that within each polypeptide chain the side chains of adjacent amino-acid residues protrude from opposite sides of the sheet (Fig. 6). Thus, polypeptide chains consisting of an alternation of glycine and alanine residues may be arranged in such a way as to form a sheet having only the hydrogen atoms of the glycine residues protruding from the front side and only the methyl groups of the alanine residues protruding from the back side. Two sheets of this type can pack together efficiently either front-to-front at a distance of 3.5 A or back-to-back at a distance of 5.7 A; a succession of these sheets would pack together at distances alternately 3.5 and 5.7 A. An arrangement of this sort would be in approximate agreement with the positions of the maxima in the Patterson function $P(w)$; it would also be consistent with a composition of four glycine, three alanine, and one serine residue in the unit cell.

The structure which we propose as a pseudo unit for silk fibroin is shown diagrammatically in Fig. 8. Two unit cells are shown, each containing eight amino-acid residues comprising portions of two antiparallel-chain pleated sheets. For simplicity, the atoms in each pleated sheet are represented as being coplanar. The methyl or hydroxymethyl side chains of the alanine or serine residues are labeled "R"; they protrude, along the c axis, backward from the front plane and forward from the rear plane, interlocking so

References p. 33/34.

as to give efficient packing. These two planes are 5.7 A apart. The hydrogen atoms of the glycine residues protrude from the front of the forward plane and from the back of the rear plane; thus, the distance between the front plane of one unit cell and the rear plane of the next unit cell is 3.5 A.

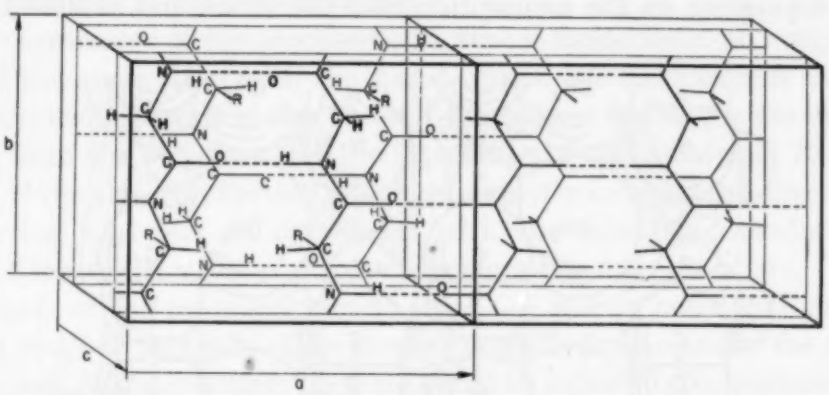

Fig. 8. A diagrammatic representation of the arrangement of the polypeptide chains within the pseudo unit of structure.

The assumption of the value 3.5 A for the distance between pairs of pleated sheets presenting glycine side chains (hydrogen atoms) toward one another is supported by the results of intensity calculations, and also by the consideration of the X-ray pattern of polyglycine. We have pointed out[23] that the powder X-ray pattern of polyglycine is compatible with a pleated-sheet structure. The strongest line of this pattern gives the spacing between adjacent pleated sheets, and its value is 3.47 A.

A schematic representation of the proposed pseudo structure projected along the *b* axis is shown in Fig. 9. In this drawing the backbones of the polypeptide chains are represented as roughly elliptical; they are bonded together by hydrogen bonds to form sheets parallel to the *a* axis. The large circles between these sheets represent methyl or hydroxymethyl side chains of alanine or serine residues and the small circles represent hydrogen atoms of glycine residues. The arrangement of the sheets at alternately 3.5 and 5.7 A is clearly shown.

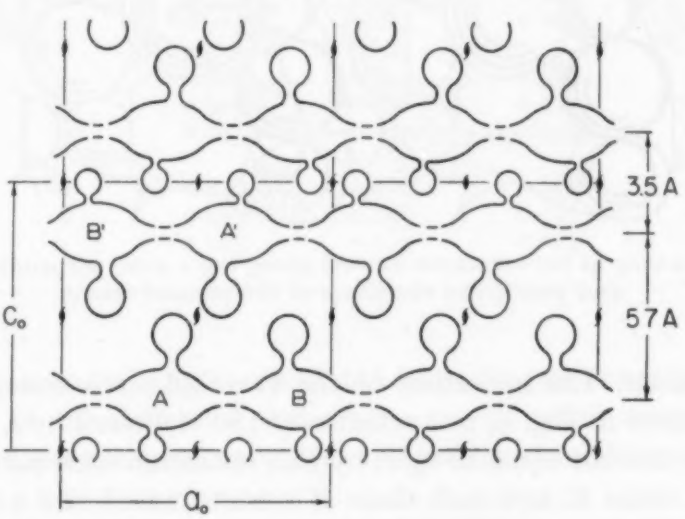

Fig. 9. A schematic representation of the proposed pseudo unit of structure projected along the fiber axis.

References p. 33/34.

Packing drawings of the structure viewed along the y and z axes are shown in Figs. 10 and 11 respectively.

Although the unit cell is orthogonal, the symmetry of the proposed pseudo structure is that of the monoclinic space group $P2_1$; furthermore, the presence of the two-fold screw axes is dependent on the assumption that the serine and alanine side chains are

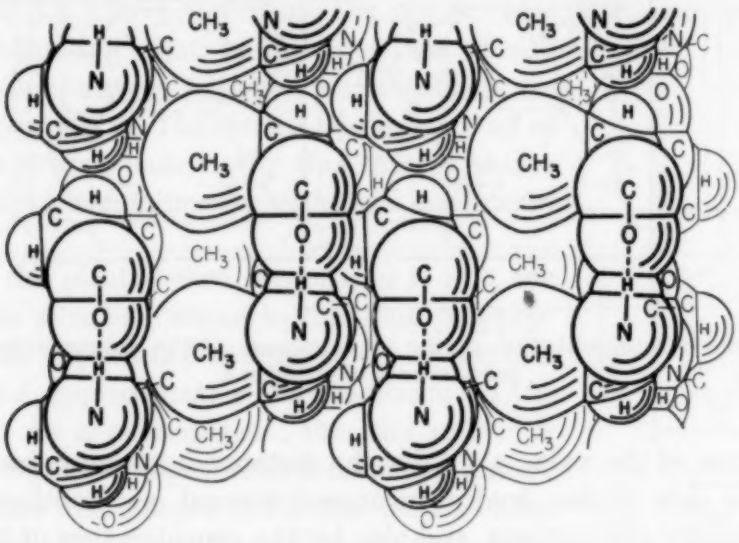

Fig. 10. A packing drawing of the structure viewed along the fiber (y) axis.

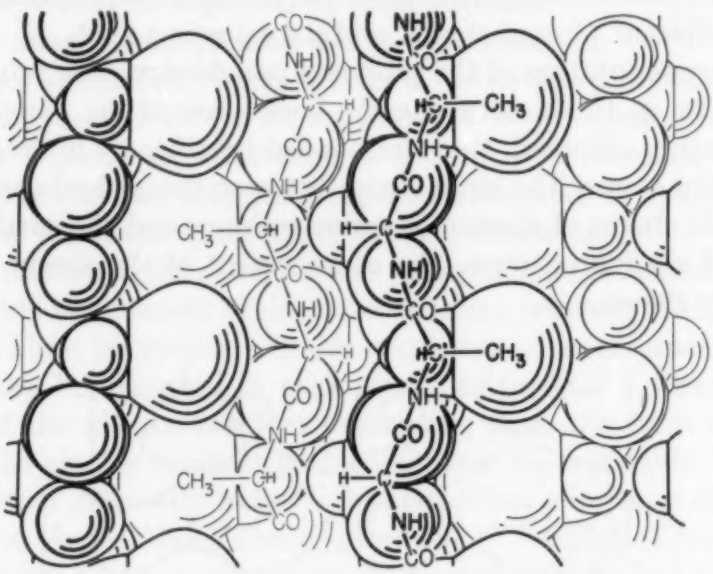

Fig. 11. A packing drawing of the structure viewed along the z axis, perpendicular to the fiber axis and parallel to the plane of the pleated sheets.

structurally equivalent. The operation of the two-fold screw axes, whose positions in the unit cell are shown in Fig. 9, is a rotation of 180° followed by a translation parallel to the b axis by an amount equal to $b_0/2$; by this operation each polypeptide chain A is transformed into a chain A′ and each chain B is transformed into a chain B′. Thus, the side chains of a pleated sheet A′ B′ are displaced from those of its neighbor A B by an amount equal to $b_0/2$; side chains from adjacent pleated sheets thus interlock.

References p. 33/34.

The detailed packing of the side chains is determined by the displacement along the *a* axis of the polypeptide chains A′ and B′ relative to chains A and B. In the pseudo structure, as shown in Fig. 9, the chains are staggered so that the center of chain A′ is midway between the centers of chains A and B. This arrangement is in agreement with the observed strength of the reflection 400.

Since the symmetry of the proposed structure is monoclinic, no restriction is placed on the size of the angle β between the *a* and *c* axes. We have chosen this angle to be 90°. The justification for this choice rests in the success of this pseudo unit of structure in explaining both the positions and the intensities of the equatorial X-ray reflections. In particular, if the 1.56-A reflection (No. 8) is correctly indexed as being a superposition of reflections 601 and $60\bar{1}$, in agreement with the intensity calculations, its small angular spread limits the value of β to 90° within a few minutes of arc.

On the basis of the proposed pseudo structure atomic positional parameters have been assigned to all of the main-chain atoms except hydrogen and to the β-carbon atoms of the alanine and serine residues; they are listed in Table VI. No parameters have been assigned to the oxygen atom of the serine residue.

TABLE VI

ATOMIC POSITIONAL PARAMETERS FOR THE PSEUDO STRUCTURE

Space group: $P2_1$
Equivalent positions: x, y, z (Chains A and B)
$\bar{x}, \frac{1}{2} + y, \bar{z}$ (Chains A′ and B′)
$a_0 = 9.40$ A
$b_0 = 6.97$ A
$c_0 = 9.20$ A
$\beta = 90°$

Chain	*Residue*		*N*	*C*	*C′*	*O*	*βC*
A	I	*x*	0.404	0.340	0.422	0.553	
		y	0.074	0.252	0.426	0.426	
		z	0.163	0.113	0.173	0.173	
A	II	*x*	0.346	0.410	0.328	0.197	0.410
		y	0.574	0.752	0.926	0.926	0.752
		z	0.215	0.265	0.205	0.205	0.430
B	III	*x*	0.904	0.840	0.922	0.053	0.840
		y	0.926	0.748	0.574	0.574	0.748
		z	0.215	0.265	0.205	0.205	0.430
B	IV	*x*	0.846	0.910	0.828	0.697	
		y	0.426	0.248	0.074	0.074	
		z	0.163	0.113	0.173	0.173	

The bond distances and angles calculated from the positional parameters are listed in Table VII. All of the distances and angles are in satisfactory agreement (within 0.02 A and 3°) with the accepted values for the fundamental dimensions of polypeptide chains[23].

The atomic positional parameters listed in Table VI were used to calculate structure factors for those reflections on the equator and first three layer lines which have inter-

References p. 33/34.

TABLE VII

INTERATOMIC DISTANCES AND BOND ANGLES FOR THE PROPOSED PSEUDO STRUCTURE

	Calculated from parameters in Table VI	*Accepted values*[3]
	Bonded distances	
N—C	1.45 A	1.47 A
C—C′	1.54	1.53
C′—O	1.23	1.24
C′—N	1.31	1.32
C—βC	1.52	1.54
N—H···O	2.76	2.8
	Bond angles	
N—C—C′	110.5°	110°
C—C′—O	120.1°	121°
C—C′—N	116.8°	114°
O—C′—N	123.0°	125°
C′—N—C	122.5°	123°
C′—N···O	122.3°	123°
C—N···O	115.1°	114°
N—C—βC	108.5°	109.5°
C′—C—βC	111.0°	109.5°

planar spacings greater than 1.0 A. The structure factor expression for the space group $P2_1$ is $F = A + iB$, where

$$\left.\begin{aligned} A_{hkl} &= \sum_j f_j \cos 2\pi(hx_j + lz_j) \cos 2\pi k y_j \\ B_{hkl} &= \sum_j f_j \cos 2\pi(hx_j + lz_j) \sin 2\pi k y_j \end{aligned}\right\} \text{for } k = 2n$$

and

$$\left.\begin{aligned} A_{hkl} &= -\sum_j f_j \sin 2\pi(hx_j + lz_j) \sin 2\pi k y_j \\ B_{hkl} &= \sum_j f_j \sin 2\pi(hx_j + lz_j) \cos 2\pi k y_j \end{aligned}\right\} \text{for } k = 2n + 1$$

The summations extend over all atoms j in the four residues (I, II, III, IV, Table VI) comprising the asymmetric unit: 10 carbon atoms, 4 oxygen atoms, and 4 nitrogen atoms. Atomic form factors f_j for carbon, nitrogen, and oxygen were taken from the tables of JAMES AND BRINDLEY[33]. The calculated values of $F^2 = A^2 + B^2$ are listed in Table VIII. Because of the orthogonality of the pseudo unit cell each reflection of the type *hkl* is superimposed on a corresponding reflection $hk\bar{l}$; for simplicity values of F^2_{calc} listed in the table comprise the sum of the contributions of the two planes *hkl* and $hk\bar{l}$. The observed intensities of reflections occurring on the equator and the first three layer lines are also listed in Table VIII. In cases where an observed reflection could not be unambiguously indexed from photographs of doubly-oriented samples, brackets have been used to include all planes compatible with the measured interplanar spacings. The observed intensities of the equatorial reflections have been corrected for Lorentz and polarization factors to give values of F^2_{obs}.

References p. 33/34.

TABLE VIII

INTENSITY DATA OBTAINED FROM SILK FIBROIN COMPARED WITH VALUES OF F^2 CALCULATED FROM THE PARAMETERS LISTED IN TABLE VI

h	l	d_{hol}	$k=0$			$k=1$		$k=2$		$k=3$	
			I_{obs}	F^2_{obs}	F^2_{calc}	I_{obs}	F^2_{calc}	I_{obs}	F^2_{calc}	I_{obs}	F^2_{calc}
0	0	—	—	—	14,400	—	0	vs	123	—	0
1	0	9.40			3		50	ms	16	ms	361
0	1	9.18	90	380	697	w	79		166		4
1	1	6.56			0		148		38	vw	639
2	0	4.70			0		55		0		21
0	2	4.59	450	3940	2460	w	424	ms	372	s	7
2	1	4.19	900	8700	2100	s	1015		33		88
1	2	4.12			17		186		52		454
2	2	3.28			208		336		43		6
3	0	3.08			10		17		214		182
0	3	3.07	180	1192	2725	vw	180	m	346	w	74
3	1	2.97			34		28		464		250
1	3	2.92			56		139		41		369
3	2	2.59			23		68		404		98
2	3	2.57			0		108		74		2
4	0	2.35	20	385	502	m	296		9		3
0	4	2.30			0		21		3		21
4	1	2.27			18		96	w	13	vw	8
1	4	2.23			66		84		55		279
3	3	2.19			4		99		284		88
4	2	2.09	< 5	< 110	116	w	348		30		26
2	4	2.07			180		552		45		10
5	0	1.88			9		35		17		166
4	3	1.87			162		332		45		8
3	4	1.85			10		102		231	vw	66
0	5	1.84	< 5	< 135	708	vvw	369		317		71
5	1	1.84			42		30		73		211
1	5	1.81			64		79		63		165
5	2	1.74			33		8		91		56
2	5	1.71			24		78		60		6
4	4	1.64			0		10		2		10
5	3	1.60			0		21		46		59
3	5	1.59			0		147		185		19
6	0	1.57			0		1		0	mw	1
6	1	1.54	18	615	612		38		47		2
0	6	1.53			61		38		266		164
1	6	1.51			86		74		54		80
6	2	1.48			238		20		47		6
2	6	1.46			32		196		152		2
5	4	1.45			24		4		89		45
4	5	1.45			20		246		99		4
6	3	1.39			46		10		23		4
3	6	1.38			22		188		100		6
7	0	1.34			7		0		17		630
7	1	1.33			17		45		91		977
5	5	1.32			7		51		119		11
0	7	1.31			1		10		110		85
1	7	1.30			126		43		35	mw	56
6	4	1.30			308		76		59		30
7	2	1.29			0		127		120		587
4	6	1.28			14		40		104		34
2	7	1.27			22		106		125		198
7	3	1.23			32		136		86		505
3	7	1.21			90		149		38		7
6	5	1.19			10		12		13		4

(continued overleaf)

TABLE VIII (continued)

h	l	d_{hol}	$k=0$			$k=1$		$k=2$		$k=3$	
			I_{obs}	F^2_{obs}	F^2_{calc}	I_{obs}	F^2_{calc}	I_{obs}	F^2_{calc}	I_{obs}	F^2_{calc}
5	6	1.19			19		126		54		24
8	0	1.18	< 5	< 250	250		1		29		1
8	1	1.17			46		2		16		0
7	4	1.16			43		80		152		423
0	8	1.15			159		12		90	w	586
4	7	1.15			16		8		57		16
1	8	1.14			129		19		35		46
8	2	1.14			184		10		44		0
2	8	1.12			4		18		4		24
8	3	1.10			274		16		61		14
6	6	1.10			44		48		39		30
7	5	1.08			29		180		207		187
3	8	1.08			102		90		19		6
5	7	1.08			111		81		2		22
8	4	1.05			0		0		0		2
9	0	1.04			5		23		55		102
9	1	1.04			24		20		132		127
4	8	1.03			0		16		65		158
0	9	1.02			0		9		0		27
9	2	1.02			22		9		137		28
1	9	1.02			100		10		37		31
7	6	1.01			149		303		108		32
6	7	1.01			44		40		33		104
2	9	1.00			0		58		38		178

In general there is good agreement between calculated and observed values of F^2 for the equatorial reflections. Indeed, the agreement would be excellent if the calculated values of F^2 were corrected with an anisotropic temperature factor of the type $\exp(-ah^2-\gamma l^2)$, where γ is considerably larger than a. A temperature factor of this type would be appropriate in view of the apparent disorder in the direction of the c axis as manifested by the diffuseness of observed reflections of the type $00l$.

The observed and calculated intensities for non-equatorial reflections are in general qualitative agreement. The most conspicuous discrepancy occurs for the meridional reflection 020; whereas this reflection is observed as being very strong, its calculated value of F^2 is only moderate. The low value of F^2 calculated for this reflection is due to the regular spacing of atoms along each polypeptide chain; the contributions of the two carbon atoms and one nitrogen atom in the chain nearly cancel one another, and the contributions of the oxygen atoms are to some extent canceled by the contributions of the β-carbon atoms. Since the extreme strength of the sixth-order meridional reflection is strong evidence in support of the basic arrangement of the polypeptide chain, it would appear that the strength of the 020 reflection must be due, in large part, to the contributions of side-chain atoms.

3. An extension of the pseudo unit and the structure of silk fibroin

Early in the course of our investigations of silk fibroin it was recognized that the complete and detailed structure of this substance could not be satisfactorily described on the basis of a unit cell as simple as the pseudo unit which we have discussed above. Nevertheless, it has seemed profitable thus far to describe the fundamental features of

References p. 33/34.

the structure in terms of the pseudo unit; indeed, the general agreement between observed values of intensities and interplanar spacing and those calculated for the pseudo unit is so striking that there can be little doubt that the real structure is closely related to the pseudo structure. It is the purpose of this section to discuss those ways in which the pseudo unit of structure must be revised and extended in order to approach more closely to the true structure of silk fibroin.

There are two major reasons why the pseudo unit cannot be the true unit of structure of silk fibroin. In the first place, the observed spectrum of the diffuse equatorial reflections—those reflections which arise from diffracting planes oriented parallel to the plane of rolling of the doubly-oriented samples, and which have been indexed as orders of 00*l*—cannot be satisfactorily explained by a *c* axis identity distance as small as 9.2 A. The presence of diffuse reflections at spacings of about 35 A and 15 A is strong evidence that the identity distance is probably very much greater than 9.2 A; furthermore, the observed spacing of the 9.7 A reflection differs from the assumed value, 9.2 A, by an amount greater than the limit of error of our observations.

A second objection to the pseudo structure is that it takes into account only the three smallest amino-acid residues present in silk fibroin—glycine, alanine, and serine; the remaining 18% of the residues, including about 5% of tyrosine, remain unaccounted for. There has been a tendency among previous investigators to ignore this 18% of the larger residues on the grounds that the X-ray diffraction pattern of silk fibroin is so simple relative to those of other proteins that only small, well-ordered amino-acid residues can be present in the crystalline portion. This viewpoint has found some support in various chemical experiments as discussed in the introduction to this paper; however, there is also considerable contradictory evidence, and at the present time there seems to be insufficient justification for assuming that the larger amino-acid residues occur only in a non-crystalline portion of the protein. It seems more likely that the diffraction pattern of silk fibroin is representative of all of the residues present in the protein.

It is reasonable to assume that the true structure of silk fibroin is based on the pseudo unit of structure so modified and extended as to satisfactorily account for the diffuse equatorial reflections and to include the larger as well as the smaller amino-acid residues. The diffuse reflections have already been interpreted as being representative of the method of packing of the antiparallel-chain pleated sheets, so that changes in the distances between adjacent sheets would affect the positions and intensities of these reflections. The distances between adjacent sheets are determined primarily by the sizes and shapes of the side chains of the amino-acid residues; in particular, the side chains of the larger amino-acid residues present in silk fibroin would require inter-sheet distances considerably larger than the 3.5 and 5.7 A distances in the pseudo structure. It seems probable, then, that the X-ray diffraction pattern of silk fibroin can be explained by assuming that the majority of the small amino-acid residues glycine, alanine, and serine are arranged in accordance with the proposed pseudo unit; the remaining 18% of the residues, which are too large to be accommodated by the pseudo unit, are nevertheless present in the crystalline component of silk fibroin and are responsible for deformations of the pseudo unit. These deformations occur in the direction of the *c* axis of the pseudo unit, and hence have a relatively large effect on the spacings and intensities of the 00*l* reflections.

Measurements made on models of antiparallel-chain pleated sheets show that a

References p. 33/34.

sheet containing the side chains of tyrosine or phenylalanine protruding from one side may pack with an adjacent sheet consisting of glycine residues at a distance of approximately 8 to 9 A. In view of the fact that the van der Waals diameter of a phenyl group is about 7 A, this distance is, at first glance, somewhat shorter than might be expected. However, since the bond connecting the α-carbon atom of the main polypeptide chain with the corresponding β-carbon atom of the side chain is oriented perpendicular to the plane of the pleated sheet, the bond connecting the β-carbon atom to the phenyl group makes an angle of only 20° with the plane of the sheet; thus, the phenyl group can conveniently lie nearly parallel to the plane of the sheet. Consequently the packing is determined predominantly by the van der Waals thickness rather than the diameter of the phenyl group.

Inter-sheet distances required by the other large amino-acid residues present in silk fibroin are more difficult to predict since there are fewer restrictions on the relative positions of the various side-chain atoms. It appears that efficient packing can be obtained if the distances are approximately the same as that required by the tyrosine residues—about 8 or 9 A if the adjacent pleated sheet consists of glycine residues or about 10 A if the adjacent sheet consists of alanine or serine residues. Thus, the introduction of the larger amino-acid residues into the crystalline part of silk fibroin would require that the strict alternation of inter-sheet distances between the values of 3.5 and 5.7 A, as derived for the pseudo unit, be interrupted occasionally by distances of about 9 A.

One might expect that definite information concerning the sequence of distances between adjacent pleated sheets, and in particular the way in which pleated sheets containing the larger residues are packed in relation to the sheets containing the smaller residues, could be derived from the positions and intensities of the reflections of the type 00*l*. However, there are so few reflections of this type that no precise conclusions as to the packing can be drawn; indeed, the diffuseness of these reflections may be taken as an indication that perhaps there is no well-ordered method of packing of the sheets, and therefore no true identity distance in the direction perpendicular to the sheets. A minimum identity distance roughly compatible with the observed spacings of all of the diffuse equatorial reflections is about 58 A.

Some additional information regarding the packing of the sheets may be derived from considerations of density. Since the larger amino-acid residues are to be included in the structure, the density of the material giving rise to the X-ray diffraction pattern must be taken as the density of silk fibroin rather than the density of a pseudo-silk containing only glycine, alanine, and serine. The most reliable value for the density of silk fibroin appears to be that reported by HEERTJES[34], 1.34 g/cm^3. From this value for the density and the average residue weight of 76.5 reported by TRISTRAM[1], the volume occupied by one residue is calculated to be 94.8 A^3. The area occupied by four residues within each pleated sheet is given by the *a* and *b* identity distances of the pseudo unit cell—$9.4 \times 6.97 = 65.5$ A^2; from these figures the average distance between adjacent sheets may be computed. The resulting value is 5.8 A, as compared with the value of 4.6 A derived for the pseudo structure. These calculations indicate that if there is a definite *c*-axis identity distance in silk fibroin it is a multiple of 5.8 A.

In an attempt to derive some conclusions as to the sequence of pleated sheets in silk fibroin, we have made intensity calculations for several different arrangements of the sheets. The method used for each of these calculations is as follows. First, an

References p. 33/34.

identity distance normal to the plane of the pleated sheets was assumed; the distances actually chosen were 58 A and 174 A, the value of 58 A having been previously derived as being the minimum spacing compatible with the positions of the diffuse equatorial reflections. Within the chosen identity distance there were placed pleated sheets consistent in number with the density calculations; thus, ten pleated sheets were placed in the assumed identity distance of 58 A and thirty in the distance 174 A. For the actual positioning of these sheets it was assumed that approximately two-thirds of the sheets are packed in accordance with the pseudo structure, that is, with inter-sheet distances alternating between the values 3.5 and 5.7 A. The remaining sheets were placed at distances of about 9 A, representing the packing distance required by pleated sheets containing the larger amino-acid residues. For each calculation it was assumed that all of the scattering material present in each pleated sheet is located in the plane of that sheet; thus, the effect of the side chains as well as that of the slight puckering of the sheets were neglected. These assumptions imply that the distance between any two adjacent sheets must remain the same throughout the structure. This implication, which arises from the necessity of performing computations on simplified models, should not be regarded as defining a structural feature of silk fibroin. It is probable that the sequence of amino-acid residues in silk fibroin requires that the distance between any two adjacent sheets vary considerably from region to region; the models upon which these calculations are based should, accordingly, be regarded as representing localized methods of packing which occur frequently throughout the structure.

In order to simplify the calculations, each sheet was represented by a point on the c axis and these points were arranged symmetrically about the origin. The structure factor expression for each plane $00l$ is then of the form

$$F_{00l} = \sum_i \cos 2\pi l \, (z_i/c_0)$$

where z_i is the distance in Ångströms of each point i from the origin and c_0 is the assumed identity distance.

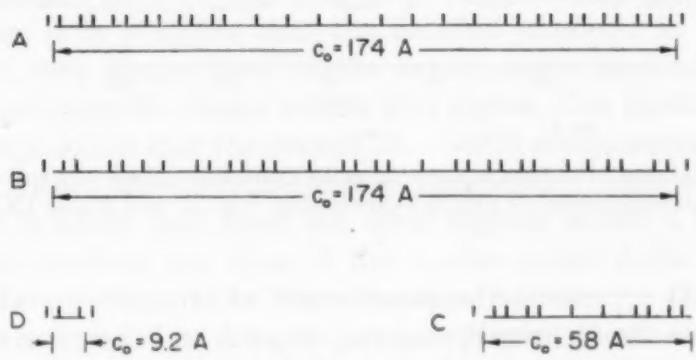

Fig. 12. Arrangements of pleated sheets assumed for intensity calculations.

Typical arrangements of pleated sheets for which intensity calculations were made are described in Table IX and Fig. 12. The results of the intensity calculations are shown diagrammatically in Fig. 13, in which the calculated values of F^2_{00l}/n^2 are plotted against sin θ/λ. For purposes of normalization, the calculated values of F^2 were divided by n^2, where n is the number of sheets within the assumed identity distance c_0. For comparison, the observed spectrum of the diffuse equatorial reflections is shown at the bottom of Fig. 13.

References p. 33/34.

TABLE IX

PARAMETERS z_i, IN ÅNGSTRÖMS, FOR ARRANGEMENTS OF PLEATED SHEETS SHOWN IN FIG. 12

A ($c_0 = 174$)		*B* ($c_0 = 174$)		*C* ($c_0 = 58$)	*D* ($c_0 = 9.2$)
1.75	91.37	2.85	89.85	2.85	1.75
7.45	100.09	6.31	93.31	6.35	7.45
10.95	108.81	15.75	102.75	12.05	
16.65	117.53	19.21	112.18	15.55	
20.15	126.25	24.91	115.64	24.55	
25.85	129.75	30.61	121.34	33.45	
29.35	135.45	40.04	124.80	42.45	
35.05	138.95	43.50	130.50	45.95	
38.55	144.65	49.20	133.96	51.65	
44.25	148.15	52.66	143.39	55.15	
47.75	153.85	58.36	149.09		
56.47	157.35	61.82	154.79		
65.19	163.05	71.25	158.25		
73.91	166.55	80.69	167.69		
82.63	172.25	84.15	171.15		

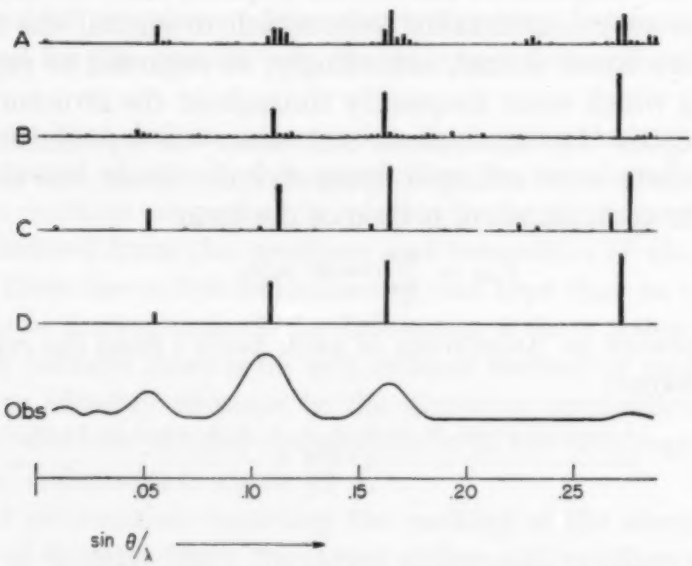

Fig. 13. Observed spectrum of diffuse equatorial reflections and values of F^2/n^2 calculated for various arrangements of pleated sheets (See Fig. 12 and Table IX).

Arrangement D represents the pseudo unit of structure in which there are two pleated sheets within the identity distance $c_0 = 9.2$ A and there is a strict alternation of inter-sheet distances between the values 3.5 and 5.7 A. It has already been pointed out that in this arrangement no provision is made for amino-acid residues other than glycine, alanine, and serine, that its density would be expected to be significantly higher than that observed for silk fibroin, that it will not explain satisfactorily the observed position of the 9.7-A reflection ($\sin \theta/\lambda = 0.053$), and that it will not account for the presence of the weak reflections at smaller diffraction angles. Arrangement C is based upon an identity distance of 58 A containing 10 pleated sheets; arrangements A and B are based on an identity distance of 174 A containing 30 pleated sheets. These three arrangements are compatible with the observed density. It should be emphasized again that these

References p. 33/34.

arrangements are not presented as being possible structures of silk fibroin, but rather as a means of exploring the effect on the diffuse equatorial reflections of the introduction of the larger residues.

Of the intensity plots shown in Fig. 13, that of arrangement C probably shows the most satisfactory agreement with the observed positions and intensities of the diffuse equatorial reflections. However, it is evident that the observed spectrum, including the weak reflections at small diffraction angles, can be approximated by the intensities calculated for any of several different arrangements of the pleated sheets and that no "best" arrangement can be decided upon.

Better agreement with the observed spectrum could be obtained by applying a temperature factor of the type $e^{-B(\sin\theta/\lambda)^2}$ to the calculated intensities; a "temperature" factor of this sort would compensate for general disorder in the packing of the sheets and also take into account, to some extent, the "pleating" of the sheets and the effects of side-chain atoms.

It should be noted that the introduction of the larger amino-acid residues can be accomplished without major changes in the 00*l* spectrum, and that their presence would have even less effect on the intensities of the general reflections of the type *hkl*. It therefore seems reasonable to conclude that the significance of the general agreement between the observed intensities and those calculated for the pseudo structure (Table VIII) may be extended to more complete structures which include all of the amino-acid residues known to be present in silk fibroin.

Two conclusions may be drawn from the agreement between observed and calculated intensities as represented in Table VIII and Fig. 13. In the first place, the diffraction pattern of silk fibroin can be explained on the basis of an arrangement of antiparallel-chain pleated sheets wherein the strict alternation of inter-sheet distances as derived for the pseudo structure is interrupted occasionally by larger spacings representative of the larger amino-acid residues; in the second place, no information as to the exact dispositon of these larger spacings within the structure can be derived. Indeed, it is reasonable to suppose that these large inter-sheet spacings do not occur in a well-defined manner; it is probable that the detailed structure in any region is not determined *a priori*, but adapts itself to the requirements imposed by the chemical composition of the polypeptide chains within that region. One further point should be stressed: it seems improbable that the overall amino-acid composition of any one particular pleated sheet within the structure differs significantly from the composition of any other sheet. It is likely that there are some regions within a given sheet where essentially all of the residues are those of the smaller amino-acids and other regions where there is a concentration of the larger residues; but there seems to be no reason and there certainly is no need to assume that one pleated sheet—or one polypeptide chain within a sheet—consists entirely of small amino-acid residues and that another pleated sheet contains the larger residues. Thus, the method of packing of adjacent pleated sheets is determined by the composition of regions within the sheets rather than by the composition of the sheets as a whole.

The structure of silk fibroin may, then, be described as consisting of antiparallel-chain pleated sheets packed together in a manner determined by the sequence of amino-acid residues within the polypeptide chains. In particular, the sequence –G–X–G–X–G–, where G is glycine and X is alanine or serine, must occur with high frequency; this is the only sequence which will account for the alternation of inter-sheet distance between the

References p. 33/34.

values 3.5 and 5.7 A. which predominates in the structure. The larger amino-acid residues such as tyrosine are also present within the crystalline portion of silk fibroin, although the precise manner in which they are arranged in the structure cannot be derived.

Just as a satisfactory description of the packing of the pleated sheets requires a modification of the *c*-axis identity distance of the simple pseudo unit of structure, so a complete picture of the distribution of the amino-acid residues within the sheets, either along the fiber axis of the polypeptide chains or in the direction perpendicular to the fiber axis, requires an abandonment of the corresponding *b*- and *a*-axis identity distances 6.97 and 9.4 A. The values for b_0 and a_0 as deduced from the X-ray diffraction pattern cannot be regarded as true identity distances in the strict crystallographic sense, but rather as repeat distances of the back-bone atoms of the polypeptide chains; true identity distances would be determined by the disposition of side-chain atoms. In view of the variety of the amino-acid residues present, it is likely that identity distances in the strict crystallographic sense do not exist in silk fibroin. The occurrence on heavily exposed photographs of weak layer lines representing first and second orders of a 21-A repeat distance in the *b* direction is undoubtedly due to some kind of ordering of side-chain atoms. It is tempting, although probably not justified, to regard these layer lines as arising from a regular repetition of serine residues in a sequence such as –G–A–G–A–G–S–.

IV. DISCUSSION OF THE STRUCTURE

The structure of silk fibroin which has been derived in the preceding section lacks complete definition in the sense that it does not assign specific coordinates to all of the atoms in the protein. Nevertheless, it is characterized by very specific structural features which are so well defined as to merit further examination and discussion.

1. Physical properties and the orientation of hydrogen bonds

The proposed structure of silk fibroin consists essentially of a lateral packing of pleated sheets composed in turn of polypeptide chains bound together in the plane of the sheet by N—H···O hydrogen bonds normal to the fiber axis. Supplementary evidence concerning the validity of this structure may be sought in studies of silk fibroin made with the electron microscope and by the techniques of infrared spectroscopy.

Mr. EDWARD D. HENDERSON of these Laboratories has made several electron micrographs of silk fibroin prepared in the following manner. Degummed natural silk fibers were cut into short lengths and were further disintegrated in water suspension by prolonged treatment with a Waring Blendor. The suspension was allowed to settle for several hours, after which time portions of the supernatant liquid containing the finer particles were removed for examination with the electron microscope. Fig. 14 shows a typical electron micrograph obtained in this way. The flat ribbonlike form of the silk fibers is similar to that reported by other workers (ZAHN[35], HEGETSCHWEILER[36]). By means of tryptic digestion, MERCER[37] obtained thin "ribbon-like fragments" of silk fibroin which in electron micrographs showed what seemed to be "long, thin, parallel microfibrils". All of this evidence appears to be favorable to a structure for silk fibroin composed of laterally packed sheets of polypeptide chains; it cannot, of course, be construed as proof of such a structure.

References p. 33/34.

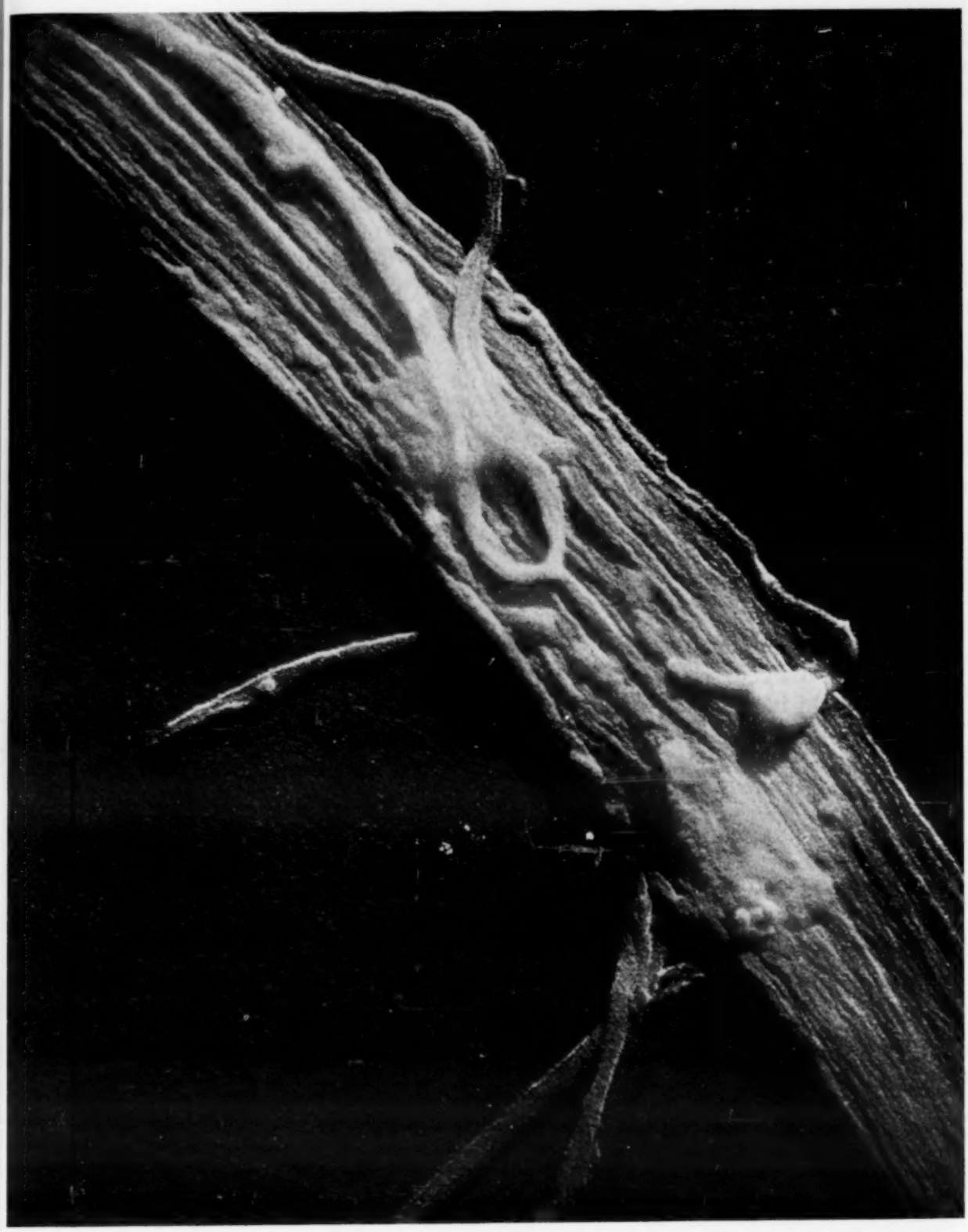

Fig. 14. An electron micrograph of a silk fiber shadowed with a 15-A film of gold-palladium alloy at the angle $\tan^{-1} = 1/3$.

The results of infrared spectroscopic measurements, especially measurements of infrared dichroism, can be interpreted more definitely in terms of structural features of silk fibroin. The approximate orientation of the C=O and the N—H bonds in fibers

References p. 33/34.

of synthetic polypeptides and in fibrous proteins have been determined by measuring the dichroic ratio observed for polarized infrared radiation (AMBROSE AND ELLIOTT[38]). By this means, AMBROSE AND ELLIOTT[39] were able to decide that these bonds are oriented approximately parallel to the fiber axis in the α-proteins such as hair and approximately perpendicular to the fiber axis in the β-proteins, including silk suture. They interpreted their infrared data as also showing that silk suture contains a component whose chains are folded in a fashion similar to that of the α-proteins. The use of dichroic ratios for determining unambiguously the precise orientations of the C=O and N—H bonds in silk fibroin and other fibrous proteins is complicated by problems of interpretation which have apparently not yet been satisfactorily solved[40, 41, 42].

2. Chemical composition and sequences of amino-acid residues

Unlike structures previously proposed for silk fibroin, which accounted for only the glycine, alanine, and serine residues, the present structure provides for the presence of nearly all of the amino-acid residues shown by analysis to be present in the protein. The only amino-acid residue which cannot be accommodated is proline, which, because of the steric restrictions imposed by the five-membered ring, would cause major distortions or interruptions of the pleated sheets. However, the proline content of silk fibroin—0.5 residue per cent—is probably too small to have a determining effect upon the structure.

A fundamental feature of the proposed structure is the frequent occurrence in the polypeptide chains of the sequence –G–X–G–X–G–X–, in which G represents glycyl and X represents alanyl or seryl residues. Evidence concerning the occurrence of this sequence is to be sought in the identity and relative amounts of the peptides isolated from hydrolysates of silk fibroin.

From chromatographic analysis of acid hydrolysates of fibroin, LEVY AND SLOBODIAN[43, 44] report the presence of large amounts of the dipeptides alanylglycine and glycylalanine, but only very small amounts of glycylglycine. In a later paper[45], these authors reported the presence of large amounts of the tripeptide glycylalanylglycine. More complete chromatographic analyses of partial hydrolysates of silk fibroin have recently been reported by KAY AND SCHROEDER[46]. The principal dipeptides found by these authors are alanylglycine, glycylalanine, serylglycine, tyrosylglycine, and glycyltyrosine; no glycylglycine or serylalanine and only small amounts of alanylalanine were reported. They also separated a number of tripeptides, the most prominent of which they believed to be serylglycylalanine, glycylalanylglycine, alanylglycylalanine, and glycylvalylglycine. The total amounts of dipeptides and tripeptides found by them account for approximately 50% of the glycine, alanine, serine, and tyrosine present in silk fibroin. Two tetrapeptides, alanylglycylanalylglycine and serylglycylalanylglycine, have also been isolated from large-scale chromatograms[47].

From the relative amounts of alanylglycine and glycylalanine which they obtained, LEVY AND SLOBODIAN proposed the sequence $-G-X_1-A-G-A-G-X_2-$ (G = glycine, A = alanine, X = other residue) as a minimum repeating unit for silk fibroin. However, KAY AND SCHROEDER raise some question as to the significance of this proposal; in particular, they point out that the effect of the relative ease of hydrolysis of the bonds X_1–A and G–X_2 might be rather great in determining the amounts of alanylglycine and glycylalanine in the hydrolysates. Indeed, if X_2 were a serine residue, the extreme ease of hydrolysis of the glycyl-seryl bond[48] would be expected to increase the observed

References p. 33/34.

amounts of alanylglycine and glycylalanylglycine. Similarly, if the assumption is made that the sequence –A–G–A–G–S–G– occurs frequently in silk fibroin, the dipeptides formed on hydrolysis would be expected to contain considerably more alanylglycine than glycylalanine, and the tripeptides would contain considerably more glycylalanylglycine than alanylglycylalanine. The observational data of KAY AND SCHROEDER are in accord with the results of this assumption; indeed, the relative amounts of the dipeptides and tripeptides of alanine, glycine, and serine obtained by them can be satisfactorily explained if one assumes that the sequence –G–X–G–X–G–, where X may be either alanine or serine, occurs frequently in silk fibroin.

Among the heavier amino-acid residues, the principal peptides isolated by KAY AND SCHROEDER are tyrosylglycine, glycyltyrosine, and gylcylvalylglycine. The presence of these sequences would indicate that the larger amino-acid residues in silk fibroin are surrounded by glycine residues; thus, in those portions of the protein which contain the larger amino-acid residues, the sequence is apparently –G–X–G–X–G–, where X may be any of the larger residues. This sequence is compatible with the proposed structure. Polypeptide chains containing sequences of this type could form antiparallel-chain pleated sheets in which the hydrogen atoms of the glycine residues protrude from one side and the side chains of the large residues protrude from the other side; two sheets of this sort could pack together front-to-front at a distance of 3.5 A, back-to-back at a distance of about 11 A, or front-to-back at a distance of about 8 A. On the basis of the present evidence, there appears to be no way to choose between the latter two arrangements; in the packing models for which we have calculated intensities of the 00*l* reflections, we have chosen a value of approximately 9 A to represent the distance between sheets containing the larger amino-acid residues without regard as to whether these sheets pack front-to-front or front-to-back, or as to whether or not the large side chains protrude from both sides of a single pleated sheet. The chemical evidence of KAY AND SCHROEDER might be considered to indicate that, in general, the large residues protrude from only one side of the sheets. On the other hand, SANGER[49] concludes from a study of the works of various investigators that "there are tetrapeptide sequences in fibroin that contain no glycine or alanine"; if this is the case, it would mean that there are at least small regions in the structure where the larger side chains protrude from both sides of a single pleated sheet.

3. Concluding Remarks

Previous investigators have proposed structures for silk fibroin comprising extended polypeptide chains oriented parallel to the fiber axis and held together by lateral hydrogen bonds[5,9,11], but no previous attempt has been made to assign definite coordinates to carbon, nitrogen, and oxygen atoms. The present structure, based on many more data, and in particular on quantitative spectrometric measurements of the intensities and interplanar spacings of the equatorial reflections, is superficially similar. Because of the greater accuracy of the data, however, it has been possible to arrive at a definite picture of the way in which the chains are packed together, and for the pseudo unit, at least, even to assign positional parameters to the principal atoms comprising the chains.

The validity of these parameters has been tested by comparison of calculated and observed X-ray spectra.

This picture fails to provide a complete and accurate description of the structure of silk fibroin in terms of the precise positions of all of the amino-acid residues and the

References p. 33/34.

coordinates of all atoms related to a definite unit of structure. Indeed, it seems reasonable to believe that the structure of silk fibroin involves some randomness and that it is not a simple repetition of identical structural units which can be precisely defined. The present clarified but still incomplete picture of the structure of silk may therefore be close to a possible limit of precision which is imposed by the nature of the material and the available chemical and X-ray data.

One definite implication of the present structure is especially interesting because of its failure to agree with a suggestion which has been put forward in many studies dealing with the structure of silk fibroin. This suggestion, which was originally made by X-ray workers, is to the effect that silk fibroin consists of at least two components, a crystalline component containing only glycine, alanine, and serine residues which is responsible for the characteristic X-ray diffraction pattern, and an amorphous component containing the larger amino-acid residues (especially tyrosine) in addition to the three residues mentioned above. By chemical and enzymatic treatment of silk DRUCKER AND SMITH[13,14] have isolated products which have been interpreted as corresponding to such crystalline and noncrystalline components. As already mentioned in this paper, the small units of structure derived from earlier X-ray data were unable to accommodate tyrosine, which comprises 5.4 residue percent of silk, or the other relatively large amino-acid residues, which make up an additional 10.4 residue percent. As pointed out in the derivation of the present structure, the recent, more accurate X-ray data are not compatible with a simple unit but require the presence of longer interplanar spacings in a way which permits ample provision to be made for tyrosine and other large residues. Quite aside from chemical reasoning, the new X-ray data alone point to the inclusion in the crystalline portion of all of the amino-acid residues, and in approximately the proportion in which they are known to occur. The present X-ray data provide no basis for conclusions concerning an amorphous component in silk fibroin.

ACKNOWLEDGEMENTS

We are indebted to Dr. MAX ROGERS for the preparation of doubly-oriented specimens of silk fibroin and for making these specimens available to us. We are also indebted to Mr. EDWARD D. HENDERSON for the preparation of electron micrographs of silk. We wish to thank Miss ANN SHERIDAN and Warner Brothers Studio for silkworms from which many of our specimens of silk were obtained.

SUMMARY

An investigation based on new X-ray diffraction data, including quantitative spectrometric measurements of X-ray intensities, has led to the derivation of the fundamental structural features of silk fibroin. The structure consists of extended polypeptide chains bonded together by lateral N—H···O hydrogen bonds to form antiparallel-chain pleated sheets. The sequence –G–X–G–X–G–X– in which G represents glycyl and X alanyl or seryl residues predominates throughout the structure, so that adjacent sheets pack together at distances of about 3.5 and 5.7 A. Longer inter-sheet distances are explained by the presence in the structure of the larger amino-acid residues, such as tyrosine.

References p. 33/34.

RÉSUMÉ

Une nouvelle étude de la diffraction des rayons X, comportant des mesures spectrométriques quantitatives des intensités des rayons, permet de proposer une structure fondamentale pour la fibroïne de la soie. Cette structure consiste en chaînes polypeptidiques allongées reliées entre elles par des liaisons hydrogène N—H···O latéraux pour former des lames plissées à chaînes antiparallèles. La séquence –G–X–G–X–G–X–, dans laquelle G représente un résidu de glycocolle et X un résidu d'alanine ou de sérine, prédomine le long des chaînes, de telle façon que des lames adjacentes sont écartées d'environ 3.5 et 5.7 A. Des distances plus élevées entre les lames s'expliquent par la présence dans les chaînes d'amino-acides plus encombrants, tels que la tyrosine.

ZUSAMMENFASSUNG

Eine auf neuen Röntgenstreuungsergebnissen, einschliesslich quantitativen spektrometrischen Intensitätsmessungen, beruhende Untersuchung hat zur Aufstellung des Strukturbildes von Seidenfibroin geführt. Die Struktur besteht aus gestreckten Polypeptidketten, die durch seitliche N—H···O Wasserstoffbrücken zusammengehalten werden und plissierte Schichten (pleated sheets) antiparalleler Ketten bilden. Die Reihenfolge –G–X–G–X–G–X–, in der G Glycin- und X Alanin- oder Serinreste darstellen, herrscht in der gesamten Struktur vor, so dass benachbarte Schichten auf einen Abstand von etwa 3.5 und 5.7 A zusammengepackt sind. Grössere Zwischenschichtabstände werden durch die Anwesenheit von grösseren Aminosäureresten in der Struktur, wie Tyrosin, erklärt.

REFERENCES

1 G. R. TRISTRAM, *Adv. Protein Chem.*, 5 (1949) 143; *The Proteins*, H. NEURATH AND K. BAILEY, Editors, Academic Press, New York, 1953, Vol. 1A, p. 220.
2 R. O. HERZOG AND W. JANCKE, *Ber.*, 53 (1920) 2162.
3 R. B. COREY AND L. PAULING, *Proc. Roy. Soc.*, B 141 (1953) 10.
4 R. BRILL, *Ann.*, 434 (1923) 204.
5 K. H. MEYER AND H. MARK, *Ber.*, 61 (1928) 1932.
6 R. O. HERZOG AND W. JANCKE, *Z. Physik*, 52 (1929) 755.
7 O. KRATKY, *Z. phys. Chem.*, B 5 (1929) 297.
8 O. KRATKY AND S. KURIYAMA, *Z. phys. Chem.*, B 11 (1931) 363.
9 M. L. HUGGINS, *Chem. Rev.*, 32 (1943) 195.
10 C. TROGUS AND K. HESS, *Biochem. Z.*, 260 (1933) 376.
11 R. BRILL, *Z. phys. Chem.*, B 53 (1943) 61.
12 K. H. MEYER, M. FULD AND O. KLEMM, *Helv. Chim. Acta*, 23 (1940) 1441.
13 B. DRUCKER AND S. G. SMITH, *Nature*, 165 (1950) 196.
14 B. DRUCKER, R. HAINSWORTH AND S. G. SMITH, *J. Textile Inst.*, 44 (1953) T 420.
15 H. FRIEDRICH-FREKSA, O. KRATKY AND A. SEKORA, *Naturwiss.*, 32 (1944) 78.
16 H. ZAHN, O. KRATKY AND A. SEKORA, *Z. Naturforsch.*, 6b (1951) 9.
17 H. ZAHN, *Melliand Textilber.*, 33 (1952) 1076.
18 C. H. BAMFORD, L. BROWN, A. ELLIOTT, W. E. HANBY AND I. F. TROTTER, *Nature*, 171 (1953) 1149.
19 O. KRATKY AND E. SCHAUENSTEIN, *Discussion Faraday Soc.*, No. 11 (1951) 171.
20 L. PAULING AND R. B. COREY, *J. Am. Chem. Soc.*, 72 (1950) 5349.
21 L. PAULING, R. B. COREY AND H. R. BRANSON, *Proc. Nat. Acad. Sci. U.S.A.*, 37 (1951) 205.
22 L. PAULING AND R. B. COREY, *Proc. Nat. Acad. Sci. U.S.A.*, 37 (1951) 235.
23 L. PAULING AND R. B. COREY, *Proc. Roy. Soc.*, B 141 (1953) 21.
24 L. PAULING AND R. B. COREY, *Proc. Nat. Acad. Sci. U.S.A.*, 37 (1951) 729.
25 L. PAULING AND R. B. COREY, *Proc. Nat. Acad. Sci. U.S.A.*, 39 (1953) 253.
26 G. ALBRECHT AND R. B. COREY, *J. Am. Chem. Soc.*, 61 (1939) 1087.
27 H. A. LEVY AND R. B. COREY, *J. Am. Chem. Soc.*, 63 (1941) 2095.
28 G. ALBRECHT, G. W. SCHWAKENBERG, M. S. DUNN AND J. D. MCCULLOUGH, *J. Phys. Chem.*, 47 (1943) 24.
29 H. L. YAKEL, Jr., *Acta Cryst.*, 5 (1952) 847.
30 J. E. LEONARD AND R. A. PASTERNAK, *Acta Cryst.*, 5 (1952) 150.
31 R. A. PASTERNAK AND J. E. LEONARD, *Acta Cryst.*, 5 (1952) 152.
32 R. B. COREY AND L. PAULING, *Review Sci. Instruments*, 24 (1953) 621.
33 R. W. JAMES AND G. W. BRINDLEY, *International Tables for the Determination of Crystal Structures*, Gebrüder Borntraeger, Berlin, 1935; Volume 2, page 571.
34 P. M. HEERTJES, *Rec. Trav. Chim.*, 60 (1941) 329.
35 H. ZAHN, *Kolloid-Z.*, 112 (1949) 91.

[36] R. HEGETSCHWEILER, *Makromol. Chem.*, 4 (1950) 156.
[37] E. H. MERCER, *Australian J. Sci. Res.*, (B) 5 (1952) 366.
[38] E. J. AMBROSE AND A. ELLIOTT, *Proc. Roy. Soc.*, A 205 (1951) 47.
[39] E. J. AMBROSE AND A. ELLIOTT, *Proc. Roy. Soc.*, A 206 (1951) 206.
[40] C. H. BAMFORD, L. BROWN, A. ELLIOTT, W. E. HANBY AND I. F. TROTTER, *Proc. Roy. Soc.*, B 141 (1953) 49.
[41] W. C. PRICE AND R. D. B. FRASER, *Proc. Roy. Soc.*, B 141 (1953) 66.
[42] A. ELLIOTT, *Nature*, 172 (1953) 359.
[43] M. LEVY AND E. SLOBODIAN, *Cold Spring Harbor Sym. Quant. Biol.*, 14 (1949) 113.
[44] M. LEVY AND E. SLOBODIAN, *J. Biol. Chem.*, 199 (1952) 563.
[45] E. SLOBODIAN AND M. LEVY, *Federation Proc.*, 11 (1952) 288.
[46] L. M. KAY AND W. A. SCHROEDER, *J. Am. Chem. Soc.*, 76 (1954) 3564.
[47] L. M. KAY AND W. A. SCHROEDER (private communication).
[48] P. DESNUELLE AND A. CASAL, *Biochim. Biophys. Acta*, 2 (1948) 64.
[49] F. SANGER, *Adv. Protein Chem.*, 7 (1952) 44.

Received September 2nd, 1954

Note added October 25, 1954

The article by J. O. WARWICKER entitled "The Crystal Structure of Silk Fibroin" (*Acta Crystallographica*, 7 (1954) 565) has just come to our attention. The structure described by WARWICKER resembles the structure of our pseudo unit in that it is based on antiparallel-chain pleated sheets packed together at spacings alternately 3.7 and 5.6 A (our values being 3.5 and 5.7 A); also, alternate residues in the polypeptide chains are glycine, the others being alanine or serine. These features of our structure were described in a report to the Solvay Congress on proteins in April, 1953 (L. PAULING, "The Configuration of Polypeptide Chains in Proteins", in *Les Protéines*, R. Stoops, Editeur, Bruxelles, 1953). However, WARWICKER's structure differs from our pseudo unit in that it is based on an orthorhombic space group. At an early stage of our investigation we had considered this orthorhombic structure and had been forced to reject it because of its failure to give even approximate agreement between the observed and calculated intensities of principal equatorial reflections. The strongest reflection on the pattern of silk fibroin is the medium-sharp equatorial reflection with spacing 4.3 A (reflection No. 3 of Table II). From photographs of doubly-oriented specimens prepared by KRATKY AND KURIYAMA (1931) and by us this reflection has been definitely shown to arise from sets of planes making an angle of approximately 70° with the plane of rolling. This reflection can be unambiguously indexed as 120 (on the basis of WARWICKER's unit cell). The intensity of 120 calculated with the parameters listed in WARWICKER's paper is practically zero; thus WARWICKER's structure does not explain the occurrence of this very strong reflection, and it must be rejected.

Received November 1st, 1954

SOME SENSITIVE AND RECORDING VOLUMETERS

by

BESSEL KOK

Carnegie Institution of Washington, Department of Plant Biology, Stanford, Calif. (U.S.A.) and T.N.O. Solar Energy Project, Laboratory for Plant Physiology, Agricultural University, Wageningen (Netherlands)*

Kinetic measurements in photosynthetic problems often put higher demands for accuracy and speed on the gasometric method used than is fulfilled by standard manometric equipment. In the course of years the present author has used several types of volumeters; some of these have proved to be quite satisfactory, and easy to construct, calibrate and operate.

In general principle a reaction- and a compensation vessel are interconnected by a capillary containing an index droplet. The index is used as zero indicator. At the moment a reading is taken, the gas exchange in the reaction vessel is compensated by a change in volume of the compensating vessel. A mercury delivery screw is turned until the drop is back in the original (zero) position and the displacement of the piston is read. Be V_c and V_r the gasvolumes of compensation and reaction vessel respectively and P_0 the initial pressure in both vessels. Suppose an amount of gas xP_0 is evolved in V_r, after which the index is readjusted by turning the screw h units, each unit representing a volume displacement of $m\mu$l. Then, if P_1 represents the final pressure in both vessels:

$$(V_r + x)P_0 = V_r P_1 \text{ and } V_c P_0 = (V_c - h.m)P_1$$

which yields, neglecting a term xhm:

$$x/V_r = h.m/V_c \qquad (1)$$

If the reacting material is suspended in a liquid phase of a volume V_f, leaving a gasvolume V_g in the reaction vessel and if α represents the Bunsen absorption coefficient of the gas studied at the prevailing temperature T, the volume of the gas evolved at a pressure P_0, reduced to 0°C:

$$x = h \frac{m}{V_c} \left(V_g \frac{273}{T} + \alpha V_f\right) \qquad (2)$$

COMPENSATION VESSEL AND DELIVERY SCREW

The limit of useful *relative* sensitivity in gasometric apparatus can be expressed as the ratio of the minimum measurable amount of gas evolved x_{min} to the total amount of gas present in the reaction vessel: V_r. This ratio is mainly limited by temperature

* Work in Wageningen was aided by a grant from the Charles F. Kettering Foundation, Yellow Springs, U.S.A.

fluctuations*. Dependent on the properties of the thermostat bath (and to a lesser extent on the symmetry of reaction and compensating vessel) a value of $x_{min}/V_r = 1:10^4$ to $1:10^5$ can roughly be taken as attainable in routine apparatus.

If m_{min} represents the smallest volume change to be read on the delivery screw, according to (1) this same ratio can be chosen for the term m_{min}/V_c. Normal micrometer-heads can be used as mercury delivery screws and significantly read down to one division (1/100 mm, ~ 0.3 μl) or less. The volume of the compensating vessel can therefore be 10 to 50 ml. This same combination may be used independently of the volume of the reaction vessel and the latter's size and shape can be chosen as demanded by experimental conditions.

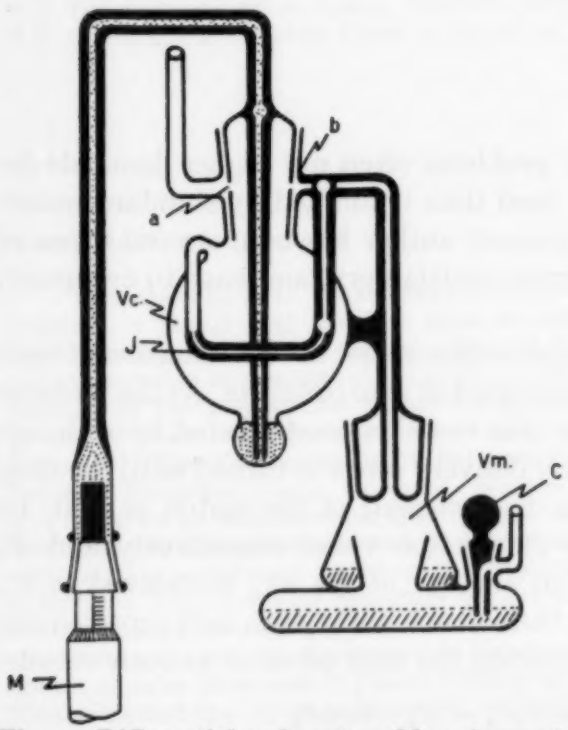

Fig. 1. Differential volumeter. M: micrometer head. V_c: compensating vessel, V_m: reaction vessel, J: index capillary (ø 0.3 to 0.5 mm, length 20 to 50 mm). Holes a and b can oppose glass tubes as shown in the drawing. By means of stopper C, V_c and V_m can be equilibrated with gas mixtures. Turning the whole vessel 90° will close a and b and measurement can start after C is closed.

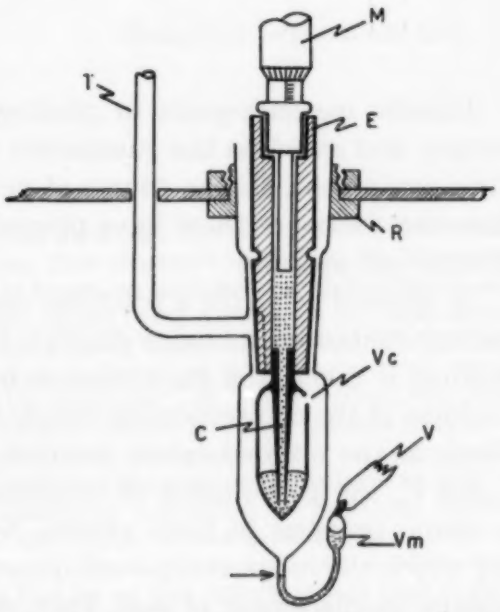

Fig. 2. Differential volumeter. Micrometer head M is sealed into a lucite extension piece E. Into the other end of E is sealed a glass capillary C, which is connected to a mercury reservoir (*ca.* 3 ml). In the lower tapered part of E a groove is cut, allowing for the connection of the compensating vessel V_c with tube T (a stopcock arrangement could be used instead). V_m: reaction vessel, V: metal rod, connected to vibrator—a piece of rubber tubing slipped over its end may be used with fragile vessels.

When filling the screw with mercury, entrapped air should be carefully removed. If it is used upside down as in the arrangement shown in Fig. 1, there will be no leakage as long as an excess pressure is maintained on the mercury (a few cm mercury suffices). In this arrangement a glass capillary connects screw and compensating vessel and the whole apparatus can be mounted on a standard manometer assembly if desired. The design shown in Fig. 2 is more compact and can be used with any type of compensating vessel. Here the delivery screw is combined with its mercury reservoir to form a removable unit. A mercury seal must be present on top of the ground spindle passage (*i.e.* inside the screw) and no leakage will occur even if the apparatus is evacuated.

* B. KOK, G. W. VELTKAMP AND W. P. GELDERMAN, *Biochim. Biophys. Acta*, 11 (1953) 7.

VOLUMETER OF HIGH RELATIVE SENSITIVITY

The volumeter illustrated in Fig. 1 was used in various modifications for accurate measurements of small gas exchanges in large or complicated reaction vessels. A few features of the index capillary combine to simplify the operation of this apparatus:

Only the middle part of the capillary is straight and horizontal; here the zero position of the drop is marked on the glass wall. Towards both ends the capillary has a smooth vertical bend. This adds to the sensitivity of the horizontal part an extension of the usable range: as soon as the gas evolution pushes the drop around the bend, its weight opposes further movement (*i.e.* it shifts towards manometric action). The capillary is suddenly, but smoothly expanded at both ends. This is very helpful in preventing the drop from escaping while placing the volumeter in the thermostat or inadvertently allowing too great pressure differences to develop. An excessive pressure change only breaks the drop at the expanded place, after which it is easily restored to its original position by moving the screw back and forth. In this way, one and the same drop (*e.g.* valeric acid), can be used for a number of days. Smooth movement of the index requires regular cleaning and especially drying of the capillary. Although shaking was usually interrupted during the readings (taken at 1′ intervals), it does not disturb the action of the index drop.

The apparatus is entirely submerged in the bath, and the index can be read through a hole in the insulation of the front wall of the tank. An extended microscope eye-piece mounted on the assembled volumeter is helpful in taking the readings.

The reaction vessel shown in Fig. 1 has two large compartments. The upper compartment holds up to 3 ml of gas absorbing or buffering agents, the lower one 5–10 ml of cellular suspension. To prevent splashing, circular shaking (350 R.P.M., 8 mm stroke) was used with this vessel.

VOLUMETER OF HIGH ABSOLUTE SENSITIVITY

For a given relative sensitivity (x_{min}/V_r cf. (1)) of volumetric apparatus, the smaller the gas phase V_r used per amount of material to be studied, the smaller will be the absolute amounts of gas which can be measured. (For photosynthetic measurements with thin suspensions it is primarily important to realize a small ratio of V_r to the irradiated surface of the vessel.)

For such studies, in which only one liquid phase is to be used in the reaction vessel, this decrease of V_r was realised to the extreme in the designs shown in Figs. 2 and 3.

A small fraction of the suspension liquid itself serves as index fluid (the zero position of the meniscus is indicated by an arrow). With not too small reaction vessels it is possible to keep the amount of suspension fluid in the capillary within one or a few percent of the total liquid phase.

In this apparatus the gas phase is an air bubble, the volume of which can be adjusted as desired by

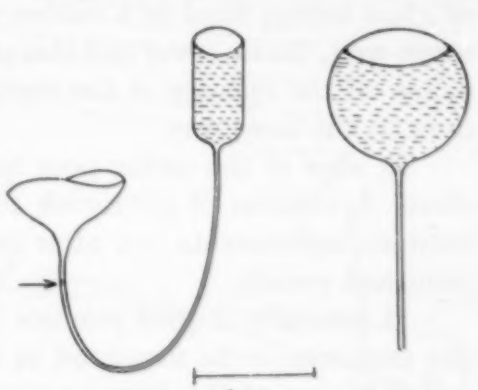

Fig. 3. Reaction vessel and index capillary of medium size (0.3 ml). The capillary is thin walled, inner ø 0.25 mm, outer ø 0.35 mm, length *ca.* 40 mm.

filling the vessel with more or less suspension fluid. Good performance was obtained with a gas phase as small as 1/6 the total volume of V_m. High sensitivity and favourable ratio's of V_r to illuminated area (see above) can be attained in this way.

The index capillary connecting V_c and V_m is rather thin walled; this allows small displacements of the reaction vessel.

A 50 or 60 cycle vibration is induced in this vessel, which causes intense mixing of fluid and gas phases. For this purpose a suitable electric razor or hair clipper can be easily adapted. A small extension rod, fixed to the moving part of the vibrator, touches the vessel or a glass rod sealed onto it. In order to have smooth performance of the index meniscus — of special importance when it is to be automatically recorded — too intense a vibration ought to be avoided. An example of the equilibration times obtained can be found in Fig. 6.

Operation of the volumeter

With the aid of brass ring R (Fig. 2), sealed onto the extension of the compensation vessel, the apparatus can be firmly mounted. Once in its desired position, it need not be removed, since all operations of cleaning and filling can be simply performed through tube T and the opening of V_c.

To fill the reaction vessel with the desired contents, the amount of suspension fluid to be used is pipetted into the compensation vessel on top of the capillary. After greasing its joint, the screw and mercury reservoir unit is placed in position, still leaving tube T connected to the vessel. A two way stopcock connects this tube to either an aspirator or to a reservoir, containing the desired gas mixture. First the stopcock is turned to the aspirator and after the apparatus is evacuated, the stopcock is turned to connect the apparatus with the reservoir containing the gas mixture. The inflowing gas pushes the suspension liquid into the reaction vessel. After a few seconds the index fluid is moved until an unbroken fluid column is obtained with the meniscus in the desired position. For this purpose a syringe, temporarily connected to tube T by means of a piece of rubber tubing, is helpful. The tube T is now closed off by turning the screw unit and measurement started when temperature equilibrium is attained.

The fluid is removed from the reaction vessel by applying suction through a piece of glass tubing fixed in a rubber stopper, which fits on top of V_c after removal of the screw unit. On its lower end this glass tube is fitted with a piece of rubber tubing, which closes off the opening of the capillary. Washing and cleaning of the reaction vessel is done in the same way.

In view of the rather poor index properties of water, the capillary has to be kept clean. A solution of potassium nitrate in strong sulfuric acid was applied over-night between experiments (*i.e.* after removal of the screw unit and preliminary cleaning of joint and vessel).

It generally is good practice to fill the reaction vessel in such a way that the total gas exchange to be measured in an experiment can be compensated by less than one full discharge of the delivery screw; if this amounts to about 1 ml mercury and if V_c is 10 to 20 ml, this represents a relative pressure change as high as 5–10%, sufficient to make corrections necessary. But larger exchanges can eventually be measured by opening T, turning the screw all the way back and restoring the meniscus with the aid of a syringe on tube T.

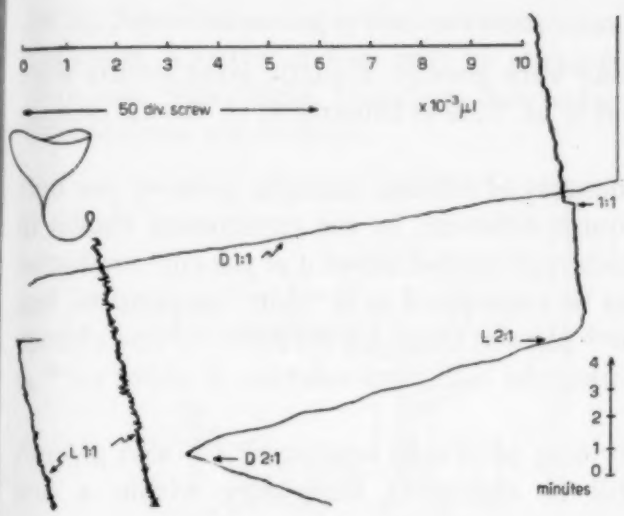

Fig. 4. Recordings made with the smallest reaction vessel used so far ($V_m = 8$ µl, $V_g = 2$ µl). Calibration of the recorder paper both as number of screw divisions and as µl volume change are given for "gear ratio" 1:1, yielding twice the sensitivity of the also used gear ratio 2:1. Gas phase: air plus 2 % CO_2. *Chlorella* cells, suspended in 6 µl carbonate buffer mixture, were exposed to either darkness (D) or a light intensity (L), which slightly over-compensated respiration. The "waves" observable in recording D 2:1 — L 2:1 correspond to small displacements of the vessel for each 180° turn of the screw. This was due to the fact that a mounting, less firm than the one shown in Fig. 2 was used for this recording and for the one given in Fig. 5.

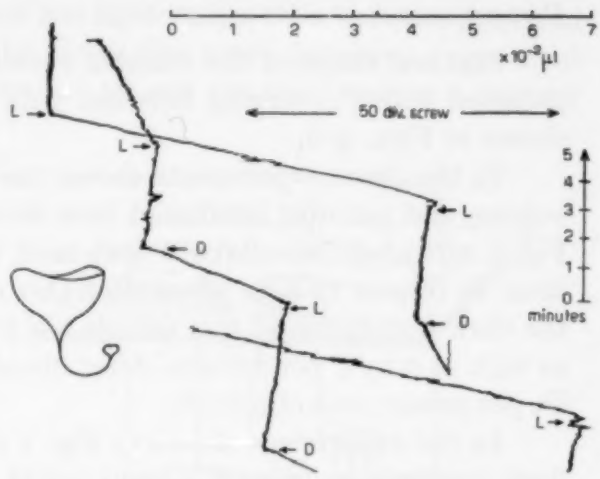

Fig. 5. Recordings made with a reaction vessel of 41 µl ($V_g = 11$ µl). Exposure of *Chlorella* cells in 30 µl carbonate buffer medium to darkness (D) and various light intensities (L). Small irregularities in the recordings are due to breaking of bubbles in the suspension.

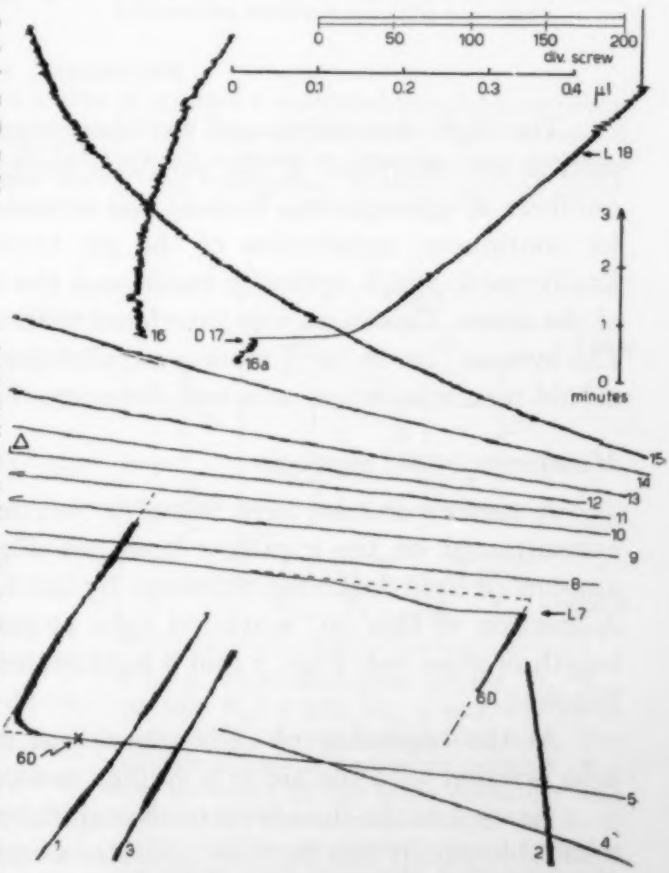

Fig. 6. An experiment made with the arrangement shown in Figs. 2 and 3. Chart speed was 25.4 mm per minute, *i.e.* twice as fast as used for expts. shown in Figs. 4 and 5. Also a different screw was used. $V_m = 290$ µl, $V_g = 60$ µl. Top right an example of calibration in screw divisions is shown: The system was manually moved over 200 screw divisions (4 turns) first to the right, thereafter to the left. Intervals of 50 divisions were marked on the paper. Backlash appears to be virtually absent. In this experiment *Chlorella* cells, resuspended in 230 µl carbonate buffer mixture, were first alternately exposed to darkness (1, 3, 6) and various light-intensities (2, 4, 5). A prolonged exposure to very intense light was then given at the moment marked L7. Each time the pen had travelled all the way across the recorder paper screw SS (see Fig. 7) was loosened and the pen relocated at the right side of the paper (8–16). The strong light caused a progressive decrease of the rate of oxygen evolution, which finally became negative and irregular (15, 16). After darkening (D 17) oxygen uptake became smooth again. At Δ the delivery screw was turned all the way down, after restoring this (see page 40) the recordings were continued (12). The fast equilibration due to vibrating the vessel may be noticed at the start of 6 and 7. The sudden volume change upon addition and removal of strong light (L7, D17) is due to heat effects.

Performance

Size and shape of the reaction vessel may vary greatly. Equally good results were obtained with V_m varying between 3 ml and 8 μl. This is illustrated in the recordings shown in Figs. 4–6.

In the three experiments shown the amounts of cellular material present per unit volume and per unit irradiated area were quite different. In the experiment shown in Fig. 4, 0.18 μl of *Chlorella* cells were used, which represented about 4 μl per cm^2 irradiated area. In respect to light absorption this may be considered as a "thin" suspension, but the dark respiration of this sample ($\sim 3 \cdot 10^{-3}$ μl/min) caused a relative volume change as high as 0.15% per minute. After illuminating the cells, an evolution of about 10^{-4} μl O_2 per minute was observed.

In the experiment shown in Fig. 5 only 0.04 μl of cells were used (~ 0.02 μl/cm^2) dark respiration ($7 \cdot 10^{-4}$ μl/min) could still be measured accurately within a few minutes.

In the experiment shown in Fig. 6, 2 μl cells were used (~ 2.5 μl/cm^2). For this type of experiment either a smaller amount of cells or a smaller liquid phase should have been used because the screw was turned all the way down in the middle of an exposure.

The two smaller reaction vessels used for these recordings were sealed onto the same compensation vessel. Both were made, calibrated and tested (see Figs. 4 and 5) within one day, which illustrates the simplicity of the method.

RECORDING VOLUMETRY

The high sensitivity and the short equilibration times characterizing volumeters such as are described in the previous paragraph, readily allow the collection of large numbers of observations. To take full advantage of these features we examined methods for continuous registration of the gas exchange. A relatively simple apparatus was finally used, which optically monitored the index meniscus and registered the turning of the screw. This in no way interfered with the sensitivity of the gasometric apparatus. The system can be used more generally to record any type of measurement, in which a fluid meniscus serves as a null detector.

Monitoring of the meniscus

A narrow, intense light beam ($\varnothing \sim 1$ mm) from a 6 V–0.5 A automobile lamp is concentrated on the capillary bore (see Fig. 7). There is a marked difference in the amount of light scattered sideways by the bore, whether filled with liquid or with air. A fraction of this 90° scattered light is guided towards a photo multiplier cell by a length of glass rod. Figs. 7 and 8 further illustrate this arrangement, which operates as follows:

At the beginning of each experiment the index meniscus is located close to its zero position with the aid of a syringe (see page 38), after which the vessel is closed.

As soon as the fluid level in the capillary rises, the photocurrent decreases. Through a suitable circuit this decrease actuates a relay or a clutch, that reverses the direction of rotation of a motor, which drives the delivery screw. This pushes back the fluid meniscus until enough light reaches the photocell to again reverse the rotation of the motor. This causes the meniscus to oscillate within narrow limits about its zero position. If a gas exchange occurs in the reaction vessel, the delivery screw automatically compensates

for it. Since balancing occurs between more and less light rather than between light and darkness, a better action will be obtained the closer the lower intensity approaches darkness. Stray light, therefore, has to be screened off and the lamp run on a battery or stabilized a.c. voltage.

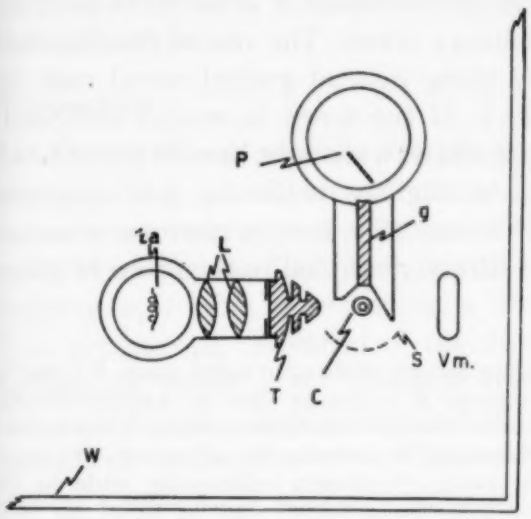

Fig. 7. Arrangement to record the position of the index meniscus. V_m: reaction vessel, C: index capillary. La: lamp, L: lenses (ø 1 cm, f 3 cm). T: lucite tip sealed onto brass tube; incisions are made in it and both outside and inside are painted black except for small circles in both centers. This serves to produce a restricted parallel light beam. g: glass rod (ø 2 mm, length 3 or 4 cm) guiding scattered light towards photocell P. To screen off stray light, the glass rod is sealed in a hole, drilled through a brass or bakelite strip fastened onto the photocell container. S: small screen, fixed onto a rod, extending through the top plate. It can be lifted to make the capillary visible through the thermostat wall W.

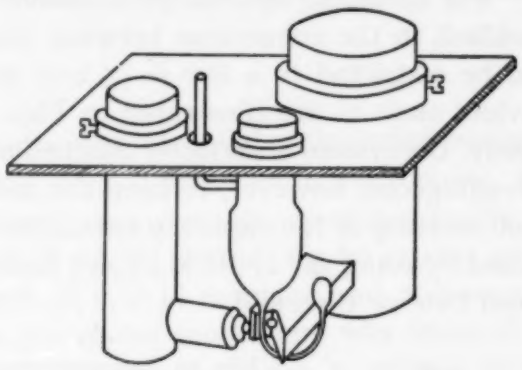

Fig. 8. From left to right: lamp housing, volumeter, photocell housing. All parts are firmly but adjustably mounted on the top plate as were all other thermostat accessories and the vibrator, the tip of which protruded through a hole in this plate. A small, glass-walled thermostat bath (25 × 15 × 15 cm) was mounted to be easily removable underneath the top plate.

Registration

A straightforward and reliable arrangement to make a record of the movement of the screw was built with the aid of a single-pen Brown recorder and is described in detail:

Fig. 9 shows a simple circuit, in which the changes in photocell current actuate the recorder *via* a cathode follower. The amplifier terminals are disconnected from the potentiometer circuit and are used directly, but no further alterations in the recorder have to be made. The recorder motor develops enough power to actuate a mercury delivery screw in addition to the pen carriage and by mechanically coupling both a reliable Servo system is obtained. This is done most simply (though with some backlash) by interconnecting the motor pinion and the screw with a length of flexible (speedometer) cable passing through a hole in the back wall of the recorder. With the aid of a set screw (see Fig. 10),

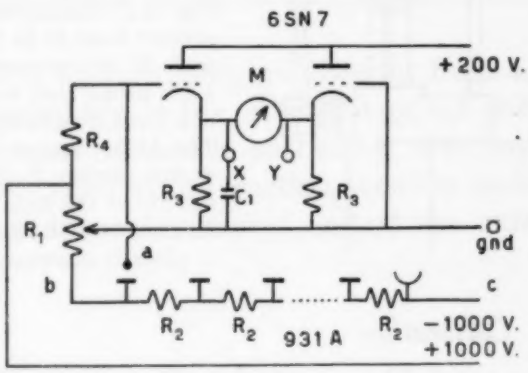

Fig. 9. Photomultiplier circuit. R_1, R_2: 50 kΩ, R_3: 2 kΩ, R_4: 3 mΩ, C_1: 25 to 100 μf. M: 0–5 mA midpoint zero. The photocell and its resistance network (R_2) are mounted in the brass container and connected with a 3-wire cable (a, b, c) with further equipment. x–y: recorder amplifier input terminals. Voltages are to be stabilized and ac components carefully removed (C_1). Meter M is helpful as a control for aligning purposes and for adjusting the meniscus to its zero position before the vessel is closed.

this cable can be easily connected to or disconnected from the micrometerhead. Before each run it may be disconnected and the pen located on a suitable spot on the paper (this can be done either by hand or by motor movement monitored by turning the screw). Connection is then restored and the recording started.

For obtaining optimal performance and cleanest recordings it is useful to minimize backlash in the connection between pen and delivery screw. The use of flexible cable can be restricted to a few (~ 5 cm) lengths by using instead guided metal rods and devices such as are illustrated in Figs. 10 and 11. If the screw is moved sufficiently slowly, the system is perfectly damped and the pen draws a straight line. It proved to be advantageous, however, to keep the index meniscus slightly oscillating, probably since good wetting of the capillary is maintained in this way. The best performance was obtained by using the 27 RPM Brown motor, either directly coupled to the screw or geared down two- or threefold.

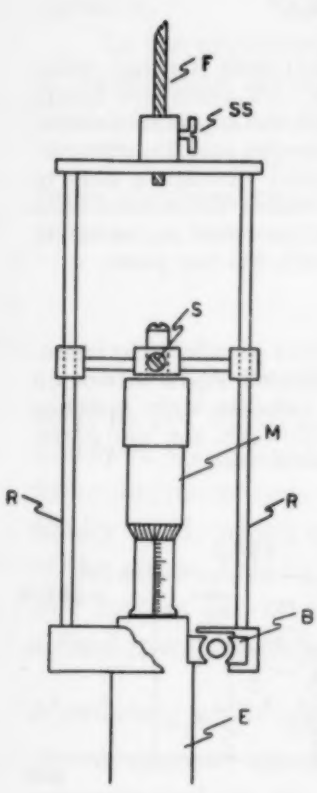

Fig. 10. Accessory to minimise the length of flexible cable used. A cross bar fastened with S onto the micrometer M is free to slide in vertical direction along two bars R, but will transmit circular movement induced *via* cable F, fastened with set screw SS. Ball bearing B, carrying the accessory, fits loosely on the extension piece E. Its inner ø is chosen sufficiently wide so that after S and SS have been loosened the accessory can be lifted up freely and removed.

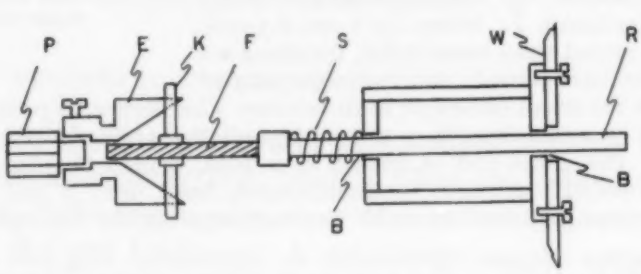

Fig. 11. Arrangement to connect the recorder motor with the delivery screw: Axle R (ø 5 mm) fits loosely in its bearings B, attached to the back wall W of the recorder (the amplifier case has to be moved upwards about 1 cm along this wall). Spring S presses the axle towards the motor. Its end is a 5 cm length of flexible cable F, on which in turn a "knife" K is attached. The latter snaps into a sleeve in the brass extension piece E fixed on the motor pinion P. This extension piece is conical inside, which serves to guide the tip of the axle (protruding *ca.* 1.5 cm beyond the knife) towards its centre. In this way the recorder mechanism can be freely swung out on its hinges; after it is swung back again the mechanical coupling is easily restored.

Calibration

Calibration is done by moving the mechanism and reading the corresponding numbers of divisions on the screw and on the recorder paper. Using this ratio and formula (2), the latter can be simply expressed in microliters gas exchange.

When widely diverging rates of gas exchange are to be measured, it may be advantageous to have a choice of sensitivities available, *i.e.* a number of ratios of screw divisions to paper divisions. This can easily be realised by arranging a set of interchangeable gears between the pen movement and the delivery screw. Such a gear train can be mounted either outside the recorder between motor and screw or inside the recorder between motor and pen movement. The second arrangement, though a little more complicated, is to be preferred, since a change of the ratio does not imply a change in speed

of movement of the screw and therefore leaves the damping of the system unaltered. In our apparatus we removed the motor pinion and remounted it on a separate axle again to drive the pen carriage. The latter axle was connected with the motor axle through the gear train, which was mounted between two brass plates and screwed onto the recorder chassis. A set of change gears ("Meccano" parts) allowed a 9-fold variation of the scale span.

Performance

The performance of the described system controlling the level of the index meniscus surpasses that of visual and manual operation, even if aided by a microscope. For instance, we may give some data as observed with an apparatus, described in Fig. 3: 27 RPM motor, capillary bore ⌀ 0.28 mm, V_c: 14,2 ml, V_m: 290 μl, V_g: 60 μl, one screw division (0.01 mm) representing a displacement of 0.36 μl mercury and a change in $V_g = 1.5 \cdot 10^{-3}$ μl. Reversal of the direction of the motor movement was induced by turning the screw < 0.2 division; this represents a relative change in volume of one part in 10^5 and a displacement of the meniscus of about 5 μ. In actual operation the continuous oscillations were within one or two divisions of the screw, which represented volume oscillations in $V_g < 3 \cdot 10^{-3}$ μl and movements of the meniscus < 50 μ. Arranged in such a way that the full scale of the recorder (100 divisions = 280 mm) corresponded to 430 screw divisions (8.5 revolutions) and therefore to 0.65 μl, short and long term zero constancy with normal shaking intensity of the reaction vessel (observed during an hour) was within one division of the recorder.

The fluctuations within this limit were correlated both in time and in magnitude with the on-off action of the thermostat heater. When the scale span was decreased 9-fold (to 0.072 μl), these temperature fluctuations appeared accordingly increased in the recordings. This indicates that the thermostat rather than the recording system limited the sensitivity; in this case to $\Delta V/V = 1:10^4$ (cf.[1]). Slight short term irregularities in the mixing of gas and fluid phases may sometimes appear in the recordings, but do not influence the accuracy of the measurement.

A few records obtained with reaction vessels of different size are given in Figs. 4, 5 and 6. Full scale deflection of the recorder (280 mm) was in the order of 0.01, 0.1 and 1.0 μl respectively. The recording system can of course be used in connection with any other type of gasometric apparatus. Shaking or vibration of the reaction vessel in such cases is best arranged as a well-aligned circular movement, centered around the axis of the index capillary.

SUMMARY

A few types of volumeters of simple construction and operation, characterized by high sensitivity (both absolute and relative) are described. A Servo-system for automatically recording gas exchanges occurring in such volumeters was constructed. Full scale span of the recorder used could be arranged to represent from 10^{-2} μl upwards, with an uncertainty in the order of one percent of full scale. The recording system can be generally used for applications in which a fluid meniscus serves as a null detector, the sensitivity amounting to a few μ displacement.

RÉSUMÉ

Quelques types de volumètres de construction et d'emploi simples, caractérisés par une grande sensibilité (à la fois absolue et relative) sont décrits. Un servo-système destiné à l'enregistrement

automatique des échanges gazeux dans ces volumètres a été construit. L'échelle de l'enregistreur utilisé a été agencée de façon à pouvoir indiquer des volumes depuis 10^{-2} μl, avec une précision de l'ordre de un pour cent de l'échelle totale. Le système d'enregistrement peut généralement être appliqué à des cas où ménisque liquide sert de détecteur de zéro, la sensibilité permettant de percevoir un déplacement de quelques μ.

ZUSAMMENFASSUNG

Einzelne Typen von Voluminometern einfacher Konstruktion und Bedienung, die sich durch ihre hohe absolute und relative Empfindlichkeit auszeichnen, werden beschrieben.

Ein automatisches System zur Registrierung des Gasaustausches, der in einem derartigen Voluminometer stattfindet, wurde konstruiert.

Der Apparat konnte so gebaut werden, dass er bei Vollausschlag 10^{-2} mm^3 oder mehr mit einer Unsicherheit von höchstens 1 % angibt.

Dieses registrierende System, dessen Empfindlichkeit wenige μ Wegdifferenz beträgt, kann man ganz allgemein dann gebrauchen, wenn ein Meniskus als Nullinstrument dient.

Received July 21st, 1954

ÉTUDE AUTORADIOGRAPHIQUE DE L'INCORPORATION DANS LE FOIE DE SOURIS DE PRÉCURSEURS DES ACIDES NUCLÉIQUES ET DES PROTÉINES

par

A. FICQ* ET M. ERRERA**

Laboratoire de Morphologie animale, Université libre de Bruxelles (Belgique)

Les méthodes autoradiographiques permettent de déceler dans les cellules les constituants qui ont été marqués par des radioisotopes[4,7]; les premiers résultats obtenus par ces méthodes s'étant montrés encourageants, il nous a paru utile d'étudier systématiquement le sort de certains précurseurs dans des tissus dont le métabolisme est déjà connu grâce aux méthodes biochimiques. C'est pourquoi nous avons choisi le foie de souris comme matériel expérimental; nous y avons étudié l'incorporation de divers précurseurs des protéines et des acides nucléiques.

Le but de toute méthode cytochimique étant d'identifier, de localiser et de doser certains constituants cellulaires, il importe d'utiliser comme marqueurs les précurseurs les plus spécifiques possibles de ces consitutants. On peut, d'autre part, en adjoignant aux observations autoradiographiques des réactions cytochimiques destinées à fixer ou à éliminer les molécules marquées de façon spécifique, espérer arriver à les identifier avec une précision accrue. C'est pourquoi nous avons étudié l'effet de fixateurs variés sur des coupes d'organes fixés préalablement par congélation sous vide à basse température[8] ou par congélation-dissolution[11] parce que ces méthodes assurent au mieux la conservation dans la cellule des substances solubles.

Une série de coupes a donc été soumise telle quelle au processus autoradiographique; d'autres ont été traitées, avant l'application de l'émulsion sensible, par les solutions suivantes;

1. l'alcool acétique, qui est un fixateur fréquemment utilisé pour l'autoradiographie;

2. l'acide trichloracétique qui est utilisé par les biochimistes pour précipiter les protéines et les polynucléotides;

3. l'acétate de plomb qui a été proposé par TANDLER[14] comme un bon fixateur des des nucléotides acidosolubles;

4. l'acide citrique a, en outre, été choisi parce qu'on l'utilise souvent pour isoler les noyaux cellulaires[5] et qu'il permet donc de comparer nos propres résultats avec les données obtenues dans le cas des tissus fractionnés par centrifugation diffèrentielle et analysés par les méthodes usuelles de dosage des radioisotopes. Rappelons que MIRSKY[1,3] a observé que l'acide citrique extrait une proportion considérable des protéines du noyau cellulaire.

* Chargée de Recherches au Fonds National de la Recherche scientifique.
** Associé au Fonds National de la Recherche Scientifique.

Bibliographie p. 50.

Nous avons choisi, comme précurseurs, le glycocolle-1-^{14}C dont le carbone marqué fournit le C_4 des purines et qui s'incorpore aussi dans les protéines; l'adénine et la phénylalanine sont, par contre, des précurseurs plus spécifiques respectivement des purines et des protéines. On sait que si le foie n'est pas en régénération, l'acide désoxyribonucléique ne s'y marque pratiquement pas[9].

MATÉRIEL ET MÉTHODES

Nous avons injecté à trois souris, par voie intrapéritonéale, du glycocolle-1-^{14}C, de l'adénine-8-^{14}C et de la DL-phénylalanine-3-^{14}C dissous dans du liquide physiologique. L'activité des différents précurseurs radioactifs utilisés était de 16 μc dans le cas de la glycine et de 4 μc dans celui de l'adénine et de la phénylalanine.

Les animaux ont été sacrifiés après 24 heures dans le cas du glycocolle et de l'adénine et après 60 heures dans celui de la phénylalanine. Bien qu'il ne s'agissait pas de foie en régénération, nous avons choisi ces durées d'expériences parce que, après hépatectomie, la synthèse des purines est maxima après 24 heures et celle des protéines après 60 heures[9]. Les foies ont été prélevés et fixés à basse température sous vide par la technique de GERSH[8] ou par la méthode de congélation-dissolution décrite par LISON[11]. Des coupes d'environ 10 μ ont été effectuées et leur épaisseur a été vérifiée dans chaque cas à l'aide de la vis micrométrique du microscope, puisque la radioactivité observée est évidemment proportionnelle au volume du tissu. L'activité a été corrigée dans chaque cas et ramenée à une épaisseur uniforme de 10 μ.

Un certain nombre de coupes fixées et déparaffinées au xylol ont été ensuite soumises aux traitements suivants:

1. Alcool acétique (3/1 en volumes) pendant 10 minutes à 20°, suivi d'un lavage à l'éthanol 70° pendant 30 minutes.
2. Acide trichloracétique 10% à 0° pendant 15 minutes, suivi de lavages répétés à l'éther.
3. Acétate de plomb 10% acidifié par de l'acide acétique (1% en volume) pendant 12 heures à 0°, suivi de plusieurs lavages à l'eau distillée, selon la méthode de TANDLER[14].
4. Acide citrique 5% (pH 3.4) à 0° pendant 12 heures, suivi d'un traitement pendant 2 heures par de l'acide trichloracétique à 10%, puis d'un lavage à l'alcool-éther (3/1 en volumes).
5. Un certain nombre de préparations témoins n'ont été traitées par aucune solution.

Les préparations histologiques ont été recouvertes d'émulsion Ilford G5 "in gel form", puis révélées, fixées et colorées par le mélange d'Unna, suivant la méthode précédemment décrite[7]. Les lames ont été développées après 24 heures d'exposition dans le cas du glycocolle et de l'adénine et après 48 heures dans celui de la phénylalanine.

Au moins mille cellules ont été comptées dans chaque cas et les traces des électrons émis par le ^{14}C (environ 300 traces pour 1.000 cellules habituellement) ont été dénombrées dans le cytoplasme et les noyaux des cellules parenchymateuses et des cellules de KUPFFER; elles ont été rapportées à la surface correspondant à chacun de ces éléments. Le diamètre moyen des noyaux des cellules parenchymateuses et des cellules de KUPFFER a été mesuré au moyen d'un micromètre. La surface du cytoplasme a été évaluée en mesurant la surface totale de tissu observée, dont on déduit la surface des noyaux et celle des espaces intercellulaires, qui peut être estimée à environ 1/5 de celle de l'ensemble des noyaux. Il n'a été tenu compte que des traces des électrons d'au moins 4 grains. Le "background" a été déterminé dans 20 champs de chaque lame; on a déduit de la radioactivité de chaque élément cellulaire, l'activité d'une surface correspondante de background. Le background des environs immédiats de la préparation histologique est environ 2 fois plus élevé que celui des régions qui en sont éloignées; il n'excède jamais 1 trace par champ microscopique de 16,000 μ^2 et il correspond à environ 10% de la radioactivité totale. Les résultats expérimentaux sont exprimés en nombre de traces pour 1,000 μ^2 de tissu; il est donc possible, si l'on connaît les teneurs relatives des diverses fractions cellulaires en protéines et en acides nucléiques, de déterminer de façon approximative la valeur de la radioactivité spécifique.

Nous avons utilisé comme étalon de la radioactivité une suspension de cellules de levures marquées au ^{14}C, dont la radioactivité par cellule avait au préalable été déterminée au compteur Geiger. Une goutte de cette suspension a été déposée sur chacune des lames et le nombre de traces pour 500 cellules a été déterminé dans chaque cas. Cet artifice permet de vérifier la constance du processus de l'autoradiographie (épaisseur de l'émulsion photographique, durée de l'exposition et conditions de développement).

RÉSULTATS EXPÉRIMENTAUX

Les résultats sont rassemblés dans le Tableau I, tandis que la microphotographie (Fig. 1) montre l'aspect d'une préparation de tissu traitée par cette technique.

Bibliographie p. 50.

TABLEAU I

	Expérience 1 Glycocolle				Expérience 2 Phénylalanine				Expérience 3 Adénine			
	Nombre de traces 10,000 μ^3				*Nombre de traces 10,000 μ^3*				*Nombre de traces 10,000 μ^3*			
	Cyto-plasme	*Noyaux*	*Noyaux / cytopl.*	*Noyaux Kupffer*	*Cyto-plasme*	*Noyaux*	*Noyaux / cytopl.*	*Noyaux Kupffer*	*Cyto-plasme*	*Noyaux*	*Noyaux / cytopl.*	*Noyaux Kupffer*
Alcool	0.8	3.7	4.6	10.6					0.41*	1.8*	4.4	7*
acétique	0.6	3.4	5.6	8.3	0.45*	1.8*	4.0	4.4*	0.51*	2.9*	5.6	7*
	0.7	4.0	5.6	10.0					0.36	1.14	3.7	15
Acide	0.6	1.7	2.8	6.1	0.13*	0.4*	3.0	0.8*	0.36*	1.1*	3.0	4*
citrique	0.7	1.9	2.7	3.8								
Acetate	0.4	3.3	8.5	5.3	0.35*	2.4*	7.0	3.5*	0.18*	1.05*	5.8	2.7*
de plomb	0.4	3.7	9.1	6.8					0.13	0.84	6.4	2.4
Acide trichloracétique	0.9	4.0	4.5	10.0	0.39*	1.5*	3.8	8.0*	0.16	0.9	5.6	3
—	0.15	1.1	7.4	4.4					0.5*	3.6*	7.2	0.4*
									0.22	0.68	3.1	1.3

Les résultats marqués d'une astérisque concernent des tissus fixés par congélation-dissolution. Les autres résultats se rapportent à des tissus fixés par congélation-dessication.

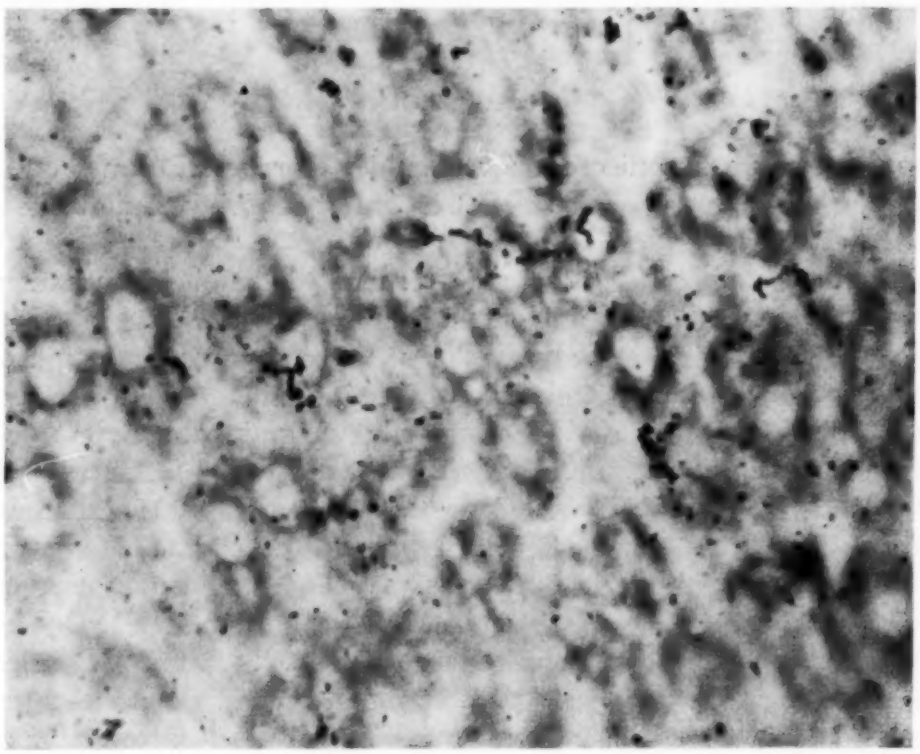

Fig. 1. Autoradiographie de tissu hépatique, coloré au mélange de Unna et photographié en lumière verte (les noyaux sont en clair et la basophilie cytoplasmique est très apparente).

On observe une radioactivité du même ordre de grandeur dans les coupes de l'animal tué 60 heures après l'injection de phénylalanine et dans celles de l'animal tué 24 heures après l'injection d'adénine. Mais, dans ce dernier cas, l'exposition de l'émulsion photographique n'était que de 24 heures alors qu'elle était de 48 heures dans le premier. On peut en conclure que l'incorporation de la base purique dans les nucléotides est plus

Bibliographie p. 50.

rapide que celle de l'acide aminé dans les protéines, puisque la radioactivité de la solution injectée était la même. On avait injecté une dose de radioactivité quatre fois plus élevée pour le glycocolle; il n'est donc pas étonnant d'observer une radioactivité spécifique plus élevée dans son cas.

Le traitement par l'alcool acétique ou par l'acide trichloracétique semble conserver une activité comparable dans le cas du glycocolle et dans celui de la phénylalanine; dans le cas de l'adénine, l'alcool acétique conserve deux fois plus d'activité que l'acide trichloracétique. Le témoin fixé par simple congélation-dissolution demeure cependant le plus actif. En général, la fixation par l'acétate de plomb entraîne une perte de radioactivité dans le cas des 3 isotopes utilisés: elle se manifeste surtout dans le cytoplasme; il faut en conclure que, dans le cas de l'adénine, la fixation des nucléotides n'est certainement pas quantitative. Le traitement par l'acide citrique s'accompagne d'une diminution notable de la radioactivité principalement au niveau des protéines (expériences 1 et 2); les noyaux cellulaires peuvent perdre jusqu'à 75% de leur activité (expérience 2). Une fraction des protéines cytoplasmiques semble également être éliminée par ce traitement. Il s'agit vraisemblablement de protéines basiques parce que, dans ce cas, la basophilie des nucléoles et celle du cytoplasme sont particulièrement évidentes.

La radioactivité des noyaux est 4 fois plus élevée que celle du cytoplasme, tant en ce qui concerne les protéines que les nucléotides; les noyaux des cellules de KUPFFER semblent très actifs dans tous les cas observés.

DISCUSSION

Il ressort des résultats qui ont été rassemblés dans le Tableau I que les noyaux hépatiques incorporent plus de glycocolle, d'adénine et de phénylalanine que le cytoplasme, par unité de volume.

Mais il importe, avant de discuter ce résultat, d'examiner les causes d'erreurs techniques qui peuvent intervenir au cours de ces déterminations.

Considérons d'abord les erreurs que l'on peut commettre en ce qui concerne la localisation de l'origine cellulaire de la radioactivité. Le diamètre apparent des noyaux hépatiques est de l'ordre de 10 μ. Le diamètre d'un grain d'AgBr est de l'ordre de 0.5 μ; la distance entre les tout premiers grains est de 1 à 0.5 μ. La perte de premiers grains d'une trace pourrait donc occasionner une erreur assez considérable dans la localisation de son point d'origine. Cette erreur peut, cependant, être négligée car le développement photographique de toutes les plaques a été homogène dans toute la profondeur de l'émulsion (environ 40 μ d'épaisseur d'émulsion sèche). Une autre erreur de localisation pourrait résulter du phénomène de "back-scattering" (l'électron peut effectuer un certain parcours dans le tissu et dans le verre du porte-objet avant de pénétrer dans l'émulsion sensible); il serait possible d'évaluer cette erreur en utilisant des porte-objets constitués par des éléments légers (matières plastiques) ou lourds (verres riches en plomb) qui diminueraient ou exagéreraient son importance. Il semble toutefois que des erreurs de ce type doivent jouer plutôt en défaveur des noyaux, puisqu'ils représentent la surface la plus petite. Cependant, si la zone cytoplasmique périnucléaire était particulièrement active, on risquerait d'attribuer aux noyaux un nombre trop considérable de traces: or on sait que cette zone est particulièrement basophile et qu'elle est donc riche en microsomes. Ces particules constituent précisément la fraction qui incorpore le plus intensément les précurseurs des acides nucléiques et des protéines.

Bibliographie p. 50.

tant *in vitro*[10,13] que *in vivo*[2]. Cependant, selon ces mêmes auteurs[2,10,13], la fraction nucléaire incorpore aussi très activement les précurseurs des protéines et des nucléotides. Il semble donc que les valeurs élevées trouvées pour les noyaux des cellules parenchymateuses et, plus encore, pour ceux des cellules de KUPFFER soient significatives. Le rapport entre l'incorporation des précurseurs dans le noyau et dans le cytoplasme est du même ordre de grandeur, quel que soit le précurseur considéré (Tableau I). SMELLIE et ses collaborateurs[13] ont observé, par des méthodes biochimiques, un enrichissement en ^{15}N plus élevé dans l'ARN et les protéines du noyau que dans les mêmes constituants du cytoplasme total.

D'après SCHNEIDER[12] la teneur en protéines et en ARN du noyau est environ 10% de celle du cytoplasme. Nos estimations montrent que le rapport nucléo-cytoplasmique des cellules hépatiques correspond à 0.1, ce qui concorde avec les observations de ALLFREY *et al*[1].

Pour que les valeurs consignées dans le Tableau I représentent des radioactivités spécifiques, il faudrait que la concentration en protéines et en acides nucléiques soient identiques dans le noyau et dans le cytoplasme. Ceci semble approximativement exact en ce qui concerne les protéines[12]; mais l'ARN est, d'après MIRSKY[1], deux fois moins concentré dans les noyaux que dans le cytoplasme.

Remarquons que les valeurs que nous avons observées par autoradiographie tendent à mettre l'accent sur le métabolisme particulièrement élevé des noyaux. Cette conclusion reste valable, que les tissus soient seulement congelés et desséchés, ou qu'ils soient ensuite fixés par l'alcool acétique ou par l'acide trichloracétique. Dans le cas de l'adénine, l'acide trichloracétique élimine, semble-t-il, une proportion assez considérable de nucléotides marqués, tant dans le noyau que dans le cytoplasme. Nous avions espéré fixer quantitativement les nucléotides acidosolubles en les précipitant à l'aide d'acétate de plomb, comme le préconise TANDLER[14]: le rapport d'incorporation nucléocytoplasmique est en effet plus marqué dans ce cas; mais il résulte d'une perte de radioactivité dans le cytoplasme, tant en ce qui concerne les protéines que les acides nucléiques. Il en résulte donc, et ceci est particulièrement évident dans le cas de l'adénine, que l'acétate de plomb ne fixe pas les nucléotides acidosolubles de manière quantitative. Enfin, le fait que la plupart des auteurs aient trouvé, par voie biochimique, une activité de la fraction nucléaire relativement moins élevée que celle que nous observons, résulte vraisemblablement de l'utilisation d'acide citrique comme milieu d'isolement: cet acide extrait, en effet, jusqu'à 75% de l'activité due aux protéines et près de 50% de celle due aux nucléotides.

MIRSKY[1] observe également que l'acide citrique peut enlever jusqu'à 55% des protéines du noyau, principalement des histones; ce fait explique la basophilie accrue des nucléoles, que nous avons observée. La baisse de la radioactivité due aux nucléotides, à la suite d'un traitement prolongé à l'acide citrique, ne peut s'expliquer que par une hydrolyse lente des bases puriques ou des polynucléotides. Ajoutons, d'autre part, que l'acide trichloracétique, même à froid pendant 15 minutes, élimine une certaine proportion des nucléotides qui ont incorporé de l'adénine. Il est difficile d'expliquer, à l'heure actuelle, pourquoi une même extraction ne s'observe pas quand la glycine est utilisée comme précurseur. Peut-être y a-t-il une incorporation plus élevée d'adénine que de glycine dans les petits nucléotides. Dans le cas des protéines, la diminution de la radioactivité, après traitement à l'acide trichloracétique, est négligeable et elle est de l'ordre des erreurs expérimentales.

Bibliographie p. 50.

Nos résultats indiquent que la méthode autoradiographique est susceptible d'apporter des renseignements d'ordre quantitatif. Il serait toutefois désirable de trouver un mode de fixation qui soit à l'abri de toute critique et qui modifie le moins possible la constitution du tissu. La méthode de congélation-dissolution semble, à ce point de vue, offrir un net avantage, en tous cas, en ce qui concerne la fixation des nucléotides. Cette conclusion concorde avec les observations de DAVIES et WALKER[15], faites par microspectrophotométrie d'absorption. Ajoutons que les images cytologiques obtenues par ce mode de fixation sont excellentes.

RÉSUMÉ

Nous avons étudié, par autoradiographie, l'incorporation *in vivo* dans le foie de souris de glycine-1-^{14}C, de DL-phénylalanine-3-^{14}C et d'adénine-8-^{14}C. La méthode est quantitative et les résultats concordent avec ceux obtenus par les méthodes biochimiques usuelles. Toutefois, dans le cas des trois précurseurs utilisés, nous avons trouvé une activité métabolique des noyaux hépatiques d'environ 4 fois supérieure à celle du cytoplasme. Les noyaux des cellules de KUPFFER ont une activité encore plus considérable.

Nous avons étudié de manière systématique par la même technique les propriétés des divers fixateurs histologiques.

SUMMARY

The *in vivo* incorporation of glycine-1-^{14}C, DL-phenylalanine-3-^{14}C and adenine-8-^{14}C in mouse liver has been studied by radioautography. Results may be given quantitatively and are in fair agreement with those obtained by the usual biochemical methods. However, in the case of all three precursors, we have found a metabolic activity of the nuclei of liver cells about 4 times that of the cytoplasm. The nuclei of the KUPFFER cells have a still greater activity.

We have investigated systematically by the same technique the properties of various fixatives.

ZUSAMMENFASSUNG

In vivo wurde der Einbau von Glycin-1-^{14}C, DL-Phenylalanin-3-^{14}C und Adenin-8-^{14}C in die Leber der Maus mittels der Radioautographie untersucht. Die Methode liefert quantitative Ergebnisse, die mit denen der gewöhnlichen biologischen Methoden übereinstimmen. Jedoch fanden wir im Falle der drei verwandten Vorläufer in den Kernen der Leberzellen eine viermal so hohe Aktivität wie im Zellplasma. Die Kerne der KUPFFER'schen Sternzellen haben eine noch grössere Aktivität. Mit der gleichen Technik haben wir die Eigenschaften verschiedener histologischer Fixierungsmittel systematisch untersucht.

BIBLIOGRAPHIE

1 V. ALLFREY, H. STERN, A. E. MIRSKY ET H. SAETREN, *J. Gen. Physiol.*, 35 (1952) 529.
2 H. BORSOOK, C. L. DEASY, A. J. HAAGEN-SMIT, G. KEIGHLEY ET P. H. LOWY, *J. Biol. Chem.*, 186 (1950) 309.
3 M. M. DALY, V. ALLFREY ET A. E. MIRSKY, *J. Gen. Physiol.*, 36 (1952) 173.
4 I. DONIACH, A. HOWARD ET S. R. PELC, *Progress in Biophysics*, 3 (1953) 1.
5 A. L. DOUNCE, G. H. TISCHKOFF, S. R. BARNETT ET R. M. FREER, *J. Gen. Physiol.*, 33 (1949) 629.
6 N. H. ELIASSON, E. HAMMARSTEN, P. REICHARD, S. ÅQUIST, B. THORELL ET G. EHRENSVÄRD, *Acta Chem. Scand.*, 5 (1951) 431.
7 A. FICQ, F. GAVOSTO ET M. ERRERA, *Exper. Cell Res.*, 6 (1954) 69 et 238.
8 I. GERSH, *Anat. Rec.*, 70 (1938) 311.
9 E. HAMMARSTEN, *Ciba Symposium. Conf. on Isotopes in Biochemistry*, (1951) 203.
10 T. HULTIN, *Exper. Cell Res.*, 1 (1950) 376.
11 L. LISON, *Histochimie et Cytochimie animales*. Gauthier-Villars, Paris, 2e Edit. (1953) 29.
12 W. C. SCHNEIDER, *Cancer Res.*, 6 (1946) 685.
13 R. M. S. SMELLIE, W. M. MACINDOE ET J. N. DAVIDSON, *Biochim. Biophys. Acta*, 11 (1953) 559.
14 C. J. TANDLER, *Arch. Histol. norm. y pathol.*, 4 (1951) 275.
15 P. M. B. WALKER, communication personnelle.

Reçu le 13 août 1954

SOME PROPERTIES OF THE MANGANESE AND COPPER CATALYZED OXIDATION OF CATECHOL AND SOME OTHER *ORTHO*-DIHYDROXYBENZENE DERIVATIVES*

by

JAMES R. GILLETTE, DEAN WATLAND AND GEORGE KALNITSKY

Department of Biochemistry, College of Medicine, State University of Iowa, Iowa City, Iowa (U.S.A.)

It has been shown by CHAIX *et al.*[1,2,3] that manganese and copper catalyze the oxidation of adrenaline and noradrenaline. In a previous paper, we have demonstrated that these metallic ions catalyze the oxidation of catechol, DOPA, N-methyl-DOPA 3-hydroxytyramine and epinine[4] in slightly alkaline solutions. It was also shown that the metallic ion catalyzed reaction differs from the tyrosinase reaction in a number of ways. The purpose of this investigation was to determine some of the properties of the metallic ion catalyzed reactions.

METHODS AND MATERIALS

The conventional WARBURG technique was used in this investigation to follow the rate of oxidation. All solutions were made with demineralized distilled water. The $MnSO_4$ and $CuSO_4$ solutions were made from C.P. grade metallic salts. The *o*-dihydroxybenzene derivatives were either obtained from commercial houses or were synthesized as were previously described[4].

In order to determine whether chelates were formed between the metallic ions and the *o*-dihydroxybenzene derivatives two methods were used. A Beckman spectrophotometer, Model D.U., was used to determine the shift in the ultra-violet spectrum due to chelate formation. The other method was the manometric method used by CHAIX *et al.*[2]. For this method a 0.03 *N* $NaHCO_3$ solution was equilibrated with a 5 % CO_2–95 % N_2 atmosphere forming a bicarbonate buffer of pH 7.6.

EXPERIMENTAL

The effect of various buffers on the manganese catalyzed oxidation of DOPA and of catechol

Using a phosphate buffer CHAIX *et al.* found that Mn^{++} catalyzed the oxidation of adrenaline only after a lag period of several minutes had elapsed[1]. Since no lag period was apparent during the Mn^{++} catalyzed oxidation of catechol or DOPA in a veronal buffer, the effect of various buffers on the Mn catalyzed reaction was studied. It was found that Mn^{++} had the greatest catalytic effect in either veronal or tris (hydroxymethyl) aminomethane buffers. Glycine, phosphate and citrate buffers inhibited the Mn^{++} catalyzed oxidation of DOPA but had little effect on the autoxidation of DOPA (Table I).

* These studies were aided by a contract between the office of Naval Research, Department of the Navy and the State University of Iowa, NR 123–327, and by a grant from the Central Scientific Fund, College of Medicine, State University of Iowa.

References p. 57.

Consequently, these buffers probably form complexes with the manganese, thereby decreasing the effective concentration of the catalyst. When borate buffers were used both the Mn^{++} catalyzed oxidation and the autoxidation of DOPA were inhibited. Since borate is known to form chelates with ene-diols, it is likely that the borate inhibited reaction could be explained at least in part by the formation of the borate-DOPA chelate thereby decreasing the effective concentration of the substrate.

The Mn^{++} catalyzed oxidation of catechol was also inhibited by glycine and phosphate buffers. On the other hand, when a small amount of threonine (twenty micromoles) was added to the veronal buffer, the rate of the Mn^{++} catalyzed oxidation of catechol was increased about twenty percent.

TABLE I

EFFECT OF VARIOUS BUFFERS ON THE Mn^{++} CATALYZED OXIDATION OF DOPA

Buffer	*pH*	*Mn^{++} (M)*	*O_2 (µl)*	*Inhibition %*
Veronal acetate	7.88	—	71	
	7.88	0.0005	389	—
Tris	7.95	—	63	
	7.95	0.0005	374	2
Sodium citrate	7.92	—	51	
	7.92	0.0005	110	81
Sodium phosphate	7.88	—	69	
	7.88	0.0005	146	76
Glycine·NaCl	7.9	—	51	
	7.9	0.0005	281	28
Sodium borate	7.88	—	0	
	7.88	0.0005	18	94

Conditions: 0.005 *M* (10 *µM*) DOPA; 0.05 *M* buffer; KOH in center well; temperature, 37° C; time, 1 h.

Effect of various Mn^{++} and Cu^{++} concentrations on the rate of oxidation of 3-hydroxytyramine and of DOPA

Both the rate and the total amount of oxygen absorbed were found to be altered by varying the Mn^{++} concentration. Using ten micromoles of 3-hydroxytyramine ($5 \cdot 10^{-3}$ *M* final concentration) buffered at pH 7.9., the rate of oxygen absorption was increased as the manganese concentration was increased to 0.5 micromole ($2.5 \cdot 10^{-4}$ *M* final concentration). The rate of oxidation was increased only slightly by higher manganese concentrations (Table II). The total amount of oxygen absorbed was inversely proportional to the concentration of Mn^{++}. Similar results were obtained for the Mn^{++} catalyzed oxidation of DOPA.

During the Cu^{++} catalyzed oxidation of 3-hydroxytyramine, it was found that the the rate of oxygen uptake was increased as the Cu^{++} concentration was increased to $2.5 \cdot 10^{-3}$ *M*. Higher Cu^{++} concentrations decreased the total amount of oxygen absorbed during the course of the reaction.

References p. 57.

TABLE II

EFFECT OF VARIOUS Mn^{++} AND Cu^{++} CONCENTRATIONS ON THE OXIDATION OF 3-HYDROXYTYRAMINE

Metal ion Conc. (M)	*O_2 uptake*		*Metal ion Conc. (M)*	*O_2 uptake*	
	Mn^{++} (µl)	*Cu^{++} (µl)*		*Mn^{++} (µl)*	*Cu^{++} (µl)*
—	61	82	$5.0 \cdot 10^{-4}$	429	163
$2.5 \cdot 10^{-5}$	135	—	$1.0 \cdot 10^{-3}$	473	202
$5.0 \cdot 10^{-5}$	182	91	$2.5 \cdot 10^{-2}$	388	293
$1.0 \cdot 10^{-4}$	251	106	$5.0 \cdot 10^{-2}$	—	254
$2.5 \cdot 10^{-4}$	363	127			

Conditions: 0.075 *M* veronal, pH 8.1; 0.005 *M* (10 µ*M*) 3-hydroxytyramine·HCl; KOH in center well; atmosphere, air; temperature, 30° C; time, 90 min.

The formation of chelates

In order to determine if a chelate were formed between DOPA and the metallic ions, the ultra-violet spectrum of a DOPA solution was compared with the ultra-violet spectrum of a solution containing DOPA and the metallic ions. The spectrum of the DOPA solution containing Mn^{++} was identical with the ultra-violet spectrum of a DOPA solution alone. On the other hand there was a marked shift in the spectrum of the DOPA solution containing Cu^{++} (Fig. 1). These data indicate that a chelate was formed between Cu^{++} and DOPA but that no chelate was formed between DOPA and Mn^{++}.

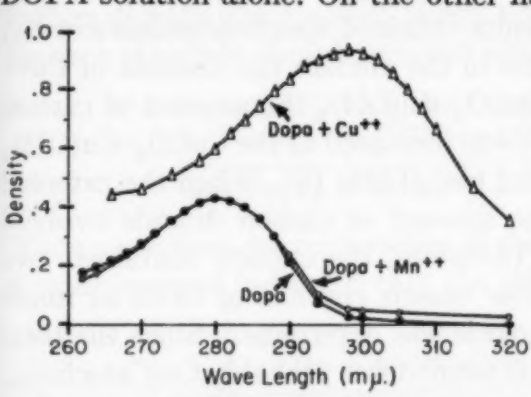

Fig. 1. Absorption spectra of DOPA with metallic ions. Conditions: 0.006 *M* veronal, pH 7.5; $1.6 \cdot 10^{-4}$ *M* DOPA; $1.6 \cdot 10^{-4}$ *M* metallic ions.

Since the spectrum of a chelate is not necessarily different from the spectrum of the ligand, the manometric method used by CHAIX *et al.*[2] was used to corroborate the spectrophotometric method. The metallic ions were equilibrated with the 0.03 *M* $NaHCO_3$ buffer in an atmosphere of 5% CO_2–95% N_2. During this phase carbon dioxide was evolved due to the formation of the metallic hydroxyides and carbonates. Under these conditions the amount of carbon dioxide evolved on the addition of Mn^{++} was negligible indicating that Mn^{++} did not form hydroxides or carbonates to any appreciable extent.

A blue-green precipitate was formed when Cu^{++} was added to the bicarbonate buffer. If this precipitate were $CuCO_3$ the amount of carbon dioxide evolved would be one micromole of carbon dioxide for every micromole of Cu^{++}. Two micromoles of carbon dioxide would have been evolved if the precipitate were $Cu(OH)_2$, while 1.5 micromoles of carbon dioxide would have been evolved if the precipitate were $CuCO_3 \cdot Cu(OH)_2$. CHAIX *et al.* found that one micromole of carbon dioxide was evolved for every micromole of Cu^{++} added. Under the conditions which we used, however, 1.5 micromoles of carbon dioxide were evolved, indicating that the precipitate was probably $CuCO_3 \cdot Cu(OH)_2$.

When catechol, DOPA, N-methyl DOPA or 3-hydroxytyramine·HCl was added to the Mn^{++}-bicarbonate mixture, little or no carbon dioxide was evolved, indicating little if any chelate formation between Mn^{++} and these *o*-dihydroxybenzene derivatives

References p. 57.

(Table III). Using this method, CHAIX *et al.* showed that there was very little chelation between Mn^{++} and adrenaline.

TABLE III

THE AMOUNT OF CO_2 EVOLVED DUE TO THE FORMATION OF METAL CHELATES

Ligand	*Ligand µmoles*	*Metal µmoles*	*Mn^{++} µl CO_2*	*Co^{++} µl CO_2*	*Cu^{++} µl CO_2*
Catechol	4	2	4	3	68
DOPA	4	4	0	30	122
N-methyl-DOPA	4	4	1	11	131
3-hydroxytyramine	5	5	3	13	99

Conditions: 0.03 *M* $NaHCO_3$ (pH 7.6); Atmosphere, 5% CO_2–95% N_2; temperature 30°. Total vol. 2.0 ml.

On the other hand, when catechol was added to $CuCO_3 \cdot Cu(OH)_2$ the precipitate dissolved and a large evolution of carbon dioxide was observed. Similar results were obtained when DOPA, N-methyl DOPA and 3-hydroxytyramine·HCl were added to $CuCO_3 \cdot Cu(OH)_2$ (Table III). This would indicate that chelates were formed between Cu^{++} and these compounds, corroborating the results obtained spectrophotometrically.

In order to determine the catechol/Cu^{++} ratio in the chelate the amount of Cu^{++} was varied. On the addition of catechol to the $CuCO_3 \cdot Cu(OH)_2$ the amount of carbon dioxide evolved due to the formation of the chelate was increased as the $CuCO_3 \cdot Cu(OH)_2$ was increased until the catechol/Cu^{++} ratio equaled two (Table IV). When the catechol was added to higher concentrations of Cu^{++}, the amount of carbon dioxide evolved due to the chelate formation was not affected. Therefore, the chelate contained two molecules of catechol for every Cu^{++} ion. In those vessels containing twice as much catechol as copper, the total amount of carbon dioxide was determined. Since the total carbon dioxide/Cu^{++} ratio was about 3.5, the chelate formed was probably $Cu(Catechol)_2$.

When DOPA or N-methyl DOPA were added to the $CuCO_3 \cdot Cu(OH)_2$ more carbon dioxide was evolved than when 3-hydroxytyramine·HCl was added to it (Table III). This would indicate that Cu^{++} formed a chelate with DOPA through the amino and the carboxyl groups as well as through the phenolic groups.

When 3-hydroxytyramine·HCl was added to various amounts of $CuCO_3 \cdot Cu(OH)_2$, the carbon dioxide evolved was stabilized when the 3-hydroxytyramine·HCl/Cu ratio was two (Table IV). Since the catechol/Cu ratio was also two, this would indicate that Cu^{++} cannot combine with the amino group to any great extent, under these conditions. On the other hand, when DOPA was added to various amounts of $CuCO_3 \cdot Cu(OH)_2$, the carbon dioxide was not stabilized when the DOPA/Cu ratio was two. This would indicate that a chelate was formed between Cu^{++} ion and the carboxyl groups of DOPA.

The effect of manganese dioxide on catechol

Since the manganous ion probably changes valence during the course of the Mn^{++} catalyzed oxidation of catechol, it was considered that a fairly stable chelate might be formed between catechol and Mn^{+3} or Mn^{+4}. In order to determine if such a chelate could be formed, catechol was allowed to react with manganese dioxide in the following manner.

References p. 57.

TABLE IV

THE EFFECT OF VARIOUS Cu^{++} CONCENTRATIONS ON THE CO_2 EVOLVED DURING Cu^{++} CHELATE FORMATION

Cu^{++} conc. (μmoles)	*Catechol 2 μmoles (μl CO_2)*	*DOPA 4 μmoles (μl CO_2)*	*3-Hydroxytyramine 10 μmoles (μl CO_2)*
0.5	24	30.7	37
0.75		33.8	
1.0	33	40.3	
1.5		59	88
2.0	35	72	
2.5		90	
3.0		102	159
4.0	35		201
5.0		133	214
10.0			197
20.0			169

Into vessels containing one micromole of potassium permanganate dissolved in 0.03 *M* sodium bicarbonate buffer under a 5% CO_2–95% N_2 atmosphere at 30° C., various amounts of manganese sulfate were added. A dark precipitate was formed and carbon dioxide was evolved. When 1.5 micromoles of manganese sulfate were added the amount of carbon dioxide evolved indicated that the precipitate was manganese dioxide.

a. $MnO_4^- + 1.5\ Mn^{++} + H_2O \longrightarrow 2.5\ MnO_2 + 2H^+$
b. $2H^+ + 2\ HCO_3^- \longrightarrow 2CO_2 + 2\ H_2O$

sum: $MnO_4^- + 1.5\ Mn^{++} + 2\ HCO_3^- \longrightarrow 2.5\ MnO_2 + 2CO_2 + H_2O$

When more than 1.5 micromoles of manganese sulfate were added, the amount of carbon dioxide evolved indicated that the following reactions took place.

c. $4\ MnO_4^- + 11\ Mn^{++} + 9\ H_2O \longrightarrow 5\ MnO_2 \cdot Mn_2O_3 + 18\ H^+$
d. $18\ H^+ + 18\ HCO_3^- \longrightarrow 18\ CO_2 + 18\ H_2O$

sum: $4\ MnO_4^- + 11\ Mn^{++} + 18\ HCO_3^- \longrightarrow 5\ MnO_2 \cdot Mn_2O_3 + 18\ CO_2 + 9\ H_2O$

When catechol was added to the insoluble manganese oxides, a rapid absorption of carbon dioxide was observed as the oxides dissolved. After about ten minutes a slow evolution of carbon dioxide was observed and a white precipitate was formed (Fig. 2). The color of the solution changes to a faint yellow when the catechol is added either to the potassium permanganate or to the insoluble manganese oxides.

Although the amount of catechol added was varied from 2.5 to 10 micromoles, neither the rate of carbon dioxide absorbed during the first ten minutes nor the subsequent rate of carbon dioxide evolution was affected. This would indicate that no stable chelate was formed between the catechol and Mn^{+3} or Mn^{+4}.

After the system came to equilibrium the total amount of carbon dioxide evolved was determined.

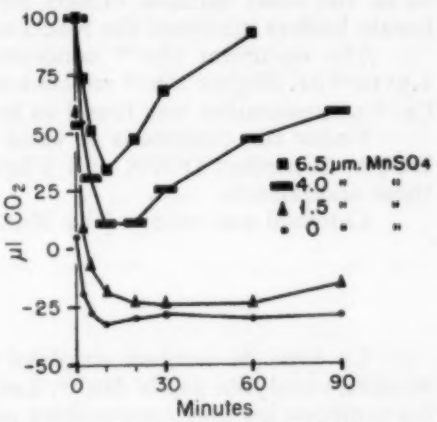

Fig. 2. The effect of $KMnO_4$ and the manganese oxides on catechol. Conditions: 0.03 *M* $NaHCO_3$; Atmosphere, 5% CO_2–95% N_2; pH 7.6; 1 μ*M*. $KMnO_4$; Mn^{++} as indicated; $5 \cdot 10^{-3}$ *M* (10 μ*M*) catechol; temp., 30° C.

References p. 57.

Although this quantity of carbon dioxide was independent of the catechol concentration, it was dependent on the Mn^{++} concentration according to the following relationship.

$$\frac{3 \text{ micromoles } CO_2 + \text{total } CO_2 \text{ evolved}}{\text{Total } Mn^{++} \text{ in micromoles}} = 1$$

In this equation the three micromoles of carbon dioxide represents the carbon dioxide absorbed during the oxidation of catechol by either potassium permanganate or the manganese oxides, according to the following equations.

e. $MnO_4^- + 1.5\ Mn^{++} + 2\ HCO_3^- \longrightarrow 2.5\ MnO_2 + 2\ CO_2 + H_2O$

f. $2.5\ MnO_2 + 2.5$ 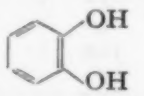 $\longrightarrow 2.5\ Mn^{++} + 2.5$ 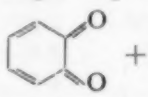 $+ 5\ OH^-$

g. $5\ OH^- + 5\ CO_2 \longrightarrow 5\ HCO_3^-$

---

sum: $MnO_4^- + 2.5$ 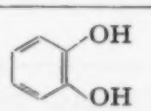 $+ 3\ CO_2 \longrightarrow Mn^{++} + 2.5$ 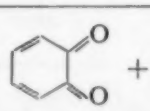 $+ 3\ HCO_3^- + H_2O$

In another experiment, it was found that sodium fluoride, which forms a complex with manganous ions, markedly inhibited the rate of the carbon dioxide evolution which occurred after the first ten minutes. It did not affect the rate of carbon dioxide absorbed during the first ten minutes.

In conclusion, it can be stated that manganese dioxide and probably manganese trioxide oxidize catechol. The evolution of carbon dioxide which follows this oxidation is due to either the formation of insoluble manganese carbonate or to the formation of a chelate between the manganous ion and an oxidation product of catechol.

SUMMARY

The type of buffer used had a profound effect on the Mn^{++} catalyzed oxidation of the *ortho*-dihydroxybenzene compounds used. Veronal or tris (hydroxymethyl) amino methane were found to be the most suitable buffers for the study of these reactions. Glycine, phosphate, citrate and borate buffers inhibited the reaction.

The optimum Mn^{++} concentration for the 3-hydroxytyramine and DOPA oxidation was $2.5 \cdot 10^{-4}$ *M*. Higher Mn^{++} concentrations increased the rate of oxidation only slightly. The optimum Cu^{++} concentration was found to be $2.5 \cdot 10^{-3}$ *M*.

Under the conditions of these experiments chelates were formed between Cu^{++} and catechol, DOPA, N-methyl DOPA and 3-hydroxytyramine. No chelation was detected between Mn^{++} and these compounds.

Catechol was oxidized by MnO_2 and $KMnO_4$.

RÉSUMÉ

Le type de tampon employé a une grande importance dans l'oxydation des orthodiphénols étudiés, catalysée par le Mn^{++}. Les tampons véronal ou tris (hydroxyméthyl) amino méthane sont les tampons les plus convenables pour l'étude de ces réactions. Les tampons glycocolle, phosphate, citrate et borate inhibent la réaction.

La concentration optimum en Mn^{++} pour l'oxydation de la 3-hydroxytyramine et de la DOPA est $2.5 \cdot 10^{-4}$ *M* des concentrations plus élevées en Mn^{++} n'augmentent que faiblement la vitesse d'oxydation. La concentration optimum en Cu^{++} est $2.5 \cdot 10^{-3}$ *M*. Dans les conditions expérimentales employées, des chélates sont formés entre le Cu^{++} et le catéchol, la DOPA, la N-méthyl DOPA et la 3-hydroxytyramine. Il n'y a pas de chélation entre Mn^{++} et ces corps.

Le catéchol est oxydé par MnO_2 et par $KMnO_4$.

References p. 57.

ZUSAMMENFASSUNG

Die Art des verwendeten Puffers beeinflusst die von Mn^{++} katalysierte Oxydation der benutzten *ortho*-Dihydroxybenzol-Verbindungen stark. Veronal oder Tris(hydroxymethyl)aminomethan eigneten sich am besten als Puffer, bei dem Studium dieser Reaktionen. Glykocoll, Phosphat, Citrat und Borat Puffer hemmten die Reaktion.

Das Mn^{++} Konzentrationsoptimum lag für die Oxydation von 3-Hydroxytyramin und DOPA. bei $2.5 \cdot 10^{-4}$ *M*. Höhere Mn^{++} Konzentrationen erhöhten die Oxydationsgeschwindigkeit nur wenig. Das Konzentrationsoptimum für Cu^{++} wurde bei $2.5 \cdot 10^{-3}$ *M* gefunden. Unter den Versuchsbedingungen bildeten sich zwischen Cu^{++} und Katechol, DOPA, N-methyl DOPA und 3-Hydroxytyramin Chelate. Kein Chelation wurde entdeckt zwischen Mn^{++} und diesen Verbindungen.

Katechol wurde oxydiert durch MnO_2 und $KMnO_4$.

REFERENCES

1 P. CHAIX, J. CHAUVET AND J. JEZEQUEL, *Biochim. Biophys. Acta*, 4 (1950) 471.
2 P. CHAIX, G. MORIN AND J. JEZEQUEL, *Biochim. Biophys. Acta*, 5 (1950) 472.
3 P. CHAIX AND C. PALLAGET, *Biochim. Biophys. Acta*, 10 (1953) 462.
4 J. R. GILLETTE, D. WATLAND AND G. KALNITSKY, *Biochim. Biophys. Acta*, 15 (1954) 526.

Received July 26th, 1954

THE ACETATE-ACTIVATING ENZYME OF *RHODOSPIRILLUM RUBRUM**

by

MAX A. EISENBERG

Department of Neurology, College of Physicians and Surgeons, Columbia University, New York (U.S.A.)

It was demonstrated in a previous investigation[1] that the acetate-activating enzyme system of *Rhodospirillum rubrum* is not identical with that found in most microorganisms[2,3]. The absence of the enzyme phosphotransacetylase and the requirement of coenzyme A indicated that the enzyme system in this organism was similar to the one first described by NACHMANSOHN AND MACHADO[4] for the acetylation of choline in brain tissue and further elaborated on by LIPMANN *et al.*[5,6] during an extensive investigation of the mechanism of acetylation in pigeon liver. It was subsequently shown by LIPMANN *et al.*[7], with a yeast preparation, that the acetate-activation involved a pyrophosphorolytic split of ATP. With the identification of "active acetate" as the thiolester of coenzyme A by LYNEN *et al.*[8], the overall equation could be formulated as follows:

$$(1) \quad \text{ATP} + \text{CoA} + \text{Acetate} \rightleftharpoons \text{Acetyl CoA} + \text{AMP} + \text{P–P}$$

A similar enzyme system has also been purified from heart muscle[9,10] and more recently it has also been found in a variety of plants and plant tissues[11]. Further information concerning the detailed mechanism of the acetate-activating reaction has recently been obtained by JONES, LIPMAN, HILZ AND LYNEN with the aid of isotopes[12].

The present investigation was undertaken with the purpose of studying the acetate-activating reaction in greater detail with purified enzyme preparations from *Rhodospirillum rubrum*. The present report concerns itself with the purification procedure and the properties of the purified enzyme system.

MATERIALS AND METHODS

Barium ATP**), coenzyme A, and adenosine-3′-phosphate were products of Pabst Brewing Co. Barium ADP, adenosine-5′-phosphate and calcium phosphate gel were purchased from Sigma Chemical Co. Potassium acetate, potassium pyrophosphate, hydroxylamine hydrochloride, and glutathione were commercial products. All acidic solutions were adjusted to pH 7.4 with KOH. Acetyl coenzyme A was prepared by the method of SIMON AND SHEMIN[13]. Crystalline yeast pyrophosphatase was generously supplied by Dr. M. KUNITZ, and a purified preparation of yeast hexokinase was kindly furnished by Dr. W. H. STEIN.

* This work was supported by the Division of Research Grants and Fellowships of the National Institutes of Health, H-740, United States Public Health Service

** The abbreviations used are as follows: ATP-adenosine triphosphate, ADP-adenosine diphosphate, AMP-adenosine 5′ phosphate, CoA-coenzyme A, AcetylCoA-acetyl coenzyme A, P–P-inorganic pyrophosphate.

References p. 65.

Inorganic phosphate was determined by the method of FISKE AND SUBBAROW[14]. Pyrophosphate was estimated by a slight modification of the procedure of KUNITZ[15], and also by the manganese precipitation method of KORNBERG[16]. ATP, ADP and AMP were separated by the column technique of COHN AND CARTER and their respective concentrations determined spectrophotometrically[17]. ATP was also determined by the hexokinase method in which the acid-labile phosphate is measured, ADP by the acid-labile phosphate after 10 minutes' hydrolysis in 1 *N* HCl at 100° C, and AMP by the absorption at 260 mμ. Coenzyme A was assayed by the arsenolysis test with acetyl coenzyme as a standard for CoA[18]. Acetyl CoA was determined spectrophotometrically by measuring the decrease in the optical density at 232 mμ in the presence of arsenate and phosphotransacetylase[19]. The method of WARBURG AND CHRISTIAN[20] was used to measure the protein concentrations. ATPase activity was assayed by the method of KIELLEY AND KIELLEY[21], and myokinase activity by the method of COLOWICK AND KALCKAR[22]. Acetyl coenzyme A deacylase activity was determined by the decrease in optical density at 232 mμ or by the formation of aceto hydroxamic acid.

Acetohydroxamic acid formation was measured by the method of LIPMANN AND TUTTLE[23]. The reaction mixture in a final volume of 1 ml was mixed with 1 ml of 12% trichloracetic acid, 2 ml of water, 1 ml of 4 *N* HCl, and 1 ml of 5% ferric chloride in 0.1 *N* HCl. The mixture was clarified by centrifugation and the adsorption of the supernatant fluid measured in a KLETT-SUMMERSON photoelectric colorimeter with a #54 filter. A reagent blank was used to set the instrument. 1 μM of acetohydroxamic acid was equivalent to 57 Klett units using as a standard a sample of acetylglutathione kindly furnished by Dr. H. SACHS.

ENZYME PURIFICATION

R. rubrum was grown for 36 hours under continuous illumination in 10–12 liter quantities according to the procedure described previously[1]. The culture was removed from the light cabinet and left for 24 hours at room temperature prior to harvesting. The yield was approximately 3–4 grams of wet cells per liter of culture medium. The cells were washed twice with distilled water and packed tightly in the Sorvall high speed centrifuge at 12,000 × gravity. The packed cells were then stored in the freezing compartment of the refrigerator over night.

Crude extract. The frozen mass of cells was broken up in a cold mortar and ground with 2.5 times its weight of alumina A-303. The tacky paste was taken up with 2.5 times its volume of cold 0.05 *M* phosphate buffer pH 7.4 and centrifuged at 900 × gravity in the International Refrigerated Centrifuge. The supernatant was decanted and the alumina resuspended twice in 10–15 ml of buffer, and recentrifuged. The supernatant fluids were combined and centrifuged at 78,400 × gravity for one hour in the Model E Spinco centrifuge. The supernatant fluid was removed and stored in the deep freeze at —20° C. The activity of the crude extracts was maintained for an extended period of time in the frozen state. Occasionally, the crude extracts showed a lower total enzymic activity than the more purified preparations and in addition increased in activity when kept in the frozen state. This suggested the presence of an inhibitor. Dialysis of these crude extracts did not increase the enzymic activity indicating the inhibitor was of a high molecular weight. The addition of fluoride to the reaction mixture to inhibit ATPase activity resulted only in a loss of activity. No further attempt was made to identify the inhibitor.

1st ammonium sulfate fractionation. To 100 ml of crude extract at 0–2° C were slowly added with continuous stirring 16.6 grams of solid ammonium sulfate to yield a 30% saturated solution. The solution was stirred for another ten minutes and then centrifuged at 8,700 × gravity for 15 minutes. The reddish precipitate contained very little activity and was discarded. Sufficient ammonium sulfate was then added to the supernatant fluid to bring the concentration up to 70% saturation. The heavy precipitate was centrifuged for 15 minutes at 35,000 × gravity. The precipitate was taken up in a

References p. 65.

minimum amount of 0.05 *M* phosphate buffer pH 7.4 and dialyzed against the same buffer over night. The dialysis was continued on the following day using 0.01 *M* phosphate buffer pH 7.4 until the dialysate was free of ammonium sulfate.

Protamine sulfate. The dialyzed 30–70% fraction was diluted with buffer to a final concentration of about 15 mg of protein per ml. A 2% solution of protamine sulfate was slowly added with continuous stirring until a final concentration of 18 mg of protamine sulfate for each 100 mg of protein was attained. The heavy flocculent precipitate was removed by centrifugation and discarded.

2nd ammonium sulfate fractionation. Solid ammonium sulfate was added to the above supernatant to bring the concentration up to 50% saturation. The precipitate was removed by centrifugation and discarded. More solid ammonium sulfate was added and the precipitate formed at 70% saturation removed by centrifugation at 35,000 × gravity and saved. A final precipitate was removed after bringing the ammonium sulfate concentration up to 90% saturation. Both precipitates were dissolved in a minimum amount of 0.05 *M* phosphate buffer pH 7.4 and dialyzed against the same buffer until the solutions were essentially free of ammonium sulfate. About 40% of the total activity was found in the 50–70% fraction as compared to 25% in the 70–90% fraction. However, the latter had about twice the specific activity of the former, and therefore was used for further purification.

Calcium phosphate gel. The pH of the 70–90% fraction was adjusted to 6.5 with 1 *N* acetic acid and then diluted with buffer to a final protein concentration of 12–15 mg per ml. The gel suspension containing approximately 15 mg of calcium phosphate by dry weight per ml was washed with distilled water until the washings were neutral to brom thymol blue. The gel was then suspended in one half the original volume and a sufficient quantity added to the protein solution to give a ratio of 1:1 of gel to protein. The mixture was stirred for 10 minutes at 0–2° C and then centrifuged for 5 minutes at 400 × gravity. The supernatant was stored in the deep freeze at —20° C under which conditions it was found to be stable for at least 3 months. This preparation was also found to be free of ATPase, acetylcoenzyme A deacylase and pyrophosphatase activity, however, it still contained appreciable quantities of myokinase activity.

In Table I are summarized some typical results obtained with the above fractionation procedure.

TABLE I

ACTIVITY OF VARIOUS FRACTIONS DURING ENZYME PURIFICATION

Fraction	*Volume ml*	*Protein mg/ml*	*Activity μM/ml/30 min*	*Total activity*	*Specific activity*	*Per cent recovery*
Crude	144	22.0	32	4,600	1.5	100
1st Ammonium sulfate (30–70%)	90	15.1	45	4,100	3.0	88
Protamine sulfate	98	8.1	43	4,200	5.2	91
2nd Ammonium sulfate (70–90)	7.4	11.9	130	960	11.2	21
Calcium Phosphate Gel	8.7	6.6	109	950	16.5	20

Hydroxamic acid assay. The absolute requirement for ATP and CoA in the hydroxamic acid assay sytem is indicated in Table II. The high activity observed in the absence of any added acetate was due to the presence of acetate in the ATP preparations

References p. 65.

TABLE II

COMPONENTS OF THE ACETATE-ACTIVATING ENZYME SYSTEM

The complete sytem contained $MgCl_2$ 10 μM, glutathione 10 μM, CoA 0.26 μM, ATP 4.1 μM, K acetate 50 μM, hydroxylamine 400 μM, Tris (hydroxymethyl) aminomethane pH 7.4 50 μM, and enzyme 0.085 mg in a final volume of 1.0 ml. The reaction was carried out at 32° C for 30 minutes.

	Aceto-hydroxamic acid μM
Complete system	0.77
Without glutathione	0.35
Without $MgCl_2$	0.22
Without CoA	0.04
Without ATP	0.03
Without acetate	0.46

used. This enzyme system has been shown to be sensitive to acetate[9]. In Fig. 1 are shown the optimum concentration curves for the various components of the system except acetate. The requirements for high concentrations of hydroxylamine and coenzyme A are in accord with the results previously obtained with the yeast and muscle enzymes. Since the relatively high saturation requirements for hydroxylamine are attributed to the non-enzymic nature of the reaction between acetyl CoA and hydroxylamine, it would appear that at the plateau in the hydroxylamine curve the rate limiting step is the formation of acetyl CoA.

The hydroxamic acid assay has been found to be linear over a ninefold increase in enzyme concentration as shown in Fig. 2. At somewhat higher enzyme concentrations

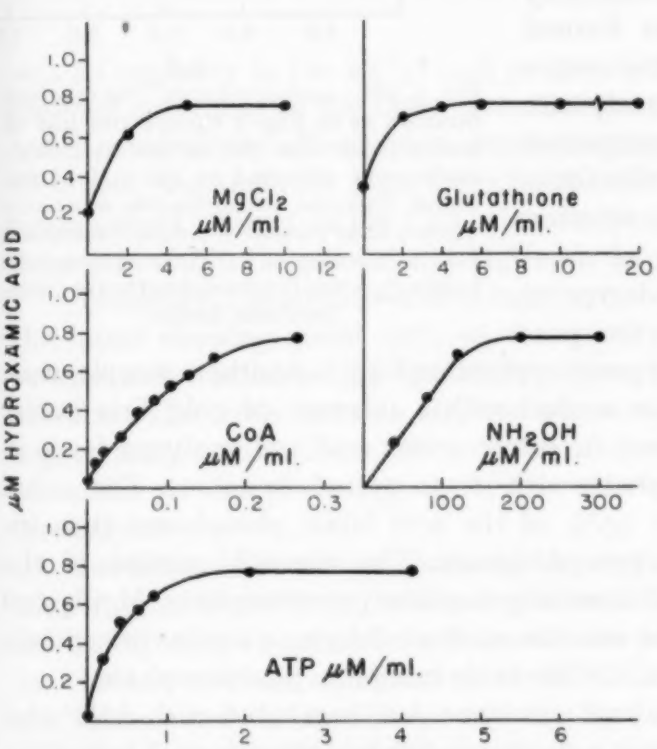

Fig. 1. The optimum concentration curves for the various components of the hydroxamic acid assay system. The standard assay is given in Table II.

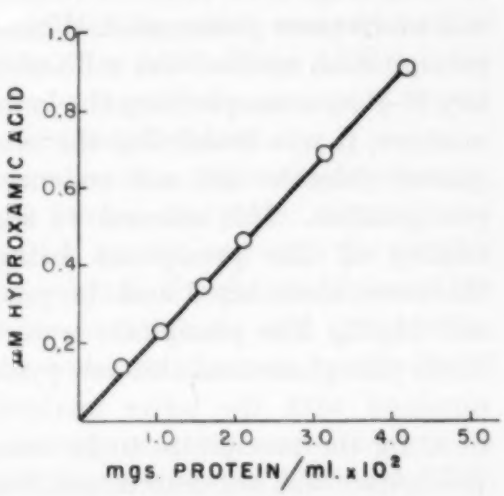

Fig. 2. Activity as a function of enzyme concentration. The reaction mixture contained $MgCl_2$ 10 μM, glutathione 10 μM, CoA 0.11 μM, ATP 3.2 μM, K acetate 50 μM, hydroxylamine 400 μM, Tris (hydroxymethyl) aminomethane pH 7.4 50 μM, in 1.0 ml. The reaction was carried out at 32° C for 30 minutes.

References p. 65.

the activity falls off and the assay becomes unreliable. This may be a reflection of a change in the rate-limiting step of the reaction. With higher enzyme concentrations the rate of acetyl CoA formation increases until essentially all of the CoA is in the form of acetyl CoA at all times. Under these conditions, the rate of the non-enzymic hydroxamic acid formation would be proportional to the hydroxylamine concentration, and since the concentration of the latter was kept constant, one can expect a decrease in activity beyond a certain enzyme concentration range. However, within the limited range of activity (0–1.2 μM hydroxamic acid formed in 30 minutes) the assay has proven to be reliable and quite satisfactory.

The pH-activity curve in Fig. 3 shows the pH optimum for the assay to to be about 7.5 with the activity falling off rapidly on the acid side of the pH optimum. A similar pH optimum was obtained for the yeast and plant enzyme systems[7,11].

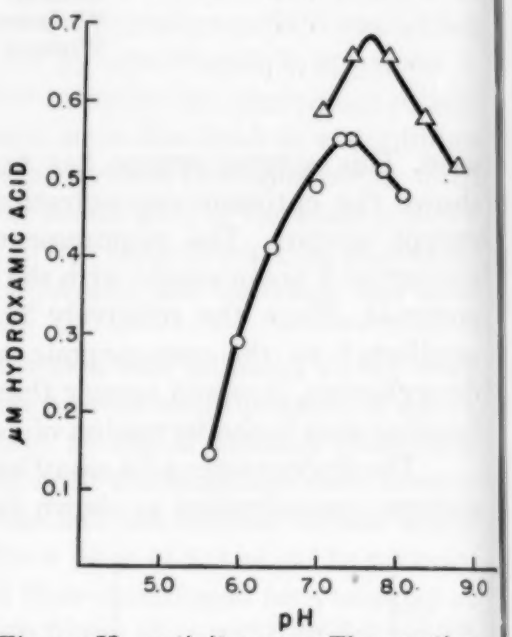

Fig. 3. pH – activity curve. The reaction mixture as in Fig. 2 except 100 μM of buffer used. The pH of the hydroxylamine was adjusted to the pH of the buffer. Enzyme concentration was 0.027 mg in a final volume of 1.0 ml. Incubated for 30 minutes at 32° C. ○ – phosphate buffer △ – tris (hydroxylmethyl) aminomethane buffer.

Balance study. It is shown in Table III that with catalytic amounts of CoA and with hydroxylamine as a trapping agent, one mole of AMP, P–P, and acetyl coenzyme A is formed for each mole of ATP disappearing. These results have been corrected for the ADP formed during the course of the reaction as the results of the myokinase activity. One half of the ADP formed was added to the ATP disappearing and AMP formed.

During the routine assays in which one ml of reaction mixture was used, it was frequently observed that a slight precipitate was formed during the course of the reaction. In the course of some large scale enzymic runs, this precipitate was much more pronounced. When the manganese precipitation method was utilized to further identify P–P in a sample from the large scale reaction mixture, it was found that the addition of manganese chloride did not enhance the degree of precipitation. This seemed to suggest the possibility of the precipitate being inorganic pyrophosphate. Another sample was, therefore, centrifuged and the precipitate washed with a mixture of cold Tris buffer and $MgCl_2$. The precipitate was dissolved in dilute acetic acid and analyzed for acid labile phosphate and also for pyrophosphate with yeast pyrophosphatase. The value obtained with the latter analysis was 95% of the acid labile phosphorus thus indicating the precipitate to be inorganic pyrophosphate. The chemical nature of the precipitate was not determined, but a mixture of potassium pyrophosphate, $MgCl_2$ and Tris buffer in the concentration used in the reaction mixture did give a similar precipitate suggesting possibly Mg pyrophosphate as the insoluble inorganic pyrophosphate.

Reversibility of the reaction. When acetyl coenzyme A is incubated with AMP and P–P in the presence of the enzyme, there is a decline in the hydroxamic acid formed as shown in Table IV. There is no decline in the absence of pyrophosphate and a small decline in the absence of AMP. The latter result would seem to indicate that AMP

References p. 65.

TABLE III

BALANCE STUDY OF THE ACETATE-ACTIVATING REACTION

The reaction mixture contained $MgCl_2$ 40 μM, glutathione 40 μM, Coenzyme A 0.9 μM, ATP 22.3 μM, hydroxylamine 1600 μM, K acetate 100 μM, Tris (hydroxymethyl) aminomethane buffer pH 7.4 200 μM, and enzyme 0.438 mg in a total volume of 3 ml. The reaction was carried out at 32 °C for one hour. The results are expressed in micromoles.

*ATP**	*ATP corr. f. ADP*	*AMP**	*AMP corr. f. ADP*	*Inorganic* P–P*	*Aceto hydroxamic acid*
—7.1	—6.1	+4.9	+6.0	+6.2	+7.0

* Corrected for the blank without added acetate.

TABLE IV

THE REVERSIBILITY OF THE ACETATE-ACTIVATING REACTION

The complete system contained $MgCl_2$ 10 μM, adenosine 5′ phosphate 9.6 μM, potassium pyrophosphate 100 μM, Tris (hydroxymethyl) aminomethane buffer pH 7.4 50 μM, acetyl coenzyme A 1.74 μM, and enzyme 0.236 mg in a final volume of 1 ml. Reaction mixture incubated at 32° C for one hour. 400 μM neutral hydroxylamine added and after 10 minutes acethohydroxamic acid determined.

	Acetohydroxamic acid µM
acetyl CoA	1.74
acetyl CoA +AMP	1.74
acetyl CoA +P–P	1.47
acetyl CoA +AMP —P–P	0.96

was an impurity in the acetyl CoA preparation. When a sample of CoA was chromatographed according to the COHN AND CARTER procedure[17], it was found that AMP was not a contaminant. However, a small quantity of a nucleotide, which was not further identified, was removed from the column with the eluant for ADP. If the ADP was the contaminant present in the CoA, then in the presence of myokinase one could expect some reversal in the presence of high concentrations of pyrophosphate.

Specificity. The acetate-activating enzyme is active only with acetate and proprionate, the latter showing about 90% of the activity of the former. Butyrate, caproate and octanoate are activated by the crude enzyme preparation but are not with the purified extracts. The crude extracts also contain most of the enzymes for the oxidation of the higher fatty acids*. Since the rate limiting step in the hydroxamic acid assay is the formation of acetyl coenzyme A, the above results indicate the true specificity of the enzyme.

Inhibition. The end products of the acetate-activating reaction were found to be inhibitory to the system. In Fig. 4 is shown the inhibitory activity of AMP and ADP; the latter being about one third as effective as AMP. P–P was also found to be about one third to one half as inhibitory as AMP. The inhibitory action of ADP may be more of a reflection of the myokinase activity than of any action of ADP *per se*. Adenylic-3′-phosphate was almost completely inactive over the same concentration range as AMP.

* Personal communication from Dr. J. STERN.

References p. 65.

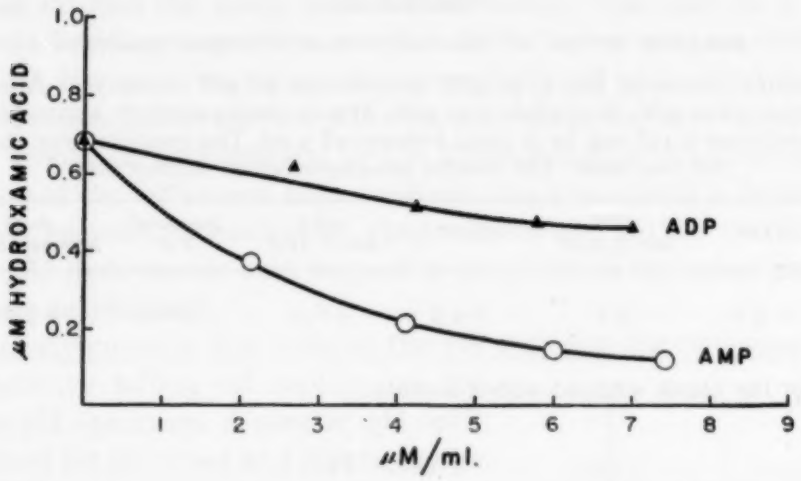

Fig. 4. Inhibition of the acetate-activating enzyme by ADP and AMP. The reaction mixture as in Fig. 2 except CoA 0.27 μM and ATP 2.3 μM. Enzyme concentration was 0.174 mg in a final volume of 1.0 ml. Reaction mixture incubated at 32° C for 30 minutes. ○ AMP. ▲ ADP.

DISCUSSION

The purified acetate-activating enzyme of *Rhodospirillum rubrum* appears in the absence of high salt concentrations to be a more stable preparation than that of yeast or heart muscle. In addition this preparation is free of pyrophosphatse activity. The presence of the enzyme myokinase still introduces a number of difficulties in many of the assays and work is now in progress to rid the purified preparation of this impurity. Many of the properties of the enzyme described are similar to those found for the yeast, heart muscle and plant enzymes. However, the question of whether the mechanism is the same for this enzyme as for the yeast enzyme must await further investigation.

ACKNOWLEDGMENT

The author wishes to express his gratitude to Dr. DAVID NACHMANSOHN for his guidance and helpful advice throughout this work.

SUMMARY

A relatively stable purified enzyme preparation has been obtained from *Rhodospirillum rubrum* which catalyzes the formation of acetyl coenzyme A form ATP, acetate and CoA.

AMP and pyrophosphate were shown to be end products of the reaction and also inhibitors of the reaction.

The properties of the enzyme system have been described and found to be similar to those described for the yeast, heart muscle and plant enzymes.

RÉSUMÉ

Une préparation enzymatique purifiée relativement stable, qui catalyse la formation d'acétyl coenzyme A à partir d'ATP, d'acétate et de CoA a été extraite de *Rhodospirillum rubrum*. L'AMP et le pyrophosphate sont des produits finaux et également des inhibiteurs de la réaction.

Les propriétés de ce système enzymatique sont décrites et sont semblables à celles des enzymes de la levure, du muscle cardiaque et des végétaux.

References p. 65.

ZUSAMMENFASSUNG

Von *Rhodospirillium rubrum* wurde eine relativ beständige Enzyme-Präparation erhalten, die die Bildung von Acetylcoenzym A aus ATP, Acetat und CoA katalysiert.

Es wurde gezeigt, dass AMP und Pyrophosphat Endprodukte und Hemmstoffe der Reaktion sind.

Die Eigenschaften des Enzymsystems wurden beschreiben und es wurde gefunden, dass sie den für Hefe-, Herzmuskel-und Pflanzenenzymen beschriebenen ähnlich sind.

REFERENCES

1 M. A. EISENBERG, *J. Biol. Chem.*, 203 (1953) 815.
2 F. LIPMANN, *J. Biol. Chem.*, 155 (1944) 55.
3 I. ROSE, M. GRUENBERG-MANAGO, S. KOREY AND S. OCHOA, *Fed. Proc.*, 13 (1954) 283.
4 D. NACHMANSOHN AND A. L. MACHADO, *J. Neurophysiol.*, 6 (1943) 397.
5 F. LIPMANN, *J. Biol. Chem.*, 160 (1945) 173.
6 N. O. KAPLAN AND F. LIPMANN, *J. Biol. Chem.*, 174 (1948) 37.
7 F. LIPMANN, M. E. JONES, S. BLACK, R. M. FLYNN, *J. Am. Chem. Soc.*, 74 (1952) 2384.
8 F. LYNEN, E. REICHERT AND L. RUEFF, *Ann.*, 574 (1951) 1.
9 H. BEINERT, D. E. GREEN, P. HELE, H. HIFT, R. W. VON KORFF AND C. V. RAMAKRISHAN, *J. Biol. Chem.*, 203 (1953) 35.
10 P. HELE, *J. Biol. Chem.*, 206 (1954) 671.
11 A. MILLERD AND J. BONNER, *Arch. Biochem. Biophys.*, 49 (1954) 343.
12 M. E. JONES, F. LIPMANN, H. HILZ AND F. LYNEN, *J. Am. Chem. Soc.*, 75 (1953) 3285.
13 E. J. SIMON AND D. SHEMIN, *J. Am. Chem. Soc.*, 75 (1953) 2520.
14 C. H. FISKE AND Y. SUBBAROW, *J. Biol. Chem.*, 147 (1943) 514.
15 M. KUNITZ, *J. Gen. Physiol.*, 35 (1952) 423.
16 A. KORNBERG, *J. Biol. Chem.*, 182 (1950) 779.
17 W. E. COHN AND H. E. CARTER, *J. Am. Chem. Soc.*, 72 (1950) 4273.
18 E. R. STADTMAN AND A. KORNBERG, *J. Biol. Chem.*, 203 (1953) 47.
19 E. R. STADTMAN, *Abstracts Am. Chem. Soc.*, 122, Meeting at Atlantic City, (September 1952) 32 C.
20 O. WARBURG AND W. CHRISTIAN, *Biochem. Z.*, 310 (1941) 384.
21 W. W. KIELLEY AND R. K. KIELLEY, *J. Biol. Chem.*, 191 (1951) 485.
22 S. P. COLOWICK AND H. M. KALCKAR, *J. Biol. Chem.*, 148 (1943) 117.
23 F. LIPMANN AND L. C. TUTTLE, *J. Biol. Chem.*, 159 (1945) 21.

Received August 2nd, 1954

THE STRUCTURE OF CILIA

by

BARBARA P. POTTS AND S. G. TOMLIN
Physics Department, University of Adelaide (South Australia)

The structure and mode of action of such fibrous organelles as cilia, flagella and sperm tails present extremely interesting biophysical problems. This paper gives the results of some investigations on the structure of cilia, using the electron microscope to examine them both whole and after thin sectioning. There are numerous publications on the electron microscopy of flagella and sperm tails, but they have usually been observed only after drying on to a collodion supporting film. This technique needs to be supplemented with electron micrographs of sectioned material, for only by this means is a reliable picture of the intact structure obtained.

The introduction of the shadow casting technique[1] so improved the results of electron microscopy that early electron micrographs of flagella were soon superseded. Among recent investigations that should be quoted are those of LEWIN AND MEINHART[2] on the flagella of *Chlamydomonas*, MANTON and co-workers[3,4,5,6,7,8,9,10] on plant cilia and flagella, and GRIGG AND HODGE[11,12] on fowl and human sperm tails. The structure of cilia has not been so extensively studied, but brief observations have been made by SCHMITT *et al*[13] on clam cilia, while ANDERSON[14], JAKUS AND HALL[15], and KRUGER AND WOHLFARTH-BOTTERMANN[16] have examined the cilia of *Paramecium*. These authors examined whole cilia dried on to collodion films. Recently WATSON[17] and CHALLICE[18] have obtained electron micrographs of sections of sperm tails in which their detailed structure can be seen, but published electron micrographs of sections of cilia have not been of high quality. While this paper was being written, a publication by FAWCETT AND PORTER[19] became available, in which sections of cilia showing fine structure are illustrated.

The observations of these authors on the structure of cilia from molluscs, amphibians and mammals, and of MANTON and co-workers[3,4,5,6,7,8,9,10] on plant cilia and flagella are in close accord with those to be presented here, on the structure of cilia from the protozoan, *Paramecium*, and from the gills of an Australian fresh water mussel, *Hyridella australis* (Lam.).

EXPERIMENTAL

Fresh water mussels, of the species *Hyridella australis*, were collected from the River Murray. Cilia were freed from the gills and labial palps by macerating for several days in distilled water or fixative. After this treatment the supernatant liquid contained a high concentration of unwanted cell debris and soluble material, from which a purified suspension of cilia, suitable for electron microscopy, was prepared by differential centrifugation.

An unidentified species of *Paramecium* was grown in an Osterhaut-vegemite culture medium[20], from which, after passing through a coarse filter, the organisms were separated by gentle centrifuga-

References p. 74.

tion. Light centrifuging several times in distilled water served to separate the cells from bacteria and other material, and harder centrifuging, or maceration in distilled water or fixative, freed sufficient numbers of cilia for examination in the electron microscope. The cilia from both sources were examined with and without fixation.

Specimens for the electron microscope were prepared in the usual way by drying a drop of the suspension on to a collodion supporting film, and shadow casting with palladium.

The technique for the preparation of thin sections was substantially that described by PALADE[21]. Pieces of gill from *Hyridella* were fixed for four hours in buffered osmic acid (pH 7.4) and embedded in *n*-butyl methacrylate containing 10–20% methyl methacrylate and 2% benzoyl peroxide for catalyst. *Paramecia* were carried through the same process using gentle centrifugation to effect the change of liquids. A microtome of the thermal expansion type[22] was used for cutting sections, which were then examined in the electron microscope while still embedded.

The electron microscope used for these investigations was a Philips instrument operated at 60 kilovolts. The magnification meter was calibrated against polystyrene latex particles.

RESULTS

Whole cilia

When detached from cells cilia are not seriously damaged as they appear to have a natural cleavage plane[19, 23]. Free, unbroken cilia could be distinguished by their slightly bulbous and denser bases.

Fig. 1 shows a group of cilia from the gills of *Hyridella* and Fig. 2 a single cilium from *Paramecium*. Most of the cilia detached from *Paramecium* were 9–12 μ long with diameter about 0.15 μ when intact and about 0.25 μ when more flattened. Those from *Hyridella* were 12–25 μ long with diameter 0.14–0.19 μ, the wide range of lengths probably being associated with the different types of cilia found on the ctenidia and labial palps. The cilia were of uniform diameter except for the base and tip regions, and frequently their fibrillar constitution could be seen (Fig. 1). The tip region of the cilia from *Paramecium* consisted of a tapering zone leading to the narrower tip. In many of the cilia from *Hyridella* the tip region was longer and narrower like a whiplash; some, however, possessed rather a tapering tip, while in others the whiplash terminated in a swollen region. Again these differences might be associated with the different types of cilia.

In over a hundred electron micrographs of the cilia from *Hyridella* there were no signs of an enveloping membrane, and some of the cilia from *Paramecium* presented much the same appearance. On the other hand, many of the cilia from *Paramecium*, especially when they had been fixed in osmic acid, were found to be surrounded by a wide, flat, low density structure (Fig. 2). In a number of cases the appearance of folds in this structure indicated clearly that it was a membrane. Although not shown in Fig. 2, this membrane sometimes extended to the tip, and frequently it appeared more swollen in one region, often at a bend in the cilium. In Fig. 3 the base of the cilium has apparently become twisted into a circular shape surrounded by a sac composed of the remnants of the sheath.

The cilia from *Hyridella* had a marked tendency to coil (Fig. 1) and, at the same time, they were often partly frayed. In order to determine whether the coiling was caused in drying, suspensions of cilia in water were examined with a phase contrast microscope. The cilia were found to have permanent configurations resembling those that had been seen in electron micrographs.

Occasional preparations from both *Hyridella* and *Paramecium* showed, without any apparent reason, more disintegration of the cilia than was normally found. The disintegration or fraying of the cilia from *Paramecium* into about eleven fibrils has been

References p. 74.

previously described[15]. In the present investigations a few cases of fraying were observed in which eleven or less fibrils could be counted. These examples were too few for general assertions to be made, but it was clear that two of the fibrils differed somwhat from the remainder by their close adherence and smaller diameter (Fig. 4). The remaining fibrils frequently lay together in a sheet or cylindrical formation (Fig. 4).

Similarly in *Hyridella* only a small proportion of the cilia completely frayed into their component fibrils. However, the large number of specimens examined and the enhancement of disintegration caused by treatment with alkaline 10% potassium chloride yielded a sufficient number of cases for some general observations to be made. A maximum number of eleven fibrils was found (Fig. 5), although quite often there were nine, or sometimes ten, in what appeared to be perfect examples of frayed cilia. As was found for *Paramecium*, two of these fibrils tended to adhere together and were of smaller diameter than the remainder, which tended to lie in sheet formations (Fig. 5). When the cilia had partly disintegrated, they were found to consist of a cylinder of fibrils surrounding a core of one or two fibrils (Fig. 6).

Figs. 6 and 7 show cilia from *Hyridella*, in which some substance appears to stretch between the fibrils. In a few instances, the fibrils of partially disintegrated cilia had regularly spaced ridges on them which suggested a cross striation. As this was observed only occasionally, and as the adhesivelike material already described gave almost the same appearance, the apparent striations may be only another manifestation of this substance between the fibrils. MANTON AND CLARKE[9] have observed somewhat similar effects in some plant flagella. No sign of a substance between the fibrils was found in the cilia from *Paramecium* but fewer specimens were examined.

Although the frayed fibrils of cilia from both *Hyridella* and *Paramecium* often had configurations suggestive of a very loose spiralling in the intact cilium, examination of intact or partially disintegrated cilia also showed the fibrils pursuing a straight and parallel course throughout the length of the cilium. Possibly the twisting of the fibrils could be produced during drying.

Individual fibrils were uniform in diameter which was in the range 350–500 A. Their appearance in cilia from both *Hyridella* and *Paramecium* was somewhat granular, and they showed a marked tendency to segment transversely (Figs. 4, 8 and 9). Some micrographs of more severely damaged cilia (Fig. 8) gave indications that the fibrils were themselves composed of finer sub-fibrils of the order of 50 A in diameter. Occasionally in the cilia from *Hyridella*, the fibrils also showed some signs of longitudinal segmentation into two or three parts (Fig. 9).

The effects of several reagents on the cilia from *Hyridella* were examined but did not yield any conclusive results regarding their composition. No recognizable remnants of cilia were found after digestion with trypsin, while they were unchanged by hyaluronidase digestion. They were completely dissolved by dilute hydrochloric acid and caustic soda, while ammonia and acetic acid produced a "blurring" of their structure as seen in electron micrographs. Slightly alkaline potassium chloride solutions were found to promote fraying and disintegration.

Sections of cilia

Sections of cilia from the cytopharynx of *Paramecium* and from the gills of *Hyridella* are illustrated in Figs. 10 and 11 respectively. Such electron micrographs showed very clearly the arrangement of the eleven fibrils, already described, within an enveloping

References p. 74.

membrane. This membrane differed somewhat in the two kinds of cilia. In the sections of *Paramecium* cilia it appeared as a very irregular structure, sometimes with prolongations of 1 μ or more in length, whereas the cilia from *Hyridella* had a less irregular membrane which was thinner, less osmiophilic and hence less conspicuous than that of *Paramecium*.

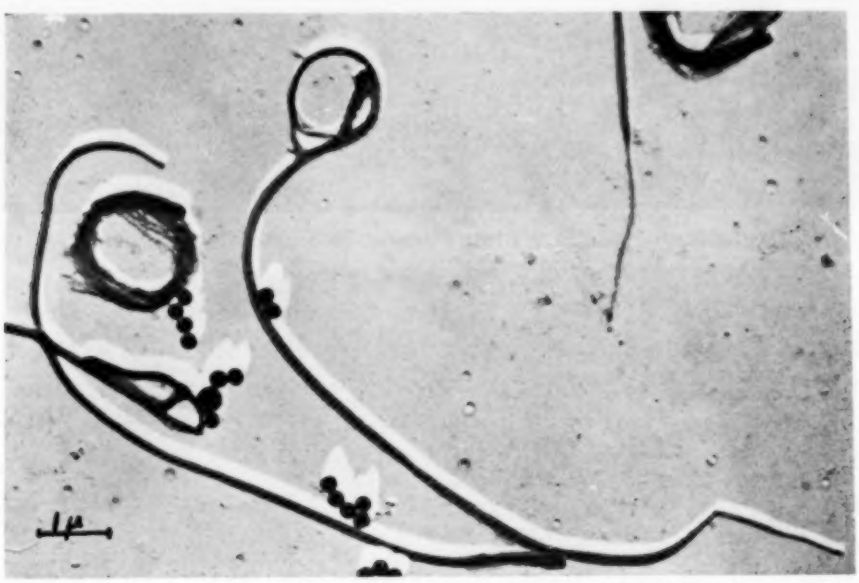

Fig. 1. A group of cilia detached from the gills of *Hyridella* (× 7,000).

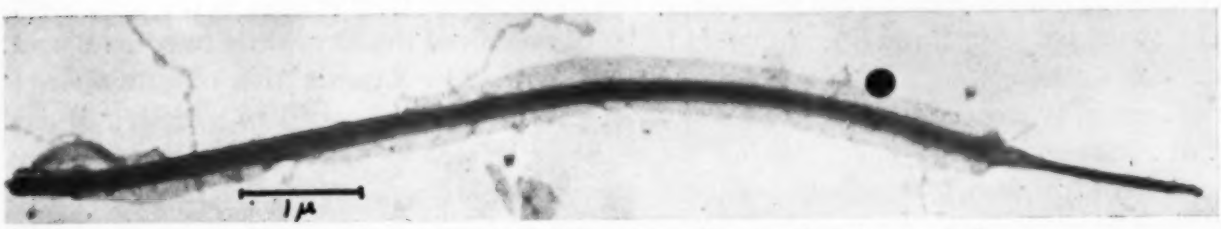

Fig. 2. A single detached cilium from *Paramecium* (× 13,000).

The thickness of the membrane for the latter varied from 100–200 A. The space around the fibrils within the membrane appeared to be occupied by some structureless substance of low density.

Both kinds of cilia showed the same fibrillar structure, namely a circular array of nine fibrils about a central pair. In a small minority of cilia it was not possible to count nine outer fibrils, but this was almost certainly due to disarrangement of the fibrils during processing; sometimes the inner pair of fibrils was not distinctly resolved.

There was no evidence that the fibrils had any kind of spiral organisation. In some longitudinal sections they were seen to follow a straight course over distances of 2–3 μ. Further, in cases where the orderly arrangement of the cilia had been preserved (Fig. 10) there was an obvious preferred orientation of the line joining the two central fibrils which would not be expected in sections cut at random if these fibrils twisted about each other.

Fig. 3. Portion of a partly coiled cilium from *Paramecium* (× 18,000).

References p. 74.

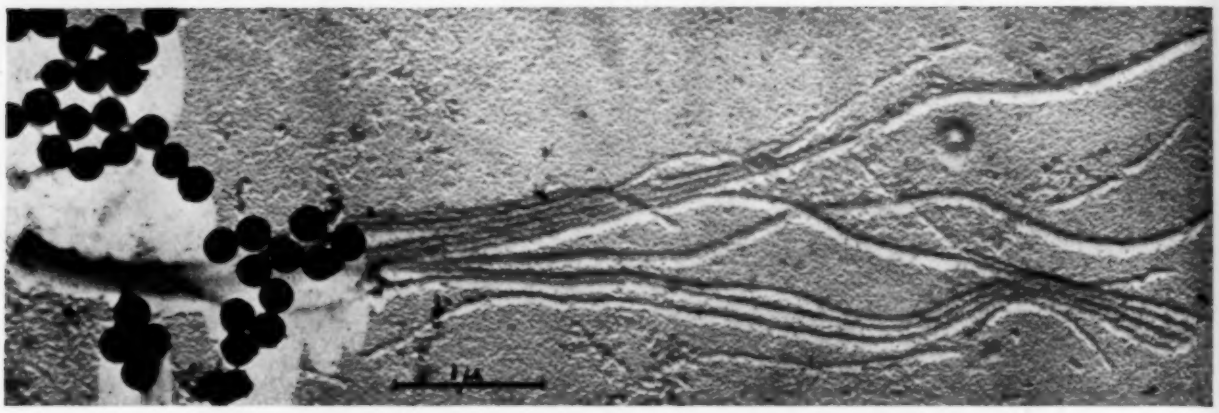

Fig. 4. Disintegration of a cilium from *Paramecium* into eleven fibrils. (× 16,000)

The diameter of the cross sections of cilia from *Hyridella* varied from about 0.12 μ to 0.24 μ while that of the fibrillar cylinder varied from about 0.1 μ to 0.2 μ. The diameter of many of the cilia from *Paramecium* was about 0.16 μ. Some much larger cilia of diameter about 0.25 μ (Fig. 10) were found, and some much smaller of diameter about 0.1 μ. The latter were probably sections through the tips of the cilia. The corresponding diameters of the fibrillar cylinder were 0.12 μ to 0.15 μ for the larger cilia and about 0.06 μ for the smaller ones.

Besides cross sections and oblique sections of cilia, Fig. 11 shows some cilia which are curved with respect to the plane of the section. Prominent features of the more longitudinally cut portions of such sections are the sharp, dense, double lines at the periphery. The space between these lines appears to be of enhanced density while in some places there is a trace of a third line adjacent to the dense pair. Examination of a number of such sections showed that these lines almost certainly corresponded to a section of one fibril. In one place in Fig. 11, two pairs of lines can be seen in the position corresponding to the central fibrils. Some of the fibrils at the ends of such sections, though cut more obliquely, also show a double-stranded character, although some appear to be composed of three strands. The oblique sections of cilia in Fig. 11 also show signs of this double-stranded appearance. Even when curved, the two lines always remain parallel, and the distance across them is about 200 A, the lines themselves being of the order of 50 A wide.

In cross sections the fibrils had a core considerably denser than the surrounding medium suggesting either that they were enveloped by a sheath or by material precipitated during fixation. (Fig. 10 and 11) In many cases their appearance also suggested a hollow structure, while occasionally they could be interpreted as double. The overall diameter of the fibrils was estimated to be 300–400 A but precise measurement was difficult. The inner core was about half this diameter.

DISCUSSION

It is clear from the work of a number of authors, and particularly of MANTON and her colleagues[3,4,5,6,7,8,9,10], and of FAWCETT AND PORTER[19], together with the results reported here, that many cilia and flagella (other than bacterial flagella) have essentially the same structural features. The fundamental pattern of structure is one of a cylindrical array of nine fibrils about a central pair. The central pair are narrower and more closely adherent than the peripheral fibrils, but all are parallel throughout the length of the cilium, with no convincing evidence for any spiral structure. Such appearances of a

References p. 74.

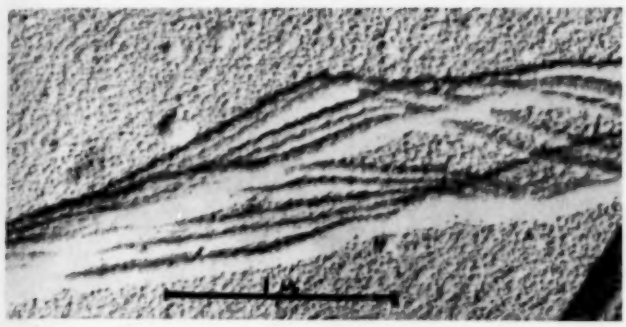

Fig. 5. Portion of a disintegrated cilium from *Hyridella* showing eleven component fibrils (× 25,000).

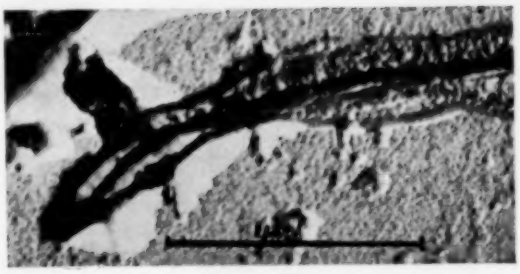

Fig. 6. Portion of a partly disintegrated cilium from *Hyridella* showing its cylindrical structure (× 28,000).

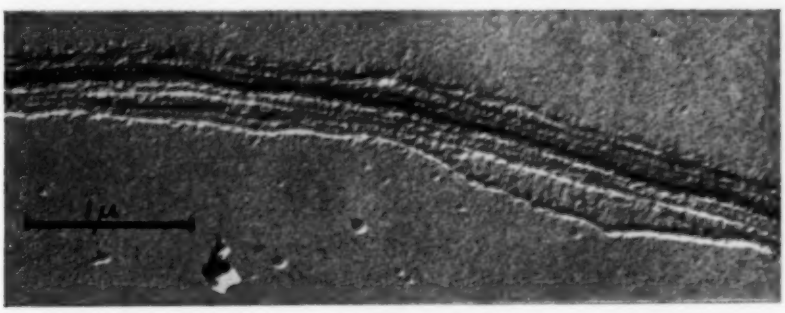

Fig. 7. Portion of a partly disintegrated cilium from *Hyridella* showing the presence of some material stretching between the fibrils (× 18,000).

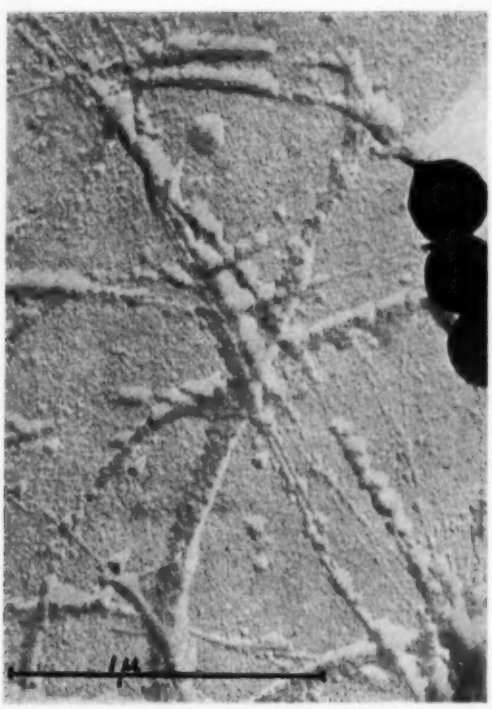

Fig. 8. Component fibrils from the cilia of *Hyridella* showing disintegration into a number of smaller subfibrils (× 34,000).

Fig. 9. Component fibrils of a cilium from *Hyridella* showing longitudinal cleavage into two or three parts (× 32,000).

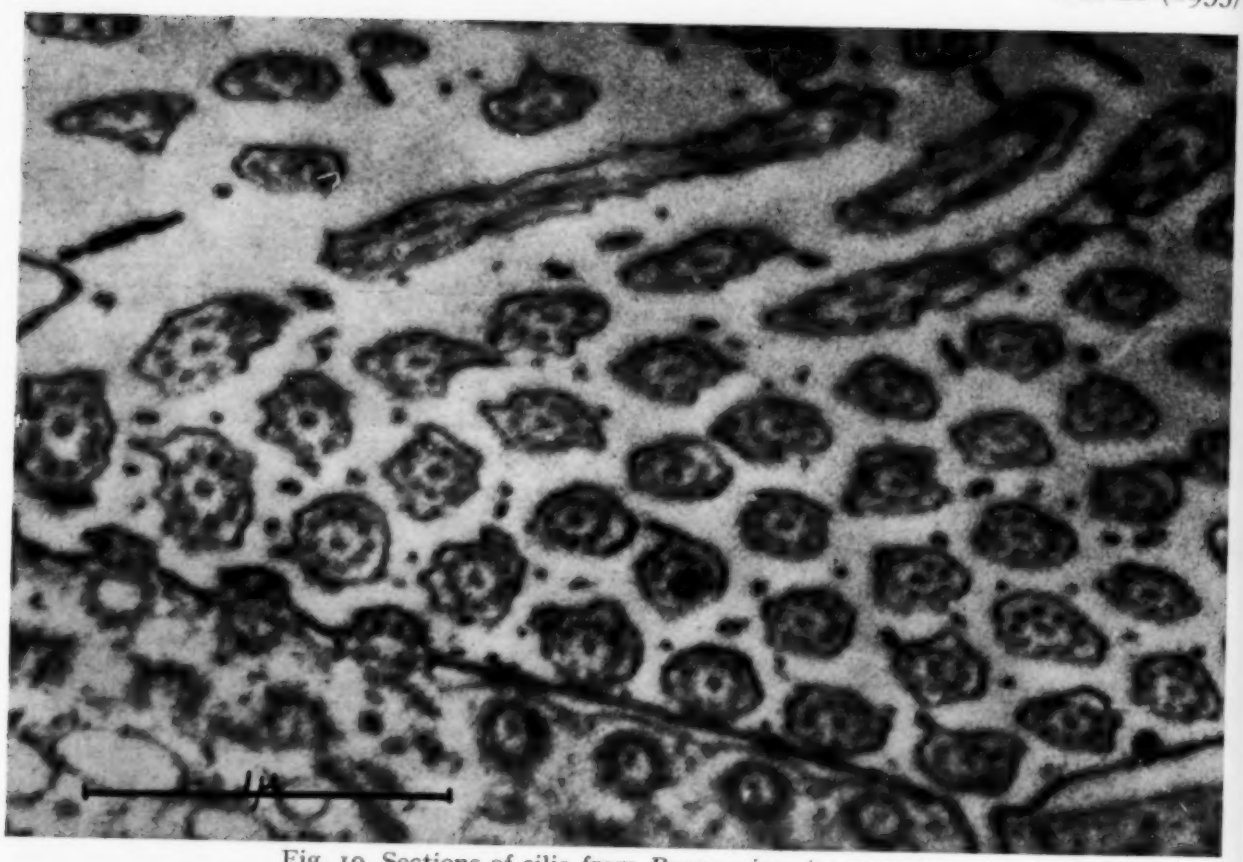

Fig. 10. Sections of cilia from *Paramecium* (× 40,000).

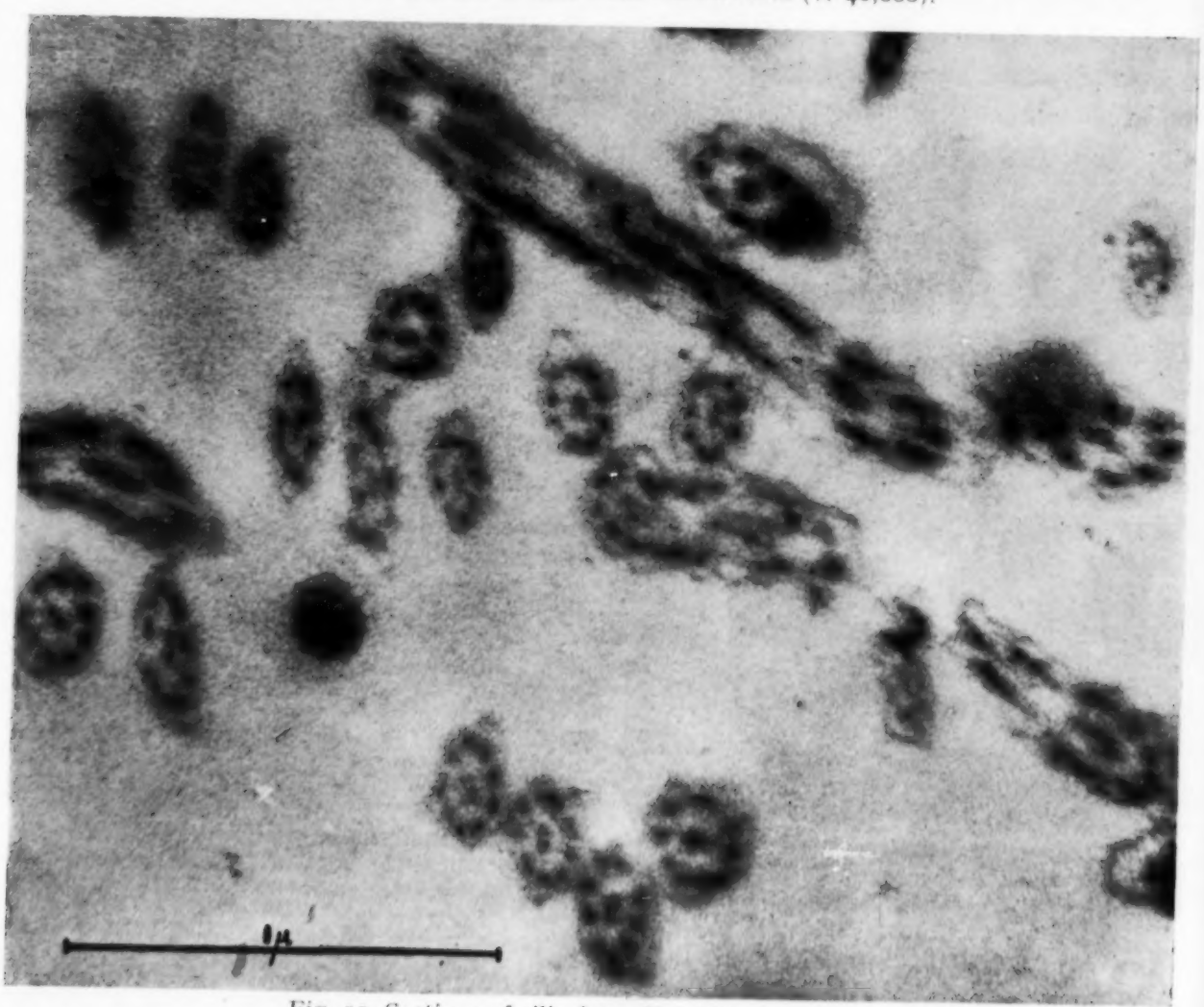

Fig. 11. Sections of cilia from *Hyridella* (× 50,000).

spiral arrangement as occur in micrographs of whole cilia may be discounted as the results of drying. The fibril system is surrounded by a thin membrane, the space within being occupied by a matrix, which, after fixation, appears as a precipitate of low electron optical density.

The main point for discussion concerns the nature of the peripheral fibrils, which are certainly composite in structure. The micrographs of frayed whole cilia usually show the nine fibrils as single threads, but occasionally as in Fig. 9 they are distinctly double or even triple. There is also evidence that extremely fine subfibrils of the order of 50 A in diameter are components of the major fibrils (Fig. 8). FAWCETT AND PORTER[19] have suggested that the appearance of fibrils from whole cilia is due to inadequate cleaning, but this seems unlikely because the fibrils themselves are of uniform diameter (Fig. 5). It is always in more damaged cilia that the composite structure of the fibrils is revealed most clearly. A more likely explanation of these observations is that the fibrils consist of a sheath of different composition surrounding the smaller units.

There is some indication of this sheath in cross sections of fibrils where the appearance of a central osmiophilic core surrounded by a less dense region is often given. None of these cross sections lead to an unequivocal picture of the complex structure of the fibrils, but the impression is often given of a hollow tubular core, or occasionally a double structure is suggested. On the other hand from some of the longitudinal and very oblique sections (Fig. 11) a clearer picture emerges. If, as suggested by FAWCETT AND PORTER[19], the outer fibrils do consist of a pair of tubular structures in contact, longitudinal or oblique sections might be expected to show two or three lines corresponding to the walls of the tubules. This is precisely what is shown in Fig. 11. However, it may be doubted that the tubular appearance is real, for it may be an artifact arising from the fixing or embedding processes. WYCKOFF[24] has obtained sections of collagen showing fibres which appear to be tubes, and in this laboratory it has been found that the embedding process often results in distension of bacteria. Be this as it may, it seems quite certain from such sections that the nine outer fibrils have each a double stranded structure. Whole fibrils show indications of breakdown into very fine units, and both whole and sectioned fibrils appear to be surrounded by a sheath of different composition.

It is a striking fact that cilia, flagella and sperm tails from so many diverse sources should have the same basic fibrillar structure, and it is interesting to speculate on the occurrence of the cylindrical array of nine fibrils. In sections these appear to be rather widely spaced, but it is not clear that this represents the state of affairs in the living cilium where they might be more closely packed. If this were so, the occurrence of nine fibrils might reflect some property of their molecular symmetry. If, on the other hand, the fibrils are really as widely spaced as their sections suggest, it is not clear what preserves the observed structure unless there is some transverse connection between the fibrils or some fairly adhesive material which holds them in place.

ACKNOWLEDGEMENTS

This work was carried out while one of the authors (B.P.P.) held a Commonwealth Scientific and Industrial Research Organization Australian Studentship. The authors wish to thank the staff of the Zoology Department, University of Adelaide, for assistance in collecting mussels and for supplying a culture of *Paramecium*.

References p. 74.

SUMMARY

The structure of cilia from *Paramecium* and from the gills of an Australian bivalve, *Hyridella australis* (Lam.), has been studied by means of electron microscopy. Both whole isolated cilia and sections of cilia have been examined and their fine structure elucidated. This fine structure is similar in both types examined, and appears to be of remarkable uniformity whatever the source of cilia. The fundamental pattern is that of a cylindrical array of nine parallel fibrils and a pair of axial fibrils. Each of the fibrils is itself a complex structure.

RÉSUMÉ

La structure des cils de *Paramécie* et des branchies d'un bivalve Australien, *Hyridella australis* (Lam.), a été étudiée au microscope électronique. Des cils entiers isolés et des sections de cils ont été examinés et leur structure fine élucidée. Cette structure fine est semblable chez les deux types examinés, et se montre d'une remarquable uniformité quelque soit l'origine des cils. Le chéma fondamental est celui d'un arrangement cylindrique de neuf fibrilles parallèles et d'une paire de fibrilles axiales. Chaque fibrille possède elle-même une structure complexe.

ZUSAMMENFASSUNG

Es wurde die Struktur der Cilien von *Paramaecien* und von den Kiemen einer australischen Muschel, *Hyridella australis* (Lam.), mit dem Elektronenmikroskop untersucht. Es wurden ganze isolierte Cilien und Schnitte von Cilien untersucht und ihre Feinstruktur aufgeklärt. Diese Feinstruktur ist für beide untersuchten Typen ähnlich und scheint von bemerkenswerter Einheitlichkeit zu sein woimmer die Cilien herstammen. Der grundlegende Bauplan ist der einer zylindrischen Anordnung von neun parallelen Fibrillen und einem Paar axialer Fibrillen. Jede der Fibrillen selbst besitzt eine komplexe Struktur.

REFERENCES

1 R. C. Williams and R. W. G. Wyckoff, *J. Applied Physics*, 17 (1946) 23.
2 R. A. Lewin and J. O. Meinhart, *Canad. J. Bot.*, 31 (1953) 711.
3 I. Manton and B. Clarke, *J. Exp. Bot.*, 2 (1951) 125.
4 I. Manton and B. Clarke, *Ann. Botany (London)*, 15 (1951) 461.
5 I. Manton and B. Clarke, *J. Exp. Bot.*, 2 (1951) 242.
6 I. Manton, B. Clarke and A. D. Greenwood, *J. Exp. Bot.*, 2 (1951) 321.
7 I. Manton, *Soc. Exp. Biol. Symp.*, 6 (1952) 306.
8 I. Manton, B. Clarke, A. D. Greenwood and E. A. Flint, *J. Exp. Bot.*, 3 (1952) 204.
9 I. Manton and B. Clarke, *J. Exp. Bot.*, 3 (1952) 265.
10 I. Manton, B. Clarke and A. D. Greenwood, *J. Exp. Bot.*, 4 (1953) 319.
11 G. W. Grigg and A. J. Hodge, *Aust. J. Sci. Res.*, ser. B., 2 (1949) 271.
12 A. J. Hodge, *Aust. J. Sci. Res.*, ser. B., 2 (1949) 368.
13 F. O. Schmitt, C. E. Hall and M. A. Jakus, *Biol. Symp.*, 10 (1943) 261.
14 T. F. Anderson, cited by R. Wichterman, *The Biology of Paramecium*, The Blakiston Co. Inc., N.Y., 1953.
15 M. A. Jakus and C. E. Hall, *Biol. Bull.*, 91 (1946) 141.
16 F. Kruger and K. E. Wohlfarth-Bottermann, *Mikroskopie*, 7 (1952) 121.
17 M. L. Watson, *Biochim. Biophys. Acta*, 10 (1953) 1.
18 C. E. Challice, *J. Roy. Microscop. Soc.*, 73 (1953) 115.
19 D. W. Fawcett and K. R. Porter, *J. Morph.*, 94 (1954) 221.
20 B. A. Humphrey and G. F. Humphrey, *Br. J. Exp. Biol.*, 25 (1948) 123.
21 G. E. Palade, *J. Exp. Med.*, 95 (1952) 285.
22 A. J. Hodge, H. E. Huxley and D. Spiro, *J. Histochem. and Cytochem.*, 2 (1954) 54.
23 L. G. Worley, E. Fischbein and J. E. Shapiro, *J. Morph.*, 92 (1953) 545.
24 C. Ragan, *Connective Tissues*, Trans. Third Conf. Josiah Macy Fn, N.Y., 1952.

Received August 4th, 1954

THIAMINE PYROPHOSPHATASE, ACID AND ALKALINE PHOSPHATASE ACTIVITY IN THE CHICKEN BRAIN IN VITAMIN B_1 DEFICIENCY

by

D. NAIDOO AND O. E. PRATT

Institute of Psychiatry (British Postgraduate Medical Federation, University of London), Maudsley Hospital, London (England)

SHIMIZU, HANDA, HANDA AND KUMOMOTO[1] examined nervous tissue of thiamine-deficient pigeons in respect to both alkaline and acid phosphatases. Acetone fixed tissue showed that thiamine-deficient nerve cells "acquired increased amounts of alkaline phosphatase" whereas "acid phosphatase of the axis cylinders and cytoplasm of the nerve cells is diminished in amount". There has been much criticism of the acid phosphatase technique when chemically fixed tissue is used particularly since loss in activity may be considerable[2,3,4,5], and since results with nervous tissue may be variable[5,6]. It is now generally agreed that freeze-drying methods are to be preferred for histological enzyme study. Further, NAIDOO AND PRATT[7] demonstrated a specific enzyme in rat brain splitting inorganic phosphate from thiamine pyrophosphate. This was active in both the acid and alkaline ranges. At pH 9.1 thiamine pyrophosphatase was present in different histological sites from the non-specific alkaline phosphatase. In the acid range, however, although the sites of activity of the thiamine pyrophosphatase were histologically similar to those of the non-specific acid phosphatase, these enzymes were functionally distinguishable by their differences in activation and inhibition.

It was considered that a study of the distribution and activity of thiamine pyrophosphatase and of the non-specific acid and alkaline phosphatases in frozen-dried nervous tissue from thiamine-deficient chickens was necessary to confirm and extend the findings of SHIMIZU, HANDA, HANDA AND KUMOMOTO[1]. This paper illustrates the histochemical findings and compares the activity of these enzymes in normal and in thiamine-deficient brain.

EXPERIMENTAL

Management of Birds. Day-old Rhode Island Red cockerels obtained from an accredited commercial hatchery were housed in an electrically heated Hover-Brooder. The brooder temperature was set at first at 35° C and progressively reduced during the first three weeks to room temperature which was maintained at 22° by thermostatically controlled steam heaters. The room was well lit by daylight. The birds were kept on a wire mesh floor, the droppings falling onto metal trays which were cleaned out twice weekly. Clean drinking water was provided and during the first three weeks a commercial baby chick mash (Spillers Ltd., London) was allowed without restriction.

At the end of the third week all weaklings or abnormal birds were rejected and the remainder was divided into two similar groups in respect of weight. The two groups were placed in smaller adjacent cages and the points of their upper beaks blunted by clipping in order to prevent feather

References p. 81.

pecking. The commercial mash was withheld and the birds fed on a synthetic diet which was mixed with water to a thick creamy consistency and introduced directly into the crop. The feeding was carried out twice daily, at 9 and 17 hours approximately, with a metal syringe of a type normally used to apply ornamental icing to cakes. The diet was prepared by grinding the mixture through a fine metal seive and mixing 100 g with 100 ml of water. A 12 cm length of rubber tubing (external diameter 6 mm, internal diameter 3 mm) was attached to the nozzle of the syringe, moistened and passed down the oesophagus into the crop. The bird was held in the left hand with the first two fingers placed upon the crop and the food mixture injected until the crop was palpably full. The birds were allowed to feed freely on a mixture of gelatin and cellulose powder.

Each bird in the control group received every second day an intramuscular injection containing 100 μ of thiamine in saline. All birds were weighed daily immediately before the morning feed. Four sets of 12 birds each were used in this work. The synthetic diet was a modification of that of COATES, KON AND SHEPHEARD[8], omitting the thiamine. The constituents were as shown in Table I.

TABLE I

COMPOSITION OF SYNTHETIC DIET

Dextrin	1200 g
Casein (B.D.H. vitamin free)	360 g
Mixed salts IV	100 g
(HEGSTED, MILLS, ELVEHJEM AND HART[9])	
$CaHPO_4$	20 g
Cystine	6 g
Inositol	2 g
Sulphite treated liver extract[10]	15 ml
Lard	100 g
Cod liver oil	20 g
Heptane extract from 60 g dried grass	
Choline chloride	3 g
Riboflavin	12 mg
Ca pantothenate	30 mg
Pyridoxin	8 mg
Nicotinamide	100 mg
2-Methyl-1:4-naphthoquinone	100 mg

The solid constituents were first ground. The last six items were dissolved in 25 ml 90% aqueous ethanol. The lard, cod liver oil and grass extract were mixed together and added to a little dextrin before incorporation with the bulk of the solid constituents. The liver extract and the alcoholic solution of vitamins were added to the mixture in a similar manner.

Each bird received 35–50 g daily of the diet mixture when forced feeding was started. The birds given the thiamine supplement continued to receive this quantity of diet daily throughout the experiment but the birds not given thiamine received less of the diet mixture towards the end of the experiment, owing to delayed emptying of the crop. Manipulation of the crop did not appear to hasten its emptying. The birds were killed when the weight had fallen sharply and they were unable to stand or hold their heads up. When placed on their backs they were unable to right themselves.

The activity of acid and alkaline phosphatases was estimated by inorganic phosphate liberation from glycerophosphate by suspensions of tectum ground in saline, as previously described[11]. The histological distribution of these enzymes was studied in sections prepared from frozen dried blocks of tissue as described elsewhere[7,12]. A modified medium was employed for the study of thiamine pyrophosphatase as follows:

	Assay medium M	*Histological medium* M
Medinal buffer (pH 8.7)	0.025	0.025
$MgCl_2$	0.020	0.020
$CaCl_2$	0.025	0.100
Thiamine pyrophosphate	0.008	0.008

References p. 81.

The substrate was added immediately before use and the final pH was 8.4 (as measured by a glass electrode). For quantitative estimation of activity, the medium included sufficient tissue suspension to give 1 mg of fresh tissue/ml.

RESULTS

The first difference seen between the two groups was a greater increase in weight of the thiamine supplemented group. Weakness of leg and neck muscles appeared first in two birds of the deficient group on the eleventh day but two did not show these symptoms until the twenty-fourth day. Enzyme activity found in suspensions prepared from the tectum of birds with and without the thiamine supplement are given in Table II. The acid or alkaline phosphatase activity did not appear to be related to the duration of the experimental feeding period, but the thiamine pyrophosphatase activity tended to fall with increasing survival on the experimental diet in both the deficient and the thiamine supplemented groups. Table III compares the mean enzyme activity of each group and shows that there was a significant increase in the alkaline phosphatase and thiamine pyrophosphatase but no significant change in acid phosphatase activity.

TABLE II

ACID AND ALKALINE PHOSPHATASE AND THIAMINE PYROPHOSPHATASE ACTIVITY IN NORMAL AND THIAMINE-DEFICIENT CHICKEN TECTUM

At 21 days of age all animals were fed the diet of Table I. One series received in addition regular thiamine injections. Deficient birds were killed when nervous symptoms were severe and controls were sacrificed at similar intervals.

Chicken No.	*Duration of experiment days*	*Change in weight g*	*Acid phosphatase units*	*Alkaline phosphatase units*	*Thiamine pyrophosphatase units*
		Basal diet + Thiamine			
99	15	+ 210	—	81	—
100	18	+ 212	26	80	59
111	21	+ 247	50	70	45
101	22	+ 270	46	65	58
102	23	+ 262	39	—	34
103	23	+ 243	37	74	—
104	24	+ 261	40	—	39
112	25	+ 287	—	—	37
113	25	+ 305	44	78	34
114	26	+ 301	46	71	38
		Basal diet only			
93	13	+ 23	40	131	65
105	15	— 13	33	119	76
94	15	— 21	38	115	63
95	18	+ 20	40	120	108
96	21	+ 14	43	107	68
97	22	— 21	42	89	34
107	22	— 10	49	—	47
98	23	— 12	40	—	44
108	25	— 28	53	—	49
109	26	— 3	—	112	52

References p. 81.

TABLE III

COMPARISON OF MEAN ENZYME ACTIVITY IN TECTUM WITH AND WITHOUT THIAMINE

Enzyme	*Thiamine*		*No thiamine*		*P-value of difference of means*
	No. expts	*Mean units*	*No. expts*	*Mean units*	
Acid phosphatase	8	41.0	9	42.0	> 0.3
Alkaline phosphatase	7	74.1	7	113.3	< 0.001
Thiamine pyrophosphatase	8	43.0	10	60.6	< 0.05

Histological. Nissl and myelin preparations of the deficient brain did not show any histological abnormality. Sections of optic tectum incubated with glycerophosphate at pH 5.3 showed no differences of staining between the normal and thiamine-deficient at incubation periods of up to 2 hours (Fig. 1 and 2). In the alkaline range at pH 9.1 definite differences of activity and distribution were evident in sections incubated for different intervals up to 2 hours. The deficient tectum showed an increase in the activity of the stratum opticum and the subjacent outer layers (Fig. 4). In the inner layers nuclei of the neurones showed moderate staining. In the layers overlying the ependyma staining was deep. In the normal control (Fig. 3) no nuclei could be made out on microscopy and the outer layer immediately below the stratum opticum stained comparatively lightly. None of the zones of the tecta showed capillary endothelial staining. The neuropile between inner layers was lighter in the deficient brain. In the sections incubated with thiamine pyrophosphate, the deepest stained layer was the stratum opticum in both control (Fig. 5) and experimental (Fig. 6) tissues. In the other layers staining of the nerve cell bodies was moderately deep in the normal, but considerably deeper in the deficient bird. The neuropile in the deficient tectum was darker than that in the control.

DISCUSSION

The synthetic thiamine-deficient diet makes possible controlled feeding of measured amounts of a diet of known constitution which is adequate for normal growth when supplemented with thiamine.

In the later stages in the experimental group delayed emptying of the crop, a phenomenon possibly inseparable from thiamine deficiency, probably accounted for some degree of inevitable interference with general nutrition. But, since crop stasis is not severe until general paralysis is so pronounced that the birds are sacrificed, it appears unlikely that the effects of this under-nutrition will complicate the picture of thiamine deficiency.

Alkaline phosphatase in the normal chicken brain appears to be much more active than in rat brain[13]. Chicken brain thiamine pyrophosphatase differs in some respects from the enzyme previously studied in rat brain[7,14]. The rat enzyme shows high activity over a wide range of H^+ concentration, including both pH 6.9 and 9.1, but the chicken enzyme only acts over a narrower range close to pH 8.4. The latter enzyme is activated only by Mg^{+2}, whereas the rat thiamine pyrophosphatase can be activated by either Ca^{+2} or Mg^{+2}. The activity of this enzyme tends to fall with survival of the birds, even in the group fed on a thiamine-supplemented diet. This finding suggests that the activity of this enzyme may alter with maturation of the nervous system.

References p. 81.

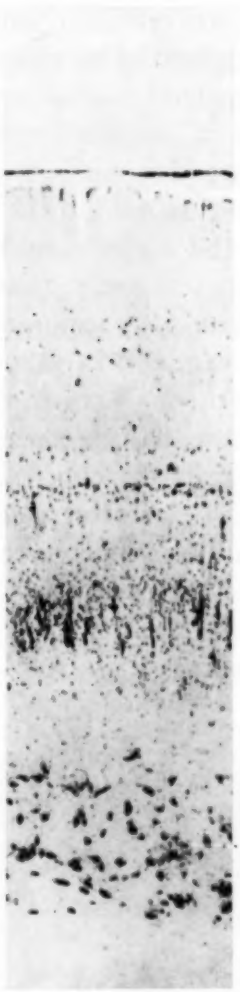

Fig. 1. × 80. Glycerophosphate substrate pH 5.3 (supplemented diet). Showing deep staining of the nerve cell and glial element throughout all layers.

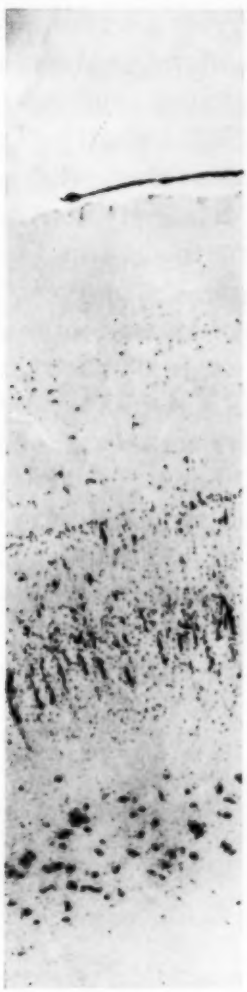

Fig. 2. × 80. Glycerophosphate substrate pH 5.3 (deficient diet). Showing no differences between cytological findings in deficient and supplemented diets.

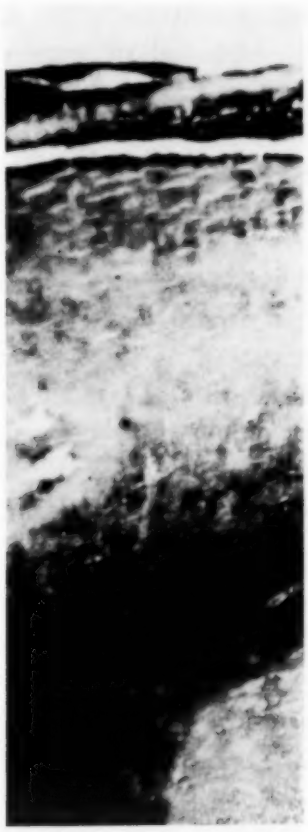

Fig. 3. × 80. Glycerophosphate substrate pH 9.1 (supplemented diet). Lightly stained outer layer and no nuclei present.

Measurement of enzyme activity clearly shows differences between the deficient and the control groups. There is a significant increase in the activity both of alkaline phosphatase and of thiamine pyrophosphatase in the thiamine-deficient brains, but no significant changes in acid phosphatase activity. The optic tectum is chosen for histological study as it is clearly laminated and changes can be described in terms of the intensity of staining of the distinct layers. The changes in the staining are consistent with the measured increase in alkaline phosphatase and in thiamine pyrophosphatase activity. The quantitative results therefore confirm the histological findings.

The change in alkaline phosphatase activity is in agreement with the findings of SHIMIZU, HANDA, HANDA AND KUMOMOTO[1], but the fall in acid phosphatase activity described by these authors is not seen in the present work. It should be noted that the frozen-dried chicken tectum shows little acid phosphatase activity in axons or dendrites, unlike the chemically fixed pigeon brain studied by SHIMIZU, HANDA, HANDA AND KUMOMOTO[1]. An explanation of this disagreement may lie in the different methods of tissue preparation, or in the probability that brain acid phosphatase activity represents more than one enzyme, as reported by LOWRY, ROBERTS, WU, HIXON AND CRAWFORD[15].

References p. 81.

Thiamine pyrophosphate undergoes a series of reversible and irreversible changes in alkaline solution[16]. If sufficient breakdown products accumulate during the incubation of the chicken brain sections at pH 8.4 suitable substrates may be provided for alkaline phosphatase action. However, not more than a small part of the increase in thiamine pyrophosphatase activity in the deficient chicken brain is likely to be accounted for in this manner.

Although in acute vitamin B_1 deficiency no structural changes are seen in the brain by the usual histological staining methods, small haemorrhages and a glio-mesodermal reaction may be found in the tecta, in the periventricular grey matter, and particularly in the mamillary bodies of chronic deficient animals. The changes in enzyme activity may possibly be a sequel to this tissue damage but the tecta examined in this study showed no evidence of histological abnormality by ordinary methods. Moreover, it is difficult to explain on this basis why activity should increase rather than decrease, and it is surprising that there is no change in acid phosphatase activity, especially as activation of this enzyme has been reported after axon section[17,18] or after electrical stimulation[19]. It has been found that alkaline phosphatase and thiamine pyrophosphatase activity does not undergo rapid changes post-mortem[13]. It seems unlikely that the changes in alkaline phosphatase and thiamine pyrophosphatase activity can be due to destruction of the tissue but rather to a more specific metabolic injury.

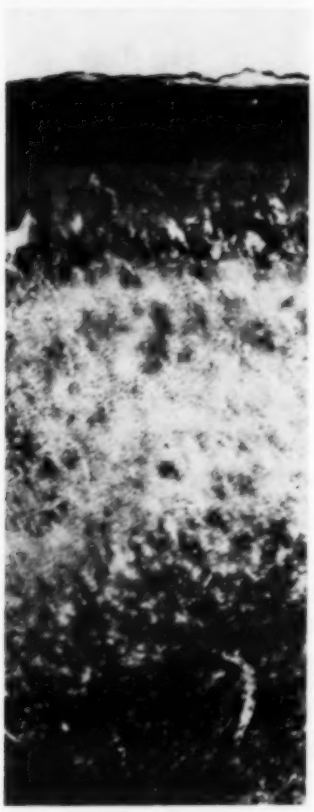

Fig. 4. × 80. Glycerophosphate substrate pH 9.1 (deficient diet). Deeply staining outer layers and nuclei present.

Fig. 5. × 80. Thiamine pyrophosphate substrate pH 8.4 (supplemented diet). Deeply staining stratum opticum and light neuropile with faintly staining nuclei.

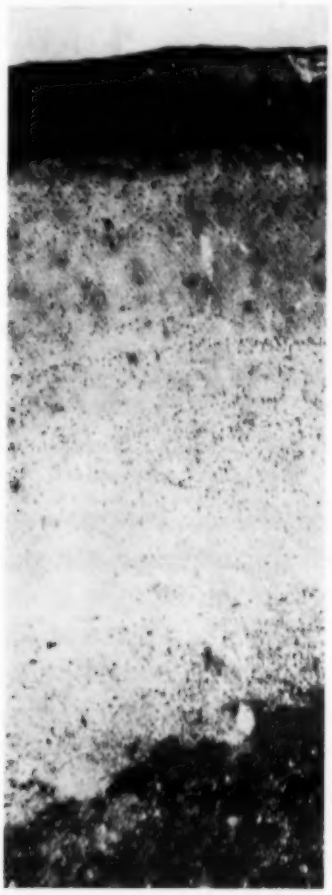

Fig. 6. × 80. Thiamine pyrophosphate substrate pH 8.4 (deficient diet). Deeply staining stratum opticum with moderately staining neuropile and more darkly staining cell bodies.

References p. 81.

ACKNOWLEDGEMENTS

We wish to thank Professor A. MEYER and Dr. H. MCILWAIN for their continued support and the Mapother Bequest (Medical Research Council) and the Bethlem and Maudsley Research Fund for financial assistance. Technical assistance was most efficiently rendered by Miss MOLLIE READ.

SUMMARY

1. The overall activity and the histological distribution of thiamine pyrophosphatase, of acid and alkaline phosphatases have been studied in nervous tissue of the normal and of the thiamine-deficient chicken.

2. A Mg^{+2}-activated thiamine pyrophosphatase with optimal activity about pH 8.4 is present in chicken brain in addition to the acid and alkaline phosphomonoesterases.

3. In the optic tectum of thiamine-deficient chickens there is a significant increase in the activity of the thiamine pyrophosphatase and of alkaline phosphatase, but no significant change in the activity of the acid phosphatase.

RÉSUMÉ

1. L'activité totale et la répartition histologique de la thiamine pyrophosphatase et des phosphatases acide et alcaline ont été étudiées dans le tissu nerveux du poulet normal et du poulet carencé en thiamine.

2. Outre les phosphomonoestérases acide et alcaline, le cerveau du poulet renferme une thiamine pyrophosphatase, activée par le Mg^{+2} et dont le pH optimum est d'environ 8.4.

3. Dans le tectum optique de poulets carencés en thiamine, on observe une augmentation significative de l'activité de la thiamine pyrophosphatase et de la phosphatase alcaline, mais aucune modification de l'activité de la phosphatase acide.

ZUSAMMENFASSUNG

1. Die Gesamtaktivität und die histologische Verteilung der Aneurinpyrophosphatase, der sauren und der alkalischen Phosphatasen wurden im Nervensystem der normalen und der an Aneurin-Mangel leidenden Küken untersucht.

2. Eine durch Mg^{++}-aktivierte Aneurinpyrophosphatase mit optimaler Aktivität bei pH 8.4 ist im Gehirn der Küken noch ausser der sauren und alkalischen Phosphomonoesterasen vorhanden.

3. Im Tectum des Mittelhirns der an Aneurinmangel leidenden Küken ist eine bemerkenswerte Zunahme der Aktivität der Aneurinpyrophosphatase und der alkalischen Phosphatasen aber keine besondere Veränderung in der Aktivität der sauren Phosphatasen zu beobachten.

REFERENCES

1 N. SHIMIZU, Y. HANDA, J. HANDA AND T. KUMOMOTO, *Proc. Soc. Exptl. Biol. Med.*, 75 (1950) 696.
2 R. O. STAFFORD AND W. B. ATKINSON, *Science*, 107 (1948) 279.
3 W. L. DOYLE, *Proc. Soc. Exptl. Biol. Med.*, 69 (1948) 43.
4 M. BERENBOM, H. O. YOKOYAMA AND R. E. STOWELL, *Proc. Soc. Exptl. Biol. Med.*, 81 (1952) 125.
5 M. RABINOVITCH, L. C. JUNQUIERA AND A. FAJER, *Stain. Tech.*, 24 (1949) 147.
6 A. M. LASSEK, *Stain. Tech.*, 22 (1947) 133.
7 D. NAIDOO AND O. E. PRATT, *Enzymologia.*, 16 (1953) 91.
8 M. E. COATES, S. K. KON AND E. E. SHEPHEARD, *Brit. J. Nutr.*, 4 (1950) 199.
9 D. M. HEGSTED, R. C. MILLS, C. A. ELVEHJEM AND E. B. HART, *J. Biol. Chem.*, 138 (1941) 459.
10 *U.S. Pharmacopoeia*, XIII (1947) 704.
11 O. E. PRATT, *Biochem. J.*, 55 (1953) 140.
12 D. NAIDOO AND O. E. PRATT, *J. Neurol. Neurosurg. Psychiat.*, 14 (1951) 287.
13 D. NAIDOO AND O. E. PRATT, *Enzymologia* (in press).
14 O. E. PRATT, *Biochem. J.*, 56 (1954) iii.
15 O. H. LOWRY, N. R. ROBERTS, M. WU, W. S. HIXON AND E. J. CRAWFORD, *J. Biol. Chem.*, 207 (1954) 19.
16 T. MATSUKAWA AND S. YURUGI, *Science*, 118 (1953) 109.
17 D. BODIAN AND R. C. MELLORS, *Proc. Soc. Exptl. Med.*, 55 (1945) 243.
18 D. BODIAN AND R. C. MELLORS, *J. Exp. Med.*, 81 (1945) 469.
19 W. M. HARD AND A. M. LASSEK, *J. Neurophysiol.*, 9 (1946) 121.

Received September 3rd, 1954

FURTHER OBSERVATIONS ON THE ELECTRON MICROSCOPE CHANGES FOLLOWING INDUCTION OF *E. COLI* K12

by

R. H. GORRILL AND C. E. CHALLICE

The Wright-Fleming Institute of Microbiology, St. Mary's Hospital Medical School, London (England)

In a previous paper[1] it was shown that induction of lysogenic *E. coli* K12 was accompanied by the production of many long forms of bacterial cell together with debris resembling collapsed spheres. These spheres are of interest as they have not been recorded when bacteria are lysed by virulent bacteriophage. This paper records our investigation into the relationship between sphere production and induction.

In order to carry out this work use was made of the fact that *E. coli* K12 can be cured of lysogenicity and then becomes an indicator for the phage lambda. Such cured strains have been used to determine the position of the prophage in the bacterial chromosome by crossing cured with lysogenic cultures[2,3].

It should be stated that all the cured strains used in this work were either obtained from Dr. E. L. WOLLMAN of the Pasteur Institute, Paris or produced by one of us (RHG) during his tenure of an Anglo-French exchange bursary at the Pasteur Institute. Cured strains of K12 can usually be reinfected with phage λ and returned to their original lysogenic state. During the process of curing a number of strains are isolated carrying a mutant of λ. Amongst these mutants some are no longer inducible in the sense that irradiation is not followed by lysis although they often show a rise in free phage count under these conditions. As well as being non-inducible some also show a difference in plaque morphology. That the K12 host is still infected with a λ phage and not a contaminant is shown by the fact that the cultures are immune to λ but are sensitive to the virulent mutant described by JACOB AND WOLLMAN[4]. Using these various strains of K12 it was possible to examine the effect of ultraviolet light on cured strains, reinfected strains and strains carrying a mutant of λ. This has allowed us to demonstrate the close relationship between induction and sphere formation.

METHODS

All technical methods were as described in the earlier paper[1]. Bacterial strains used were:

(a) K12 S a cured culture of wild type K12.

(b) K12[1] a reinfected culture of K12 S.

(c) W677[1] and[7] two cured strains of W677.

(d) W705 SR21 carrying a mutant of λ, not inducible showing a small increase in free phage on irradiation, and giving a tiny plaque.

(e) *E. coli B.* as representative of a non lysogenic coliform which has been previously studied under the electron microscope[5].

References p. 86.

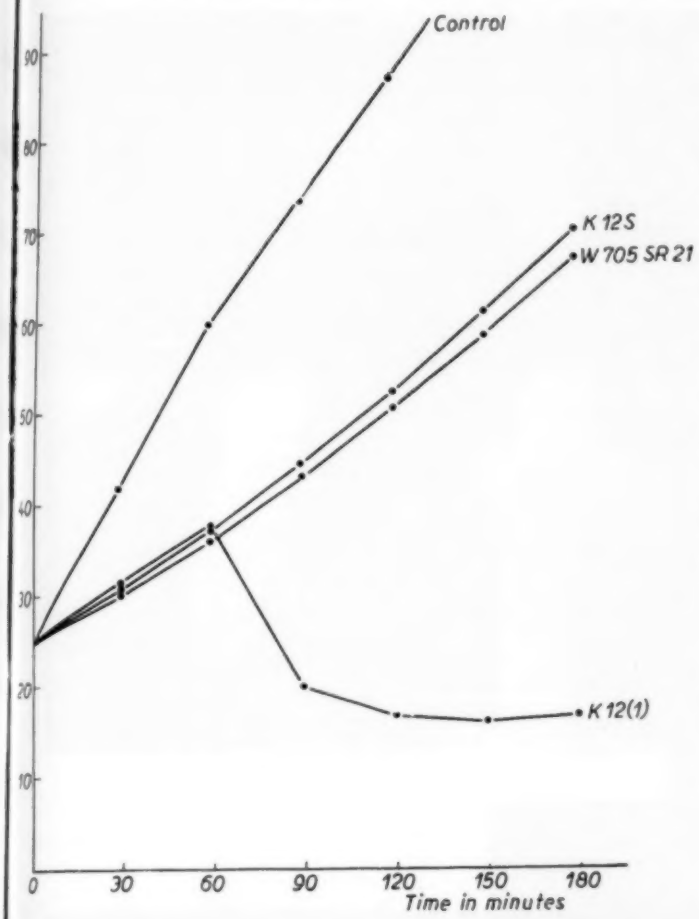

RESULTS

In Fig. 1 is shown the growth curves of K12 S, K12[1] and W705 SR21 following 120 sec irradiation with UV light. The curves have been reduced to a common starting density. The control curve is representative of all three strains growing in the medium used. As will be seen neither K12 S or W705 SR21 were inducible while K12[1] behaved as did Y10 in the earlier paper[1]. *E. coli B.* and W677[1,7] have been omitted for clarity but they had a growth curve similar to K12 S.

Electron microscopical examination of the cured strains and of *E. coli B.* following irradiation showed a considerable proportion of long bacillary forms but at no time were any collapsed spheres seen. Two illustrations of these

Fig. 1. Growth curves of K12S, K12(1) and W705 SR21 following 120 sec UV irradiation.

Fig. 2. K12 S two hours after 180 sec irradiation × 12,000.

References p. 86.

Fig. 3. *E. coli B.* three hours after 120 sec irradiation × 11,000.

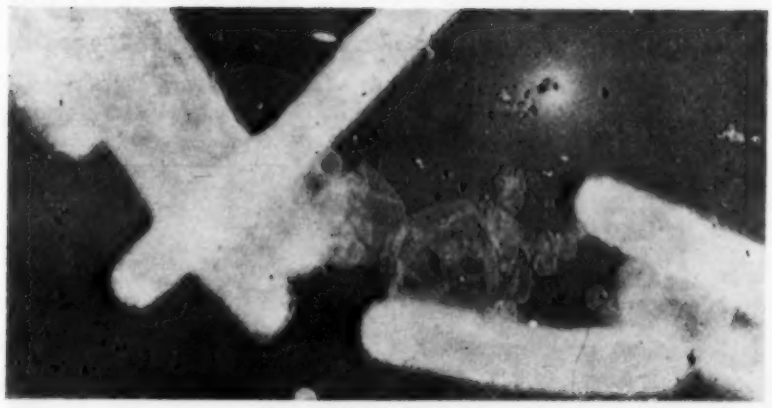

Fig. 4. K12(1) one hour after 120 sec irradiation × 11,000.

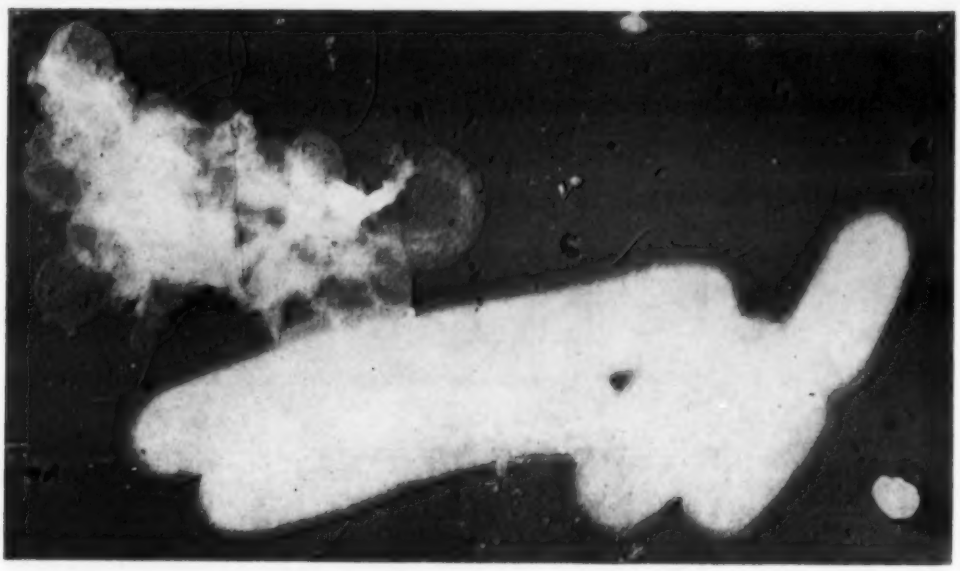

Fig. 5. K12(1) two hours after 120 sec irradiation × 14,000.

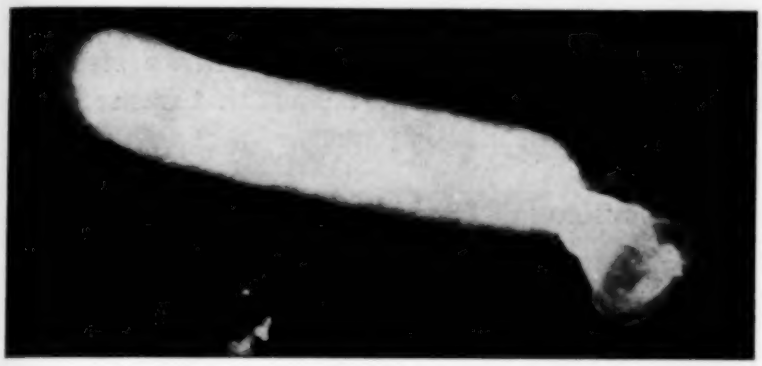

Fig. 6. W705 SR21 two hours after 60 sec irradiation × 16,000.

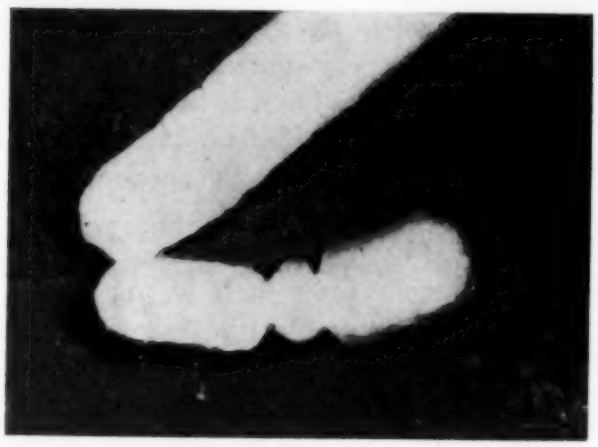

Fig. 7. W705 SR21 two hours after 180 sec irradiation × 15,000.

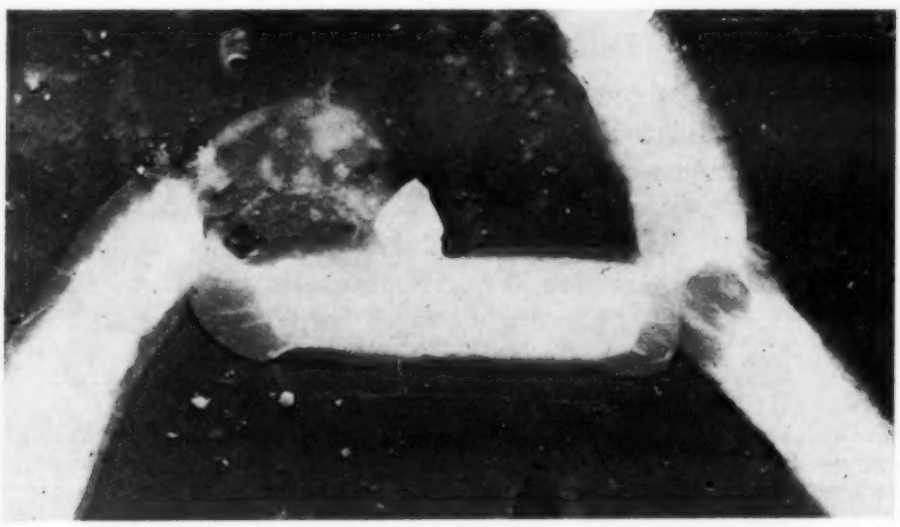

Fig. 8. W705 SR21 one hour after 180 sec irradiation × 15,000.

strains are given; Fig. 2 shows K12 S two hours after 180 sec of irradiation while Fig. 3 shows *E. coli B.* three hours after 120 sec irradiation.

When the irradiation specimens of K12[1] were examined it was found that the appearance was very similar to that recorded earlier[1]. Thus Fig. 4 shows a specimen 1 hour after 120 sec irradiation while Fig. 5 shows the appearance seen 2 hours after the same dose. With K12[1] as with Y10 120 sec irradiation gave the best pictures. The debris contains besides the large collapsed spheres smaller structures which may be likened to foam.

Finally the appearance of W705 SR21 was examined and some rather unusual

References p. 86.

pictures were seen. As well as the usual long forms some bacteria showed evidence of swelling at the ends, Fig. 6 (2 hours after 60 sec) and some showed a spherical structure in the middle, Fig. 7 (2 hours after 180 secs). Fig. 8 shows the nearest that was seen to a collapsed sphere in this strain (1 hour after 180 sec).

DISCUSSION

It will be seen that in this investigation the appearance of spheres in the debris is only found after induction. They are not produced by the same organism rendered non-inducible nor in normally non-inducible strains.

It is not possible from these pictures to determine the nature of the spherical object but it is possible that it represents the outer layer of a bacterium which has for some reason been greatly distended at the time the specimen was made. This suggests that before the bacteria burst to liberate the mature phage particles the control of the osmotic barrier is lost, the cell distends and normally bursts and that the forms we see are those in that state at the time the specimen was fixed.

The origin of the foam is obscure and one can postulate that it represents some inner structure of the bacterium which has been similarly distended.

The structures seen in W705 SR21, coupled with the fact that this strain is not inducible but does have an increase in phage count following irradiation, leads one to suggest that they are modified cellular disintegration.

The pictures support the view that it is the mechanical bursting of the cells at induction and not the presence of a prophage that leads to sphere formation.

ACKNOWLEDGMENTS

One of the authors (R.H.G.) is indebted to the Ciba Foundation for the award of an Anglo-French Exchange Bursary and to Drs. LWOFF and WOLLMAN of the Pasteur Institute for their help and encouragement.

SUMMARY

Irradiation of cured strains of *E. coli* K12 gave pictures similar to that of *E. coli B*. When the bacteria were rendered lysogenic the appearance changed and was marked by collapsed sphere formation. Strains of K12 carrying a mutant of phage λ gave an intermediate picture.

RÉSUMÉ

L'irradiation de souches guéries de *E. coli* K12 donne des images semblables à celles de *E. coli B*. Quand on a rendu les bactéries lysogènes, l'apparence change et ce changement se signale par la formation de sphères. Des souches de K12 portant un mutant de phage λ présentent un aspect intermédiaire.

ZUSAMMENFASSUNG

Die Bestrahlung von geheilten Stämmen von *E. coli* K12 ergab ähnliche Bilder wie diejenige von *E. coli* B. Wenn die Bakterien lysogen gemacht wurden, änderte sich ihr Aussehen und auf den Bildern wurden Kugeln sichtbar. Stämme von K12, die einen Mutant des Phagen λ enthielten, ergaben Bilder, welche zwischen den zwei erstgenannten Arten die Mitte hielten.

REFERENCES

1 C. E. CHALLICE AND R. H. GORRILL, *Biochim. Biophys. Acta*, 14 (1954) 482.
2 E. M. LEDERBERG AND J. LEDERBERG, *Genetics*, 38 (1953) 51.
3 E. L. WOLLMAN, *Ann. Inst. Pasteur*, 84 (1953) 281.
4 F. JACOB AND E. L. WOLLMAN, *Cold Spring Harb. Symposium Quant. Biol.*, 18 (1953) 101.
5 L. W. LABAW, V. M. MOSLEY AND R. W. G. WYCKOFF, *Biochim. Biophys. Acta*, 5 (1950) 327.

Received August 25th, 1954

THE TRANSFER OF POTASSIUM BETWEEN MAMMALIAN MUSCLE AND THE SURROUNDING MEDIUM

by

H. McLENNAN

Donner Laboratory of Experimental Neurochemistry, Department of Neurology and Neurosurgery, McGill University, and the Montreal Neurological Institute, Montreal (Canada)

There are in the literature a number of reports on the movement of sodium and potassium ions across the boundaries of muscle cells; these investigations have however largely been confined to frog muscle. CREESE[1] and GOURLEY AND JONAS[2] have investigated the K exchange in mammalian (rat) muscle *in vitro:* these authors have reported that all of the muscle K is capable of undergoing exchange with the K of the medium in which the muscle is incubated. HEVESY AND HAHN[3] and NOONAN, FENN, AND HAEGE[4] have studied the uptake of K by muscle *in vivo* following injection of ^{42}K. The latter group found that the whole of the muscle K was exchanged under these conditions, while the former found that only a portion of the K will so exchange. HAHN AND HEVESY[5] further showed that the proportion of K undergoing exchange could be increased by muscular excercise; complete exchange was however still not attained.

As a preliminary to the investigation of the effects of certain drugs and other conditions on the normal K movements, it appeared necessary to study more fully the transport of K in normal mammalian muscle *in vitro*. This has been done with muscles of two different shapes, incubated in Ringer-type solutions and in solutions of K phosphate; under the latter condition the K content of the muscle cells tends slowly to increase, in contrast to the former where the tendency is to a decrease. The use of phosphate solutions eliminates swelling of the tissue during incubation, since the cell wall is only slowly permeable to phosphate ion.

EXPERIMENTAL

Materials: The muscles used in this study were the extensor digitorum longus and the sartorius of young hooded rats. The former muscle is easily dissected without damage to the tissue; cotton loops were tied around the tendons at each end of the muscle prior to its removal from the body. The sartorius of rodents is closely fused to the tensor fasciae latae (GREENE[6]). In young animals it was, however, found possible to dissect the sartorius with minimal damage to its margins; again loops were attached to the ends of the muscle before it was removed. After excision the muscles were weighed on a torsion balance. At the end of the experiment the loops were cut off and weighed separately, and the final weight of the muscle was also determined.

Radioactive ^{42}K was obtained in the form of carbonate from the Brookhaven National Laboratory, Upton., U.S.A.; and from Atomic Energy of Canada, Limited, Chalk River, Ont.

Methods: In order to measure the uptake of K from a saline solution, the muscle with its attached loops was placed in a large volume, *ca.* 50 ml, of solution of the following composition: for 20° C, HCO_3 37, Cl 103.5; for 37° C, HCO_3 24.5, Cl 116; plus in both cases Na 131.5, K 5, Ca 2, Mg 2, SO_4 2, glucose 10 (all in mmol/l). The pH of these solutions when bubbled with 95 % O_2–5 % CO_2 was near 7.4. Any changes in the K content of these media, such as were necessary for some experiments, were

References p. 95.

balanced by changes in the Na concentration in order to preserve isotonicity. To prepare a solution containing ^{42}K, the $^{42}K_2CO_3$ was neutralized with HCl, made up to give an isotonic solution (154 mmol/l), and used in place of the inactive KCl solution in the preparation of the above media.

K phosphate solution was prepared by adding to the $^{42}K_2CO_3$ enough dilute H_3PO_4 to give a solution which contained 225 mmol/l K and 150 mmol/l phosphate. On the day of receipt of the isotope this phosphate solution was diluted 20 × with an inactive solution of the same composition; the dilution with inactive material was reduced as decay diminished the radioactivity. The phosphate solution had a pH of about 7.0.

The radioactivity of the muscle was measured at various times during incubation by removing the tissue from the solution and washing it for exactly 1 min in inactive medium of the same composition in order to remove adhering drops of radioactive saline. The cotton loops were placed over pegs set in a flat plastic base, and the whole slid beneath an end-window Geiger tube (Tracerlab type TGC–1). This method ensured a reasonable degree of reproducibility with respect to the geometrical position of the muscle under the counter. Counts of the muscle radioactivity were determined for three 1 min periods, at the end of which time the muscle was returned to the radioactive medium.

After a sufficient period of soaking in radioactive medium (at least 4 h), the rate at which the radioactive K was lost from the muscle could be followed by transferring the tissue to an inactive solution of the same composition, and assaying the radioactivity at intervals as above. The only change required in the procedure was that it was no longer necessary to wash the tissue prior to assay, since the fluid in which the muscle was now placed had a negligible activity.

At the end of the experiment the muscle was dissolved in a few drops of HNO_3 freshly distilled in silica vessels. An aliquot of the solution so obtained was assayed for radioactivity, and this activity compared with that of the radioactive saline used in the first half of the experiment, thus providing a direct relation between number of counts and amount of K.

All radioactivity measurements were corrected for blank, decay, and resolution time of the scaler-Geiger counter combination.

K analyses were performed with the aid of a flame photometer (Perkin-Elmer type 52C). The nitric acid solution of the muscle was taken to dryness, the residue taken up in water and an aliquot appropriately diluted for the measurement.

RESULTS

In the investigation of the rate of movement of an ion it is of importance first of all to determine whether the time barrier imposed between equilibration of the ions inside and outside the tissue is due to the resistance of the cell boundaries or to some diffusion barrier. In the case where the rate of transfer of an ion is determined by the permeability of the cell boundary, the probability of entry of an ion will be proportional to the external concentration of that ion $[x_o]$; the probability of transfer from inside to outside will be proportional to the internal concentration $[x_i]$. In a cell with surface area A, then, the net amount of ion entering will be $\varkappa_1 A[x_o] - \varkappa_2 A[x_i]$ per unit time, $\varkappa_1$ and $\varkappa_2$ being constants. If the volume of the cell is V, the rate of increase of concentration inside will be $(\varkappa_1[x_o] - \varkappa_2[x_i])A/V$. Putting $\varkappa_1 A/V = k_1$ and $\varkappa_2 A/V = k_2$, we have

$$\frac{d[x_i]}{dt} = k_1[x_o] - k_2[x_i],$$

which is the normal permeability equation. It will be noted that the transfer rate constants k_1 and k_2 are independent of the number of cells in the aggregate comprising the tissue, and vary only with the surface/volume ratio of the cells. If, therefore, the rate constants determined experimentally are found to vary with the size or shape of the tissue sample employed, then the limiting factor may be expected to be the rate of diffusion of the ions into the interstices of the tissue.

In the present experiments an attempt has been made to decide between these two possibilities by using two muscles of different shape, although of about the same overall volume. The extensor digitorum longus is nearly circular in cross-section, tapering somewhat towards each end; the sartorius is a thin flat sheet of muscle of fairly uniform

References p. 95.

width. Both have an average total volume of about 100 mm³, and both have fibres of 30 μ diameter for the most part. Assuming that the fibres are cylindrical and run the whole length of the muscle (30 mm for the extensor), the volume of an "average" fibre will be 0.021 mm³, and its surface area 2.83 mm².

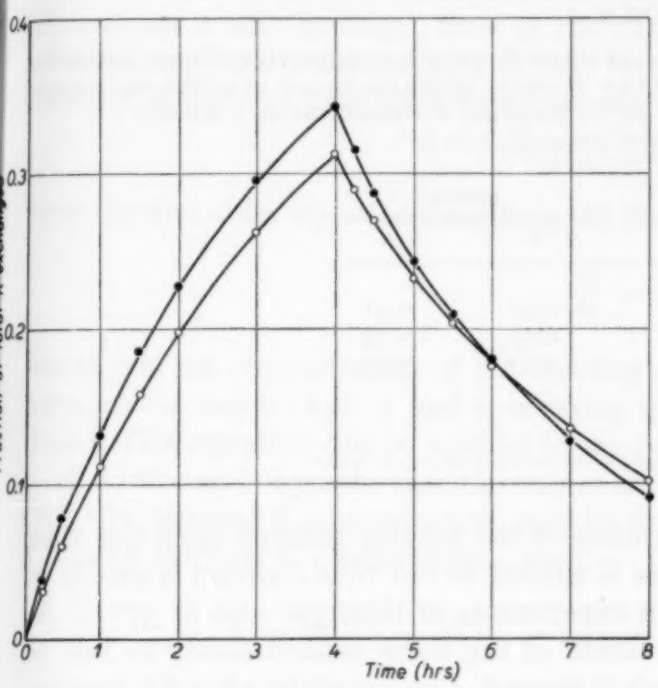

Fig. 1. The exchange of ^{42}K in two muscles from the same rat. Temperature 20° C. External K concentration 5 mmol/l. After 4 h the muscles were permanently transferred to inactive medium.

—○——○— Extensor digitorum longus.
—●——●— Sartorius.

Fig. 1. shows the results of typical experiments in which the uptake of K from a Ringer-type solution containing ^{42}K was measured, and where after some hours the muscles were placed in an inactive solution of the same composition and the time course of the loss of radioactivity followed. The figure also gives a comparison between the extensor digitorum longus and the sartorius. Empirically the uptake curves can be fitted by a simple exponential function of the type $K^* = B(1-\exp(-bt))$, where K^* is the amount of labelled K in the tissue, B is a constant representing the fraction of the total tissue K which is undergoing exchange, and b is the time constant governing the process. Strictly the equation for K^* should involve two terms, *i.e.* one for the extracellular K as well as the above, but as will be discussed below the amount of K contained in the extracellular space in these muscles is too small to be detected within the overall errors of measurement. If a steady state with respect to the total K content of the tissue pertains, then according to the superposition theorem the equation for the loss of K^* when the tissue is placed in an inactive medium at time t_1 should be

$$K^* = B(1-\exp(-bt)) - B(1-\exp(-b(t-t_1))).$$

With the medium used in these experiments the K content of the tissue remains reasonably constant. The average K content of fresh muscles was 101 ± 13 μequiv/g (S.D., 6 determinations); that of muscles incubated for periods up to 8 hr 96 ± 10 μequiv/g (S.D., 9 determinations): it has further been found that the average rate of net loss of K was less than 2% of the total per h at 20° C for periods of incubation up to 16 h. It is therefore permissible to use the steady state equations. In the experiments shown in Table I the constants B and b were derived from equations of the above type, which fitted the experimental curves closely.

From Table I it is clear that the time constant b governing the movement of about one half of the total tissue K is of the same order of magnitude for both of the muscles investigated. It may be inferred, therefore, that the constant describes a permeability rather than a diffusion process. If diffusion were the limiting factor determining the penetration of K, then the rate of penetration into the sartorius would be expected to

References p. 95.

be greater than into the extensor digitorum longus, inasmuch as the thickness of the sartorius is of the order of 0.5 mm, while that of the extensor is 3.5 mm.

TABLE I

PARAMETERS OF THE EQUATIONS FOR UPTAKE OF LABELLED K FROM A RADIOACTIVE SALINE SOLUTION BY RAT MUSCLES, AND FOR THE LOSS OF LABELLED K FROM MUSCLES TO AN INACTIVE SOLUTION. For equations, see text. Temperature 20° C. External K concentration 5 mmol/l
B as fraction of total tissue K; b in h^{-1}.

Extensor digitorum longus		*Sartorius*	
B	b	B	b
0.49	0.22	0.37	0.41
0.59	0.26	0.47	0.33
0.41	0.40	0.37	0.19
0.42	0.41		
0.46	0.17		

The effect of changing the K concentration of the bathing solution upon the time constant b and upon the amount B of tissue K subject to this time constant is shown in Table II. Attempts were made to perform experiments of this type also at 37° C. At this temperature, however, the total K content of the tissue tended slowly to fall to about one half of the initial value (45 μequiv/g instead of 96 μequiv/g) after 8 h incubation. It is therefore not permissible to apply the steady state equations given above. It was found that qualitatively the picture is the same at 20° as at 37°, but the value of b falls from an average of 0.52 h^{-1} at 37° to 0.32 h^{-1} at 20° (both with 5 mmol/l external K).

The results in Table II show that the effect of increasing the external K concentration is to raise the amount of K which undergoes exchange, without at the same time increasing the rate at which the process is carried on. As the K concentration in the medium is raised, the exchangeable fraction of the K is raised until in a concentration of 20 mmol/l the exchange is almost complete.

TABLE II

FEFECT OF EXTERNAL K CONCENTRATION ON THE TURNOVER OF RAT MUSCLE K AT 20° C. PARAMETERS B AND b DETERMINED BOTH FROM MEASUREMENTS OF INFLUX AND EFFLUX

B as fraction of total tissue K; b in h^{-1}

Extensor digitorum longus			*Sartorius*		
K conc. mmol/l	B	b	*K conc. mmol/l*	B	b
5	0.45	0.17	5	0.37	0.19
10	0.61	0.22	10	0.72	0.20
20	0.89	0.27	20	1.00	0.36
5	0.46	0.28			
10	0.59	0.26			
20	0.88	0.24			
10	0.66	0.17			
20	0.77	0.24			

References p. 95.

The figure which it is of the most interest to know is the amount of ion being transferred per unit of cell surface. An estimate of this may be obtained by considering the dimensions of an "average" fibre of the extensor muscle given above, *i.e.* a volume of 0.021 mm^3 and a surface area of 2.83 mm^2. With the muscle in a steady state the influx of K per unit time must equal the efflux, that is

$$k_1[K_o] = k_2[K_i].$$

Now the first order equation describing the disappearance of a reactant from a system is

$$-\frac{dc}{dt} = k_2 c,$$

where c is the concentration of the reacting substance. This can be integrated in the form $c_t = c_o \exp(-k_2 t)$, c_o and c_t referring to the concentrations of c initially and at time t. This equation can be applied to the present problem in the form $K^*_t = B \exp(-k_2 t)$, whence it appears that the values of b determined above are identical with k_2. $[K_i]$, the internal K concentration, may be found from B, and $[K_o]$ is also known. For 5 mmol/l external K concentration, then,

$$k_1 = \frac{k_2\,[K_i]}{[K_o]} = \frac{0.32 \cdot 38}{5} = 2.43\ h^{-1} \text{ (average of 4 measurements).}$$

The amount of K being transferred per unit of cell surface is equal to the flux of K $\times$ the ratio V/A. That is,

$$\text{Influx/mm}^2 = k_1\,[K_o]\,V/A = \frac{2.43 \cdot 5 \cdot 10^{-3} \cdot 0.021}{2.83 \cdot 3600} = 2.5 \cdot 10^{-8}\ \mu\text{equiv/mm}^2\text{/sec}$$

With an external K concentration of 10 mmol/l (5 determinations), the corresponding values are $k_1 = 1.18\ h^{-1}$, flux $= 2.4 \cdot 10^{-8}$ μequiv/mm^2/sec; and with 20 mmol/l external K (3 determinations), $k_1 = 0.94\ h^{-1}$, flux $= 3.9 \cdot 10^{-8}$ μequiv/mm^2/sec. Thus although the external K concentration is greatly increased, the amount of ion being transported across the cell boundary is not much raised. It may be that the system responsible for K transport is normally working at near capacity, and large changes in the external K concentration produce only small alterations in the total K flux.

The extracellular space of the rat gastrocnemius is given as 12% by volume (MANERY AND HASTINGS[7]); assuming that the concentration of ion in this space is the same as that in the external solution at equilibrium, the amount of K which would be expected in the extracellular phase of these muscle is 0.6 μequiv/g of tissue, *i.e.* less than 1% of the total K. In experiments involving the exchange of K with a Ringer-type solution, this small amount of K exchanging in the extracellular space is unlikely to be capable of measurement. Nevertheless the equation covering the overall K movement must consist of two terms; one a diffusion term for the equilibration of the extracellular fraction, and the second a permeability term for the movement of the ion across the cell wall. Only if the time constants governing these two processes are substantially different can movement in the two phases be dissociated.

Experiments with K phosphate made it possible to measure the volume of the extracellular space of the muscle as well as the rate of turnover of the extracellular K. These experiments were performed as follows. The muscle was placed in a solution of K^* phosphate for 1–2 h, at which time all the tissue K determined by analysis had undergone

References p. 95.

exchange. In addition, the normal high Na content of the extracellular space had been replaced by the K* ions of the solution. The muscle was then transferred to a solution of K* Ringer of the same specific activity, and the tissue radioactivity was determined at short intervals. The result was a sudden outpouring of the K* of the extracellular space in exchange for Na; the intracellular K on the other hand remained almost constant or fell very slowly, since the intracellular K level in K phosphate was found to be slightly above that found after incubation in saline medium. In three experiments of this type the extracellular space of the extensor muscle was found to be 0.10–0.15 of the total volume, and the K contained in this space turned over with a half time of 5–7 mins. This rate of exchange is very much faster than that of the intracellular K, where the half time is of the order of 1½ h. A typical experiment is shown in Fig. 2.

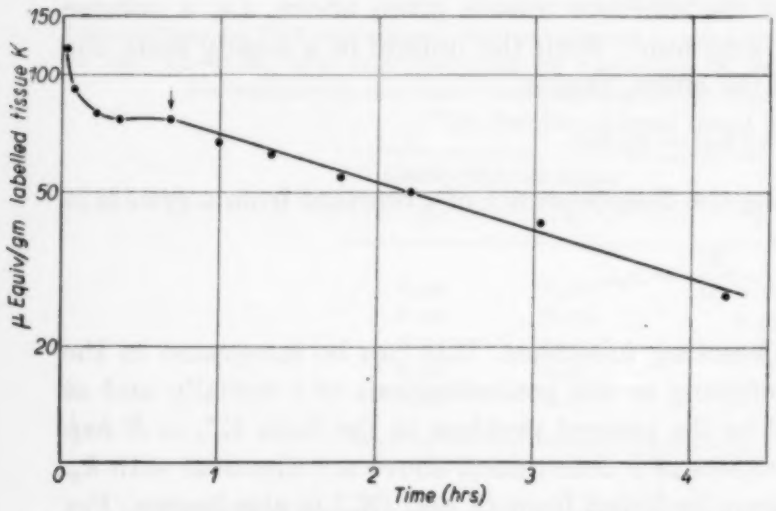

Fig. 2. Effect of incubation for 1.3 h in K* phosphate solution (external K concentration 225 mmol/l) At time o the muscle was transferred to K* Ringer (external K concentration 5 mmol/l) of the same specific activity; at the arrow the muscle was permanently transferred to inactive Ringer.

Having made the above measurements, the muscles could then be transferred from K* Ringer to inactive Ringer of the same composition, and the time constants for the efflux of intracellular K determined in the usual way. Pretreatment with K phosphate did not cause any change in the rate of K efflux in saline solution; however the K, which in saline was inexchangeable (see Table I), and which had been rendered "accessible" by the application of K phosphate, did not appear to become re-fixed when the muscle was returned to saline solution. In other words, B, the amount of exchangeable K in the intracellular phase, now approached unity. The results are given in Table III.

TABLE III

VALUES OF THE PARAMETERS B AND b DETERMINED FOR THE EFFLUX OF K FROM MUSCLE TO AN INACTIVE RINGER SOLUTION AFTER TREATMENT OF THE TISSUE WITH K* PHOSPHATE

Temperature 20° C. B as fraction of the total tissue K; b in h^{-1}.
All measurements on extensor digitorum longus.

B	b
0.93	0.26
0.92	0.24
0.91	0.38
0.93	0.32
0.95	0.23

That this effect was not due to the presence of a high concentration of phosphate was shown by the fact that pre-incubation of the muscle in a solution of Na phosphate of the

References p. 95.

same concentration produced no alteration in the subsequent uptake of K^* ($B = 0.44$, $b = 0.34\ h^{-1}$). Pre-incubation for 1 h in inactive K phosphate caused an increase in the value of B to 0.71 when the influx of K^* was measured subsequently.

The effect of stretch on frog muscle metabolism was investigated by FENG[8], who found that the resting metabolism was increased by the application of tension. Fig. 3 shows the effect of applying stretch on the K transport of the extensor digitorum longus. The stretch was given to 115% of the resting length by slipping the loops at the ends of the muscle over a U-shaped wire frame, such that the separation at the mouth of the U could be varied, and with it the length of the muscle. Otherwise the experiment was performed as before. Three such experiments were done at 20° C and one at 37°, all with the same lack of effect on either K influx or efflux. This is in accord with the results of HARRIS[9], who found a similar lack of effect of stretch on K movement in frog muscle.

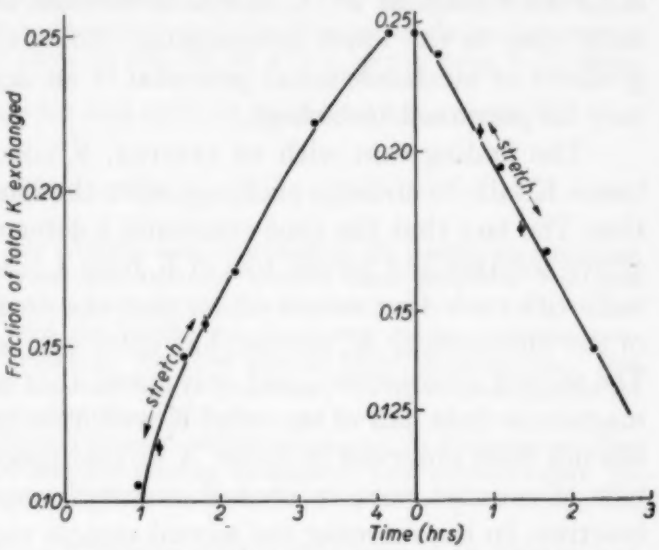

Fig. 3. The effect of stretch on K exchange in muscle. Stretch to 115% of the resting length applied between the times indicated.

DISCUSSION

These experiments, which were designed to provide information on the movement of K in resting mammalian muscle fibres *in vitro*, have shown that qualitatively there is little difference between rat muscles and those of the frog (HARRIS[9]). Thus in both species the exchange of the total tissue K is incomplete if the tissue is incubated in saline medium containing a physiological concentration of K, complete exchange only being attained if the external K concentration is much increased.

That the measured K exchange in these muscles is not being limited by a diffusion barrier is indicated both by the fact that the rate and extent of the exchange is the same in muscles of differing shape (extensor digitorum longus and sartorius), and as well from the determination of the movement of the extracellular K after incubation in K phosphate. At 20° C this equilibration of fast moving K is 50% complete in about 6 mins. Assuming that the extensor is a cylinder of radius $r_0 = 0.18$ cm, then half saturation is reached at time t when $kt/r_0^2 = 0.062$ (HILL[10]), where k is the diffusion constant governing the process. From this equation it can be calculated that $k = 5.6 \cdot 10^{-6}$ cm²/sec. The diffusion constant for K ions in free solution is given as $1.6 \cdot 10^{-5}$ cm²/sec at 17.5° C for 0.1 M KCl; the diffusion of K into the extracellular space of these muscles is thus only reduced to one third of that holding in free solution. The fact that the bulk of the tissue K exchanges much more slowly than this is indicative of the permeability barrier imposed between the cellular contents and the extracellular space.

Values reported in the literature for the cell permeability constant $\varkappa_1$ of rat muscle *in vivo* vary between 1.6 and $5 \cdot 10^{-2}$ cm/h (calculated from HAHN AND HEVESY[5], and

References p. 95.

NOONAN, FENN AND HAEGE[4]). The value of $\varkappa_1$ in the present experiments can be calculated from the values obtained for k_1, since $k_1 = \varkappa_1 A/V$. The figure for $\varkappa_1$ so obtained is $1.8 \cdot 10^{-3}$ cm/h at 20° C, the difference between this and the older values being partially due to the lower temperature. Since the uptake of K by the cell against the gradient of electrochemical potential is an active process, the temperature coefficient may be presumed to be high.

The finding that with an external K concentration of 5 mmol/l some 50% of the tissue K fails to undergo exchange with the ions of the solution requires some consideration. The fact that the time constants b determined both for uptake of K from a radioactive solution and for the loss of K from a labelled muscle to an inactive solution agree well with eachother means either that the constant cannot govern the movement of all of the intracellular K, or else that there is a large imbalance between influx and efflux. The second alternative could only mean that a *net* loss of K was taking place of such a magnitude that half of the total K would be lost during three hours of incubation. This has not been observed to occur. A further proof was given by an experiment in which a pair of muscles were incubated overnight, one in radioactive saline and the other in inactive. In the morning the second muscle was placed in active medium, and the time course of the uptake of K measured in the usual way; at the same time the first muscle was continued in active medium to ensure that no further K exchange was taking place. The results were: muscle incubated overnight in radioactive medium, $B = 0.46$; muscle pre-incubated in inactive medium, $B = 0.41$, $b = 0.40$ h^{-1}. The extent to which the K of the muscle was able to undergo exchange was thus not affected by a 10 h pre-incubation; the value of b is also within the limits found for "fresh" muscles. It seems certain, therefore, that there is a fair proportion of the cellular K of muscle which is not free to exchange *in vitro*. Whether raising the temperature would have the effect of increasing the proportion of exchangeable K, as is the case with frog muscle[9], cannot be determined from these experiments, where incubation at 37° brought about the gradual loss of tissue K. It is interesting in this connection that STONE AND SHAPIRO[11] have reported that one third of the total K of rat muscle is not ultrafilterable.

SUMMARY

The rates of uptake and loss of tracer-labelled potassium by isolated muscles of the rat have been studied. The rates were found to be of the same order in two muscles (extensor digitorum longus and sartorius) of different shape but of similar total volume.

In Ringer's solution at 20° C one half of the total tissue K exchanged with first-order kinetics, the remainder being apparently inexchangeable. The proportion of exchangeable K could be increased by increasing the K concentration of the bathing medium, complete exchange being attained with a concentration of 20 mmol/l.

The rate of exchange of the K contained in the extracellular space of the tissue, and the volume of the space, were measured following incubation of the tissue in isotonic K phosphate solution. The extracellular K exchanged with an average half time of 6 min, in contrast to the 1½–2 h period required for half exchange of the exchangeable intracellular K.

The application of mechanical stretch was without effect on the influx or efflux of K in the muscle.

RÉSUMÉ

Les vitesses d'entrée et de sortie du potassium dans les muscles isolés de rats ont été étudiés au moyen de potassium marqué. Les vitesses étaient semblables pour deux muscles de forme différente mais de même volume (extensor digitorum longus et sartorius).

Dans une solution de Ringer, la moitié de la quantité totale de K présente dans le tissu fut échangée suivant la cinétique d'une reaction du premier ordre, le reste étant apparemment non

References p. 95.

échangeable. La proportion du K échangeable put être augmenté par élévation de la concentration du milieu extérieur en K. Lorsque cette concentration était de 20 mmol/l la totalité du K fut échangé.

Le volume de l'espace extracellulaire et la vitesse d'échange de son K ont été mesurés après incubation du tissu dans une solution isotonique de phosphate de K. Le K extracellulaire s'échangeait avec une demi-periode moyenne de 6 minutes alors qu'elle est de 1½–2 heures pour le K intracellulaire échangeable.

Une tension mécanique exercé sur le muscle fut sans effet sur l'entrée ou la sortie du K.

ZUSAMMENFASSUNG

Die Geschwindigkeit der Aufnahme und der Abgabe von markiertem K wurde an isolierten Muskeln der Ratte studiert. In zwei Muskeln von verschiedener Gestalt aber gleichem Volumen (Extensor digitorum longus und Sartorius) ist die Geschwindigkeit des K-Austausch von der gleichen Grössenordnung. In Ringer Lösung bei 20° C wird die Hälfte des Gesamten K des Gewebes ausgetauscht in einer kinetischen Reaktion erster Ordnung, der Rest scheint nicht austauschbar. Das Verhältnis des austauschbaren K konnte erhöht werden, durch Erhöhung der K-Konzentration im Bad, vollständiger Austausch wurde erhalten bei einer Konzentration von 20 mmol/l.

Die Austauschgeschwindigkeit des K, in extrazellulären Gewebsspalten und ihr Volumen wurden nach Einlegen des Gewebes in isotonische K-Phosphat-Lösung gemessen. Der extrazelluläre K-Austausch mit einer Halbwertszeit von 6 Min. steht im Gegensatz zu der Zeit von 1½ bis 2 Stunden für den Austausch des intrazellulären K.

Die Anwendung mechanischen Zugs blieb ohne Wirkung auf die Aufnahme und die Abgabe von K im Muskel.

REFERENCES

1 R. CREESE, *J. Physiol.*, 115 (1951) 23P.
2 D. R. H. GOURLEY AND H. JONAS, *Fed. Proc.* 13 (1954) 59.
3 G. HEVESY AND L. HAHN, *Klg. Danske Videnskab. Selskab. Biol. Medd.*, 16 #1 (1941).
4 T. R. NOONAN, W. O. FENN AND L. HAEGE, *Am. J. Physiol.*, 132 (1941) 474.
5 L. HAHN AND G. HEVESY, *Acta Physiol. Scand.*, 2 (1941) 51.
6 E. C. GREENE, Anatomy of the Rat, *Trans. Am. Philosph. Soc.* (1935).
7 J. F. MANERY AND A. B. HASTINGS, *J. Biol. Chem.*, 127 (1939) 657.
8 T. P. FENG, *J. Physiol.*, 74 (1932) 441.
9 E. J. HARRIS, *J. Physiol.*, 120 (1953) 246.
10 A. V. HILL, *Proc. Roy. Soc.*, B 104 (1929) 39.
11 D. STONE AND S. SHAPIRO, *Am. J. Physiol.*, 155 (1948) 141.

Received July 12th, 1954

THE BIOSYNTHESIS OF RADIOACTIVE ESTRADIOL

I. SYNTHESIS BY SURVIVING TISSUE SLICES AND CELL-FREE HOMOGENATES OF DOG OVARY

by

JOSEPH L. RABINOWITZ AND ROBERT M. DOWBEN

Radioisotope Unit, Veterans Administration Hospital, Philadelphia, Pa. (U.S.A.)

The comparative biosynthetic pathways of closely related sterols are of particular interest in consequence of recent studies on precursors of cholesterol[1–4]. This study is concerned with the biosynthesis of estrogens. ^{14}C-labelled estradiol and estrone have been obtained from ovaries perfused with ^{14}C-acetate[5]. We are reporting an *in vitro* system in which ^{14}C-acetate is incorporated into estradiol and estrone. This system lends itself to investigation of intermediates, co-factors and conditions influencing synthesis.

EXPERIMENTAL

The ovaries used in these experiments were obtained from mongrel dogs. Adhering tissue was carefully removed and the ovaries placed immediately in an isotonic phosphate buffer solution at 1° C. Surviving tissue slices, 0.5 mm thickness, were prepared with a Stadie slicer. About one half gram of tissue was placed in each incubating flask together with two and a half volumes of buffer and 1 mg each of adenosine monophosphate, diphosphopyridine nucleotide and 2-^{14}C sodium acetate (1 mc/m*M*).

Homogenates were prepared after mincing ovaries in two and a half volumes of buffer containing K_2HPO_4 0.067 *M*, KH_2PO_4 0.042 *M*, $MgCl_2$ 0.006 *M* and nicotinamide 0.03 *M* at pH 7.0 at 0° C. The mince was then homogenized quickly in a loose-fitting Potter-Elvehjem glass homogenizer. The homogenate was centrifuged for seven minutes at 500 *g* to remove cells, nuclei and cell debris. The homogenate was divided among flasks containing the same co-factors and precursor as for the slices, so that the total volume of each flask was 5 ml.

The flasks were incubated at 37° C for 3 hours with gentle shaking; the gaseous phase was 100% oxygen. After incubation 10 mg of carrier estradiol, estrone or cholesterol was added separately to each flask. Metaphosphoric acid was added to pH 2. The material was extracted continuously with ether for 24 hours. The ether extract was evaporated to dryness and placed in a desiccator over KOH for several days. One ml of 10% acetic acid was added to each residue which was again dried in a desiccator over KOH. Each residue was dissolved in a minimum amount of absolute ether, decolorized with charcoal and alumina, and filtered. Petroleum ether was added to incipient turbidity and the material was kept at —20° C for 48 hours. The solid obtained was recrystallized until the specific radioactivity and melting points were constant and mixed melting point with authentic material showed no depression (m.p. 259° C for estrone; m.p. 176° C for estradiol). Aliquots of the obtained estrone and estradiol were chromatographed on celite by the method of BITMAN AND SYKES[6]. The samples followed the described elution rates and the specific radioactivity was not altered.

The *m*-bromobenzoate and 1-naphthoate derivatives of estradiol and estrone were prepared by the method of DOISY *et al.*[7] The materials obtained had correct melting points and mixed melting points with authentic material were not depressed (m.p. 195° C for di-1-naphthoate of estradiol; m.p. 155° C for *m*-bromobenzoate of estradiol; m.p. 208° C for mono-1-naphthoate of estrone, m.p. 221° C for *m*-bromobenzoate of estrone). Cholesterol was obtained as the digitonide. The radioactivity of all materials was determined, corrected to infinite thinness and for dilution, and expressed as cpm/mg C. Variations in the activity of derivatives of the same sample were within the counting error.

References p. 98.

RESULTS

Labelled estradiol, estrone and cholesterol were obtained in all experiments. The activity of the estradiol was greater in all cases than that of the estrone. The activity of both estradiol and estrone was far greater in ovaries obtained from animals during proestrus than in ovaries obtained during anestrus. The activity of the cholesterol obtained was about the same during the various phases of the oestrus cycle. The results are summarized in Tables I and II.

TABLE I

INCORPORATION OF 2-^{14}C ACETATE INTO ESTRADIOL AND ESTRONE BY TISSUE SLICES AND HOMOGENATES OF DOG OVARIES

	Recovered radioactivity							
	Estradiol (Cpm/mg C)				*Estrone (Cpm/mg C)*			
	Diluted, and recovered	*di-1-naphthoate*	*mono-m-bromobenzoate*	*Chromatographed*	*Diluted and recovered*	*mono-1-naphthoate*	*mono-m-bromobenzoate*	*Chromatographed*
Exp. 1	374	351	314	366	40	47	32	38
Exp. 2	285	295	256	—	19	14	—	—

TABLE II

INCORPORATION OF 2-^{14}C ACETATE INTO ESTRADIOL AND ESTRONE BY TISSUE SLICES AND HOMOGENATES OF DOG OVARIES IN PROESTRUS AND ANOESTRUS

		Recovered radioactive		
		Estradiol Cpm/mg C (range)	*Estrone Cpm/mg C (range)*	*Cholesterol Cpm/mg C*
Proestrus dogs	Tissue slices	760–896	31–46	—
	Homogenates	96–134	14–23	76
Anoestrus dogs	Tissue slices	71–94	3–17	—
	Homogenates	19–63	1–5	77

DISCUSSION

The conditions and techniques for liver slices and homogenates found to be optimum for cholesterol synthesis[1] were employed with success in this study.

The higher activity of estradiol than estrone in our experiments lends support to the idea that estradiol is the primary estrogen synthesized by the ovary.

The optimum conditions and co-factors for estradiol synthesis are under investigation and a particle-free, water soluble system is being developed.

References p. 98.

ACKNOWLEDGEMENTS

We are indebted to Dr. R. BRODEY, School of Veterinary Medicine, University of Pennsylvania, for making dog ovaries available to us, and to Dr. S. GURIN, Dr. C. BACHMAN and Dr. H. VARS for their suggestions and encouragement.

SUMMARY

1. 2-^{14}C-acetate is incorporated into estradiol, estrone and cholesterol by surviving tissue slices and homogenates of dog ovary.

2. Under comparable conditions more acetate was incorporated into estradiol than into estrone.

3. The activity of estradiol and estrone obtained from tissues of animals in proestrus was greater than that of animals in anestrus.

RÉSUMÉ

1. L'acétate-2-^{14}C est incorporé dans l'oestradiol, l'oestrone et le cholestérol par des tranches de tissus survivants et des homogénats d'ovaire de chienne.

2. Dans des conditions comparables l'oestradiol incorpore davantage d'acétate que l'oestrone.

3. L'activité de l'oestradiol et de l'oestrone préparés à partir de tissus d'animaux en pro-oestrus est plus élevée que celle d'animaux en anoestrus.

ZUSAMMENFASSUNG

1. 2-^{14}C-Azetat wird durch überlebende Gewebeschnitte und Homogenate von Hundenovaria in Östradiol, Östron und Cholesterol eingebaut.

2. Unter vergleichbaren Bedingungen wurde in Östradiol mehr Azetat eingebaut als in Östron.

3. Die Aktivität von Östradiol und Östron, die aus Geweben von Tieren in der Pro-Östrusperiode hergestellt worden waren, war grösser als diejenige der Tiere in der Anöstrusperiode.

REFERENCES

1 J. L. RABINOWITZ AND S. GURIN, *J. Biol. Chem.*, 208 (1954) 307.
2 J. L. RABINOWITZ, *J. Am. Chem. Soc.*, 76 (1954) 3037.
3 J. L. RABINOWITZ AND S. GURIN, *J. Am. Chem. Soc.*, 76 (1954) 5168.
4 L. C. CLARK, I. HARARY, O. REISS AND K. BLOCH, *Fed. Proc.*, 13 (1954) 640.
5 H. D. WERTHESSEN, E. SWENK AND C. BAKER, *Science*, 117 (1953) 380.
6 J. BITMAN AND J. F. SYKES, *Science*, 117 (1953) 356.
7 D. W. MCCORQUODALE, S. A. THAYER AND E. A. DOISY, *J. Biol. Chem.*, 115 (1936) 439.

Received May 29th, 1954

STUDIES ON THE INDUCED SYNTHESIS OF β-GALACTOSIDASE IN *ESCHERICHIA COLI*: THE KINETICS AND MECHANISM OF SULFUR INCORPORATION*

by

DAVID S. HOGNESS**, MELVIN COHN*** AND JACQUES MONOD

Service de Physiologie microbienne, Institut Pasteur, Paris (France)

INTRODUCTION

The present paper is concerned with the question of the origin and kinetics of incorporation of the elements of an inducible (*i.e.* adaptive) enzyme-protein. The data also present some bearings on the more general problem of protein interrelationships and protein turnover within growing cells.

The inducible enzyme β-galactosidase of *E. coli* was chosen as object of these experiments because of the exceptionally convenient properties of this system[22,1,2,3].

A culture of *E. coli* growing in a medium of mineral salts with a non-galactosidic carbon source, such as succinic acid, produces only a trace of β-galactosidase. The addition of a suitable galactoside to the growing culture is immediately followed by a sharp increase of up to 5000 fold in the rate of synthesis of β-galactosidase. This high rate of synthesis is maintained as long as the bacteria grow in the presence of the inducing galactoside (inducer). However, if the inducer is removed, the rate of synthesis falls immediately to the original trace value, and any enzyme present at that time is thereafter diluted in the increasing bacterial mass. Thus we have a system in which the formation of a given protein can be initiated and stopped at will. Furthermore in this system, it is possible to use inducers which are not hydrolysed by the enzyme nor utilized as carbon and energy source by the bacteria and which apparently do not affect the synthesis of the bulk of the other protein.

The questions we have sought an answer to in the present work are:

(a) to what extent do other *proteins* of the cell contribute, either directly (as specific precursors) or indirectly (as sources of amino acids or peptides) to the synthesis of β-galactosidase;

(b) whether there is any significant turnover of β-galactosidase within growing cells.

These questions were clearly formulated, albeit only partially answered, through previous immunochemical and nutritional studies[3,4,5] the results of which should be briefly recalled here.

---

* This work has been supported by a grant of the National Cancer Institute of the National Institutes of Health, Bethesda, Maryland.

** Ely-Lilly research fellow of the National Research Council, 1952–1954.

*** U.S. Public Health fellow, 1952–1954.

References p. 116.

Immunochemical analysis of the β-galactosidase system[4,5], has shown that:

1. the induced biosynthesis of β-galactosidase (Gz) corresponds to the appearance of a new protein molecule identifiable as a distinct antigen, not detectable in non-induced bacteria;

2. the non-induced as well as the induced cells contain a structurally related protein (Pz) which cross-reacts with the antibody to the enzyme (Gz);

3. the induction of β-galactosidase synthesis is accompanied by a decrease in the overall rate of synthesis of the Pz protein;

4. among diverse species of *Enterobacteriaceae* only those which possess the Pz protein are capable of synthesizing the enzyme (Gz).

These results led to the conclusion that the mechanisms for the synthesis of the enzyme (Gz) and of the Pz protein were related and that the two proteins were either successive or twin members of the same biosynthetic pathway:

$$\text{1. am.ac.} \longrightarrow \text{Pz} \longrightarrow \text{Gz}$$

$$\text{or 2. am.ac.} \longrightarrow \begin{cases} \text{Pz} \\ \text{Gz} \end{cases}$$

However, nutritional and kinetic studies on β-galactosidase synthesis[6] have shown that:

1. virtually all indispensable amino acids are immediately required for β-galactosidase synthesis;

2. the rate of β-galactosidase synthesis is a constant fraction of the rate of synthesis of total bacterial protein, from the time of addition of the inducer.

These results suggested that the elements of the β-galactosidase molecule are not derived from other proteins, and also that β-galactosidase synthesis is essentially irreversible, *i.e.* that the enzyme molecule is not in a "dynamic state" within the cells.

However these conclusions could be directly tested only by studying the incorporation of radioactive atoms into β-galactosidase. The present paper presents the results of such a study. Some preliminary data have already been discussed in a general report by MONOD AND COHN[7].

MATERIALS AND METHODS

Strain

The mutant (ML 32400) of *E. coli* ML[8] was used throughout these experiments.

Media

Unless otherwise specified all cultures were grown in the sulfur deficient medium 61 (13.6 g KH_2PO_4; 2.0 g NH_4Cl; 0.2 g magnesium citrate; 0.01 g $Ca(NO_3)_2$; 0.005 g $FeCl_3$; 1000 ml H_2O; and sufficient KOH to bring the pH to 7.0. The carbon source (succinic acid) and the sulfur source ($(NH_4)_2SO_4$) were added separately in the amounts specified in each experiment.

When desired this medium was made radioactive by the addition of ^{35}S "carrier-free" sulfate obtained from the Isotope Division, A.E.R.E., Harwell, England. All of the radioactivity of this material was precipitable with barium ion. The amount of sulfur thus added constituted an insignificant fraction of the total present in the medium.

Inducer

The inducer used in these experiments was methyl-β-D-thiogalactoside (MTG) synthesized by Prof. HELFERICH (Bonn, Germany)[9] to whom we should like to express our thanks. MTG is not hydrolyzed by the β-galactosidase of *E. coli*, nor is it metabolized as a carbon source by the bacteria. The kinetics of induction by MTG under the conditions used here are similar to those exhibited

References p. 116.

by methyl-β-D-galactoside[6] in that the increase in enzyme is directly proportional to the increase in bacterial protein from the moment the inducer is added, provided a "saturating" concentration of inducer is used ($> 10^{-4}$ *M*).

Method of culture and measurement of growth

The cultures were grown in conical flasks shaken in a 37° C water bath. The methods used for following bacterial growth have been described elsewhere[6]. Under the conditions employed here, the generation time in the exponential phase of growth is one hour.

Determination of β-galactosidase activity

β-galactosidase activity of toluenized suspensions of bacteria and of extracts was determined in $2.7 \cdot 10^{-3}$ *M* *o*-nitrophenyl-β-D-galactoside (NPG) and 0.05 *M* sodium phosphate buffer (pH = 7.0) at 28° C by previously described methods[8]. The unit of β-galactosidase activity is defined as the amount of enzyme which hydrolyzes 1 mμ mole of β-NPG in one minute under the above conditions.

Preparation of the crude extracts

Crude extracts were prepared from bacteria which had been harvested by centrifugation and washed three times with 0.05 *M* sodium phosphate buffer (pH = 7.0). The volume of culture employed for each extract was sufficiently large to contain a total of $6 \cdot 10^5$ units of β-galactosidase or approximately 2 mg of enzyme protein. The wet bacteria were then mixed with an equal weight of dry alumina and the mixture ground for five minutes in a mortar. The ground material was then taken up in an equal volume of 0.05 *M* sodium phosphate buffer (pH = 7.0), centrifuged and the supernatant saved, while the precipitate was ground for five more minutes in the same mortar and then taken up in an equal volume of buffer. This was centrifuged and the supernatant mixed with the previous one and centrifuged for one hour at 12,000 r.p.m. in a Sorvall SS-1 centrifuge. The resulting, clear supernatant constitutes the crude extract. All of the above operations were carried out in the cold room (0–3° C).

Isolation of β-galactosidase

There are four different stages in the purification procedure: 1. precipitation of nucleic acids with streptomycin; 2. fractionation with $(NH_4)_2SO_4$; 3. fractionation by means of electrophoresis in starch; and 4. specific precipitation of the enzyme with an antiserum. Unless otherwise specified all operations were carried out in the cold room (0–3° C).

1. When one volume of a 10% solution of streptomycin was added to ten volumes of crude extract a stringy precipitate formed which, after standing overnight, was separated by centrifugation and the supernatant saved. The precipitate is largely nucleic acid[10]. The ratio of the optical density at 280 mμ to that at 260 mμ changed from 0.55 in the crude extract to 1.2 in this supernatant. No β-galactosidase is precipitated by this treatment.

2. A saturated solution of $(NH_4)_2SO_4$ (700 g + 1 liter H_2O) was added to the above supernatant to a final concentration of 40% saturation and the mixture allowed to stand for 12 hours. After centrifugation the precipitate was taken up in about 2 ml of 0.02 *M* tris-(hydroxymethyl)aminomethane-HCl (TRIS) buffer (pH = 8.1). This solution was centrifuged for one hour at 12,000 r.p.m. in the Sorvall SS-1 centrifuge and the supernatant subjected to dialysis against 6 l of 0.02 *M* TRIS buffer (pH = 8.1). The overall yield of enzyme at this point was about 70%.

3. The dialysed extract was fractionated by electrophoresis in starch, a method for purifying β-galactosidase that was suggested to us by SPIEGELMAN. The electrophoresis apparatus consisted of a rectangular trough of lucite 50 cm long, 3 cm wide and 2 cm high with walls 2 mm thick and open at the top. This trough was mounted horizontally and to each end was fastened a section of glass wool which made contact with an electrode vessel containing 4 l of 0.02 *M* TRIS buffer (pH = 8.1) and a carbon electrode. Rhone-Poulenc potato starch was washed four times with twice its weight of water and then with 0.02 *M* buffer (pH = 8.1) until the pH of the wet starch was 8.1. This thixotropic, wet starch was then poured into the lucite trough to form a layer of 1.5 cm high, making contact at each end with the glass wool. The levels of the buffer in the two electrode vessels were then made equal with a siphon and the system allowed to equilibrate for 3–4 hours at 0–5° C. Approximately 1 ml of the dialysed extract was mixed with washed, dried starch to form a paste of the same consistency as that of the starch in the trough and the mixture was placed in a hole which had been cut in the starch trough 15 cm from the cathode end. The electrodes were then connected to a 450–500 volt D.C. source and a current of 6 to 7 mA passed through the starch. After 15–18 hours the position of the β-galactosidase in the trough was determined by punching the starch at 1 cm intervals along the length of the column with thin-walled glass capillary tubing (diam. = 1 mm), adding a drop of 0.01 *M* *o*-nitrophenyl-β-D-galactoside (β-NPG) in 0.25 *M* sodium phosphate (pH = 7.0) to the starch removed with the capillary tube, and observing the appearance of the yellow color resulting from the enzyme catalysed hydrolysis of the β-NPG. Those 1 cm sections of starch that contained the enzyme were then removed and each section placed in a glass tube

References p. 116.

(14 mm in diameter and 10 cm long) which was constricted at the bottom and had a small amount of glass wool placed in this constriction to prevent the starch from leaking out of the tube. The enzyme was then eluted from the starch by passing 2.0 ml of 0.05 *M* sodium phosphate buffer (pH = 7.0) through the starch in the tube.

The enzyme activity and radioactivity of the eluates were determined and that eluate with the lowest radioactivity to enzyme activity ratio constituted the purified enzyme extract, this generally also being the eluate with the maximum amount of enzyme. The results from two typical electrophoresis fractionations are shown in Fig. 1. The total amount of enzyme recovered in the eluates was about 70% of that added to the starch, whereas the enzyme in the eluate that contains the maximum amount of enzyme constituted about 15% of that added. Thus the overall yield from crude to purified extract was about 10%.

The purification factor, or the ratio of the specific enzyme activity (units per mg sulfur) for the purified extract to that for the crude extract, was about 20 for extracts derived from fully induced bacteria (100 enzyme units per mg bacterial N). The approximate purification factors for steps 1, 2 and 3 of the procedure was 1.6, 4 and 3 respectively. Extracts from partially induced bacteria (enzyme units per bacterial N less than 100) obviously exhibit larger purification factors.

4. The specific precipitation of the enzyme was carried out with anti-enzyme sera absorbed with Pz[4]. This technique is discussed later (Table III).

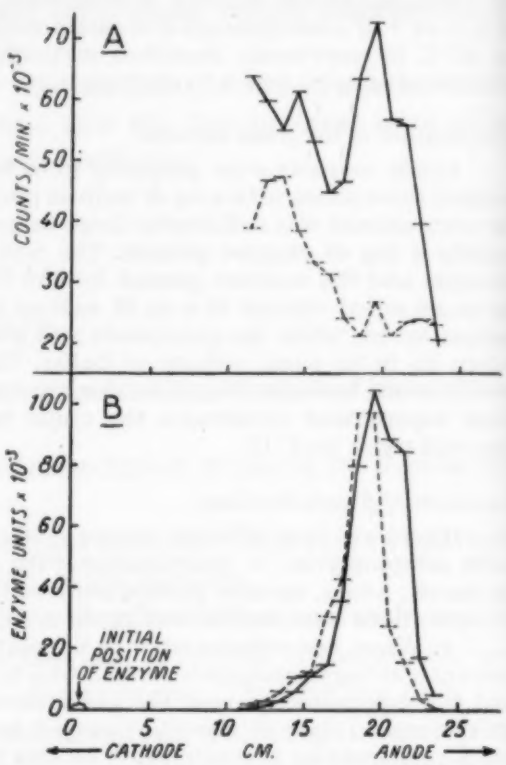

Fig. 1. Electrophoresis in starch of the fully labelled enzyme (full line) and its isolation control (dotted line). See the precursor experiment for an explanation of these extracts. A. Radioactivity in eluate versus distance along the column. B. Enzyme activity in eluate versus distance along the column. The total enzyme placed on the column was $8.0 \cdot 10^5$ units for the fully labelled enzyme and $5.2 \cdot 10^5$ units for its isolation control. The conditions under which the electrophoresis took place were as follows: voltage gradient = 9.2 volts per cm; current = 6 mA; duration of run = 16 hours for the fully labelled enzyme and 15 hours for its isolation control; temp. of column = 5–10° C.

Determination of radioactivity

The radioactivity of a given sample was determined by adding 0.30 ml of the sample to an aluminium cup (15 mm in diam. and 3 mm high) which was then placed under the infra-red lamp to dry. The dried sample was placed 12 mm under the window of a shielded Geiger Muller counter (General Electric Company, England-Type EHM2S with a mica window of 2–3 mg per cm^2 weight) and the number of counts per minute determined. The efficiency of this counter was approximately 5% and the shielded background 12 counts per min. All samples were analysed in duplicate and the total number of counts observed was always greater than 1000. Under these conditions the counts per min were proportional to the concentration of the radioactive component up to $3 \cdot 10^3$ counts per min and the reproducibility better than 5%. Consequently the samples were always diluted so that the radioactivity put on the aluminium cup was less than $2.5 \cdot 10^3$ counts per min.

EXPERIMENTAL

The specific labelling of the protein fraction of the bacteria with radioactive ^{35}S

If the synthesis of β-galactosidase were induced in a culture in which the only source of radioactivity was the bacterial proteins, then the isolation of the enzyme and the determination of its radioactivity would provide a sensitive means of evaluating what proportion of the elements of β-galactosidase is contributed by other proteins. Let us therefore first direct our attention towards the problem of specifically labelling the

References p. 116.

non-β-galactosidase proteins (*i.e.* those produced in the non-induced state) with a radioactive isotope.

Since *E. coli* grows well in a synthetic medium containing sulfate as the sole source of sulfur, it is convenient to use the radioactive isotope of sulfur, ^{35}S, as the labelling atom. The experiment described in Fig. 2 illustrates the manner in which the bacteria incorporate sulfur. During the logarithmic phase of growth, the incorporated sulfur consists of two fractions: the trichloracetic acid (TCA) soluble fraction (25% of incorporated sulfur) and the TCA insoluble or protein fraction (75% of incorporated sulfur). When approximately 90% of the total sulfur has been incorporated, the growth diminishes and sulfur incorporation comes to a halt. At this point the ratio between the TCA insoluble and soluble fractions begins to increase until all of the incorporated sulfur is in the TCA insoluble or protein fraction, at which point growth ceases. That growth ceases because of a lack of sulfur is evident from the fact that growth will resume immediately upon the addition of sulfate to the culture.

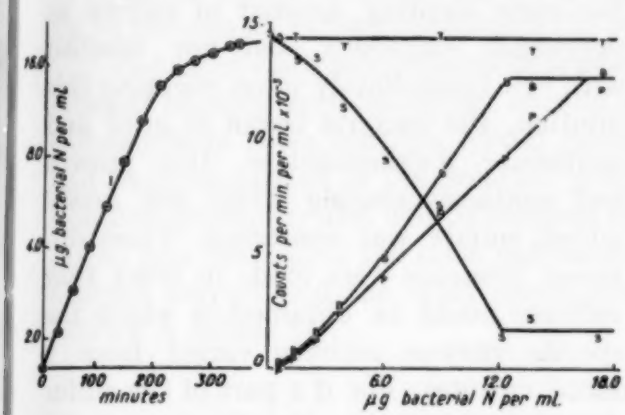

Fig. 2. Incorporation of radioactive ^{35}S by *E. coli*. ML 32400 grown in medium 61 containing a limiting amount of $(NH_4)_2SO_4$ labelled with ^{35}S. Samples taken at various times and analysed as follows. Left: total bacterial nitrogen per ml (curve I). Right: – curve T, total radioactivity per ml of culture; – curve B, radioactivity of bacteria after three washings; – curve P, radioactivity of bacteria after above washing, treatment with 5% trichloracetic acid (TCA) for 15 minutes at 0–5° C, and three washings with 5% TCA; – curve S, radioactivity of supernatant after centrifugation of culture.

These results confirm the work of COWIE, BOLTON AND SANDS[11] who found that the incorporation of ^{35}S of sulfate into the proteins of *E. coli* is proportional to the growth. Similarly ROBERTS AND BOLTON[12] found that 25% of the incorporated sulfur of *E. coli* is TCA extractable and consists primarily of glutathione, which can be incorporated into the protein fraction. That sulfur which remains in the supernatant after growth ceases has not been identified but it apparently consists of non-utilizable sulfur since it is not incorporated by bacteria growing in this supernatant supplemented with a limiting amount of non-radioactive sulfate.

From the above data, it is evident that the non-β-galactosidase proteins can be specifically labelled with the radioactive isotope ^{35}S by simply allowing the culture to grow to starvation in a non-inducing medium which contains a limiting amount of ^{35}S labelled sulfate, the other components being kept in excess. If non-radioactive sulfate and an inducer are added to such a starved culture, β-galactosidase will then be synthesized in cells whose other proteins are labelled with ^{35}S although the medium contains no utilizable ^{35}S sulfur. This is the system we desire.

The de novo synthesis of β-galactosidase. Precursor experiment

Employing the above system, the precursor experiment schematized in Fig. 3 was performed. Cells in phase I were obtained by inoculating a synthetic medium that contained a limiting amount of ^{35}S-labelled sulfate and no inducer. This culture was allowed to grow to a maximum (*i.e.* until all of the sulfate had been utilized) and was kept in this starvation state for one hour so that all of the incorporated sulfur was in the

References p. 116.

protein fraction. These cells in phase I were then allowed to pass into phase II by diluting the starved culture into a non-radioactive medium that contained the inducer, methyl-β-D-thiogalactoside (MTG), and the same limiting amount of sulfate as previously employed, but not labelled with ^{35}S. Immediately upon effecting this dilution, the bacteria began to grow and synthesize β-galactosidase, this growth and synthesis ceasing when the newly added sulfate was consumed. Three different dilutions were made in order that cultures could be obtained in which the specific enzyme activity varied from 5 to 58% of the maximum found in fully induced cultures. For if a part of the sulfur of β-galactosidase were derived from pre-existing proteins, then the fraction of the enzyme synthesized initially should contain the highest proportion of ^{35}S and consequently the β-galactosidase isolated from cultures of lower specific enzyme activity should have the higher ratio of radioactivity per enzyme unit. These three starved cultures were then harvested by centrifugation and the bacteria washed and ground up to make the crude extracts from which the enzyme was isolated. The details and results of this culture phase of the precursor experiment are presented in Table I.

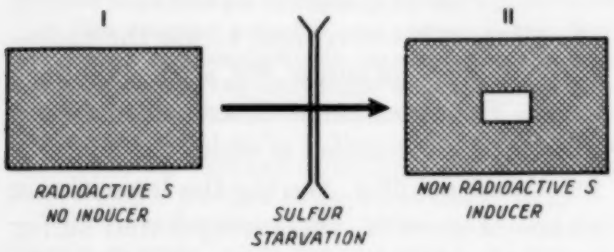

Fig. 3. Schematic of the precursor experiment. Rectangles represent total bacterial protein. Central rectangle represents β-galactosidase. Shading indicates radioactivity.

TABLE I

PRECURSOR EXPERIMENT – CULTURES

Cultures	Bacterial concentration			Enzyme concentration			
	Initial (μg N/ml)	*Final-starved (μg N/ml)*	*% Total growth occurring in phase II*	*Initial (units/ml)*	*Final-starved (units/ml)*	*100 Initial/Final*	*Final specific activity (units/μg N)*
Phase I	< 0.1	118	—	0	7	—	0.06
Phase II A	106	126	16	6	630	1.0	4.8
B	89	124	28	5	3,900	0.13	32
C	67	118	43	4	6,800	0.06	58
Fully labelled Enzyme control	< 0.1	112	—	0	11,200	—	100

Medium for phase I was the medium 61 plus 10 mg succinic acid per ml and 38 μg of ^{35}S labelled $(NH_4)_2SO_4$ per ml (9.2 μg S per ml). The specific radioactivity of the sulfur was $1.9 \cdot 10^4$ counts per minute per μg S. The medium added to achieve phase II was the medium 61 plus 10 mg succinic acid per ml, 38 μg non-radioactive $(NH_4)_2SO_4$ per ml, and sufficient methyl-β-D-thiogalactoside (MTG) to obtain a final concentration of $1.0 \cdot 10^{-3}$ *M*. The medium used for the fully labelled enzyme control was the same as that employed in phase I but contained in addition MTG at $5.0 \cdot 10^{-4}$ *M*.

Before considering the results obtained upon isolating the enzyme from these extracts, we must discuss the controls that were used. The first control was designed to obtain ^{35}S-labelled β-galactosidase in which the specific radioactivity of the sulfur was the same as that of the radioactive medium employed in phase I above. We shall call this the *fully labelled* enzyme. It served as a standard of comparison whereby the radioactivity of the enzyme isolated from the three extracts could be evaluated. Thus a

References p. 116.

medium identical with that used in phase I except that it contained the inducer MTG, was inoculated with a trace of *E. coli* (see Table I). This culture was allowed to grow to its sulfur limit, was harvested by centrifugation and the bacteria washed and ground up to provide an extract containing the fully labelled enzyme.

The other controls consisted of artificial mixtures of an extract of non-induced ^{35}S-labelled bacteria with an extract of fully induced non-radioactive bacteria. The enzyme isolated from these controls should contain no radioactivity if all the other proteins had been eliminated in the isolation procedure. Consequently these controls check the isolation technique and will be referred to as *isolation controls*. Two such controls were made: one containing the same radioactivity and enzyme activity as the fully labelled enzyme extract and the other duplicating the radioactivity and enzyme activity of extract A (phase II).

TABLE II

PRECURSOR EXPERIMENT – EXTRACTS

Extract		*Enzyme activity (units/ml)*	*Radioactivity (counts/min/ml)*	$C = \frac{\text{Radioactivity}}{\text{Enzyme activity}}$ *(counts/min/enzyme unit)*
Phase II		× 10^{-4}	× 10^{-4}	
A – crude		1.40	109	78
– purified		0.42	0.91	2.1
B – crude		6.8	130	19.1
– purified		2.64	1.38	0.52
C – crude		12.0	84	7.0
– purified		8.0	0.95	0.118
Controls				
1. Fully labelled enzyme	– crude	10.1	110	10.9
	– purified	4.2	2.78	0.66
2. Isolation control for fully labelled enzyme	– crude	10.5	109	10.4
	– purified	5.0	1.33	0.27
3. Isolation control for phase II-A	– crude	1.37	91	66
	– purified	0.60	0.45	0.76

The preparation of the crude extracts and their purification are described in MATERIALS AND METHODS.

The essential element in the isolation procedure consisted of a specific precipitation of the enzyme by anti-β-galactosidase serum. This serum was completely absorbed with an extract of non-induced bacteria, and then fractionated[4] to isolate the antibody-containing γ globulin. This preparation would not precipitate with Pz, or for that matter with any other protein in the inactive extract, but it continued to precipitate the enzyme. Since the antibody did not inactivate the enzyme it was possible to determine the enzymic activity as well as the radioactivity on the washed specific precipitate. With the purification procedure which was finally adopted the isolation control contained only 0.4% of the radioactivity of the fully labelled enzyme (Table III). Thus a technique was realized whereby β-galactosidase could be isolated from an extract containing only 2–3 mg of enzyme, representing less than 0.2% of the total material.

Bearing in mind the significance of these controls, let us now turn our attention to

References p. 116.

PRECURSOR EXPE

Purified extract	Totals			
	Enzyme activity (units × 10^{-3})			Radioactivity (counts/min ×
	from extract	carrier	total	
Phase II				
A	6.0	26.8	32.8	12.9
B	29.0	—	29.0	15.2
C	28.0	—	28.0	3.3
Controls				
1. Fully labelled enzyme	25.4	—	25.4	16.7
2. Isolation control for fully labelled enzyme	27.5	—	27.5	7.3
3. Isolation control for state 2, I	8.3	24.0	32.3	6.3

β-galactosidase was precipitated from the extracts by adding 1.00 ml of antiserum capable of precipitating $4 \cdot 10^4$ units of enzyme (MATERIALS AND METHODS) to 2.00 ml of extract containing approximately $3 \cdot 10^4$ units of enzyme. In the case of phase II-A and its isolation control it was necessary to add carrier enzyme (partially purified non-radioactive enzyme extract) because of the small amount of enzyme recovered in the purification procedure. Immediately after mixing the antiserum and the enzyme extract, a 0.100 ml sample was withdrawn and analysed for enzyme activity and radioactivity (totals). The mixture was then allowed to stand in a 37° C bath until the precipitate

the results of the precursor experiment, summarized in the last column in Table III which gives the radioactivity per enzyme unit for the β-galactosidase in the various extracts, relative to that of the fully labelled enzyme. In considering the relative radioactivity of the enzyme in the three experimental extracts A, B and C, the amount of radioactivity corresponding to the trace amount of enzyme synthesized in the non-inducing radioactive medium employed in phase I must be taken into account. Thus in the case of sample A, 1.0% of the total enzyme extracted would be expected to be fully labelled since this percentage was synthesized in phase I (see Table I). In samples B and C only 0.13 and 0.06% of the total enzyme would be expected to be fully labelled as a result of synthesis in phase I (Table I). The relative value for the radio-activity per enzyme unit found in the specific precipitates should therefore be corrected by substracting the percentage of enzyme in the extracts that is fully labelled due to synthesis in phase I. Such a correction shows that for samples A, B and C, the amount of radioactivity associated with the enzyme synthesized in phase II is respectively 0.1, 0.8 and 0.1% of that of the fully labelled enzyme. Since there is no definite order to the values (*i.e.* A > B > C) and since these values are within the range of reproducibility of the isolation controls, we may conclude that in each sample less than 0.8% of the sulfur of the sulfur of the enzyme synthesized in phase II was derived from non-β-galactosidase proteins synthesized in phase I. This result, taken in conjunction with the fact that in sample A the enzyme level was only 5% of that found in the fully induced bacteria, indicates that if any protein precursor of β-galactosidase exists in the non-induced bacteria, its level (expressed as amount of sulfur per bacterial nitrogen) must be less than 0.04% of that for β-galactosidase in fully induced bacteria.

Thus the possibility that the Pz protein is a precursor of β-galactosidase is effectively

References p. 116.

CIFIC PRECIPITATES

Supernatants		Precipitates			
Enzyme activity (units × 10^{-3})	Radioactivity (counts/min × 10^{-3})	Enzyme activity (units × 10^{-3})	Radioactivity (counts/min × 10^{-3})	$C = \frac{\text{Radioactivity}}{\text{Enzyme activity}}$ $\left(\frac{\text{counts/min}}{\text{enzyme units}}\right)$	Percent of C for fully labelled enzyme
0.48	12.6	29.6 (5.4)	0.027	0.0050	1.1
1.29	14.4	26.0	0.112	0.0043	0.9
0.085	3.0	26.2	0.019	0.00072	0.16
0.093	5.4	25.9	11.6	0.45	100
0.120	7.3	27.8	0.052	0.0019	0.42
0.35	6.4	28.3 (7.2)	0.013	0.0018	0.40

had flocculated (*ca.* 2 hours). It was centrifuged and the supernatant withdrawn for analysis. The precipitate was washed three times with cold (0–5° C) 0.85% NaCl solution, suspended in 1.00 ml of 0.05 *M* sodium phosphate buffer, pH = 7.0, and the enzyme activity and radioactivity of this suspension determined.

The values in the parentheses in the column for enzyme activities of the precipitate equal the amount of enzyme from the extract (*i.e.* after correction was made for carrier enzyme). The *C* values in the next to last column are calculated from these corrected enzyme activities.

eliminated. For the Pz protein level in non-induced bacteria (expressed as immunological combining units per bacterial nitrogen) is approximately 30% of the enzyme (Gz) level in fully induced bacteria[5] and consequently if the Pz protein were a precursor of the enzyme, one would be forced to the highly improbable conclusion that the amount of sulfur per unit of Pz protein would have to be less than 0.1% of that for the enzyme.

More generally, the results of the precursor experiment indicate that β-galactosidase is synthesized exclusively from material that is assimilated after the addition of the inducer and hence proteins existing in the non-induced bacteria play no significant role as precursors.

The stability of proteins in vivo

A second conclusion can be drawn from the results of the precursor experiment, namely, that non-β-galactosidase proteins are stable, not being degraded to amino acids by any mechanism. For if the state of the proteins within the cell consists of a continual synthesis from and breakdown to their constituent amino acids (*i.e.* state of "dynamic equilibrium"), then one would expect the β-galactosidase synthesized in phase II of the experiment to be labelled with ^{35}S as a result of the breakdown of the radioactive proteins. Since the amount of radioactivity found in the enzyme synthesized in phase II was less than 0.8% of that for the fully labelled enzyme, we can conclude that the rate of breakdown of the non-β-galactosidase proteins must be less than one percent of the rate of synthesis. That this is true is clear from a consideration of the following diagram:

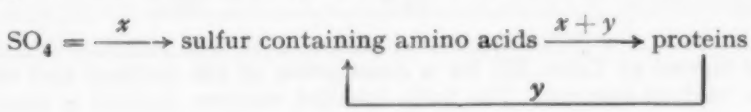

References p. 116.

in which x equals the rate of net synthesis of the proteins and y equals the rate of breakdown. The specific radioactivity of the sulfur in the non-β-galactosidase proteins in sample A is 84% of that of the proteins in phase I or of that of the fully labelled enzyme (see Table I). Hence the minimum specific radioactivity of the sulfur in the amino acids resulting from any breakdown of these proteins would be 84% of that of the fully labelled enzyme. Since the sulfur-containing amino acids synthesized directly from the sulfate of the medium during phase II cannot be radioactive and since there is no appreciable amino acid pool in *E. coli*, then the specific radioactivity of the sulfur in the total amino acids which act as precursors to protein synthesis would have a minimum specific radioactivity that was $84y/(x + y)$ percent of that of the fully labelled enzyme. Thus the β-galactosidase synthesized from these amino acids would have a minimum specivc radioactivity that would also be $84/(x + y)$ percent of that of the fully labelled enzyme. Since the enzyme in sample A that was synthesized in phase II was found to contain less than 0.8% of the radioactivity of the fully labelled enzyme, then $84y/(x + y$ must be less than 0.8, or $y/(x + y)$ must be less than 0.01, *i.e.* the rate of breakdown of

TABLE IV

STABILITY OF β-GALACTOSIDASE DURING BACTERIAL GROWTH IN THE ABSENCE OF AN INDUCER

I. Cultures

Culture	*Bacterial concentration*		*Enzyme concentration (units/ml)*	
	Initial (μg N/ml)	*Final (μg N/ml)*	*Initial*	*Final*
Phase I	< 0.1	95	0	10,150
Phase II	12.0	126	1,309	1,290

Medium for phase I was the medium 61 plus 10 mg succinic acid per ml, 38 μg $(NH_4)_2SO_4$ per ml and $5 \cdot 10^{-4}$ *M* MTG. The medium for phase II was the same except that the MTG was omitted and the $(NH_4)_2SO_4$ was labelled with ^{35}S such that the specific radioactivity of the sulfur was $1.9 \cdot 10^4$ counts per min per μg S, *i.e.* the same as that employed in the precursor experiment.

II. Extracts

Extract	*Enzyme activity (units/ml × 10⁻⁴)*	*Radioactivity (counts/min/ml × 10⁻⁴)*	$C = \frac{\text{Radioactivity}}{\text{Enzyme activity}}$ *(counts/min/enzyme unit)*
Phase II – crude	1.74	126	72
– purified	1.29	0.98	0.76

See MATERIALS AND METHODS for the preparation of the crude extract and the purification procedure.

III. Specific precipitates

Purified extract	*Total*			
	Enzyme activity (units × 10⁻³)			*Radioactivity (counts/min × 10⁻⁴)*
	from extract	*carrier*	*total*	
Phase II	15.7	20.7	36.4	11.9

See the legend of Table III for a description of the method and an explanation of the data given in the various columns. The fully labelled enzyme control is that given in Table III since

References p. 116.

the non-β-galactosidase proteins must be less than one percent of the rate of synthesis.

The validity of this interpretation is dependent upon the assumption that all of the amino acids derived from the proteins are re-utilized for protein synthesis. That this assumption is reasonable is supported by the work of COWIE, BOLTON AND SANDS[11] who showed that amino acids once incorporated into the protein of *E. coli* are not released to any significant extent into the medium. This result, which we have confirmed, is also a striking demonstration of stability of the proteins of *E. coli* during growth.

This conclusion, surprising in view of the generally accepted idea of the "dynamic state" of proteins *in vivo*, led us to investigate the stability of the β-galactosidase by the very simple and sensitive experiment schematized in Fig. 4. Cells in phase I were obtained by allowing the bacteria to grow to a limit on non-radioactive sulfate in the presence of the inducer, MTG. These starved cells were washed to remove the inducer and were then placed in a non-inducing, ^{35}S-labelled sulfate medium in which a ten-fold increase in bacterial mass took place before growth stopped due to lack of sulfate (phase II). It can be seen from Table IV that the total enzyme in the culture remained constant during growth in phase II. Thus any incorporation of ^{35}S into the enzyme is a measure of both the amount of synthesis and of the amount of breakdown of the β-galatosidase in phase II, *i.e.* in bacteria growing in the absence of the inducer. From Table IV it can be seen that the amount of radioactivity in the enzyme isolated from phase II bacteria is only 0.4% of that of the fully labelled enzyme. The isolation control for sample A of the precursor experiment also applies to this experiment since the enzyme activity and radioactivity of the crude extracts are approximately the same. The fact that the phase II enzyme has the same radioactivity per enzyme unit as its isolation control makes it highly improbable that the radioactivity in the phase II enzyme is significant. In any case it must be less than 0.4% of that of the fully labelled enzyme. This means that less than 0.4% of the enzyme could have been broken down while the total bacterial mass increased by 900%. Since in the presence of an inducer such as MTG the increase in the enzyme is proportional to the increase in bacterial mass, then the rate of breakdown of the enzyme during bacterial growth in the absence of the inducer is less than 0.2% of the rate of synthesis of the enzyme in the presence of the inducer.

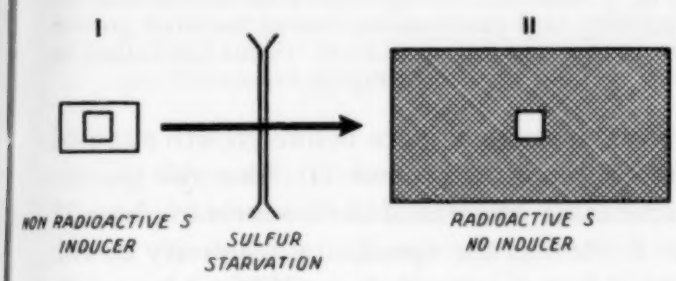

Fig. 4. Schematic of experiment for determining the stability of β-galactosidase during bacterial growth in the absence of an inducer. (Same symbolism as in Fig. 3).

Supernatant		*Precipitate*			
Enzyme activity (units × 10⁻³)	*Radioactivity (counts/min × 10⁻³)*	*Enzyme activity (units × 10⁻³)*	*Radioactivity (counts/min × 10⁻³)*	$C = \frac{\text{Radioactivity}}{\text{Enzyme activity}}\left(\frac{\text{counts/min}}{\text{enzyme units}}\right)$	*Percent of C for fully labelled enzyme*
0.44	11.8	30.3 (13.1)	0.024	0.0018	0.40

sulfur of the same specific radioactivity was used in the two experiments.

References p. 116.

While the above experiment indicates a very high degree of stability of β-galactosidase in bacteria in which no synthesis of the enzyme occurs (*i.e.* in the absence of the inducer), it tells us nothing of the stability of β-galactosidase in bacteria in which active β-galactosidase synthesis occurs (*i.e.* in the presence of the inducer). Since the inducer functions much like a catalyst in promoting the synthesis of the enzyme, one could imagine that the inducer also acts to catalyse the breakdown of the enzyme. It was therefore necessary to determine if any breakdown of the enzyme occurs during synthesis in the presence of the inducer. The experiment schematized in Fig. 5 was designed for this purpose. Bacteria in phase I were obtained by inoculating a radioactive medium containing the inducer MTG and allowing the bacteria to grow till starved on sulfur. The inducer was removed by washing and the bacteria were then placed in a non-radioactive medium in which a ten-fold increase in bacterial mass took place before growth stopped as a result of exhaustion of the carbon source, succinic acid (phase II). Thus the specific radioactivity of the sulfur in the non-β-galactosidase proteins of the bacteria in phase II decreased to nine percent of that in phase I whereas the specific radioactivity of the sulfur in the enzyme remained constant at the phase I value. Inducer MTG and succinic acid were then added, growth and β-galactosidase synthesis beginning immediately upon effecting this addition and ceasing when the succinic acid was again used up (phase III). Three different samples of phase III bacteria, in which the percentage of the enzyme that was synthesized in phase I varied form 13 to 68%, were obtained by the addition of different amounts of succinic acid to the starved phase II culture. The data for these cultures are given in Table V and for the extracts derived from them in Table VI, while Table VII gives the results of the specific precipitation of the enzyme from the purified extracts.

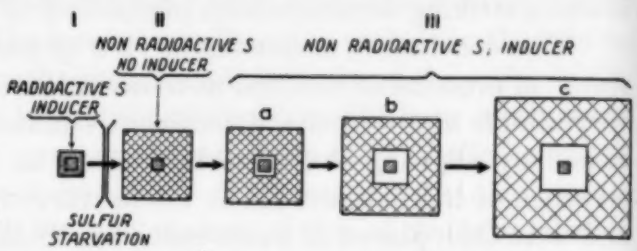

Fig. 5. Schematic of experiment for determining the stability of β-galactosidase during bacterial growth in the presence of an inducer. (Same symbolism as in Fig. 3).

TABLE V

STABILITY OF β-GALACTOSIDASE DURING BACTERIAL GROWTH IN THE PRESENCE OF AN INDUCER CULTURES

Culture	*Bacterial concentration*			*Enzyme concentration (E)*		
	Initial (μg N/ml)	*Final (μg N/ml)*	*% total growth occurring in phase I*	*Initial (units/ml)*	*Final (units/ml)*	*% total enzyme synthesized in phase I*
Phase I	< 0.1	132	100	0	13,700	100
Phase II	10.1	115	8.8	1,050	1,020	100
Phase III						
A	115	122	8.3	1,020	1,500	68
B	115	130	7.8	1,020	4,930	20.7
C	115	160	6.3	1,020	8,100	12.6

The medium used in phase I was the medium 61 plus 10 mg succinic acid per ml and 42 μg of ^{35}S labelled $(NH_4)_2SO_4$ per ml (10.2 μg S per ml) and $5 \cdot 10^{-4}$ *M* MTG. The specific radioactivity of the sulfur was $1.35 \cdot 10^4$ counts per min per μg S. The medium for phase II was medium 56(7) plus 3.5 mg succinic acid per ml. When the phase II culture had ceased to grow due to lack of succinic acid, it was divided into three parts (cultures A, B and C) and the inducer, MTG, and succinic acid were added such that the MTG concentration was $1.0 \cdot 10^{-3}$ *M* for each of the three cultures and the succinic acid concentration was 0.2, 0.5 and 1.6 mg per ml for cultures A, B and C respectively.

References p. 116.

TABLE VI

STABILITY OF β-GALACTOSIDASE DURING BACTERIAL GROWTH IN THE PRESENCE OF AN INDUCER EXTRACTS

Extract	Enzyme activity (units/ml × 10^{-4})	Radioactivity (counts/min/ml × 10^{-4})	$C = \frac{\text{Radioactivity}}{\text{Enzyme activity}}$ (counts/min/enzyme unit)
Phase I – crude	32	256	8.0
– purified	9.5	3.4	0.36
Phase II – crude	2.5	20.8	8.3
– purified	1.9	0.78	0.41
Phase III			
A – crude	3.8	25.4	6.7
– purified	2.2	0.66	0.30
B – crude	6.7	14.4	2.1
– purified	1.9	0.20	0.105
C – crude	10.3	13.4	1.3
– purified	6.9	0.56	0.081

See MATERIALS AND METHODS for the preparation and purification of the crude extracts.

If there were no breakdown of β-galactosidase in phase III of the experiment, then the total amount of radioactivity associated with enzyme should remain constant and hence the enzyme radioactivity per ml should be the same for cultures in phase II, and phase III, (samples A, B and C). The enzyme radioactivity per ml of these cultures is equal to the enzyme concentration in the culture (E) multiplied by the radioactivity per enzyme unit (C) found in the specific precipitate. If no breakdown took place during active enzyme synthesis, then $E.C = K$, a constant, and consequently a plot of C versus $1/E$ should yield a straight line with slope K and intercept at the origin. When the data are plotted in this fashion (Fig. 6) it is clear that they fit such a straight line. The curved dashed line in Fig. 6 is the curve that would be expected if the rate of breakdown of β-galactosidase were ten percent of the rate of net synthesis. This curve definitely lies outside the limits of experimental error associated with the determination of the C and E values, these errors being such that the lowest breakdown rate detectable would be 5% of the rate of net synthesis. Therefore the rate of breakdown of β-galactosidase during bacterial growth in the presence of the inducer must be less than 5% of the rate of net synthesis of the enzyme.

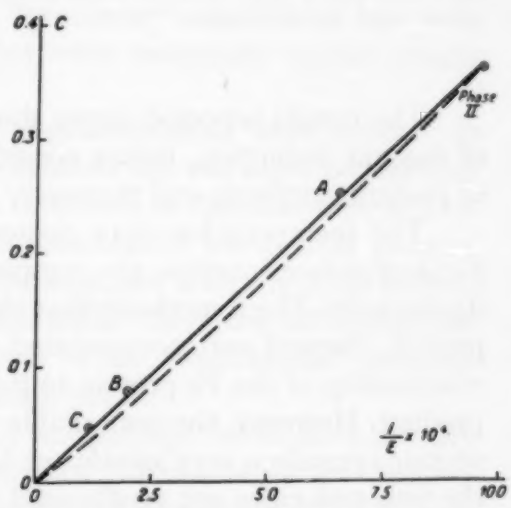

Fig. 6. Stability of β-galactosidase during bacterial growth in the presence of an inducer. Abscissa: Inverse of enzyme activity (units per ml) in the cultures during phase II and phase III (A, B, C) of the experiment schematized in Fig. 5. Ordinate: radioactivity to enzyme activity ratio of the specific precipitates given in counts per min. The dashed-line represents the expected curve if the rate of breakdown were 10% of the net rate of synthesis. The errors involved in the determination of C and E are approximately seven and five percent respectively. [5]

Although this latter experiment is less sensitive than the previous two it nevertheless indicates that β-galactosidase synthesis in

References p. 116.

STABILITY OF β-GALACTOSIDASE DURING BACTERIAL GRO

Purified extract	Totals		Supernatants	
	Enzyme activity (units × 10^{-3})	Radioactivity (counts/min × 10^{-3})	Enzyme activity (units × 10^{-3})	Radioactivity (counts/min ×
Phase I	27.5	9.8	0.110	0.98
Phase II	28.0	11.7	0.120	2.25
Phase III				
A	28.0	8.5	0.160	1.78
B	28.2	3.0	0.30	0.96
C	27.5	2.25	0.078	1.09

See the legend of Table I for a description of the method and an explanation of the data given in the various columns. Note that the average *C* value for the specific precipitate of phase I and phase II (fully labelled enzyme) is 78% of that found for the fully labelled enzyme in the precursor experiments (Table III). This is due to the fact that the sulfur used in this experiment had a specific radioactivity that was 71% of that used in the precursor experiment (Tables I and V).

the presence of the inducer is an essentially irreversible process. Therefore we must conclude that the proteins of *E. coli* are extremely stable molecules *in vivo*, synthesized by essentially irreversible reactions.

DISCUSSION

The results reported above should be discussed in relation to the specific problems of enzyme induction, before considering their bearings on the more general problems of protein synthesis and turnover.

The incorporation data demonstrate conclusively that the induced synthesis of β-galactosidase involves the complete, *de novo*, formation of the protein molecule from its elements. The hypothesis that the induced enzyme is a conversion product of another protein, formed and accumulated in the absence of inducer, is eliminated. Thus the relationship of the Pz protein to β-galactosidase can not be one of a precursor to a final product. However, the remarkable structural and physiological relationships of the two proteins remain a very significant fact, which can be understood on the assumption that the two molecules are synthesized by the same mechanisms, or at the same sites. This invites certain interesting speculations concerning in particular the analogy between the Pz-Gz system and the normal and antibody globulin[13, 14] systems. However these aspects need not be considered now, since the data presented here have no specific bearings upon them.

It should be noted that our experiments involved a step of sulfur starvation during which sulfur from the TCA soluble fraction was incorporated into protein. The experiments do not exclude, therefore, the possibility that such materials might function as a source of elements for β-galactosidase. COWIE *et al.*[15] have observed that *E. coli* B normally contains a certain alcohol-soluble "protein" fraction which disappears during sulfur starvation. If such material could serve as reserve of sulfur for β-galactosidase, it would not have been detected by our experiments. However the same workers have found that under normal conditions of growth, no sulfur from this particular fraction went into other proteins.

References p. 116.

RESENCE OF AN INDUCER. SPECIFIC PRECIPITATES

Precipitates			
Enzyme activity (units × 10^{-3})	Radioactivity counts/min × 10^{-3})	$C = \frac{\text{Radioactivity}}{\text{Enzyme activity}}$ $\left(\frac{\text{counts/min}}{\text{enzyme unit}}\right)$	Percent of C for phase II
26.4	9.0	0.34	95
25.4	9.2	0.36	100
26.8	6.6	0.25	69
26.2	2.08	0.079	21.9
25.0	1.18	0.047	13.0

Thus if the C values are converted to the more absolute quantity, the number of sulfur atoms per enzyme unit, with the aid of the specific radioactivities, then the values $4.6 \cdot 10^{11}$ and $4.9 \cdot 10^{11}$ atoms S/enzyme unit are found for the precursor experiment and the above experiment respectively. These two values are within the experimental error involved in the determination of the C values (*ca* 7%) and the specific radioactivity (*ca* 10%).

It should also be remarked that our experiments were carried out with labelled sulfur and therefore the conclusions apply rigorously only to the sulfur-containing precursors. However an experiment similar to our "precursor" experiment has been carried out by SPIEGELMAN using carbon-14 as a label, with essentially similar results (personal communication).

The incorporation data also demonstrate that β-galactosidase, once formed, is stable within the cells. These observations therefore confirm the tentative conclusions drawn from previous kinetic and nutritional studies[6]. Induction in the case of β-galactosidase, results in the initiation or acceleration of an esssentially irreversible process. The enzyme is evidently not in "equilibrium" with a precursor, nor with any other protein within the cells, nor with a pool of precursors or amino acids. Therefore, all interpretations of enzyme adaptation in terms of the alteration of an "equilibrium" between proteins within the cell[16,17,18,23,24], are shown to be inadequate.

This leads us to considering the broader aspects of our findings. As we have already noted, the results demonstrate not only that β-galactosidase is irreversibly synthesized, stable, and static within the cells, but that this must be true of essentially all, or at least of the bulk of *E. coli* proteins. A simple calculation (p. 107) shows that if there is any degradation of proteins, or exchange of amino acids between proteins within the growing cells, the rate of such a process must be so low that it plays no role in fixing the net rates of protein synthesis. Nor does this process contribute appreciably to determining the relative composition and structure of the growing cells, as far as proteins are concerned. In other words, all or most proteins, within *E. coli* cells, are in a static, not in a dynamic state.

These results might therefore appear, at first, to be at variance with the classical findings of SHOENHEIMER and his school on the turnover of proteins in the body or tissues of higher organisms. Rather than concede that this inconsistency implies that the cellular state of the proteins in mammalian tissues is essentially different from that in *E. coli*, we have sought an explanation for this inconsistency in the different properties of the two systems.

References p. 116.

One objection that we should like to dismiss before considering the different properties of the two systems is that our experiments were of too short a duration to detect degradation rates of the order of magnitude of those found in mammalian system. It is obvious that the rate of degradation must be a significant fraction of the rates of synthesis if the concept of a "dynamic state" is to have any general physiological significance at the cellular level. Therefore it is the rate of degradation relative to that of synthesis which is of importance and not the absolute rate of degradation.

The critical question appears to be the *interpretation* of the incorporation data in the case of the mammalian systems. The interpretations of such data in terms of a "dynamic state" of the protein molecules within the cells involve some inherent ambiguities. The nature of this difficulty is evident when one considers the degree of homogeneity of the cellular populations in the two systems.

The bacterial system used in our experiments consists of a homogeneous population of cells in which there is no observable cell lysis or secretion of proteins from the cells and where all the cells are placed in an identical environment. The incorporation data are therefore interpretable in terms of the synthesis and of the state of the proteins within the cells. Any renewal would have to be interpreted as reflecting a dynamic state of the protein within the cells. However, as we see, no such renewal is detected with these homogeneous systems.

Mammalian systems on the other hand consist of heterogeneous populations of cells placed under different environmental conditions in which some cells grow and multiply, some die and lyse, others secrete large amounts of proteins while still others appear to remain very stable. Thus there are three possible pathways by which tissues of such systems may lose proteins: 1. intracellular degradation; 2. secretion; and 3. cell lysis.

Labelling experiments with mammalian systems do not by themselves give the information necessary to determine by which of the above three paths the protein is lost from the tissue. That secretion and cell lysis play a dominant role in the mechanism by which proteins are removed from the tissue is indicated by the fact that tissues with high turnover rates are those in which the mitotic rate (*i.e.* cellular replacement) is very high (intestinal mucosa) or which are known to secrete proteins actively (liver) whereas very low turnover rates are associated with tissues in which both cellular replacement and protein secretion are minimal [muscle and nerve (cf. [19])]. This suggests very strongly indeed that turnover rates measured under these conditions, express the dynamic state of the tissue, rather than the state of the protein molecules within the cells. In any case, there is, to our knowledge, no experimental evidence that the proteins within the cells of mammals are any more "dynamic" than those of *Escherichia coli*. And it should be pointed out that it is not easy even to imagine an experiment which would test intracellular turnover with mammalian tissue systems. Possibly the best illustration of these difficulties can be drawn from the beautiful experiments of VELICK and coworkers on the synthesis of the three enzymes aldolase, phosphorylase and glyceraldehyde-3-phosphate dehydrogenase in muscle tissue*[20,21]. These workers found that the extremely low rate of incorporation of several amino acids into the dehydrogenase of rabbit muscle, was significantly lower than the rate of incorporation into the two other enzymes. This might of course be interpreted as expressing a difference in the intracellular turnover of the different molecules. It might however, just as well, be interpreted

* It should be noted that these experiments were designed to study the intermediates in protein synthesis, not to test the dynamic state hypothesis.

References p. 116.

as resulting from differences in composition, and rates of net synthesis in different parts, or at different levels in the tissue. Wherever there may exist metabolic gradients of any sort, a heterogeneity of the cell population as regards the rates of synthesis of various proteins is to be expected. The experience gained in the study of enzyme make-up of homogeneous bacterial populations renders such an hypothesis very likely, since it is commonly observed that even slight changes in conditions (nutritional and other) may profoundly alter the relative rates of synthesis of different proteins within the cells, as well as the net rate of cell growth.

To sum up: there seems to be at present no conclusive evidence that the protein molecules within the cells of mammalian tissues are in a dynamic state. Moreover our experiments have shown that the proteins of growing *E. coli* are static. Therefore, it seems necessary to conclude that the synthesis and maintenance of proteins within growing cells is not necessarily or inherently associated with a "dynamic state".

The experimental work on this problem was begun by Dr. A. M. PAPPENHEIMER Jr. during his stay with us at the Pasteur Institute. We should like to gratefully acknowledge his early and decisive contribution.

We would like to thank Mr. RAYMOND BARRAND for his competent and enthusiastic technical assistance.

SUMMARY

A study of the kinetics of sulfur incorporation into the molecule of β-galactosidase during the induced synthesis of this enzyme in *E. coli* brings proof that the enzyme-protein is synthesized entirely *de novo* without any appreciable participation of materials coming from other cellular proteins. Furthermore, there is no measurable renewal of β-galactosidase sulfur in growing cells whether or not the enzyme is being synthesized. The induced synthesis of β-galactosidase appears as a virtually irreversible process. The bulk of the other cellular proteins in *E. coli* are equally stable and do not undergo any appreciable degradation and resynthesis during growth.

The apparent contradiction between these results and the generally accepted concepts regarding the dynamic state of intracellular proteins is discussed.

RÉSUMÉ

L'étude de l'incorporation du ^{35}S dans la molécule de β-galactosidase, au cours de sa synthèse induite chez *Escherichia coli*, apporte la preuve que la protéine enzymatique est synthétisée *de novo* à partir des éléments du milieu, et sans participation appréciable d'éléments provenant d'autres protéines cellulaires. En outre, il n'y a pas de renouvellement mesurable du soufre de la β-galactosidase intracellulaire. La synthèse induite de la β-galactosidase est un processus pratiquement irréversible. Les autres protéines cellulaires, chez *E. coli*, sont également extrêmement stables et ne subissent pas de dégradation et de renouvellement appréciable au cours de la croissance.

L'apparente contradiction entre ces résultats et les conceptions courantes sur l'état dynamique des protéines intracellulaires fait l'objet d'une discussion.

ZUSAMMENFASSUNG

Das Studium des Einbaues von ^{35}S in das β-Galaktosidase-Molekül, im Verlauf der Synthese dieses Moleküls durch *Escherichia coli*, erbringt den Beweis, dass das Enzymprotein völlig *neu* synthetisiert wird, ohne nennenswerte Beteiligung von Elementen, die aus anderen Zellproteinen stammen. Ferner ergibt sich, dass der Schwefel der intrazellulären β-Galaktosidase nicht messbar erneuert wird. Die induzierte Synthes von β-Galaktosidase ist ein praktisch irreversibeler Process. Die anderen zellulären Proteine von *E. coli* sind gleich extrem stabil. Sie werden im laufe des Wachstums weder wesentlich abgebaut noch restituiert.

Der sichtbar Widerspruch zwischen diesen Resultaten und den allgemeinen Annahmen über den dynamischen Zustand der intrazellulären Proteine wird diskutiert.

References p. 116.

REFERENCES

1 J. LEDERBERG, *J. Bact.*, 60 (1950) 381.
2 S. A. KIRBY AND H. A. LARDY, *J. Am. Chem. Soc.*, 75 (1953) 890.
3 J. MONOD AND M. COHN, *Adv. Enzymol.*, 13 (1952) 67.
4 M. COHN AND A. M. TORRIANI, *J. Immunol.*, 69 (1952) 471.
5 M. COHN AND A. M. TORRIANI, *Biochim. Biophys. Acta*, 10 (1953) 280.
6 J. MONOD, A. M. PAPPENHEIMER Jr. AND G. COHEN-BAZIRE, *Biochim. Biophys. Acta*, 9 (1952) 648.
7 J. MONOD AND M. COHN, *Symposium on Microbial Metabolism, VIth Intern. Congress Microbiol.*, Rome (1953) 42.
8 J. MONOD, G. COHEN-BAZIRE AND M. COHN, *Biochim. Biophys. Acta*, 7 (1951) 585.
9 B. HELFERICH, H. GRUNEWALD AND F. LANGENHOFF, *Chem. Ber.*, 86 (1953) 873.
10 S. S. COHEN, *J. Biol. Chem.*, 168 (1947) 511.
11 D. B. COWIE, E. T. BOLTON AND M. K. SANDS, *J. Bacteriol.*, 60 (1950) 233; *Ibid.*, 62 (1951) 63.
12 R. B. ROBERTS AND E. T. BOLTON, *Science*, 115 (1952) 479.
13 P. GROS, J. COURSAGET AND M. MACHEBOEUF, *Bull. soc. chim. biol.*, 34 (1952) 1070.
14 H. GREEN AND H. S. ANKER, *Biochim. Biophys. Acta*, 13 (1954) 365.
15 D. B. COWIE, R. B. ROBERTS AND E. T. BOLTON, *Science*, 119 (1954) 579.
16 J. YUDKIN, *Biol. Rev.*, 13 (1938) 93.
17 S. SPIEGELMAN, *Cold Spring Harbor Symposium Quant. Biol.*, 11 (1946) 256.
18 J. MONOD, *Growth*, 11 (1947) 223.
19 D. M. GREENBERG AND T. WINNICK, *J. Biol. Chem.*, 173 (1948) 199.
20 M. V. SIMPSON AND S. F. VELICK, *J. Biol. Chem.*, 208 (1954) 61.
21 M. V. SIMPSON AND S. F. VELICK, *J. Biol. Chem.* (in print).
22 J. MONOD, A. M. TORRIANI AND J. GRIBETZ, *Compt. rend. Acad. Sci.*, 227 (1948) 315.
23 J. MANDELSTAM, *Biochem. J.*, 51 (1952) 674.
24 J. MANDELSTAM AND J. YUDKIN, *Biochem. J.*, 51 (1952) 686.

Received July 23rd, 1954

OBSERVATIONS ON NUCLEIC ACID AND POLYPHOSPHATE IN *TORULOPSIS UTILIS*

by

R. CHAYEN†, SONJA CHAYEN* AND E. R. ROBERTS†

† *Department of Inorganic and Physical Chemistry, Imperial College, London (England), and*
* *Botany Department, University College, London (England)*

INTRODUCTION

In the course of investigations into the role of ribose nucleic acid (RNA) in the biosynthesis of protein, we have been interested in measuring the quantity of RNA and of protein nitrogen present in yeast cultures at various times during the growth cycle, as a preliminary to isotopic work. Phosphorus determinations have been complicated, however, by the association with the RNA of another phosphorus compound (labile phosphate) which was readily hydrolysed by hot acid, and was thought to be the metaphosphate described by WIAME[1]. This necessitated the development of a method for estimating nucleic acid phosphate (NAP) in the presence of the labile phosphate. By application of this method, certain aspects of the metabolism of the labile phosphate and of RNA have been observed, and the findings have stimulated interest in the general structure of these compounds.

METHODS AND MATERIALS

Growth experiments were carried out using the yeast *Torulopsis utilis* (now classified as *Candida utilis*[2]). This was grown in shake culture in 250 ml conical flasks at 25° C in a Warburg tank, each flask containing 100 ml of culture. The culture medium used was as follows:

D-Glucose ($C_6H_{12}O_6$)	3 %
Potassium dihydrogen phosphate (KH_2PO_4)	0.2 %
Ammonium sulphate $(NH_4)_2SO_4$	0.3 %
Calcium chloride ($CaCl_2 \cdot 2H_2O$)	0.05 %
Magnesium sulphate ($MgSO_4 \cdot 7H_2O$)	0.07 %
Sodium chloride (NaCl)	0.05 %

For the inoculum in growth experiments, yeast of the required age was centrifuged, and resuspended in fresh medium in concentration sufficient to give a turbidity reading (extinction), at tenfold dilution, of about 0.15 at 420 mμ in a Unicam absorptiometer S.P. 400. (This corresponds to about 1 mg dry weight of yeast in 1 ml of culture.) 20 ml samples of the suspension were then taken at intervals during the growth cycle, and each sample was fractionated using SCHNEIDER'S[3] technique. The nucleic acid fraction was made up to 25 ml, and the absorption of an aliquot measured at 260 mμ and 310 mμ in a Beckman spectrophotometer. Other aliquots were used to determine orthophosphate and total phosphate by ALLEN'S[4] method. Protein nitrogen determinations were performed by the micro-Kjeldahl procedure of WILLITS AND OGG[5].

The condensed phosphates used in hydrolysis experiments, *viz.* sodium pyrophosphate, tripolyphosphate, trimetaphosphate and Glass 696 (a polyphosphate of chain length about 30) were kindly supplied by Albright and Wilson, Ltd. A highly condensed sodium polyphosphate was provided by Dr. P. ALEXANDER. This had been prepared as follows: potassium dihydrogen phosphate was heated

References p. 125/126.

to 640° C for 1 hour, and then cooled. An aqueous suspension of the condensed potassium phosphate thus formed was shaken with the sodium form of an anionic resin, and the resulting solution was freeze-dried to give a soluble white powder. The product, which was considered to be a linear sodium polyphosphate, was stated to have a molecular weight of the order of 10^5 as determined by light-scattering.

The commercial yeast nucleic acid used was a sample of BDH "Nucleic Acid from Yeast. Sodium Salt". A portion was reprecipitated twice with 10 volumes of glacial acetic acid.

EXPERIMENTAL AND RESULTS

Heterogeneity of nucleic acid fraction

A culture of *T. utilis* was grown for 36 hours in the synthetic medium described, starved of nitrogen by transference for 36 hours to similar medium devoid of nitrogen, and then inoculated into fresh medium. The nucleic acid and protein in samples taken during the following 24 hours of growth were measured, and the results are shown in Fig. 1.

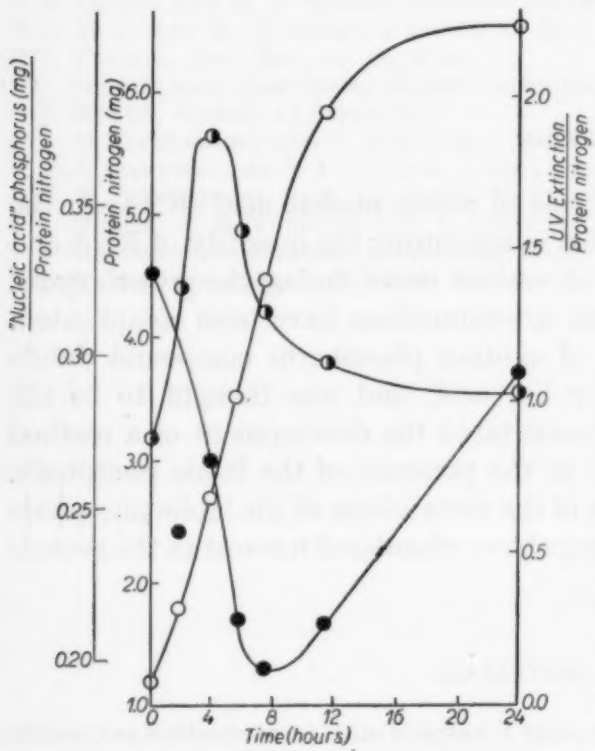

Fig. 1. ○ Protein Nitrogen (mg); ◑ UV Extinction (of nucleic acid fraction) per mg of protein nitrogen; ● mg Phosphorus (of nucleic acid fraction) per mg of protein nitrogen.

In view of the demonstration by WIAME[1] of the occurrence of a labile phosphate in the nucleic acid fraction of baker's yeast, it is not surprising that the phosphorus determinations of the nucleic acid fraction gave results differing from the UV values. As a rough guide to the nature and quantity of the phosphorus compounds in this fraction, the trichloracetic acid (TCA) SCHNEIDER extracts were allowed to stand for a period of about six weeks, and the resulting orthophosphate measured. By subtracting orthophosphate from total phosphate, values were obtained for the strongly bound "Fixed Phosphate", and the figures are given in Table I.

The UV values are roughly proportional to fixed phosphate, giving a ratio of about 11, and it appears probable that the fixed phosphate is, in fact, nucleic acid phosphate.

TABLE I

Time (h)	*Total P (mg)*	*Labile P (mg)*	*Fixed P (mg)*	*UV (extinction)*	*UV / Fixed P*
0	0.39	0.28	0.11	1.04	9.5
4	0.72	0.27	0.45	5.06	11.2
5¾	0.81	0.28	0.53	5.90	11.1
7½	0.89	0.39	0.50	5.80	11.6
11½	1.25	0.62	0.63	6.60	10.4
24	1.94	1.28	0.66	6.80	10.3

The above method, however, is inelegant and long; a speedier and more refined analysis was therefore sought. Since the SCHNEIDER extraction of the nucleic acid involves a

References p. 125/126.

15 minute hydrolysis with 5% TCA at 90° C, whereby much of the labile phosphate is hydrolysed, it seemed that continued hydrolysis under the same conditions, making use of the differing rates of hydrolysis of the labile phosphate and nucleic acid phosphate might be employed. WIAME's[6] work had indicated that the labile phosphate was probably a condensed phosphate; in particular the kinetics of its hydrolysis by *N* HCl were typical of this class of compound. The hydrolysis of four different condensed phosphates was therefore examined, using 5% TCA at 90° C; they all gave similar rate curves, and were 94% hydrolysed to orthophosphate after 75 minutes.

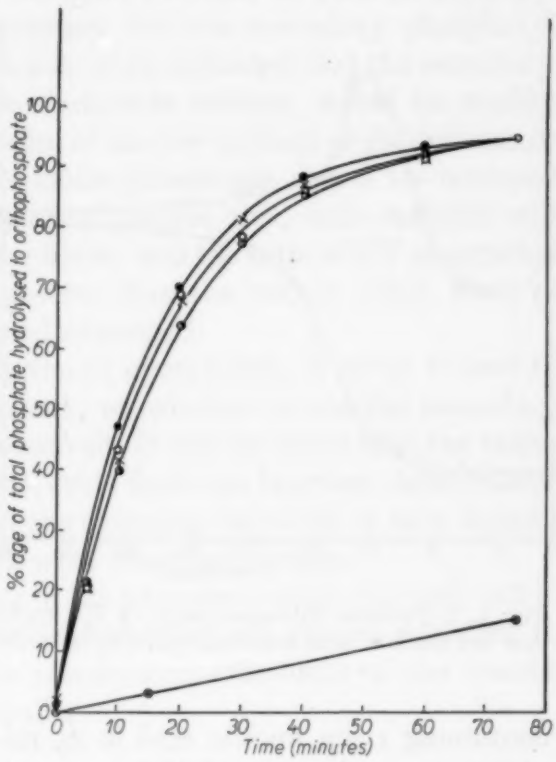

Fig. 2. Rate of hydrolysis of condensed phosphates and of bakers yeast nucleic acid. × Pyrophosphate; ◑ Tripolyphosphate; ○ Trimetaphoshate; ● Glass 696; ⊗ Baker's yeast nucleic acid.

Since four different condensed phosphates were hydrolysed to the same degree by the 75 min hydrolysis, it seems reasonable to suppose that the hydrolysis under these conditions is typical of condensed phosphates in general, and may be due merely to the fission of the P–O–P bond. Under similar conditions, a SCHNEIDER nucleic acid extract of baker's yeast, free from labile phosphate, and a sample of herring sperm deoxyribosenucleic acid (DNA) were hydrolysed only to the extent of 15%. It may be considered that this low degree of hydrolysis is typical of fission of the nucleotide C–O–P bond, and that hydrolysis of such bonds in a similar molecular environment would always liberate the same percentage of phosphorus.

The method of analysis therefore adopted was to continue the SCHNEIDER hydrolysis (5% TCA at 90° C) on an aliquot of the nucleic acid fraction for a further hour, and the orthophosphate produced (1 hour P) was determined. Another aliquot was analysed for total phosphate. From these data, the nucleic acid phosphate (N) and labile phosphate (M) could be calculated from the simultaneous equations:

$$\begin{aligned} 1\text{ Hour P} &= 0.94\,\text{M} + 0.15\,\text{N}. \\ \text{Total P} &= \text{M} + \text{N}. \end{aligned}$$

Application of hydrolysis method and composition of yeast nucleic acid

The differential hydrolysis technique was applied to a growth experiment in order to substantiate the constant ratio of UV absorption to nucleic acid phosphorus (NAP) found previously in the nucleic acid fraction. For this experiment a two-week-old culture was used as inoculum, which was found to have a low content of labile phosphate.

The growth curve (Fig. 3) shows a long lag in protein synthesis, during which time there was a drop in nucleic acid content measured by UV absorption. Table II demonstrates an unexpected change in ratio of UV absorption to NAP, and it seems that the magnitude of the ratio may be correlated with synthetic activity.

References p. 125/126.

If the differential hydrolysis technique is valid, the change in ratio of the nucleic acid fractions at different times during the growth cycle must reflect either a change in composition of nucleic acid or a variation in lability of some of the phosphorus. To determine the nature and degree of variation in the composition of the nucleic acid, it is necessary to know the composition of an authentic sample of yeast nucleic acid, about which there appears to be some contradiction in the literature. Thus WIAME[7] obtained an extinction of 0.61 for a solution of reprecipitated RNA containing 0.57 m$M \cdot 10^{-4}$ of phosphorus per ml. Converting the latter into mg P per 25 ml solution (the units used in this communication), the ratio of extinction to phosphorus is 13.9.

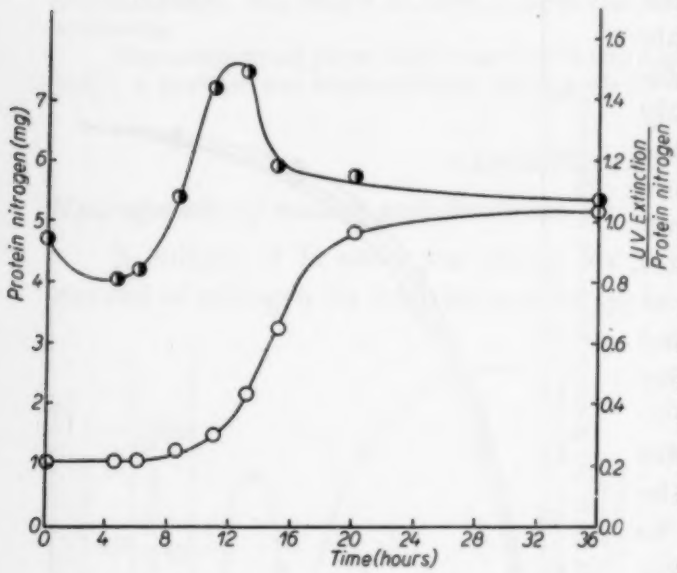

Fig. 3. ○ Protein Nitrogen (mg); ◑ UV Extinction (of nucleic acid fraction) per mg of protein nitrogen.

On the other hand, DI CARLO AND SCHULTZ[8] have given a calibration graph for the UV absorption of yeast nucleic acid; by extrapolation, an extinction value of about 1.05 may be derived for a solution containing 1 mg nucleic acid in 25 ml of solution. Since the theoretical value for the phosphorus content of RNA is considered to be about 9.5%[3], the UV to phosphorus ratio is about 11.0.

TABLE II

Time (hours)	*UV Extinction (A)*	*NAP (B)*	*Ratio A/B*
0	1.00	0.070	14.3
4½	0.865	0.084	10.3
6	0.910	0.092	9.9
8½	1.37	0.123	10.9
11	2.17	0.218	10.0
15	3.78	0.31	12.0
20	5.55	0.386	14.4
36	5.50	0.42	13.1

In view of the discrepancy in composition between the values given by the two different sources, it seemed advisable to analyse a sample of yeast nucleic acid which had not been subjected to the usual harsh extraction treatments of the commercial material. A piece of commercial baker's yeast was therefore fractionated by SCHNEIDER's technique, and labile phosphate was shown to be absent by the fact that the nucleic acid fraction contained only 3% of the total phosphate in the form of orthophosphate after the 15 minute TCA hydrolysis. The UV absorption and the total phosphate were then measured, and the ratio found to be 10.3. This was therefore taken to be the true value for yeast nucleic acid. The ratio was also determined for a sample of BDH "Nucleic Acid from Yeast. Sodium Salt", and for the reprecipitated material. The figures obtained were 13.7 and 13.8 respectively. The percentage of phosphorus in the sodium salt was 6.9, which is equivalent to 7.4% of the free acid.

References p. 125/126.

We therefore have two conflicting ratios for yeast nucleic acid, 10.3 for the native material and 13.9 for the commercially extracted sample. This difference may possibly be explained on the basis of the electrometric titration evidence of FLETCHER[9] *et al.*, who showed that yeast RNA contains three primary and one secondary phosphoryl -OH dissociations for every four atoms of phosphorus. They indicated that the secondary phosphorus atoms, being only singly bound in nucleotide linkage, would be readily labile, and suggested that this lability was the cause of the low content of phosphorus in many commercial samples of RNA. Now if all the labile phosphorus atoms are removed entirely during the alkaline extraction of commercial nucleic acid, such material will contain only 75% of the requisite amount of phosphorus, and the ratio of UV absorption to phosphorus will correspondingly be $33^1/_3$% greater than the normal value. Both of these effects are observed in the BDH nucleic acid examined.

It is thus seen that two ratios of UV absorption to phosphorus, of about 10 and 14 respectively, may be obtained, depending apparently on whether or not the secondary phosphoryl group of the nucleic acid has been removed. It will be noted that the ratios obtained during the different stages of the growth cycle fluctuate between these values, and it might not be unreasonable to suggest that the changing ratios do, in fact, demonstrate an *in vivo* variation in the binding of this same phosphate group.

It must be emphasised that both in the case of the literature values quoted, and in all the experimental work described, the nucleic acid fraction was always subjected to the SCHNEIDER hydrolysis prior to analysis. In consequence, the state of the nucleic acid in all the cases cited should be precisely similar.

The behaviour of labile phosphate during the growth cycle

Early experiments had been carried out in which only UV measurements and total phosphorus determinations had been performed on the nucleic acid fraction. In view of the demonstration of the proportionality of UV absorption to nucleic acid phosphorus being 10.3, the labile phosphate could be determined by calculating NAP from UV values and subtracting the resulting figures from the total phosphate. Data obtained in this manner showed a decrease in the total amount of labile phosphate during the early part of growth, followed by an increase during the decline of protein synthesis, with continued increase after nitrogen assimilation had ceased. As a rough approximation, it may be said that the labile phosphate reached a minimum at the time of maximum rate of protein synthesis, at which time the nucleic acid extinction per unit protein was at its maximum value. An example of this effect is shown in Fig. 4, in which labile phosphate has been calculated from the results of the experiment represented by Fig. 1.

The behaviour of labile phosphate during the growth cycle has also been followed by the differential hydrolysis technique, applying the hour's TCA hydrolysis to the SCHNEIDER nucleic acid fraction. The results are shown in Fig. 5, and it will be seen that they are in accordance with the expected effect.

Metachromasy

WIAME[10,11] has suggested, on the basis of the metachromatic reaction with toluidine blue given by the acid-insoluble labile phosphate and the fact that sodium "hexametaphosphate" prepared by the method of JONES[12] also gives the reaction, that the labile phosphate might be a hexametaphosphate, possibly in polymerised form.

References p. 125/126.

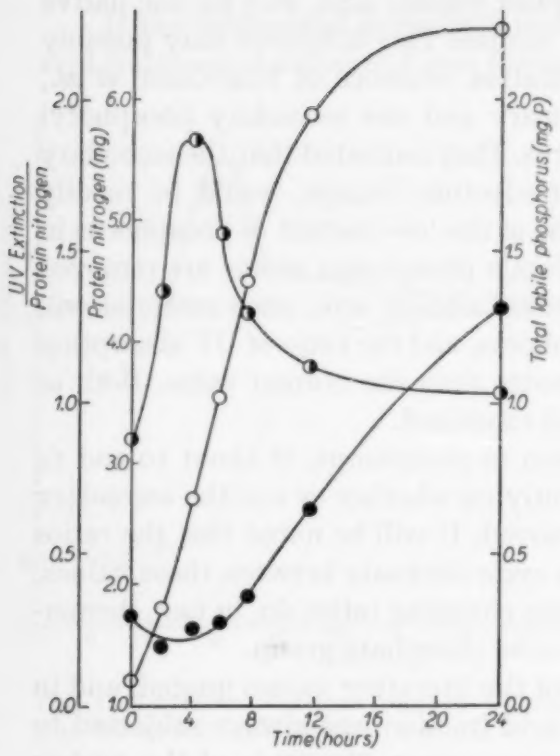

Fig. 4. ○ Protein Nitrogen (mag); ◑ UV Extinction (of nucleic acid fraction) per mg of protein nitrogen; ● Total labile phosphorus (mg).

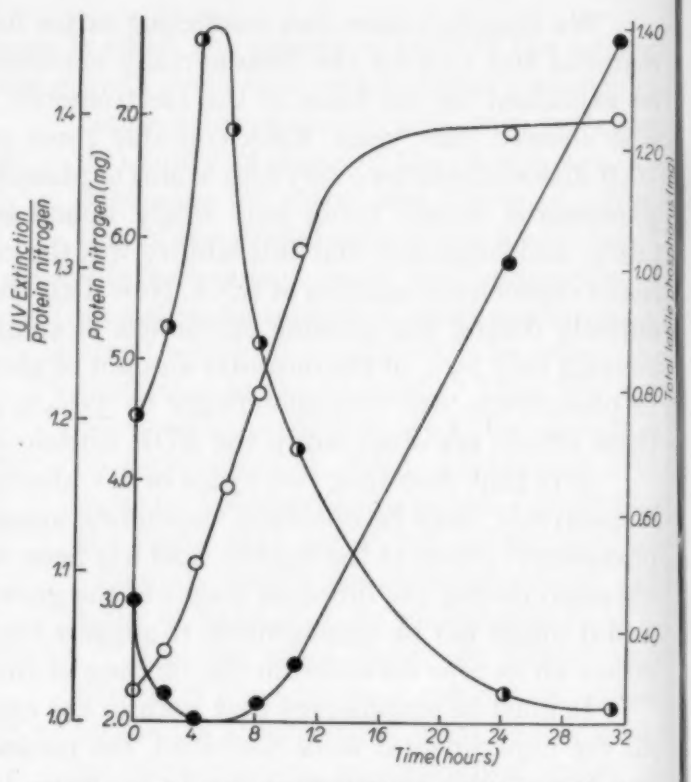

Fig. 5. ○ Protein Nitrogen (mg); ◑ UV extinction (of nucleic acid fraction) per mg of protein nitrogen; ● Total labile phosphorus (mg).

The metachromatic reaction with toluidine blue was performed on the following sodium phosphates: pyrophosphate, tripolyphosphate, trimetaphosphate, Glass 696, and a polyphosphate of molecular weight about 100,000. Both Glass 696 and the high molecular weight polyphosphate gave the reaction. It would therefore appear that the metachromatic reaction is given by highly condensed phosphates in general. In addition, metachromasy was obtained using alginic acid, sodium polymethacrylate, and the sodium salt of deoxyribosenucleic acid, which indicates that the reaction is a property of polyanions. Furthermore, "sodium hexametaphosphate" is a term applied generally to Graham's salt, or "Glassy metaphosphate", the material obtained by rapid cooling of a phosphate melt from above 628° C—the term does not imply a view about the degree of polymerisation[13,14,15], and, in fact, end-group determinations indicate that "metaphosphate" glasses have a molecular weight of the order of 10,000–20,000[16]. Both Glass 696 and the sodium "hexametaphosphate" prepared by the method of JONES are therefore similar compounds, being polyphosphates of high molecular weight.

It seems reasonable, therefore, to suggest that the labile phosphate occurring in the SCHNEIDER nucleic acid fraction of yeast is a highly condensed polyphosphate. In this respect it is of interest to note that high molecular weight "polymetaphosphate" has been isolated from the mould *Aspergillus niger*[17]. In addition, EBEL[18] has investigated a number of micro-organisms containing metachromatic granules, and has shown in all cases that the material responsible for the metachromatic reaction is, in fact, a polyphosphate.

The term "metaphosphate", although often used as synonymous with polyphos-

References p. 125/126.

phate, may be considered misleading when applied to such a compound. Thus metaphosphates have the formula $(MPO_3)_n$, where M is a univalent cation. There are only two proven metaphosphates, the sodium tri- and tetra-metaphosphates, which have cyclic structures and therefore correspond exactly to $(NaPO_3)_3$ and $(NaPO_3)_4$ respectively. The sodium polyphosphates have the formula $(Na,H)_{n+2}P_nO_{3n+1}$ and form a series of linear molecules. Admittedly, as the chain length of a polyphosphate increases and n tends to infinity, the formula tends to $[(Na,H)PO_3]_n$, *i.e.* to the composition required for metaphosphates. Such a compound, however, cannot be classed as a true metaphosphate since the chain must always start and terminate with a secondary phosphoryl group.

DISCUSSION

SPIEGELMAN AND KAMEN[19] have shown that when yeast is grown in a medium containing only glucose and phosphate labelled with P^{32}, the "nucleoprotein" fraction builds up a store of labelled phosphate. This flows out of the fraction when ammonium salts are added, but the outflow is stopped when agents such as sodium azide and dinitrophenol are added in concentrations which prevent enzyme formation and protein synthesis without inhibiting fermentation. In later experiments[20, 21], it was shown that most of the activity of the "nucleoprotein" fraction was due to the acid-insoluble "metaphosphate".

LINDEGREN[22] suggests that volutin, which WIAME[23] has identified with "metaphosphate", is essential for cell division. He considers that the loss of volutin in yeasts after division ceases is responsible for the lag period that often occurs when "dissimilated" cells are introduced into fresh medium.

All these observations are consistent with the view that the nucleic acid-associated polyphosphate of yeast is involved in protein synthesis, and it has often been suggested that the function of this material is to act as an energy supply by virtue of the high standard free energy associated with the hydrolytic fission of the P–O–P bonds. Our observations may be interpreted in accordance with such a hypothesis. Thus it has been shown that the polyphosphate decreases in quantity during the early growth phase. When the rate of protein synthesis decreases, polyphosphate is stored, and apparently is not utilised again until the yeast is suspended in fresh culture medium. Furthermore, it has been observed in experiments where there is a low content of labile phosphate initially that there is a correspondingly long lag phase as regards protein synthesis, and it may well be that the length of the lag phase in yeast cultures can be correlated with the initial amount of labile phosphate present.

A further significant feature in the phosphorus metabolism of the nucleic acid fraction is the change in ratio of UV extinction to NAP during the growth cycle. High ratios are obtained at the end of the cycle, after the cessation of protein synthesis, the low values being reached soon after inoculation. This effect also may be connected with energy relationships, since it has been found[24] that nucleic acid from an actively growing culture of *T. utilis* is capable of supporting luminescence in firefly extracts, whereas that from a dormant culture will not. Since luminescence depends on the expenditure of energy, the low-ratio nucleic acid may be considerd an "energy-rich" form. If analogy with adenosine triphosphate (ATP) is permissible, such a compound might be expected to act by transference of phosphate; *i.e.* donation of phosphate, followed by replacement of the deficiency from a phosphorus store. In this respect, it has been shown that the

References p. 125/126.

acid-insoluble polyphosphate becomes depleted during the early growth phase, namely during the same period as the low-ratio nucleic acid form is attained. In addition, the nucleic acid and polyphosphate occur in the same fraction (acid-insoluble, non-lipid, non-protein fraction) possibly as a complex[25,6], which BRACHET[26] has termed "phosphorylated nucleic acid". It would therefore not be surprising if there existed a nucleic acid phosphate which served as a phosphorylating agent in the same way as ATP, yet provided specificity in protein synthesis by aligning the amino acids along the polynucleotide chain. This is basically the hypothesis proposed by CHANTRENNE[27] (see also DOUNCE[28], and KONINGSBERGER AND OVERBEEK[29]) in which he suggests that the carboxyl groups of the amino acids could be activated by acylphosphate formation prior to peptide synthesis. The importance of such phosphorylations in peptide bond formation has been stressed by LIPMANN[30,31], and referred to by many authors recently[32].

ACKNOWLEDGEMENTS

We wish to thank PROFESSOR J. BRACHET for his kind interest in this work, for his advice and for reading the manuscript. We also wish to acknowledge our gratitude to Professors H. CHANTRENNE, J. N. DAVIDSON, J. M. WIAME, and Mr. C. A. VERNON for helpful criticism of the manuscript; to Dr. P. ALEXANDER for helpful discussion in connection with metachromasy; and to Mr. J. E. SUCH and Mr. M. G. PEARD of Albright and Wilson, Ltd., for guidance on the chemistry of polyphosphates and for reading the manuscript. We are grateful to Dr. J. CHAYEN of the Wheatstone Physics Laboratory, King's College, London, for helpful discussions and advice throughout all phases of the work and for reading the manuscript.

Two of us (R.C. and E.R.R.) wish to acknowledge our gratitude to the British Empire Cancer Campaign for a grant which made this work possible.

SUMMARY

1. The nucleic acid fraction of yeast as obtained by the SCHNEIDER technique contains an additional phosphorus compound; it is suggested that it is a linear polyphosphate of high molecular weight.

2. This has necessitated the development of a modified phosphorus determination for the Schneider fraction whereby the nucleic acid phosphate and the polyphosphate are determined in the presence of each other. The method evolved consists of a differential hydrolysis in 5% trichloracetic acid at 90° C for 1 hour. The rate of hydrolysis of the two phosphates has been determined.

3. By the application of the hydrolysis technique, the behaviour of the two phosphorus components of the nucleic acid fraction has been followed throughout the growth cycle. It has been shown that the total amount of polyphosphate decreases during the early active growth phase, then increases rapidly, increasing even after protein synthesis has finished. Fluctuation in the ratio of UV absorption to NAP, as determined by this method, has suggested that the composition of the nucleic acid itself may vary during the growth cycle; the highest values for this ratio were obtained at the termination of protein synthesis, and the lowest values during early growth. The significance of these observations is discussed.

4. Studies have been made on samples of yeast nucleic acid which were free from polyphosphate. The evidence regarding the ratio of UV to P in these investigations and in those on *T. utilis* is discussed with respect to the structure of the nucleic acid.

5. It has been demonstrated that the metachromatic reaction with toluidine blue is given by a number of polyanions and is not restricted to "hexametaphosphate". The structure and nomenclature of this substance are discussed.

RÉSUMÉ

1. La fraction acides nucléiques obtenue à partir de levure par la méthode de SCHNEIDER contient aussi un autre composé phosphoré; les auteurs pensent que c'est un polyphosphate à poids moléculaire élevé.

References p. 125/126.

2. La méthode de dosage du phosphore dans cette fraction a dû être modifiée, afin de pouvoir doser le phosphore nucléique et celui du polyphosphate en présence l'un de l'autre. La méthode mise au point dans ce but repose sur une hydrolyse différentielle d'une heure à 90° dans l'acide trichloracétique 5%. La vitesse d'hydrolyse des deux composés phosphorés a été déterminée.

3. Grâce à cette technique, il a été possible de suivre le comportement des deux composés phosphorés pendant toute la croissance de la levure. Les résultats montrent que la quantité totale de polyphosphates décroît au début de la phase de croissance active, puis qu'elle augmente rapidement et continue même à augmenter après l'arrêt de la synthèse des protéines. La variation du rapport de l'absorption dans l'U.V. à la teneur en phosphore nucléique suggère que la composition de l'acide nucléique lui-même changerait pendant le cycle de croissance; les valeurs les plus élevées de ce rapport sont atteintes à la fin de la période de synthèse des protéines, les valeurs les plus basses se placent au début de la croissance. Les auteurs discutent la signification possible de ces observations.

4. Des échantillons d'acide nucléique de levure exempt de polyphosphates ont été examinés également. Les auteurs considèrent la signification, en ce qui regarde la structure de l'acide nucléique, des valeurs du rapport de l'absorption dans l'U.V. à la teneur en phosphore obtenues pour ces acides nucléiques et pour ceux de *T. utilis*.

5. La réaction métachromatique avec le bleu de toluidine est obtenue avec plusieurs substances polyanioniques, elle n'est pas limitée au cas de l'hexamétaphosphate.

ZUSAMMENFASSUNG

1. Die Nukleinsäurefraktion aus Hefe, wie sie mit der Methode nach SCHNEIDER gewonnen wird, enthält ausser den Nukleinsäuren noch eine andere phosphorhaltige Verbindung. Es wird vermutet, dass es sich dabei um ein lineares Polyphosphat höheren Molekulargewichtes handelt.

2. Die Methode zur Bestimmung des Phosphats in dieser Fraktion musste modifiziert werden, um das Phosphat der Nukleinsäuren und des Polyphosphates in beider Gegenwart bestimmen zu können. Die entwickelte Methode besteht in einer einstündigen Differentialhydrolyse in 5% Trichloressigsäure bei 90° C.

3. Durch die Anwendung der Hydrolysentechnik war es möglich, das Verhalten der beiden Phosphatkomponenten während des Wachstums der Hefe zu verfolgen. Es konnte gezeigt werden, das die Gesamtmenge des Polyphosphates zu Beginn der Phase des aktiven Wachstums abnimmt dann schnell zunimmt und selbst nach Abschluss der Proteinsynthese noch weiter anwächst. Die Schwankungen im Verhältnis der UV Absorption zum Gehalt an Nukleinsäurephosphat lassen vermuten, dass sich die Zusammensetzung der Nukleinsäuren während des Wachtumzyklus ändern, die höchsten Werte dieses Verhältnisses wurden am Ende der Periode der Proteinsynthese erhalten, und die niedrigsten Werte zu Beginn des Wachstums. Die Bedeutung dieser Beobachtungen wird diskutiert.

4. In gleicher Weise wurden Proben von Hefenukleinsäuren untersucht, die keine Polyphosphate enthielten. Die Bedeutung des Verhältnisses der UV Absorption zu dem Gehalt an Phosphor bei diesen Nukleinsäuren und bei denen von *T. utilis* wird im Hinblick auf die Struktur der Nukleinsäuren diskutiert.

5. Es wird gezeigt, dass die metachromatische Reaktion mit Toluidin-Blau bei einer Reihe von Polyanionen auftritt und nicht auf "Hexametaphosphat" beschränkt ist. Struktur und Nomenklatur dieser Substanz wird diskutiert.

REFERENCES

1 J. M. WIAME, *Bull. soc. chim. biol.*, 28 (1946) 552.
2 J. LODDER AND N. J. W. KREGER-VAN RIJ, *The Yeasts: A Taxonomic Study*, North Holland Publ. Co., Amsterdam, 1952, p. 546.
3 W. C. SCHNEIDER, *J. Biol. Chem.*, 161 (1945) 293.
4 R. J. L. ALLEN, *Biochem. J.*, 34 (1940) 858.
5 C. O. WILLITS AND C. L. OGG, *J. Assoc. Offic. Agri. Chemists*, 33 (1950) 179.
6 J. M. WIAME, *Biochim. Biophys. Acta*, 1 (1947) 234.
7 J. M. WIAME, *J. Biol. Chem.*, 178 (1949) 919.
8 F. J. DI CARLO AND A. S. SCHULTZ, *Arch. Biochem.*, 17 (1948) 293.
9 W. E. FLETCHER, J. M. GULLAND AND D. O. JORDAN, *J. Chem. Soc.* (1944) 33.
10 J. M. WIAME, *Fed. Proc.*, 6 (1947) 302.
11 J. M. WIAME, *J. Amer. Chem. Soc.*, 69 (1947) 3146.
12 L. T. JONES, *Ind. Eng. Chem., Anal. Ed.*, 14 (1942) 536.
13 B. TOPLEY, *Quart. Rev. (London)*, 3 (1949) 359.
14 E. P. PARTRIDGE, *Chem. Eng. News*, 27 (1949) 214.
15 J. R. VAN WAZER, *J. Amer. Chem. Soc.*, 72 (1950) 644.

[16] O. SAMUELSON, *Svensk. Kem. Tidskr.*, 56 (1944) 343.
[17] B. INGELMAN AND H. MALMGREN, *Acta Chem. Scand.*, 4 (1950) 478.
[18] J. P. EBEL, *Bull. soc. chim. biol.*, 34 (1952), 321, 330, 491, 498.
[19] S. SPIEGELMAN AND M. D. KAMEN, *Science*, 104 (1946) 581.
[20] E. JUNI, M. D. KAMEN, S. SPIEGELMAN AND J. M. WIAME, *Nature*, 160 (1947) 717.
[21] E. JUNI, M. D. KAMEN, J. R. REINER AND S. SPIEGELMAN, *Arch. Biochem.*, 18 (1948) 387.
[22] C. C. LINDEGREN, *Nature*, 159 (1947) 63.
[23] J. M. WIAME, *Compt. rend. soc. biol.*, 140 (1946) 897.
[24] B. L. STREHLER AND J. R. TOTTER, *Arch. Biochem. and Biophys.*, 40 (1952) 28.
[25] M. G. MACFARLANE, *Biochem. J.*, 30 (1936) 1369.
[26] J. BRACHET, *Chemical Embryology*, Interscience Publ. Inc., New York, 1950, p. 242.
[27] H. CHANTRENNE, *Biochim. Biophys. Acta*, 4 (1950) 487.
[28] A. L. DOUNCE, *Enzymologia*, 15 (1952) 251.
[29] V. V. KONINGSBERGER AND J. TH. G. OVERBEEK, *Koninkl. Ned. Akad. Wetenschap. Proc.*, 56B (1953) 248.
[30] F. LIPMANN, *Advances in Enzymology*, 1 (1941) 99.
[31] F. LIPMANN, *Fed. Proc.*, 8 (1949) 597.
[32] W. D. MCELROY AND H. B. GLASS (Editors), *Phosphorus Metabolism*, Vols. I and II. Baltimore, The Johns Hopkins Press, 1951–52.

Received July 29th, 1954

THE RELATIONSHIP BETWEEN TOBACCO MOSAIC VIRUS AND AN ACCOMPANYING ABNORMAL PROTEIN*,**

by

C. C. DELWICHE, PHILIP NEWMARK***, WILLIAM N. TAKAHASHI AND MARY J. NG

Department of Plant Biochemistry, Virus Laboratory, and Department of Plant Pathology, University of California, Berkeley, California (U.S.A.)

The occurrence of a nucleic acid-free abnormal protein in plants infected with tobacco mosaic virus (TMV) was reported by TAKAHASHI AND ISHII (protein "X")[18], by COMMONER, NEWMARK, AND RODENBERG ("component B")[1], and by JEENER AND LEMOINE ("crystallizable antigen")[9]. Although somewhat different methods of preparation were used by these three groups of workers, the product obtained in each case is evidently the same. The protein was isolated for the present work by a procedure similar, in some respects, to that of COMMONER, NEWMARK AND RODENBERG. When this protein is mixed with protein "X" prepared by the procedure of TAKAHASHI AND ISHII, the two migrate as one electrophoretic component. Other similarities in physical and chemical properties are the subject of a separate report[15].

TAKAHASHI AND ISHII demonstrated that this protein can be caused to polymerize into rods which have the same cross section as TMV but are of varying lengths[19]. The immunological similarity which this protein bears to TMV[19,9,3] and the identity of amino acid composition [15] strongly emphasize the close structural relationship between the two. TMV has a molecular weight in the neighborhood of $5 \cdot 10^7$ whereas that of this protein in its least aggregated from appears to be less than $5 \cdot 10^4$. Its polymerization and combination with nucleic acid *in vitro* to yield infective virus particles has not been demonstrated[4,15].

The present study was undertaken to elucidate further the relationship which this protein bears to TMV insofar as its synthesis in the plant is concerned; and to determine whether it could be a degradation product of TMV resulting either from fragmentation in the extraction process or as a normal *in vivo* reversal of the synthetic mechanisms, or whether it may be a direct precursor or a by-product of the synthetic process.

MENEGHINI AND DELWICHE[14] found that ^{15}N labelled ammonium ion, when infiltrated into TMV infected leaves, was rapidly incorporated into the virus protein. From distribution of the isotope in various fractions they concluded that TMV was formed from a low molecular weight nitrogenous fraction (*e.g.*, amino acids) which was

* Reported before the thirty-eighth meeting of the American Society of Biological Chemists April, 1954[15].

** Supported by grants from the Lederle Laboratories, the Rockefeller Foundation, and the Atomic Energy Commission.

*** Research Fellow of the National Foundation for Infantile Paralysis. Present address: Department of Biochemistry, University of Kansas, Lawrence, Kansas.

References p. 136.

in more rapid equilibrium with ammonium ion than were the normal plant proteins. Recent work of COMMONER, SCHEIBER AND DIETZ[2] substantiates this view although these authors conclude that "amino acid residues of TMV are not derived from the corresponding free amino acids of the host".

It appeared likely that, using a similar technique, a comparison of labelling between TMV and other protein fractions could yield information as to whether the abnormal protein accompanying TMV infection could be ruled out as either a direct precursor or a degradation product of TMV. Direct proof that such a protein is a precursor would be difficult unless the labelled protein could be introduced at the site of synthesis and the formation of labelled TMV therefrom demonstrated.

MATERIALS AND METHODS

Six weeks old *Nicotiana tabacum* plants of a Turkish variety were greenhouse-grown in four inch clay pots. Growing points and all but three or four median leaves were removed. The leaves remaining on the plants were inoculated by rubbing their top surfaces with a gauze pad soaked in a centrifugally isolated and purified solution of TMV in 0.01 M, pH 7 phosphate buffer.

At intervals after inoculation the leaves were detached and ^{15}N-labelled ammonium ion was introduced by placing their petioles in 0.02 *M* solutions of ammonium chloride containing 32 atom percent excess of the isotope and buffered at pH 7.0 with 0.01 *M* phosphate. In order to accelerate transpiration the leaves were illuminated with artificial light of about 2,000 luces intensity. When all the culture solution had been taken up, distilled water was added as needed to prevent wilting. After 24 hours, the leaves were homogenized and fractionated, and nitrogenous fractions were assayed for total nitrogen and ^{15}N content.

In one experiment after the leaves had taken up the isotopic ammonium ion they were split in half for sampling and the halves floated on large volumes of buffered solution containing unlabelled ammonium ion in order that the rate at which isotope was leached from the several fractions could be followed.

Leaf fractionation procedure

The fractionation procedure used (Fig. 1) was based on the fact that when solutions of clarified homogenate at pH 7 are subjected to high speed (80,000 × *g*.) centrifugation, the TMV can be pelleted out without significant contamination by the abnormal nucleic acid-free protein. The remaining supernatant solution when adjusted to pH 4.7 will aggregate a large bulk of proteins, characteristic of both healthy and infected plants, which can be sedimented in comparatively weak centrifugal fields (6,000 × *g*.). The abnormal protein is partially (and reversibly) polymerized at this pH and can be pelleted out at 80,000 × *g*. A further lowering of the pH to 3.8 yields another protein fraction characteristic of both healthy and infected plants. Remaining is a final supernatant solution composed principally of non-protein nitrogen.

The leaves were ground with mortar and pestle in twice their weight of 0.1 *M* pH 7.0 phosphate buffer, and further homogenized in an all glass homogenizer. Equipment and solutions were kept cold by immersion in crushed ice. Further steps in the fractionation procedure, except for adjustment of pH, were carried on in a cold room at 3–4° C., or in a refrigerated Spinco ultracentrifuge.

The homogenate was clarified at 10,000 × *g*. for 15 min, the precipitate (P_1) washed with 0.1 *M* pH 7.0 phosphate buffer, recentrifuged under the same conditions, and the supernatant solution combined with that of the first centrifugation (S_1).

P_1 is composed of cell wall debris, and the larger fragments of chloroplasts, nuclei, and other cytoplasmic particles which are insoluble in 0.1 *M* phosphate buffer. Extraction of P_1 with 2 *M* sodium chloride yielded comparable amounts of a nucleoprotein from both uninfected and infected leaves, in accord with findings of COMMONER, *et al.*[3]

Centrifugation of supernatant solution S_1 at 80,000 × *g*. for 2 hours sedimented the TMV together with some chloroplast grana and smaller cytoplasmic fragments (P_2). The P_2 pellets were resuspended in 0.01 μ, pH 7.0 cacodylate/sodium chloride (0.2/0.8) buffer, and the TMV purified by heating the buffered solution to 60° for 15 minutes or by dropping the pH to 3.8. In either case the non-TMV, protein-containing fragments were coagulated and readily sedimented by low speed centrifugation as P_3, and a nucleic acid fraction was released. Washes of precipitate P_3 with 0.01 μ pH 7.0 cacodylate buffer were combined with solution S_3. When this solution was centrifuged at 100,000 × *g*. for 1 hour, the TMV was pelleted out, leaving the nucleic acid (as determined by ultraviolet absorption spectrum) as supernatant solution S_{3a}.

References p. 136.

Fig. 1. Leaf Fractionation Procedure

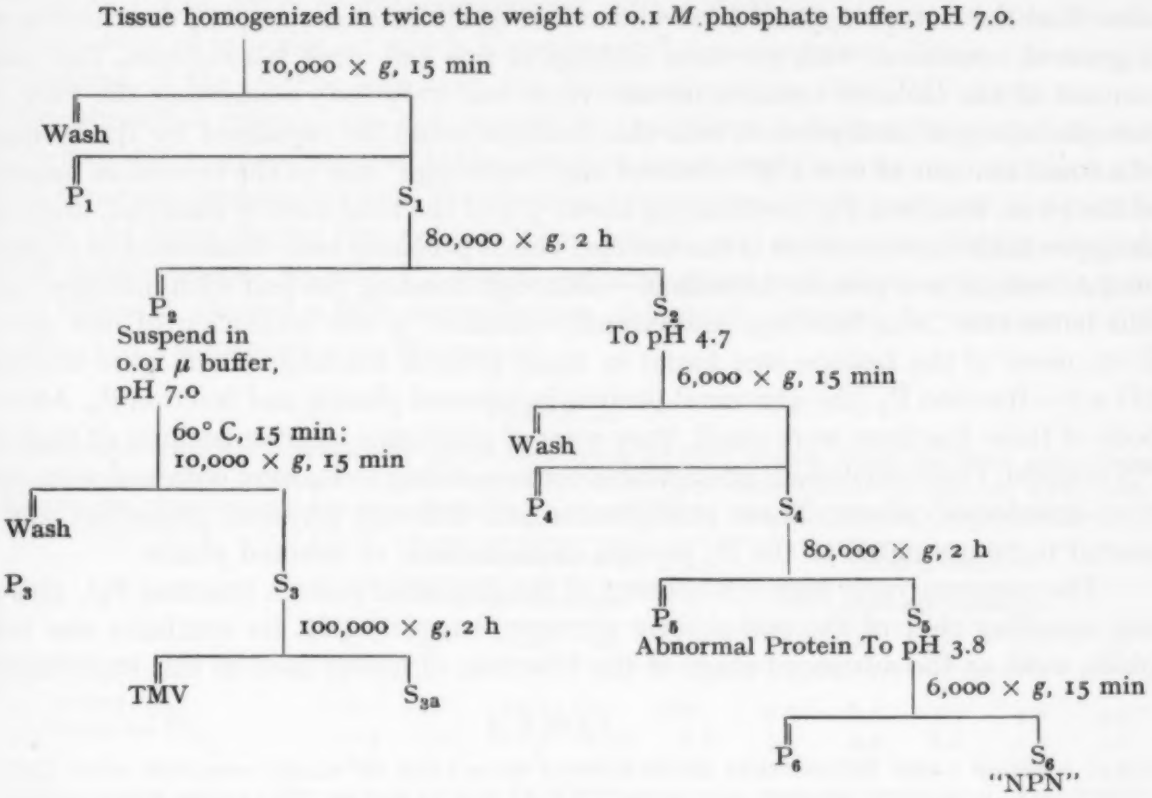

The clear, amber-colored solution S_2, at pH about 6.5, contained the soluble non-protein and low molecular weight protein constituents. By dropping the pH to 4.7 with 1 *N* sulfuric acid the bulk of the soluble proteins were precipitated isoelectrically within an hour and removed by low speed centrifugation as P_4.

Precipitate P_4 contained the 18 S protein component of EGGMAN, SINGER AND WILDMAN[5] as well as a group of proteins which have sedimentation constants of 3 S or less. A portion of precipitate P_4 redissolves in 0.1 *M* pH 7.0 phosphate or cacodylate/sodium chloride buffers.

When the remaining solutions S_4 was centrifuged at 80,000 × *g*. for 2 hours, the abnormal protein partially polymerized at this pH was sedimented as a clear TMV-like pellet (P_5). No comparable protein was obtained from uninfected leaf tissue. Resuspension of the abnormal protein in 0.1 μ, pH 7.0 cacodylate/sodium chloride buffer, followed by clarification of the solution though low speed centrifugation and dialysis against the cacodylate buffer, yielded a solution in which over 90% of the protein migrated as a single component in the electrophoresis apparatus[15].

The solution remaining, S_5, contained those low molecular weight protein and non-protein constituents which were still soluble at pH 4.7. Most of the proteins were precipitated isoelectrically by taking the pH to 3.8 with 1 *N* H_2SO_4 and allowing the solution to stand overnight. Centrifuging at low speed yielded precipitate P_6. The nitrogen in solution S_6 was mostly non-protein (NPN), but a small amount of protein could be recovered as a denatured precipitate by heating at 60° for 15 minutes.

RESULTS

The incorporation of ^{15}N into abnormal protein

A preliminary experiment was designed to determine whether at an advanced stage of infection the abnormal protein received a label from isotopic ammonia. Four basal leaves of approximately 10 cm length, showing no external signs of mosaic, were selected from an eight week old systemically infected greenhouse-grown Turkish tobacco plant 31 days following inoculation. After administration of the isotopic ammonium ion for 24 hours as outlined above, the leaves were ground and a partial fractionation was made

References p. 136.

of the homogenate yielding the fractions indicated in Table I. The data of Table I show that the isotope appeared to some extent in all fractions, and the distribution was, in general, consistent with previous findings of this and other laboratories. The isotope content of the isolated tobacco mosaic virus was very low, confirming the view that isotopic nitrogen incorporated into this fraction could be explained by the formation of a small amount of new TMV without any "exchange" due to the reversible formation of the virus. Fraction P_4, constituting about 5% of the total soluble material, underwent an appreciable incorporation of the isotope. This is probably more than could be explained on the basis of new protein formation—although flooding the leaf with nitrogen, which had heretofore been limiting, undoubtedly resulted in the formation of new protein. Even more of the isotope was found in those protein fractions which were soluble at pH 4.7—fraction P_5 (the abnormal protein in infected plants) and fraction P_6. Although both of these fractions were small, they were of particular interest because of their high ^{15}N content. Only very small precipitates corresponding to P_5 were obtained with leaves from uninfected plants. These precipitates had different physical properties and appeared to be unrelated to the P_5 protein characteristic of infected plants.

The comparatively high ^{15}N content of the abnormal protein (fraction P_5), although not equalling that of the non-protein nitrogen, suggests that its synthesis was taking place, even at the advanced stage of the infection of leaves used in this experiment.

TABLE I

TOTAL NITROGEN AND ^{15}N CONTENT OF FRACTIONS FROM LEAF OF PLANT INFECTED WITH TMV FOR THIRTY-ONE DAYS, THEN EXCISED AND GIVEN $^{15}NH_4Cl$ FOR 24 HOURS. ^{15}N VALUES WERE CALCULATED ON THE BASIS OF 100 ATOM PERCENT EXCESS ^{15}N IN THE SUBSTRATE AMMONIUM ION.

Fraction	*μAtoms N per g wet weight*	*Atom % excess ^{15}N*
Total homogenate	250.0	6.8
Clarified homogenate (S_1)	13.0	11.0
TMV	39.5	0.22
pH 4.7 ppt. (P_4)	6.3	3.4
Abnormal protein (P_5)	0.9	7.8
pH 3.8 ppt. (P_6)	0.9	7.5
pH 3.8 sol., "NPN" (S_6)	35.0	26.2

Comparison of abnormal protein and TMV protein

In view of the above results, a more detailed study of the process was undertaken in Experiment II. In this case, the leaves were supplied with isotope at varying intervals after inoculation of the plant with TMV, the times being selected to cover the period of rapid formation of virus.

Twelve uniform Turkish tobacco plants, approximately six weeks old, were selected and their growing points and all leaves except the median three removed. These leaves were then inoculated with TMV. At successive intervals, one leaf was removed from each alternate plant, giving a total of six samples of six leaves each. Upon abscission from the plants, the leaves were supplied with ammonium chloride ^{15}N and allowed to stand for 24 hours. At the end of the 24 hour interval they were fractionated according to the procedure outline in Fig. 1, with the exception of one sample at the end for which the fractionation procedure was modified with ammonium sulfate precipitation of the proteins of various supernatant solutions for the purpose of electrophoretic analysis.

References p. 136.

Results of this experiment are presented in Table II. The general observations of Experiment I also apply to this experiment, although there was no sample for the advanced stage of infection at which Experiment I was conducted. There was a rapid incorporation of the isotope into both the abnormal protein and TMV fractions.

The abnormal protein was not present in quantities sufficient for detection and analysis until the 144 hour sample. As the infection progressed there was an increase in the ratio of abnormal protein to virus. The abnormal protein was being produced at a greater rate than the virus during the 144–240 hour period, and it was more highly labelled.

The heterogeneous fraction P_3, which includes grana and other cytoplasmic particulate material, showed a high incorporation of isotopic nitrogen, in agreement with the findings of JAGENDORF AND WILDMAN[7].

TABLE II

TOTAL NITROGEN AND ^{15}N CONTENT OF FRACTIONS FROM LEAVES WHICH WERE EXCISED AND GIVEN $^{15}NH_4Cl$ FOR 24 HOURS AT VARIOUS TIMES AFTER INOCULATION WITH TMV. ^{15}N VALUES WERE CALCULATED ON THE BASIS OF 100 ATOM PERCENT EXCESS ^{15}N IN THE SUBSTRATE AMMONIUM ION.

Fraction	*μ atoms N per g wet weight*					*Atom % excess N^{15}*				
	Hours after inoculation					*Hours after inoculation*				
	48	*98*	*144*	*195*	*240*	*48*	*98*	*144*	*195*	*240*
Clarified homog. (S_1)	236	187	129(?)	161	160	9.6	6.1	5.7	4.6	4.0
Small particulates (P_3)	12.3	19.5	10.7	21.9	8.1	3.2	3.4	3.0	1.8	2.2
TMV	0.1	3.2	9.8	16.9	33.3	—	14.7	11.1	6.0	3.5
protein	—	—	—	—	—	—	—	11.6	6.0	3.6
nucleic acid	—	—	—	—	—	—	—	4.4	3.3	2.2
pH 4.7 ppt (P_4)	55.9	35.0	62.5(?)	34.8	25.3	2.6	2.4	1.7	1.1	1.1
Abnormal protein (P_5)	—	—	0.1	1.2	4.0	—	—	—	10.0	9.2
pH 3.8 ppt (P_6)	1.7	1.1	1.9	1.9	2.8	6.4	2.5	2.2	1.9	2.1
pH 3.8 sol. "NPN" (S_6)	—	61.3	51.2	64	46.4	23.4	13.6	11.1	8.3	8.4

Metabolic stability of TMV and abnormal protein

In order to compare the metabolic stability of the living leaf of fractions already considered, as well as to gain information concerning the relationship of nucleic acids to other fractions, an experiment of a somewhat different nature was conducted. In this case (Experiment III) the median leaves of ten uniform plants were inoculated with TMV. After 72 hours all the leaves were removed from the plants and provided with isotopic ammonia for the next 47 hours. The midribs were then removed and the half leaves were divided into five similar samples. These were floated on large volumes of solutions of unlabelled ammonium chloride and phosphate buffer, and the solutions were changed daily. Leaf samples were removed at successive intervals and fractionated as before. In addition fractions of nucleic acid were obtained from TMV by the procedure of KNIGHT[10] and from the particulate fraction (P_3) by extraction with hot 5% trichloroacetic acid.

Results of this experiment are shown in Fig. 2 and 3. As was anticipated there was a rapid leaching of the isotope from the NPN fraction upon exposure of the leaf halves to the unlabelled solution. There was also a large increase in toal NPN. The total amount of isotopic nitrogen in TMV and the abnormal protein increased; the drop in $^{15}N/^{14}N$ ratio of these fractions with time being readily explained by the dilution resulting from the synthesis of new protein having a lower isotope content.

References p. 136.

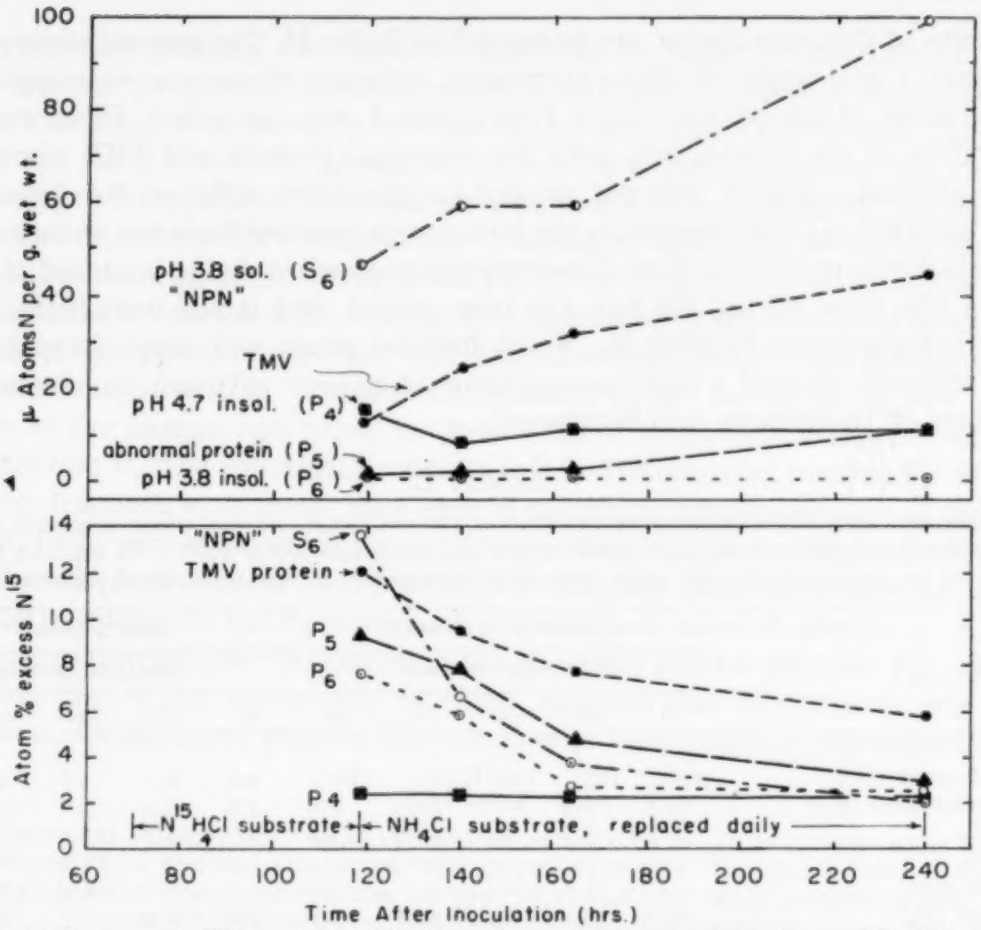

Fig. 2. Total nitrogen and ^{15}N content of leaf fractions which are soluble in 0.1 *M*, pH 7 phosphate buffer. Leaves were excised 74 hours after inoculation with TMV, floated on $^{15}NH_4Cl$ for 47 hours, and then floated on unlabelled NH_4Cl for varying times. ^{15}N values were calculated on the basis of 100 atom percent excess ^{15}N in the initial substrate ammonium ion.

These results are consistent with the results of Experiment II and with the earlier findings of MENEGHINI AND DELWICHE[13]. All point to the metabolic inertness of the bulk of the TMV synthesized in the leaf. Although, the data on the abnormal protein are not conclusive, they suggest that the protein is relatively stable.

The protein precipitable at pH 4.7 (P_4), characteristic of both infected and uninfected plants, remained more or less constant in both ^{15}N content and total nitrogen for the duration of the experiment whereas that fraction precipitated at pH 3.8 (P_6) showed a rapid loss of the isotope. It appears that the metabolic activity of this smaller fraction (P_6) was considerably greater than that of the pH 4.7 insoluble fraction (P_4).

The particulate fractions P_1 and P_3 both retained the label with little loss during the 120 hours that unlabelled ammonium ion was provided and indeed did not reach their maximal label until 24 hours after transfer to the unlabelled solution.

Incorporation of isotope into nucleic acid

A time lag was observed in the appearance of isotope in the nucleic acid fractions (Fig. 3). The extent to which the TMV nucleic acid differs from the protein portion of the virus in this regard emphasizes the non-parallel synthetic pathways of these two moieties. The time lag in the case of the nucleic acid could represent a large nitrogenous pool between the purine and pyrimidine precursors and the finished nucleic acid. Work

References p. 136.

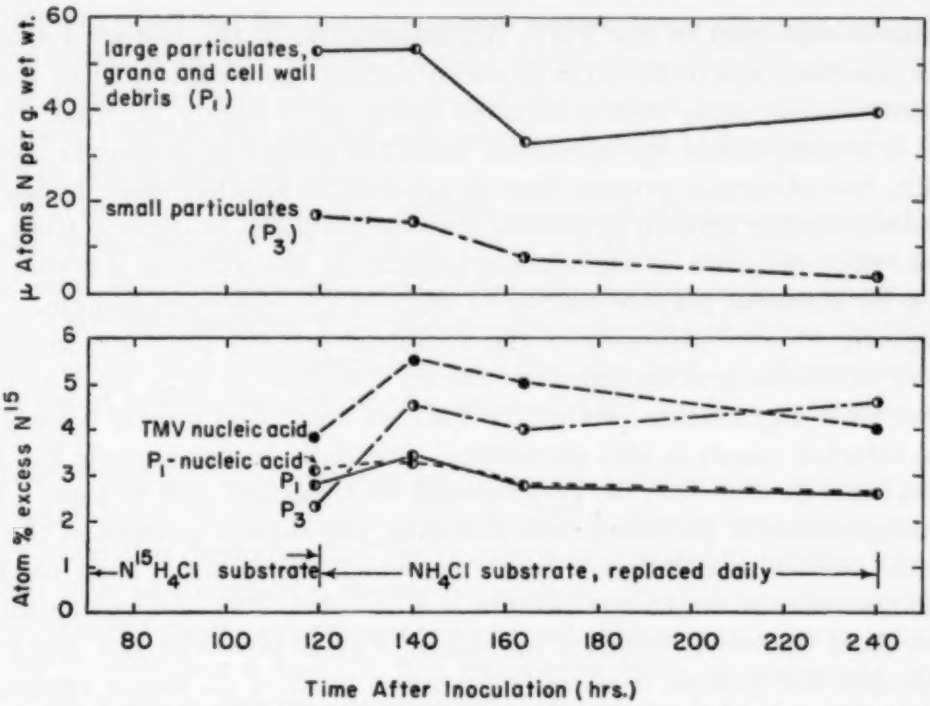

Fig. 3. Total nitrogen and ^{15}N content of leaf fractions which are insoluble in 0.1 *M*, pH 7 phosphate buffer. Values for TMV nucleic acid included for purposes of comparison. Leaves were excised 72 hours after inoculation with TMV, floated on $^{15}NH_4Cl$ for 47 hours, and then floated on unlabelled NH_4Cl for varying times. ^{15}N values were calculated on the basis of 100 atom percent excess ^{15}N in the initial substrate ammonium ion.

on the alga *Nostoc muscorum* by MAGEE AND BURRIS[12] suggests that the labelling of purines and pyrimidines probably takes place rapidly, so that the time lag in incorporation of isotope into the nucleic acid may lie between the bases and the polynucleotide.

The nucleoproteins of cell particulates

The possible implication of particulates in these synthetic processes was supported by another experiment (Experiment IV) in which uninfected and infected tobacco leaves, 19 days after inoculation with TMV, were given $^{15}NH_4Cl$ for 24 hours and then fractionated as in the earlier experiments. In addition, fraction P_1 was extracted with 2 *M* sodium chloride to yield nucleoprotein. Fraction P_3 and the residue of fraction P_1 after extraction with sodium chloride were extracted with cold and hot 5% trichloroacetic acid (TCA) to yield nucleotides and nucleic acids. There was no essential difference in the magnitude of these additional fractions between infected and noninfected plants. However, the nucleoprotein fraction was more highly labelled in both infected and uninfected plants than were the nucleotides, nucleic acids or any of the other soluble protein fractions obtained by the initial 0.1 *M* phosphate buffer extraction.

In view of the high label found earlier in the S_5 solution and succeeding fractions, a more detailed fractionation of this solution was resorted to in this experiment, using pH and temperature denaturation to obtain a number of small protein precipitates. In none of these was there found any precipitate characteristic only of the infected plant.

DISCUSSION

The nucleic acid-free abnormal protein found in TMV infected plants undergoes an incorporation of isotopic nitrogen from the non-protein nitrogen of the plant at a

References p. 136.

rate comparable with that of the TMV. Administration of the isotope for an interval early in the infection, when the virus is accumulating more rapidly than the abnomal protein, results in the virus that is isolated being more highly labelled. However, if the interval is chosen late in the infection, when the abnormal protein is being formed more rapidly, the abnormal protein that is isolated is labelled more highly than the virus. Therefore, neither protein *as isolated from the plant* can be derived from the other; the abnormal protein is not a degradation product of the virus *as a whole*, nor is the virus formed by a *general* polymerization of units of the abnormal protein.

Although the close relationship of the abnormal protein and virus insofar as their structure and synthesis are concerned is evident, the question as to whether the protein is a precursor or a degradation product of TMV *in vivo*, or is merely a second protein produced in infected plants is still unresolved. Our data do not exclude the possibility that the abnormal protein may be polymerized with nucleic acid to form TMV at the sites of virus synthesis in the plant cell. However, the isotope content of the abnormal protein which was isolated differed from that which would have been used for virus synthesis at the time at which the protein was isolated. The abnormal protein which was isolated could therefore represent an excess of virus precursor not utilized in virus synthesis because the protein was being produced at sites no longer synthesizing the intact virus, or because the protein had been lost by some other means from the sites of active virus synthesis to the protoplasm in general.

If the abnormal protein were an *in vivo* degradation product of the virus, the data in Table I would require that protein containing 7.8 atom percent excess ^{15}N be derived from TMV containing 0.22 atom percent excess ^{15}N. Only that portion of the virus synthesized in the period during which the leaf was exposed to the isotope would be labelled highly enough to serve as the source of the abnormal protein. The data in Table II would therefore require that during the 195–240 hour interval less than six virus particles be synthesized for every virus particle broken down. In Experiment III (Fig. 2), during the 140–240 hour interval, only three virus particles would have been synthesized for every particle broken down. Such degradation of the virus may occur as part of the process whereby the infection spreads from site to site within the cell or from cell to cell in the leaf. The spreading might be carried on only by a portion of the newly synthesized virus, with the bulk of the extant TMV being sequestered at sites no longer producing virus. Fragmentation of the infecting TMV particles into protein and nucleic acid moieties may occur in a manner analogous to the behavior of infecting bacteriophage particles, as discussed previously[14]. The abnormal protein may also result from a degradation of "superinfecting" TMV particles through a mechanism analogous to the degradation of "superinfecting" bacteriophage[6]. Alternatively, degradation of the final TMV particles synthesized at a site of virus production may occur as part of the mechanism regulating the amount of virus produced. In every case those protein fragments not re-utilized in the plant metabolism would represent the abnormal protein isolated.

It is highly unlikely that the abnormal protein could be an *in vitro* degradation product of TMV resulting from the isolation procedure. As shown previously[19], when purified TMV is carried through the isolation procedure for abnormal protein no abnormal protein is detected. In addition, when TMV is split into protein and nucleic acid moieties by heating[10], sodium dodecyl sulfate[16], urea[11] or alkali[16], the protein recovered no longer has the physical properties of the virus nor of the abnormal protein.

References p. 136.

The time lag observed for the appearance of isotope in the nucleic acid moiety of TMV as compared with the protein moiety emphasizes the differences in synthetic pathways of these moieties. The synthesis of the nucleic acid may involve large nitrogenous pools, possibly the nucleic acid associated with cell particulates, in addition to the pools of non-protein nitrogen.

If the final protein unit precursor of TMV possessed the dimensions of the abnormal protein then approximately 10^3 of these units would go into the virus particle. In view of the ease and rapidity with which the abnormal protein may be polymerized *in vitro* into TMV-like particles it is tempting to speculate that the nucleic acid may be synthesized to its final dimensions first and that the final act of virus synthesis may consist of a rapid polymerization of the units of TMV protein precursor around the nucleic acid core.

It is possible that the appearance of such abnormal proteins is a general phenomenon in plant virus infections; for in the case of turnip yellow mosaic virus infections MARKHAM AND SMITH[13] have also demonstrated the presence of a nucleic acid-free, non-infectious protein which otherwise resembles the virus closely in physical and chemical properties. JEENER[8] has reported upon experiments with turnip yellow mosaic virus infected plants similar to our experiments I and IV, but employing $^{14}CO_2$ as the tracer. His results, paralleling ours, show a greater incorporation of isotope into the abnormal protein than into the virus at a relatively advanced stage of infection. Here also the data do not exclude the RNA-free antigen as a possible precursor of the virus, but JEENER does not consider that they demonstrate unequivocally such a role.

SUMMARY

1. Experiments are reported in which the rate of assimilation of isotopic ammonium ion into various protein containing fractions of TMV-infected leaves was followed. Particular attention was given to an abnormal nucleic acid-free protein accompanying infection.

2. The protein sedimented by 80,000 × *g*. at pH 4.7, termed P_5, and corresponding to the protein "X" of TAKAHASHI AND ISHII, is the major abnormal protein other than the virus accompanying infection.

3. A close corresondence in isotope content appears to exist between the precursors of this protein and TMV.

4. Earlier observations on the metabolic stability of the bulk of TMV in the host cell are substantiated. The abnormal protein also appears to be relatively stable *in vivo*.

5. The extracted abnormal protein, P_5, cannot be a representative sample of a precursor of TMV, but the possibility of the same protein at the sites of synthesis being precursive is not excluded.

6. It is highly unlikely that the abnormal protein is a degradation product of TMV resulting from the extraction procedure, but the possibility is not excluded that the protein may result from an *in vivo* fragmentation of a specific portion of the total virus.

7. Isotopic ammonium ion is incorporated more slowly into the nucleic acid moiety of TMV than into the protein moiety.

8. The high activity of the particulate fractions in the incorporation of labelled nitrogen makes them suspect as the sites of virus synthesis.

RÉSUMÉ

1. Les auteurs ont suivi la vitesse d'assimilation de l'ion ammonium isotopique dans diverses fractions protéiques de feuilles infectées par le virus de la mosaïque du tabac (TMV). Une protéine anormale, sans acide nucléique, et dont la présence est liée à l'infection, a retenu particulièrement leur attention.

2. Cette protéine, qui sédimente sous 80,000 *g*. à pH 4,7 et qui est désignée par P_5, est identique à la protéine "X" de TAKAHASHI ET ISHII. C'est la principale protéine anormale, autre que le virus qui accompagne l'infection.

3. Il existe une correspondance étroite entre la teneur en isotope du précurseur de cette protéine et celle du précurseur du TMV.

References p. 136.

4. Les observations antérieures sur la stabilité métabolique de la masse du TMV dans la cellule hôte sont confirmées. La protéine anormale se montre également relativement stable *in vivo*.

5. La protéine anormale extraite, P_5, peut ne pas être un échantillon représentatif d'un précurseur du TMV, mais la possibilité que cette même protéine le soit sur les lieux de la synthèse n'est pas exclue.

6. Il est peu vraisemblable que la protéine anormale soit un produit de dégradation du TMV, résultant des méthodes d'extraction, mais il n'est pas impossible que cette protéine résulte d'une fragmentation *in vivo* d'une partie spécifique du virus entier.

7. L'ion ammonium isotopique est incorporé plus lentement dans la fraction nucléique du TMV que dans sa fraction protéique.

8. L'activité élevée des fraction particulaires au cours de l'incorporation de l'azote marquée amène à penser qu'elles peuvent être le lieu de la synthèse du virus.

ZUSAMMENFASSUNG

1. Es wird über Experimente berichtet, in denen die Geschwindigkeit der Assimilation des isotopen Ammoniumions in verschiedene Proteine, die in Fraktionen von TMV infizierten Blättern enthalten sind, verfolgt wird. Besondere Aufmerksamkeit wurde einem abnormen nukleinsäure-freien Protein, das die Infektion begleitet, gewidmet.

2. Das Protein sedimentiert bei 80,000 *g* bei pH 4.7. Es wird P_5 genannt und entspricht dem Protein "X" von TAKAHASHI UND ISHII. Es ist das bedeutendste abnorme Protein und ist verschieden von dem die Infektion begleitenden Virus.

3. Es scheint eine enge Beziehung im Isotopengehalt zwischen dem Vorläufer dieses Proteins und dem TMV zu bestehen.

4. Frühere Beobachtungen über Stoffwechselstabilität des Hauptanteiles des TMV in den Wirtszellen werden erhärtet. Das abnorme Protein scheint auch *in vivo* relativ stabil zu sein.

5. Das extrahierte abnorme Protein, P_5, kann kein repräsentativer Anteil des Vorläufers des TMV sein, aber die Möglichkeit, dass das gleiche Protein an den Orten der Synthese Vorläufer ist, wird nicht ausgeschlossen.

6. Es ist höchst unwahrscheinlich, dass das abnorme Protein ein während des Extraktionsprozesses entstehendes Abbauprodukt des TMV ist, aber es wird die Möglichkeit nicht ausgeschlossen, dass das Protein bei einer Fragmentation *in vivo* eines spezifischen Anteils des Gesamtvirus entstehen kann.

7. Das isotope Ammoniumion wird in den Nukleinsäureanteil des TMV langsamer eingebaut als in den Proteinanteil.

8. Die hohe Aktivität der besonderen Fraktionen beim Einbau von gezeichnetem Stickstoff in lässt es wahrscheinlich erscheinen, dass sie die Orte der Virussynthese sind.

REFERENCES

[1] B. COMMONER, P. NEWMARK AND S. RODENBERG, *Arch. Biochem. Biophys.*, 37 (1952) 15.
[2] B. COMMONER, D. L. SCHEIBER AND P. M. DIETZ, *J. Gen. Physiol.*, 36 (1953) 807.
[3] B. COMMONER, M. YAMADA, S. D. RODENBERG, T-Y. WANG AND E. BASLER, *Science*, 118 (1953) 529.
[4] C. C. DELWICHE, P. NEWMARK AND W. N. TAKAHASHI, *Federation Proc.*, 13 (1954) 197.
[5] L. EGGMAN, S. J. SINGER AND S. G. WILDMAN, *J. Biol. Chem.* 205 (1953) 969.
[6] A. F. GRAHAM, *Ann. inst. Pasteur*, 84 (1953) 90.
[7] A. JAGENDORF AND S. G. WILDMAN, 1953. Private communication.
[8] R. JEENER, *Biochim. Biophys. Acta*, 13 (1954) 307.
[9] R. JEENER AND P. LEMOINE, *Nature*, 171 (1953) 935.
[10] C. A. KNIGHT, *J. Biol. Chem.*, 197 (1952) 241.
[11] M. A. LAUFFER AND W. M. STANLEY, *Arch. Biochem.*, 2 (1943) 413.
[12] W. E. MAGEE AND R. H. BURRIS, *A.I.B.S. Bull.*, 2 (1952) 51.
[13] R. MARKHAM, R. E. F. MATHEWS AND K. M. SMITH, *Nature*, 162 (1948) 88.
[14] M. MENEGHINI AND C. C. DELWICHE, *J. Biol. Chem.*, 189 (1951) 177.
[15] P. NEWMARK, R. T. HERSH, W. N. TAKAHASHI AND C. C. DELWICHE, *Abstr. 125th Am. Chem. Soc. Meeting* (1954) 9c.
[16] G. SCHRAMM, *Z. Naturforsch.*, 2b (1947) 249.
[17] M. SREENIVASAYA AND N. W. PIRIE, *Biochem. J.*, 32 (1938) 1707.
[18] W. N. TAKAHASHI AND M. ISHII, *Nature*, 169 (1952) 419.
[20] W. N. TAKAHASHI AND M. ISHII, *Am. J. Bot.*, 40 (1953) 85.

Received August 6th, 1954

THE INTERACTION OF POLYMYXIN E WITH BACTERIAL AND OTHER LIPIDS

by

A. V. FEW

Department of Colloid Science, The University, Cambridge (England)

INTRODUCTION

In previous studies on the bactericidal action of polymyxin E[1,2,3] it has been shown that the treatment of suspensions of susceptible bacteria with the antibiotic results in a leakage of soluble cellular material from the organisms. To account for this effect, it has been suggested that polymyxin E combines with and thereby disorganises a cellular membrane within the organisms[4]. Such a mechanism presumes the presence of a membrane within the cell wall, which is capable of retaining low molecular weight cell solutes. The work of WEIBULL[5] has provided direct evidence for the presence of such a membrane underlying the cell wall of *Bacillus megaterium*. In addition, the examination of mechanically disrupted bacterial cells in the electron microscope has indicated the existence of a cellular membrane in other Gram positive[6] and Gram negative bacteria[4].

There is very little information concerning the chemical composition of bacterial membranes or of the nature of the sites which may be involved in the reaction with polymyxin E. Such information as is available suggests the presence of both lipid and protein in the membranes[7,8]. Whilst from a comparison of the competition between polymyxin and certain metallic cations for sites within the bacterial cell, NEWTON[9] has suggested that the polymyxin-combining groups in *Pseudomonas aeruginosa* may be polyphosphates.

In order to obtain further information on the mechanism by which polymyxin E exerts its bactericidal action, an investigation has been made of the interaction of polymyxin E with orientated monolayers of phospholipids and lipids of bacterial origin. The effects of the lipids in antagonizing the bactericidal action of polymyxin E has also been studied.

MATERIALS AND METHODS

Polymyxin E. A crystalline sample of polymyxin E sulphate, kindly given by Dr. J. F. TREVAN, was used.

Organisms. A polymyxin E sensitive strain of *Pseudomonas denitrificans* and a resistant strain of *Staphylococcus aureus*, previously investigated[1,3,4], were used. The growth conditions and harvesting were as described elsewhere[3,4].

Phospholipids. Highly purified samples of lecithin and cardiolipin were supplied by Dr M. PANGBORN. Cephalin was obtained from a chloroform extract of ox red cell stroma by precipitation with ethanol[10]. Paper chromatography of acid hydrolysates of this lipid fraction demonstrated the

References p. 145.

presence of serine in addition to ethanolamine. Thus this preparation contained both phosphatidyl serine and phosphatidyl ethanolamine but has been referred to as cephalin.

Preparation of bacterial fractions for lipid extraction

Suspensions of *Ps. denitrificans* in 0.01 *M* phosphate buffer pH 6.3 were disrupted in a Mickle disintegrator by the method described previously[3,4]. Care was taken to limit the shaking process so that the inner secondary layer, (cytoplasmic membrane[4]) was retained largely within the cell walls of the organism. The disrupted bacteria were washed free from contaminating cell cytoplasm and intact cells by differential centrifugation with the phosphate buffer, and were finally resuspended in distilled water and freeze dried.

Buffered suspensions of *Staph. aureus* were similarly disrupted. On centrifugation of the suspension at 3000 *g* for 20 min two layers were deposited, the lower being white and opaque and the upper dark yellow and opalescent. The pigmented layer was redispersed in the supernatant fluid, which was then decanted. The lower layer, which consisted of cell walls and a small quantity of intact cells, was submitted to differential centrifugation with the phosphate buffer to remove the intact cells. The cell walls were then resuspended in distilled water and freeze dried. The original supernatant, obtained after centrifugation of the suspension of disrupted *Staph. aureus*, was then centrifuged at 18,000 *g* for 1 h. This caused the deposition of the pigmented material, which was washed by centrifugation with the phosphate buffer, resuspended in distilled water and freeze dried. This dark yellow fraction has been isolated previously from *Staphylococci* by MITCHELL AND MOYLE[8] and COOPER[11] and has been shown by these authors to consist mainly of very small spherical particles. It has been suggested by MITCHELL AND MOYLE[8] that this small particle fraction, which contains a large proportion of lipid, may form a continuous layer or membrane beneath the cell wall of the intact *Staphylococci*.

Lipid extraction

The lipid extraction procedure was carried out on approximately 100 mg samples of the three bacterial fractions.

The lipids were obtained by first refluxing each of the bacterial fractions with 2 ml of 95% methanol for 1 h to disrupt any lipo-protein complexes (REICHERT[12]). The methanol was distilled off and the fractions dried *in vacuo* over P_2O_5 for 2 h. They were then each refluxed with 4 ml of Na dried diethyl ether for 30 min. After this time the ethereal extracts were collected and the process of refluxing repeated with fresh samples of ether. It was found that three extractions were sufficient to remove the ether soluble lipids from the fractions. The ethereal extracts from each fraction were transferred quantitatively to weighing bottles. After evaporation of the ether, the lipids were dried for 16 h *in vacuo* over P_2O_5, weighed, and dissolved in ether.

It was found that only a very small amount of lipid could be ether-extracted from the *Staphylococcal* cell walls, and it was possible only to investigate the properties of monolayers of this lipid and their interaction with polymyxin E.

Total nitrogen and total phosphorus analyses were made in duplicate on 1 mg samples of the lipids using the micro-methods described by UMBREIT, BURRIS AND STAUFFER[13]. These analyses were not carried out on the *Staphylococcal* cell wall lipid.

Paper chromatography

2 mg samples of the bacterial lipids were hydrolysed in sealed tubes containing 1 ml of 6 *N* HCl for 48 h at 100°. The chilled and filtered hydrolysates were evaporated and dried *in vacuo* over P_2O_5 and KOH pellets, redissolved in a small volume of distilled water and again dried. The residues were then dissolved in 0.025 ml of distilled water and samples submitted to uni-dimensional paper chromatography. Chromatograms were run for 18 h using Whatman No. 1 filter-paper with the solvent system *n*·butanol/acetic acid (10:3 v/v) saturated with water. Test mixtures of serine, ethanolamine and choline were also run with the lipid hydrolysates. The primary amino compounds were detected by the ninhydrin method. Choline was detected on separate chromatograms by the phosphomolybdic acid method of CHARGAFF, LEVINE AND GREEN[14].

Monolayer technique

Monomolecular films of the lipids were studied at the air/liquid interface using a Langmuir-Adam surface balance. Spreading solutions of the phospholipids were prepared using a mixed alcohol/benzene (1:9 v/v) solvent; the bacterial lipids were generally spread from 60–80° petroleum ether. Measurements were made at 20° ± 1. The reactions of spread monolayers of the lipids were investigated by injecting aqueous solutions of polymyxin E, with thorough mixing, into the trough solution underlying the monolayers. The reactions were followed by noting the increase in surface pressure (decrease of interfacial tension) with time at a constant monolayer area, *i.e.* "constant area penetration"[15]. Where necessary, corrections were applied to the observed surface pressure readings to compensate for the change in surface tension on the reference side of the surface balance

References p. 145.

when polymyxin E was added to the trough solution. Since polymyxin E is only slightly surface active at the air/liquid interface[3] this correction, added to the observed surface pressure, amounted to only 0.8 dyne/cm at the highest concentration of polymyxin E used in the penetration experiments.

Bulk reactions of the lipids with polymyxin E

The lipids were dissolved at 1 mg/ml in a mixed ether/alcohol solvent. 0.05 ml samples were added to a series of 1 ml sterile solutions of polymyxin E (0–80 μg/ml) in 0.01 *M* phosphate buffer, pH 6.3, contained in 1 × 7.5 cm tubes. After 15 min the tubes were inoculated with 1 ml suspensions of the polymyxin sensitive strain of *Ps. denitrificans* at 0.02 mg bacterial dry wt/ml, and the tubes incubated at 25° for 20 min. Suitable controls without the addition of the lipids were also set up and incubated. Dilutions of the suspensions were then made in nutrient broth, and the broth suspensions plated out on agar medium. The plates were read after 24 h incubation at 37°.

RESULTS

Table I shows the results obtained for the lipid extraction of the bacterial fractions and some properties of the lipids. Choline was not detected among the nitrogenous constituents of the *Pseudomonas* lipid and *Staphylococcal* small particle fraction lipid, whereas both serine and ethanolamine were identified in hydrolysates of these lipids. In addition to these two constituents another unidentified ninhydrin-reacting substance was present in hydrolysates of the *Staph. aureus* small particle fraction lipid. In the solvent system used for the chromatography this substance had an R_F value approximately half that of ethanolamine. LEVINE AND CHARGAFF[16] have also reported the presence of minor nitrogenous constituents, in addition to choline, ethanolamine and serine, in hydrolysates of beef brain phosphatides.

TABLE I

LIPID EXTRACTION OF THE BACTERIAL FRACTIONS

Bacterial fraction	*Lipid* extracted*	*Total N***	*Total P***	*Choline*	*Ethanolamine*	*Serine*
Disrupted cells of *Ps. denitrificans*	12.8	1.1	4.3	—	+	+
Cell walls of *Staph. aureus*	0.8	not determined				
Small particle fraction of *Staph. aureus*	22.3	0.8	1.8	—	+	+

* Lipid extraction expressed as the percentage dry wt of the appropriate bacterial fraction.
** N and P analyses given as the percentage contained in the lipid material.

The lipid material isolated from the disrupted cells of *Ps. denitrificans* was found to contain a high percentage of phosphorus, this being of the same order as that found in many phosphatides. However, the nitrogen analyses indicated that this lipid cannot consist entirely of nitrogen-containing phosphatides, and it is probable that a significant proportion (c. 50%) of this lipid mixture consists of phosphatidic acids. It is relevant here to mention that FOLCH[17] has identified phosphatidyl inositol as a constituent of the phosphatides present in brain cephalin.

The nitrogen and phosphorus analyses of the lipid mixture isolated from the small particle fraction of *Staph. aureus* show that these elements were present in equimolecular amounts. The quantities of these elements present would suggest that phosphatides could account for only approximately 50% of the lipids in the mixture. Other ether-soluble materials such as the sterols and fatty acids may contribute to this lipid mixture.

References p. 145.

Monolayer characteristics of the lipids

The properties of monolayers of lecithin, cephalin and cardiolipin have been reported elsewhere[10].

Monolayers of the bacterial lipids were investigated on trough sub-solutions of 0.145 *M* NaCl adjusted with HCl or NaOH to give solutions at pH 2, 6 and 10. Fig. 1 gives the force/area (F/A) curves of the *Ps. denitrificans* lipid. The monolayers were progressively expanded as the trough solution pH was increased from 2 to 10, although at surface pressures greater than 16 dynes/cm the F/A curves converged and above this surface pressure showed little if any dependence upon pH. This effect of pH can be ascribed to the ionization of acidic groups (phosphate, carboyxl) present in the monolayer, which results in an increased electrostatic repulsion between these groups when the trough solution pH is increased. A similar pH dependence has been observed with monolayers of cardiolipin and cephalin[10].

The F/A curves of the lipid isolated from the small particle fraction of *Staph. aureus* are given in Fig. 2. Monolayers of this lipid were unaffected by a change of the sub-solution pH from 2 to 6, whilst at pH 10 expansion of the monolayer occurred. Fig. 3 shows the F/A curves of the lipid obtained from the cell walls of *Staph. aureus*. Very little dependency upon trough sub-solution pH was observed with this lipid, although slightly greater areas were found for the monolayers at pH 2 when compared with those at pH 6 and 10.

It was considered that in view of the very low lipid content of the *Staphylococcal* cell wall preparation this lipid might have been derived from a contamination of the cell walls with traces of the lipid-rich small particle fraction. However, the properties of monolayers of the two *Staphylococcal* lipids demonstrate that these lipids differ considerably in their overall composition. The presence of very small quantities of lipid material in the cell walls of several other Gram positive bacteria has been reported by SALTON[18].

Constant area penetration of lipid monolayers by polymyxin E.

For the penetration experiments, the lipids were spread upon 0.01 *M* phosphate buffer at pH 6.8 and the monolayers compressed to a surface pressure of 5.6 dyne/cm. The effect of adding polymyxin E to the trough sub-solution underlying monolayers of the *Ps. denitrificans* lipid compressed initially to 5.6 dyne/cm. is recorded in Fig. 4. After the addition of polymyxin E the surface pressure rose rapidly. This occurred as a result of the electrostatic binding of the lipid polar groups with those of the polymyxin E, and the association between the non-polar portions of the lipid and the penetrating molecule. The surface pressure continued to rise for several minutes, and then reached a steady value. Similar results were obtained for the other lipids, with the exception of monolayers of lecithin which were found to be unreactive to the injected polymyxin E. The polymyxin E/lipid monolayer reactions were studied with a range of polymyxin E concentrations and the resultant surface pressure rises (interfacial tension decreases) noted by extrapolating the linear portions of the reaction isotherms to zero time. By this means penetration isotherms were obtained by plotting the extrapolated pressure rises against the concentration of polymyxin E present. Fig. 5 shows the constant area penetration isotherms for all the lipids studied. The small surface pressure changes observed with lecithin monolayers are no greater than those expected for the free adsorp-

References p. 145.

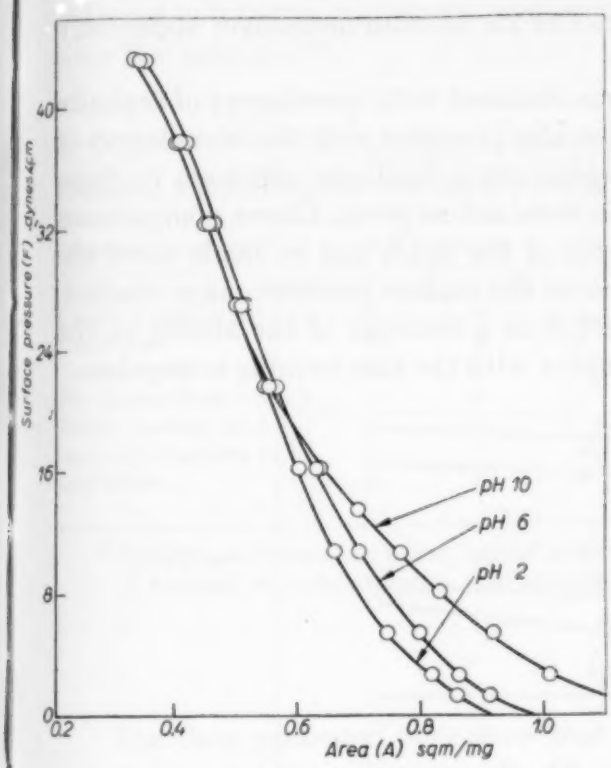

Fig. 1. Force/area curves of lipid derived from disrupted cells of *Ps. denitrificans*, spread upon 0.145 *M* NaCl, pH adjusted with NaOH or HCl. T = 20°.

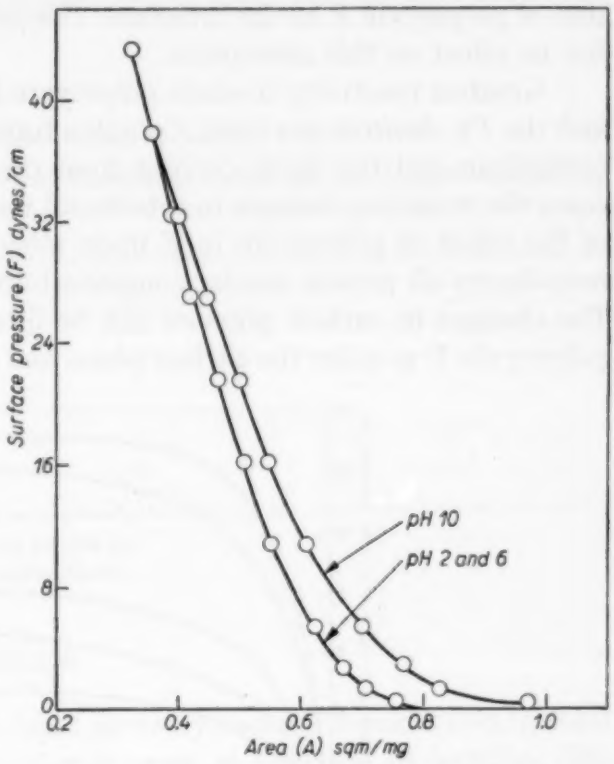

Fig. 2. Force/area curves of lipid derived from the small particle fraction of *Staph. aureus*, spread upon 0.145 *M* NaCl, pH adjusted with NaOH or HCl. T = 20°.

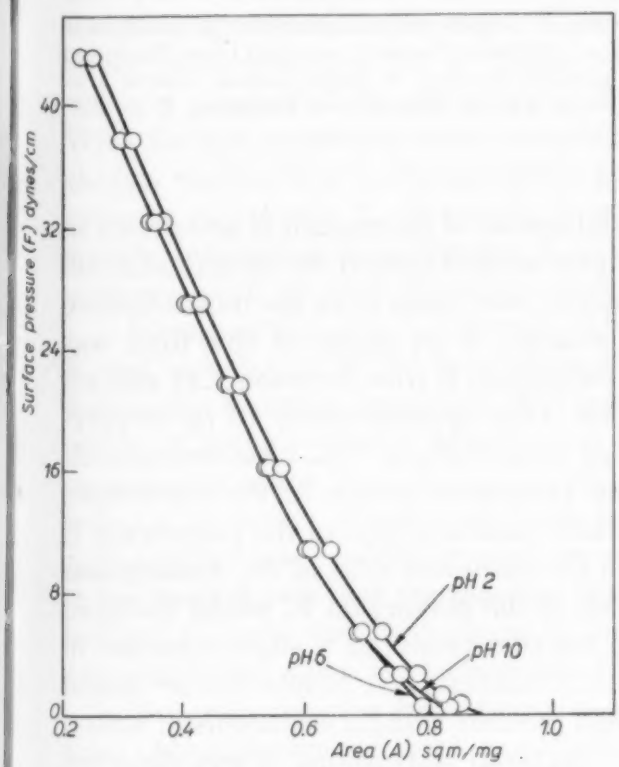

Fig. 3. Force/area curve of lipid derived from the cell walls of *Staph. aureus*, spread upon 0.145 *M* NaCl, pH adjusted with NaOH or HCl. T = 20°.

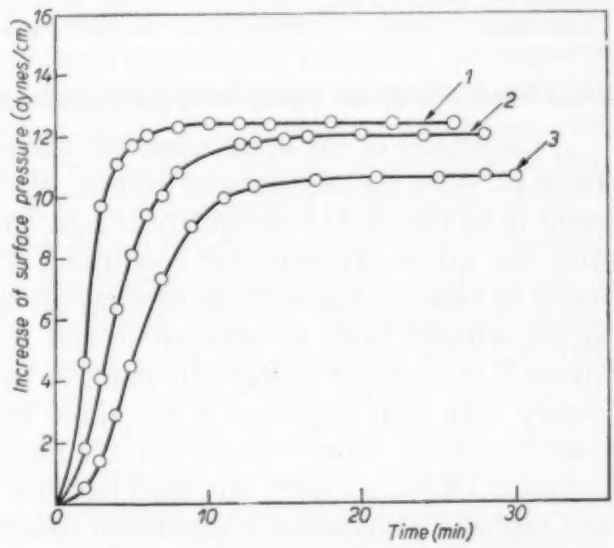

Fig. 4. The penetration of polymyxin E into monolayers of the lipid isolated from disrupted cells of *Ps. denitrificans*. Lipid monolayers spread on 0.01 *M* phosphate buffer pH 6.8 and compressed initially to 5.6 dynes/cm. Polymyxin E added to the trough solution to give concentrations of 5 μg/ml (Curve 1), 2.5 μg/ml (Curve 2), and 1.25 μg/ml (Curve 3). T = 20°.

tion of polymyxin E at the interface. The presence of the lecithin monolayer apparently has no effect on this adsorption.

Greatest reactivity towards polymyxin E was obtained with monolayers of cephalin and the *Ps. denitrificans* lipid. Complex formation also occurred with the monolayers of cardiolipin and the lipids derived from the *Staphylococcal* fractions, although in these cases the resulting changes in interfacial tension were not so great. Direct comparisons of the effect of polymyxin in E upon monolayers of the lipids can be made since the monolayers all possess similar compressibilities over the surface pressure range studied. The changes in surface pressure can be interpreted as a measure of the ability of the polymyxin E to enter the surface phase and complex with the film forming molecules.

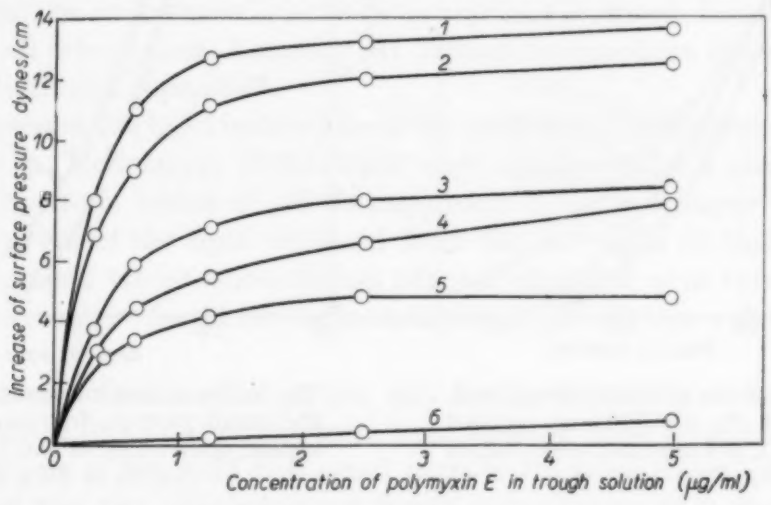

Fig. 5. The penetration of lipid monolayers by polymyxin E. Lipids spread upon 0.01 *M* phosphate buffer pH 6.8 and compressed to 5.6 dynes/cm. Curve 1 = Cephalin, Curve 2 = Lipid from disrupted cells of *Ps. denitrificans*, Curve 3 = Lipid from small particle fraction of *Staph. aureus*, Curve 4 = Cardiolipin, Curve 5 = Lipid from the cell walls of *Staph. aureus*, Curve 6 = Lecithin. T = 20°.

Bulk reactions of the lipids with polymyxin E

The effects of the lipids upon the bactericidal action of polymyxin E are shown in Table II. With the exception of lecithin, all the lipids studied caused the bactericidal end point to be raised. The phosphatidic acid, cardiolipin, was found to be the most effective with the given experimental conditions. The presence of 25 μg/ml of this lipid was found to raise the bactericidal concentration of polymyxin E from between 1.25 and 2.5 μg/ml, without lipid, to between 10 and 15 μg/ml. Thus approximately 10 μg of polymyxin E is rendered biologically inactive by 25 μg of cardiolipin. This ratio corresponds closely with that expected if the three ionizing phosphate groups in the cardiolipin molecule (M.W. 2,200)[19] react with the four available amino groups of the polymyxin E molecule (M.W. 1,250)[20]. The lipid isolated from the disrupted cells of *Ps. denitrificans* and cephalin also caused a significant inactivation of the polymyxin E, whilst the lipid obtained from the *Staphylococcal* small particle fraction produced a slight increase in bactericidal end point. In this connection, BLISS, CHANDLER AND SCHOENBACH[21] found that soap and phospholipid extracts of soya bean exerted a slight antagonistic action towards polymyxin. Prior to the addition of the bacterial suspensions, it was observed that insoluble complexes were formed between the lipids and polymyxin E in the tubes containing the higher concentrations of polymyxin E. This occurred in all cases with the exception of systems containing lecithin. The formation of water insoluble complexes

References p. 145.

between polymyxin and unspecified phospholipids has also been reported by LATTERADE AND MACHEBOEUF[22].

TABLE II

EFFECT OF LIPIDS ON POLYMYXIN E ACTIVITY

Bacteria: *Ps. denitrificans* 0.01 mg dry wt/ml., 0.01 *M* Phosphate buffer pH 6.3. Lipids at 25 μg/ml.

Polymyxin E conc. μg/ml	0	0.31	0.63	1.25	2.5	5.0	10	20	40
Control (no lipid)	+	+	+	+	—	—	—	—	—
Lecithin	+	+	+	+	—	—	—	—	—
Cardiolipin	+	+	+	+	+	+	+*	—*	—*
Ps. denitrificans lipid	+	+	+	+	+	+	—*	—*	—*
Staph. aureus small particle fraction lipid	+	+	+	+	+	—	—*	—*	—*
Cephalin	+	+	+	+	+	+	—*	—*	—*

* Precipitate formed in tubes before addition of bacteria.
+ Growth on subculture; — No growth on subculture.

DISCUSSION

The data presented here show that the lipid monolayers vary considerably in their reactivity towards polymyxin E. Of particular interest is the case of lecithin. The absence of any surface complex formation with the lecithin monolayers indicates that the positively charged choline group effectively shields the ionized phosphate group. This prevents an electrostatic bonding between the monolayer phosphate groups and the amino groups of the polymyxin E molecule, which would be necessary for penetration of the monolayer to occur. It has been observed that monolayers of cephalin are more strongly penetrated by polymyxin E than those of the phosphatidic acid, cardiolipin. With the pH conditions used, monolayers of both these lipids possess a net negative charge, which is due to the phosphate groups, and which facilitates interaction with the cationic polymyxin E. However, it is evident that, with cephalin monolayers, the specific interaction of polymyxin E with other hydrophilic groups, in addition to that occurring with the lipid phosphate group, leads to an enhancement of the penetration.

Strong surface complex formation has been shown to take place between polymyxin E and monolayers of the lipid derived from the disrupted cells of *Ps. denitrificans*, a polymyxin sensitive organism. It is possible, therefore, that the observed bactericidal action of polymyxin E[1,3] may be due to the reaction of the antibiotic with the lipid components of the bacterial membrane. It is considered that this reaction produces an increase in surface pressure (decrease in interfacial tension) at the membrane which is sufficient to cause a modification of the membrane structure. In support of this suggestion it has been shown that the reaction between polymyxin E and monolayers of the lipid isolated from the disrupted cells of *Ps. denitrificans* occur, and are completed, at antibiotic concentrations which are bactericidal for susceptible organisms[1].

Moderate complex formation also occurs with polymyxin E and monolayers of the lipid obtained from the small particle fraction (cellular membrane[8]) of *Staph. aureus*, an organism resistant to polymyxin E. However, the demonstration of a reaction between polymyxin E and isolated structural components of the bacterial cell does not necessarily imply that such a reaction will occur in the intact cell. The antibiotic must be able to

References p. 145.

penetrate readily to the susceptible site. For the case of polymyxin E, it has been observed previously[1,3] that whereas sensitive bacteria rapidly absorb large quantities of the antibiotic, resistant organisms, under the same conditions, only poorly absorb polymyxin E. In addition, a study of haemolysis by ionic detergents[23], a process analogous to the action of ionic surface active agents upon bacteria[24], has shown that complete lysis only occurs when a critical surface pressure is attained at the red cell surface. The critical surface pressure is reached by complex formation between the stroma cholesterol and detergent lysin. If a similar mechanism applies for bacteriolysis by surface active compounds, the absence of any rapid cytolytic action when resistant bacteria are exposed to polymyxin E can be attributed to both the poor absorption of the antibiotic and to the inability of polymyxin E to produce a sufficient increase in surface pressure at the membrane.

The ability of the lipids to antagonize the bactericidal action of polymyxin E did not follow exactly the reaction sequence found for the penetration of the lipid monolayers by polymyxin E. This is not unexpected in view of the differences in particle size and accessibility of the reactive groups of the lipids when present in aqueous dispersions. Thus the polymyxin E reactivity sequence found for the penetration of the lipid monolayers, which are orientated at the interface, must be regarded as giving a more precise indication of the molecular associations. It has been suggested by BAKER, HARRISON AND MILLER[25] that phospholipids may protect the bacterial cell from the toxic effects of detergents by altering the structure of the cellular membrane so as to prevent penetration by the detergents. It does not appear necessary to suggest such a mechanism in the present case. The action of the lipids can be adequately explained by the formation of biologically inactive complexes with polymyxin E in the suspension medium. Similarly, SCHULMAN AND RIDEAL[26] have shown that haemolysis by sodium cetyl sulphate is inhibited by the simultaneous addition of cholesterol, the inhibition being due to the formation of a strong complex between cholesterol and the detergent.

ACKNOWLEDGEMENTS

The author wishes to thank the Medical Research Council for a personal grant, and Dr. J. H. SCHULMAN, O.B.E., for helpful discussions.

SUMMARY

The reactions of polymyxin E with several lipids have been investigated using the monolayer technique. Strong complex formation has been shown to occur between polymyxin E and monolayers of a cephalin preparation and with monolayers of the lipid material isolated from disrupted cells of *Ps. denitrificans*, a polymyxin-susceptible organism. Moderate complex formation also occurred between polymyxin E and monolayers of cardiolipin and the lipid material obtained from two *Staphylococcal* fractions, whilst lecithin monolayers were unreactive towards polymyxin E. The relationship of these results with the suggestion that polymyxin E causes a disorganisation of the cellular membrane of susceptible organisms is discussed.

The antagonistic effects of several of the lipids upon the bactericidal action of polymyxin E has been ascribed to the formation of biologically inactive complexes in the bacterial suspension medium.

References p. 145.

RÉSUMÉ

Les réactions de la polymyxine E avec divers lipides ont été étudiées par la technique des couches monomoléculaires. La polymyxine E forme aisément des complexes avec des couches monomoléculaires de céphaline, ainsi qu'avec des couches monomoléculaires d'un lipide isolé de cellules désagrégées de *Ps. denitrificans*, organisme sensible à la polymyxine. Elle forme moins facilement des complexes avec des couches monomoléculaires de cardiolipine et d'un matériel lipidique extrait de deux fractions de *staphyloccoques*; des couches monomoléculaires de lécithine ne réagissent pas avec la polymyxine E. La relation entre ces résultats et l'hypothèse selon laquelle la polymyxine E provoquerait la désorganisation de la membrane cellulaire des organismes sensibles est discutée.

L'action antagoniste de quelques lipides sur l'activité bactéricide de la polymyxine E est attribuée à la formation de complexes biologiquement inactifs dans le milieu de suspension des bactéries.

ZUSAMMENFASSUNG

Es wurden die Reaktionen von Polymixin E mit verschiedenen Lipoiden unter Verwendung der Oberfächenfilmtechnik untersucht. Starke Komplexbildung wurde beobachtet zwischen Polymixin E und Filmen einer Cephalinpräparation und Filmen aus Lipoiden, die aus zerstörten Zellen von *Ps. denitrificans*, einem Polymyxin empfindlichen Organismus, hergestellt wurden. Eine mittlere Komplexbildung trat auf zwischen Polymyxin E und Filmen aus Cardiolipin und Lipoiden, die aus *Staphylococcen*-Fraktionen erhalten wurden. Filme aus Lezithin dagegen reagierten nicht mit Polymyxin E. Es werden diese Ergebnisse mit der Vorstellung, dass Polymyxin E eine Zerstörung der Zellmembran der empfindlichen Organismen hervorruft, diskutiert.

Die antagonistischen Wirkungen einiger Lipoide auf die baktericide Wirkung von Polymyxin E wird der Bildung von biologisch unwirksamen Komplexen in dem Suspensionsmedium zugeschrieben.

REFERENCES

1 A. V. Few and J. H. Schulman, *Nature*, 171 (1953) 644.
2 B. A. Newton, *J. Gen. Microbiol.*, 9 (1953) 54.
3 A. V. Few and J. H. Schulman, *J. Gen. Microbiol.*, 9 (1953) 454.
4 A. V. Few, *J. Gen. Microbiol.*, 10 (1954) 304.
5 C. Weibull, *J. Bact.*, 66 (1953) 688 and 696.
6 I. M. Dawson and H. Stern, *Biochim. Biophys. Acta*, 13 (1954) 31.
7 G. Knasyi, *J. Bact.*, 51 (1946) 113.
8 P. Mitchell and J. Moyle, *J. Gen. Microbiol.*, 5 (1951) 981.
9 B. A. Newton, *J. Gen. Microbiol.*, 10 (1954) 491.
10 A. V. Few and J. H. Schulman, *Biochim. Biophys. Acta*, 10 (1953) 302.
11 P. D. Cooper, *Biochem. J.*, 54 (1953) XX.
12 R. Reichert, *Helv. Chim. Acta*, 27 (1944) 961.
13 W. W. Umbreit, R. H. Burris and J. F. Stauffer, *Manometric Techniques and Tissue Metabolism*, Burgess Pub. Co., Minneapolis, p. 161 and 190.
14 E. Chargaff, C. Levine and C. Green, *J. Biol. Chem.*, 175 (1948) 67.
15 E. D. Goddard and J. H. Schulman, *J. Colloid Sci.*, 8 (1953) 309.
16 C. Levine and E. Chargaff, *J. Biol. Chem.*, 192 (1951) 465.
17 J. Folch, *J. Biol. Chem.*, 177 (1949) 497.
18 M. R. J. Salton, *Biochim. Biophys. Acta*, 10 (1953) 512.
19 M. C. Pangborn, *J. Biol. Chem.*, 168 (1947) 358.
20 A. V. Few and J. H. Schulman, *Biochem. J.*, 54 (1953) 171.
21 E. A. Bliss, C. A. Chandler and E. B. Schoenbach, *Ann. N.Y. Acad. Sci.*, 51 (1949) 944.
22 C. Latterade and M. Macheboeuf, *Ann. Inst. Pasteur*, 78 (1950) 753.
23 B. A. Pethica and J. H. Schulman, *Biochem. J.*, 53 (1953) 177.
24 R. D. Hotchkiss, *Ann. N.Y. Acad. Sci.*, 46 (1946) 479.
25 Z. Baker, R. W. Harrison and B. F. Miller, *J. Exp. Med.*, 74 (1941) 621.
26 J. H. Schulman and E. K. Rideal, *Proc. Roy. Soc.*, B 122 (1937) 29.

Received August 21st, 1954

GEISSELMODELLE UND ADENOSINTRIPHOSPHAT (ATP)

von

HARTMUT HOFFMANN-BERLING

Max-Planck-Institut für medizinische Forschung, Institut für Physiologie, Heidelberg (Deutschland)

I

Die Entscheidung darüber, ob das vorhandene ATP Kontraktion oder Erschlaffung bewirkt, ist im lebenden Muskel einem Membranmechanismus übertragen, der durch unbekannte Zwischenreaktionen die ATP-Spaltung zu enthemmen und dadurch die Kontraktion freizugeben vermag. Die rhythmische Tätigkeit der lebenden Muskelfaser bei tetanischer Kontraktion ist Ausdruck rhythmisch ablaufender Membranprozesse. Werden diese durch Zerstörung der Zellmembran ausgeschaltet, so ist je nach den Bedingungen anhaltende Kontraktion oder anhaltende Erschlaffung die Folge, wenn das kontraktile Protein mit ATP zusammengebracht wird[1]. Das beweisen die sog. Faser-[2] und Fadenmodelle[1], die aus Muskeln hergestellt sind.

Die durch Extraktion mit Glycerin-Wassermischungen hergestellten Modelle von Zellen und Zellteilen[3] zeigen, dass die Einzelzelle das Zusammenspiel von Kontraktion, Erschlaffung und Streckung auch noch auf andere Weise regulieren kann. So erklärt sich die Gleichzeitigkeit von Plasmadurchschnürung und Zellstreckung während der Telophase durch lokale Unterschiede in den Eigenschaften der beteiligten funktionellen Proteine[4].

Auch Spermatozoengeisseln und *Trypanosomen* können mit wässrigem Glycerin extrahiert und dadurch ihrer löslichen Eiweisse, Fermente und Betriebsstoffe beraubt werden. Solche Geisselmodelle arbeiten trotz der Membranzerstörung rhythmisch: wird ATP zugesetzt, so wechseln in ihnen Kontraktion und Erschlaffung und laufen als Wellenbewegung über die Modelle hin[5].

Soweit untersucht, lassen sich funktionsfähige Geisselmodelle aus *Trypanosomen** und aus den Spermatozoen von Vertebraten (Maus, Hahn) wie von Wirbellosen (Schmeissfliegen*, Heuschrecken) herstellen. Für quantitative Untersuchungen besonders geeignet sind die riesigen Spermiengeisseln grosser Heuschreckenarten (*Tachycines**), die ihre Kontraktilität in den Extraktionslösungen bei —18° C bis zu 40 Tagen bewahren**.

---

* Herrn Prof. KRAUSE, Tübingen, danke ich für die freundliche Überlassung von Heuschrecken, Herrn Prof. PRIGGE, Frankfurt a.M., für *Trypanosoma brucei*-infizierte Mäuse, Herrn Prof. STEINER, Heidelberg, für die Überlassung von *Phormia regina*.

** Dass ATP Betriebsstoff der Cilien- und Geisselbewegung sei, ist schon von ENGELHARDT[6] vermutet worden. Versuche, eine Wirkung des ATP auf abgetrennte Cilien nachzuweisen[7], blieben jedoch umstritten, und auch die Beschleunigung, die die Geissel[8]- und Ciliarbewegung[9] lebender Zellen durch ATP erfährt, ist vieldeutig, denn es kann sich um einen Einfluss des ATP auf die Zellmembran oder die ganze Zelle handeln.

Literatur S. 154.

II

An Geisselmodellen laufen rhythmische Bewegungen selbst dann ab, wenn die Geisseln von Mittelstück und Kopf abgetrennt sind: also muss in Geisselmodellen das kontraktile Protein selbst die Bewegung steuern. Da jedoch die terminalen Abschnitte von Spermiengeisseln an den Bewegungen mehr passiv teilnehmen, führt ein abgetrenntes Geisselende unter ATP Bewegungen nur aus, wenn die Abtrennung nicht weiter distal als zwischen mittlerem und letztem Drittel der Geissel erfolgte. — Werden die drei lichtmikroskopisch gut sichtbaren Fibrillen, die in den Spermiengeisseln von *Tachycines* umeinandergewunden sind, durch Behandlung mit hoher Ionenstärke bei schwach alkalischem pH voneinander getrennt, so bewegt sich jede einzeln liegende Fibrille ebenfalls noch rhythmisch.

Diese Beobachtungen sind beschränkt auf die Geisseln der Spermien von *Tachycines**, denn nur diese grossen Geisseln können an beliebiger Stelle durchschnitten und aufgespalten werden. Für *Trypanosomen*geisseln sind analoge Verfahren noch nicht gefunden worden.

Die Umschaltung von Kontraktion auf Erschlaffung (oder Streckung) wird anscheinend lokal ausgelöst durch die jeweilige Verformung der Geissel an der betreffenden Stelle. Bewegung und Gegenbewegung scheinen sich gegenseitig auszulösen. Für diese These sprechen die Wirkungen, die bei Behinderung der Bewegung auftreten: werden Geisseln an umschriebener Stelle mechanisch festgelegt, so findet man häufig zu beiden Seiten des Fixierungspunktes einen verschiedenen Rhythmus. Geisseln, die durch Retraktion des von der Unterlage abgelösten Einbettungsmediums (vgl. im method. Teil) gestaucht und in enge Windungen gelegt sind, bewegen sich nicht mehr.

Die Einbettung der Spermatozoen und *Trypanosomen* in ein dünnes Fibrinkoagulum, die es ermöglicht, das gleiche Modell unter wechselnden Bedingungen zu beobachten, erlaubt der fixierten Geissel nur wellenförmige Kontraktionen. Gelegentlich wurden freischwimmende Modelle untersucht, um die Wirksamkeit der Geisseltätigkeit für die Fortbewegung zu prüfen. Nur bei kurz extrahierten Zellen findet eine — wenn auch wenig gerichtete — Lage- und Ortsänderung statt, bei lang extrahierten Modellen ist der Geisselapparat hierfür zu starr. Bei kurz extrahierten *Trypanosomen*modellen sind die für die lebende Zelle charakteristischen schnellenden Körperbewegungen zu beobachten, an vieltägig extrahierten Modellen laufen nur noch wellenförmige Kontraktionen an Geissel und undulierender Membran ab**.

Auch unter optimalen Bedingungen bleibt die Bewegung der Modelle hinter den Bewegungen lebender Geisseln zurück. Sie kommt diesen umso näher, je kürzer die Modelle extrahiert und je länger sie mit ATP behandelt werden. Ursache der regressiven Veränderungen sind anscheinend Denaturierung und zunehmende Verfestigung, die sich ähnlich auch bei anderen Modellen einstellt[10].

III

Alle quantitativen Angaben der Figs. 1–7 beziehen sich auf Modelle aus den Spermiengeisseln von Tachycines, da diese über Stunden gleichmässig reagieren. Jede Kurve gibt das Verhalten einer Geissel wieder. Da Schlagfrequenzen > 8/sec nicht mehr sicher auszuzählen sind, wurden die Kurven in den hohen Frequenzbereichen nur gestrichelt und das Einsetzen von Messwerten wurde zumeist unterlassen.

Die minimale ATP-Konzentration, die in Suspensionen von Muskelfibrillen mit einem Fibrillendurchmesser von 1–1,5 μ maximale Kontraktion erzeugt, d.h. gerade

* Der Durchmesser des Spermatozoenkopfes ist bei *Tachycines* nicht grösser als der Geisseldurchmesser; Kopf und Geisselende der Spermien sind jedoch durch ihre unterschiedliche Zuspitzung auseinanderzuhalten.

** Auch eine von der Membran abgerissene Geissel bewegt sich noch; gänzlich aus dem Körper herausgelöste *Trypanosomen*geisseln wurden nicht beobachtet.

Literatur S. 154.

gross genug ist, um trotz der Spaltung des eindringenden ATP auch die zentralen Anteile der Fasern zu durchtränken, ist wenig grösser als 10^{-5} *M*[11] und beträgt für *Tachycines*-geisseln mit einem Durchmesser von 0.9 μ etwa $5 \cdot 10^{-6}$ *M*. Schon hierin findet sich eine Übereinstimmung entwicklungsgeschichtlich weit auseinanderliegender Prozesse.

Die Bewegungsgeschwindigkeit der Geisselmodelle ist temperaturabhängig und verdoppelt sich jeweils zwischen 0° und 10° und zwischen 10° und 20° C (Fig. 1). Ähnlich verhalten sich Muskelmodelle, deren Verkürzungsgeschwindigkeit mit der Temperatur zunimmt, weil sie ATP bei höheren Temperaturen schneller spalten[1]. Vermutlich dürfte dieselbe Erklärung auch für Geisselmodelle zutreffen. Dazu passen die Angaben NELSON's[12], der in isolierten Spermiengeisseln eine wirksame, strukturgebundene ATPase auffand.

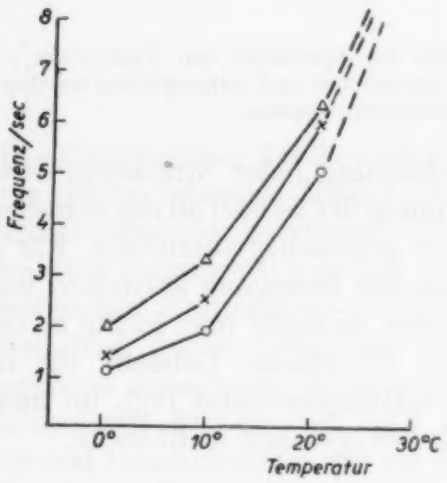

Fig. 1. Schlagfrequenz und Temperatur. 19 Tg. extr. Modelle, 10^{-3} *M* ATP, pH 7.2, I = 0.18 μ.

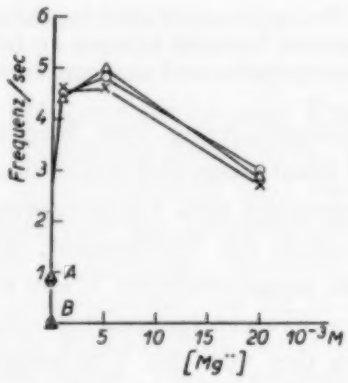

Fig. 2. Schlagfrequenz und Mg^{++}-Konzentration. 2 Tg. extr. Modelle, 10^{-4} *M* ATP, pH 6.8, I = 0.20 μ. A = ohne Mg^{++}-Zusatz; B = mit $5 \cdot 10^{-3}$ *M* Äthylendiaminotetraacetat.

Für die rhythmische Bewegung der Geisselmodelle sind geringe Mengen Mg^{++} erforderlich — wie für die Kontratktion von Muskel- und Fibroblastenmodellen. Die Kontraktilität aller Modelle erlischt, wenn diese Spuren durch $5 \cdot 10^{-3}$ *M* Aethylendiaminotetraacetat gebunden werden. Regelmässigkeit und Frequenz der Geisselbewegung werden durch Zugabe von 10^{-3} *M* Mg^{++} gesteigert und durch Konzentrationen $> 10^{-2}$ *M* gehemmt (Fig. 2).

$5 \cdot 10^{-5}$ *M* Salyrgan* unterdrückt die Bewegung der Geisselmodelle und 10^{-2} *M* Monojodacetat verringert zwar die Bewegungsgeschwindigkeit, hebt die Beweglichkeit aber nicht auf. Die Giftempfindlichkeit der Geisselmodelle ist also ähnlich abgestuft wie die Empfindlichkeit der Muskelmodelle. Dagegen kann bei Geisselmodellen das Salyrgan nur unvollkommen durch $2 \cdot 10^{-2}$ *M* Cystein entgiftet werden.

Die Intensität der Kontraktion aller Muskel-[13,14] und Zellmodelle[5] nimmt ab, wenn die ATP-Konzentration über ein Optimum hinaus erhöht wird, das je nach der Art des Modells (und der Extraktionsdauer, Ionalität und Temperatur) verschiedene Werte hat. Diese Optima liegen in der Regel zwischen 10^{-3} *M* und $> 10^{-2}$ *M* ATP. Die *Trypanosomen*modelle stellen bei Gegenwart von $5 \cdot 10^{-3}$ *M* ATP ihre Bewegungen sogar vollständig ein. Spermatozoengeisseln sind dagegen durch ATP-Konzentrationen bis $2.5 \cdot 10^{-2}$ *M* nicht zu lähmen (bei Ionenstärken bis 0.3 μ).

* Salicyl (hydroxymercuri-methoxypropyl-)amidoorthoacetat.

Literatur S. 154.

Es ist bisher nicht gelungen, an Geisselmodellen Kontraktion ohne Erschlaffung ablaufen zu lassen. Dauerverkürzung der Geisseln wird auch dann nicht erreicht, wenn durch niedrige Ionenstärken (um 0.10 μ) und ein schwach saures pH Bedingungen eingestellt werden, die nach den Erfahrungen an anderen Modellen kontraktile Prozesse begünstigen und Erschlaffung oder Streckung ausschalten[5]. Allerdings könnte die Stauchung der elastischen Geisselelemente, die durch symmetrische Anspannung der kontraktilen Geisselanteile bewirkt wird, zu gering sein, um erkennbar zu werden — während asymmetrisch auftretende kontraktile Kräfte durchaus in der Lage sein mögen, die elastischen Elemente rhythmisch zu verbiegen.

IV

Das kontraktile Protein der Spermatozoengeissel ist schwerer zu extrahieren als das kontraktile Protein des Muskels[10] und der Fibroblastenzelle. Zwar wird die Kontraktilität der Spermatozoenmodelle durch Ionenstärken $> 0.4\ \mu$ aufgehoben, doch ist dieser Effekt durch Verdünnen selbst dann noch reversibel, wenn eine Lösung von 1 M KCl + $2 \cdot 10^{-2}\ M$ Pyrophosphat ($I \approx 1.1\ \mu$) 30 min bei 0° C auf die Modelle einwirkt. Also kommt die durch hohe Ionenstärken erzeugte Kontraktionshemmung nicht deshalb zustande, weil das kontraktile Protein in Lösung geht. Das Verhalten der Geisselmodelle bestätigt die an Muskelmodellen gemachte Erfahrung[10], dass ein Intervall der Ionenstärke existiert, in dem das kontraktile Protein unfähig zur Kontraktion (bezw. Superpräzipitation) ist, aber noch im Gelzustand verharrt.

Erst durch mehrstündige Behandlung mit Lösungen einer Ionenstärke von 1 μ wird die Beweglichkeit der Spermatozoenmodelle irreversibel zerstört. *Trypanosomen*modelle sind empfindlicher, in 0.4 M KCl-Lösung verlieren sie schon in kürzester Zeit die Fähigkeit, in verdünnten Lösungen auf Zusatz von ATP mit Bewegung zu reagieren.

V

Als Betriebssubstanz der Geisselbewegung wirkt ATP spezifisch und ist weder durch Adenosinmonophosphat, Creatinphosphat noch durch anorganisches Pyrophosphat, Triphosphat und sog. Hexametaphosphat zu ersetzen. Bereits $5\text{–}10 \cdot 10^{-6}\ M$ ATP genügen, um Geisselmodelle aus Spermatozoen in Bewegung zu setzen. Wird die ATP-Konzentration erhöht, so steigt die Bewegungsgeschwindigkeit, — und zwar bei kurz extrahierten Modellen rascher als bei lang extrahierten Modellen (Fig. 3). Diese ATP-Wirkung ist unspezifisch und durch Erhöhung der Ionenstärke (Fig. 4), durch Zusätze von Pyrophosphat (Fig. 5), Polysulfosäuren (Fig. 5 und 6) oder allgemein durch solche Massnahmen zu imitieren, die Muskelmodelle "weichmachen", d.h. ihren Dehnungswiderstand senken. Hochfrequente Geisselbewegung ist mithin auch bei niedriger ATP-Konzentration möglich, wenn die mangelhafte Plastizität der Modelle durch hohe Ionenstärken (Fig. 4) oder durch Weichmacher (Fig. 6) verbessert wird. Ähnlich wird in mehrwöchig extrahierten und daher verfestigten Modellen durch ATP-Konzentrationen $> 10^{-4}\ M$ Bewegung vielfach erst dann erzeugt, wenn Pyrophosphat oder $2\text{–}10 \cdot 10^{-6}\ M$ Germanin zugesetzt werden (Fig. 5). Zwischen Schwelle und Optimum beruht die frequenzfördernde Wirkung des ATP offenbar auf seiner Wirksamkeit als Weichmacher.

Die Amplitude der Geisselbewegung steht in umgekehrtem Verhältnis zur Bewegungsfrequenz (Fig. 3). Diese Tatsache macht es unmöglich, an den Spermienmodellen von *Tachycines* zu beurteilen, ob der Elementarvorgang der Bewegung bei Anwesenheit hoher ATP-Konzentrationen und Ionenstärken ebenso wieder nachlässt, wie dies bei allen anderen Modellen[5,14] beobachtet wird. Denn die mittlere Geschwindigkeit der

Literatur S. 154.

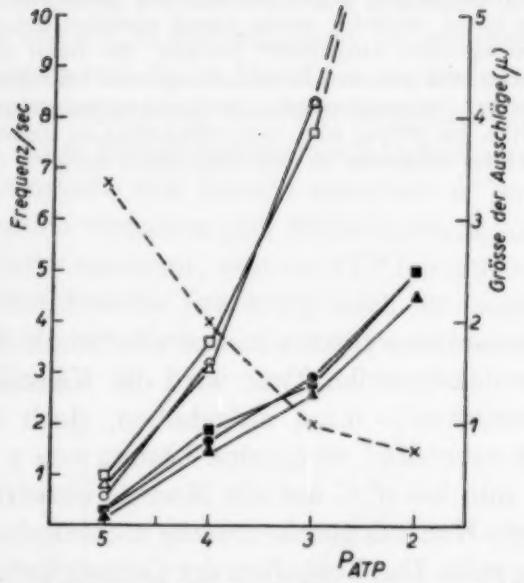

Fig. 3. Abhängigkeit der Schlagfrequenz und der Bewegungsgrösse von der ATP-Konzentration. ○ △ □ 2 Tg. extr. Modelle; ● ▲ ■ 16 Tg. extr. Modelle. Schlagfrequenz = ausgezogene Kurven; Bewegungsgrösse = gestrichelte Kurve (Mittelwerte der 2 Tg. extr. Modelle) pH 7.2, I = 0.20 μ.

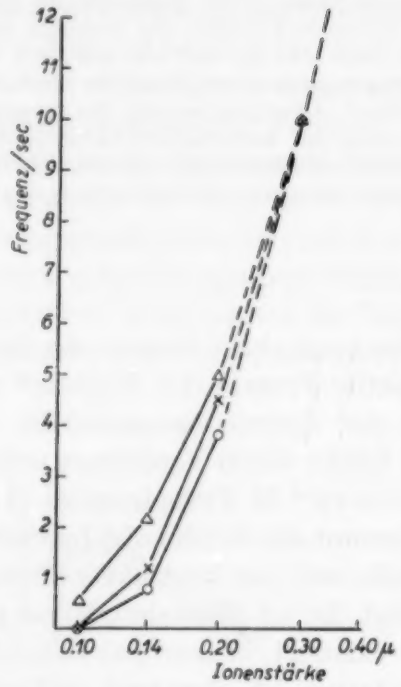

Fig. 4. Schlagfrequenz und Ionenstärke. 9 Tg. extr. Modelle; $5 \cdot 10^{-4}$ *M* ATP, pH 7.2.

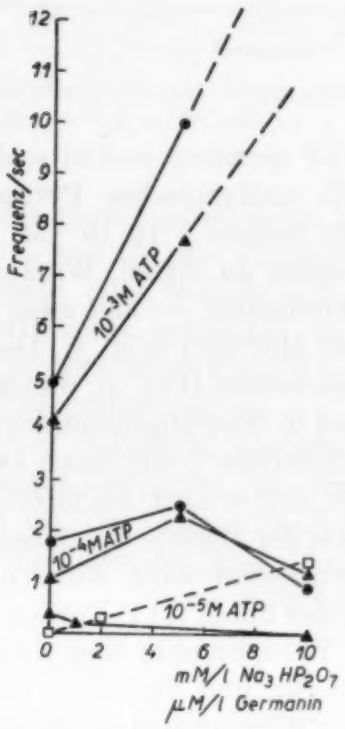

Fig. 5. Wirkung von Pyrophosphat bei verschiedenen ATP-Konzentrationen und von Germanin bei 10^{-5} *M* ATP. 11 Tg. extr. Modelle, pH 6.8, I = 0.15 μ. ● ▲ bei Pyrophosphatzusatz; □ bei Germaninzusatz. Abscisse: Konzentration von $Na_3HP_2O_7$ in mMol/liter, Konzentration von Germanin in μMol/liter.

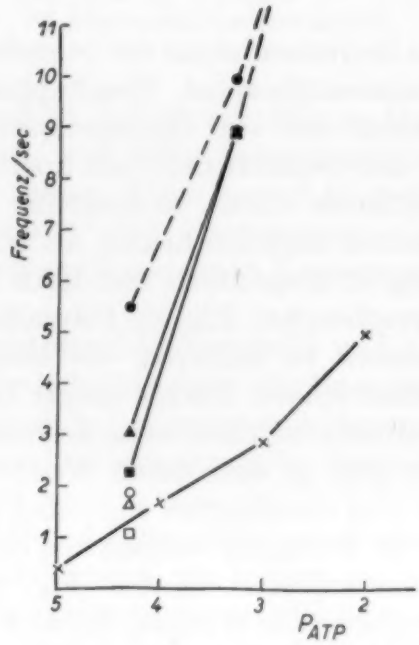

Fig. 6. Wirkung der gleichen Germaninkonzentration bei verschiedenen ATP-Konzentrationen. 28 Tg. extr. Modelle, pH 7.2, I = 0.12 μ. ○ △ □ ohne Germanin; ● ▲ ■ mit $2 \cdot 10^{-6}$ *M* Germanin. Die Kontrollkurve ohne Germanin (×) ist Fig. 3 entnommen (16 Tg. extr. Modelle).

Bewegung des einzelnen Geisselquerschnitts ergibt sich als Produkt aus Frequenz und Amplitude. Bei ATP-Konzentrationen $> 10^{-3}\,M$ kann zwar die Amplitude des Geisselausschlags noch gemessen werden, aber die Frequenz wird zu gross, um ausgezählt werden zu können (vgl. Fig. 3 und method. Teil). Infolgedessen lässt sich nur sagen, dass bis zur Konzentration $10^{-3}\,M$ ATP die Geschwindigkeit der Querschnittsbewegung zunimmt. Das gleiche gilt für die Steigerung der Ionenstärke über das optimale Mass hinaus, das — jeweils verschieden — bei allen anderen Modellen eine Abnahme der Bewegung zur Folge hat. Andererseits steht fest, dass durch Ionenstärken $> 0.4\,\mu$ *Tachycines*geisseln (ähnlich wie Muskel- und Zellmodelle) völlig stillgelegt werden — ohne dass mit der Annäherung an diesen Wert eine Frequenzabnahme und eine Vergrösserung der unmessbar klein gewordenen Bewegungen zu beobachten wären.

Dies gilt für langextrahierte Spermatozoenmodelle (Fig. 4). Dagegen ist bei kurz (< 2 Tage) extrahierten Spermatozoenmodellen und bei allen *Trypanosomen*modellen starke Erweichung durch hohe ATP-Konzentrationen oder Ionenstärken von Unregelmässigkeiten der Bewegung und Frequenzabfall gefolgt bevor die Modelle vollständig gelähmt sind.

Nicht unter allen Bedingungen scheint Pyrophosphat auf Spermienmodelle nur als Weichmacher zu wirken. Ist die molare Konzentration des ATP 100mal kleiner als die des Pyrophosphat, so verlangsamt Pyrophosphat die Bewegung oder unterdrückt sie vollkommen. Diese Hemmung wird sofort beseitigt, wenn die ATP-Konzentration erhöht wird (Fig. 5). Sie kann also nicht durch übermässige Erweichung des Modells zustande kommen, denn solche Hemmungen werden durch Erhöhung der ATP-Konzentration verstärkt. Offenbar unterdrückt Pyrophosphat, wenn es in sehr viel höherer Konzentration als ATP anwesend ist, die Kontraktion durch kompetitive Hemmung der ATP-Bindung an das kontraktile Eiweiss. Giftwirkungen des Pyrophosphat sind auch an den Modellen von glatten[15] und quergestreiften[16] Muskeln beobachtet worden.

VI

Polysulfosäuren (Trypanrot, Germanin (Bayer 205)*, Heparin, Liquoid Roche) hemmen die Bewegung von Geisselmodellen ähnlich wie sie die Kontraktion von Zell[5]- und Muskelmodellen hemmen. $2\text{–}5\cdot10^{-6}\,M$ Germanin genügt, um kurz extrahierte Trypanosomenmodelle unbeweglich zu machen, $5\cdot10^{-5}\,M$ Germanin und $5\cdot10^{-5}$ g/ml Heparin sind erforderlich, um die gleiche Wirkung an kurzextrahierten Spermatozoenmodellen zu erzielen. Die Germaninwirkung ist bei Spermatozoenmodellen völlig, bei *Trypanosomen*modellen nur schlecht durch Auswaschen reversibel.

Polysulfosäuren sind zugleich wirksame Weichmacher[17]. Sie beschleunigen daher zunächst die Bewegung solcher Geisselmodelle, die durch lange Extraktion verfestigt sind. Um diese Modelle unbeweglich zu machen, sind 10mal höhere Germaninkonzentrationen erforderlich, als sie für kurz extrahierte Modelle genügen. Mit zunehmender ATP-Konzentration steigt die Gift-Wirksamkeit aller Germaninkonzentrationen beträchtlich an (Fig. 6).

Germanin wirkt auch auf andere Modelle je nach der Extraktionsdauer verschieden: $10^{-5}\,M$ Germanin hemmt die Kontraktion einstündig extrahierter Fibroblastenmodelle und beschleunigt die Kontraktion vieltägig extrahierter Modelle auf das 4–8fache.

* Na_6-*sym.*-bis(*m*-aminobenzoyl-*m*-amino-*p*-methylbenzoyl-l-naphthyl-amino-4,6,8-trisulfonat).

Literatur S. 154.

Ähnlich wie Germanin verhalten sich Heparin und Liquoid Roche. $5 \cdot 10^{-5}$ g/ml Heparin beschleunigen die Geisselbewegung lang extrahierter Spermatozoenmodelle und höhere Heparinkonzentrationen bringen sie zum Stillstand.

Vermutlich bestehen Beziehungen zwischen der Wirksamkeit der Polysulfosäuren als Kontraktionsgifte und ihrer Wirksamkeit als Weichmacher. Weil etwa physiologische ATP-Konzentrationen genügen, um kurz extrahierte Geisselmodelle optimal oder fast optimal plastisch zu machen, hemmen schon Schwellenkonzentrationen Germanin in kurz-extrahierten Modellen die Kontraktion. Dagegen werden die gleichen Germaninkonzentrationen bei lang-extrahierten Modellen benötigt, um die Weichheit der Präparate den Verhältnissen in kurzextrahierten Modellen anzugleichen[9] Und erst wenn die Germaninkonzentration weiter gesteigert wird, lockert sich das Gefüge der Modelle so sehr, dass die Kontraktilität leidet.

Die hohe Germaninempfindlichkeit der *Trypanosomen*modelle hängt offenbar zusammen mit ihrer hohen Empfindlichkeit gegen alle Weichmacher (z.B. auch das ATP). Lähmung der *Trypanosomen*modelle tritt schon bei Germaninkonzentrationen ein, die kleiner sind als diejenigen, die sich bei der Umrechnung therapeutischer Dosen auf das menschliche Körpervolumen ergeben. Daher ist die therapeutische Wirkung des Germanin vielleicht unter anderem eine Wirkung auf den Geisselapparat — wie dies von früheren Untersuchern schon vermutet wurde[18]. Doch ist seine therapeutische Wirkung spezifisch, seine Wirkung auf das Geisselmodell dagegen nur an seinen Charakter als Polysulfosäure gebunden.

Die allgemeine Vergiftung aller Kontraktionsprozesse durch Polysulfosäuren scheint im besonderen Fall der Geisselbewegung auch eine biologische Bedeutung zu haben. Für die Besamung von Seeigeleiern ist die Agglutination der Spermien an der Eioberfläche Voraussetzung. Sie wird erreicht durch — dem Heparin ähnliche — Polysulfosäuren, die das Ei aus seinen äusseren Hüllen (jelly coat) abscheidet[19]. Unter der Voraussetzung, dass die Polysulfosäure in die Spermiengeisseln wirklich eindringt, ist deren Stillegung auf Grund der Modellbeobachtungen zu fordern.

Der Wirkung von Weichmachern entgegengesetzt ist die Wirkung von Protamin[17]. Protamin verfestigt die Geisselmodelle wahrscheinlich ebenso, wie es Zellmodelle verfestigt: daher verlangsamt es in Konzentrationen $< 2 \cdot 10^{-5}$ g/ml (als Sulfat) die Bewegung und verringert — insbesondere bei langextrahierten Modellen — die Bewegungsgrösse. Dieser Effekt kann nicht durch Auswaschen, wohl aber durch Steigerung der ATP-Konzentration oder Ionenstärke bei solchen Modellen ausgeglichen werden, die noch nicht vollständig gelähmt waren (Fig. 7). Die Reaktivierung bewegungslos gewordener Modelle gelingt nur selten. Konzentrationen $> 5 \cdot 10^{-5}$ g/ml lähmen alle Modelle irreversibel. Die Protaminwirkung ist durch Arginin bis 10^{-3} *M* und durch Polyaminovinylalkohol* bis $5 \cdot 10^{-4}$ g/ml nicht zu imitieren.

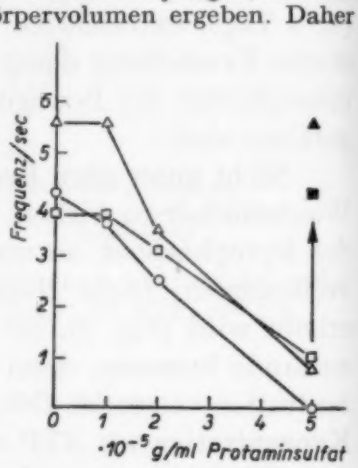

Fig. 7. Protamin und Schlagfrequenz. 28 Tg. extr. Modelle; pH 7.4, I = 0.20 μ. ○△□ $5 \cdot 10^{-4}$ *M* ATP; ▲■ Reaktivierung durch $2.5 \cdot 10^{-2}$ *M* ATP.

Ähnlich wie Protamin wirken Ca-Ionen auf Geisselmodelle. $5 \cdot 10^{-3}$ *M* Ca^{++} verringert ihre Bewegungsgeschwindigkeit und Bewegungsgrösse. Auch diese Wirkung st durch Steigerung der ATP-Konzentration auszugleichen. Im Gegensatz zu der Wirkung des Protamin ist der Ca^{++}-Effekt durch Auswaschen reversibel.

Hemmende Verbindungen mit unbekanntem Wirkungsmodus sind Strophanthin und Diäthylstilböstrol. $5 \cdot 10^{-5}$ g/ml Strophanthin senken die Schlagfrequenz und Bewegungsgrösse von Spermienmodellen auf etwa die Hälfte, 10^{-4} *M* Diäthylstilböstrol hemmt die Bewegung vollständig. Auswaschen hebt die Wirkung beider Stoffe auf.

TECHNIK

Zur Herstellung der Modelle und um das Verhalten des gleichen Modells gegenüber variierten Bedingungen zu prüfen, empfiehlt es sich, vor der Extraktion die geisseltragenden Zellen durch ein dünnes Fibrinkoagulum auf Deckgläsern zu fixieren. Die eingebetteten Modelle ragen während des

* Das Präparat verdanke ich Herrn Dr. GRUBHOFER, Heidelberg.

Literatur S. 154.

Versuchs in eine mit der Versuchslösung gefüllte Kammer mit seitlichem Zu- und Abfluss und werden in dieser Anordnung mikroskopiert.

Heuschreckenhoden sind das Ausgangsmaterial für die Gewinnung von Spermatozoen. Sie werden im Einbettungsmedium zerzupft und als Suspension mit einer Pipette auf Deckgläsern aufgestrichen. — *Trypanosomen* enthaltendes Blut infizierter Mäuse (gewonnen durch Kupieren der Schwanzspitze) wird mit dem Einbettungsmedium 1:20 bis 40 gemischt und wie die Hodensuspension ausgestrichen. Nach Gerinnen des Mediums in einer feuchten Kammer werden die Deckgläser in Gefässe mit Extraktionslösung versenkt. Sterile Arbeitsbedingungen erübrigen sich bei der Einbettung. Geprüft und verwendbar für die Herstellung von *Trypanosomen*modellen sind *Tr. brucei* und *Tr. gambiense*.

Das Einbettungsmedium für die Spermatozoen besteht aus 10% Hühnerplasma (gewonnen aus der A. carotis in paraffinierten Gläsern ohne Zusätze) und 80% Tyrodelösung. Unmittelbar vor dem Ausstreichen werden 10% Hühnerembryonalextrakt (1:3) zugegeben, um die Gerinnung des Mediums in Gang zu bringen. Bei der Herstellung von *Trypanosomen*modellen wird die Tyrodelösung durch Pferdeserum ersetzt. Die eintretende Agglutination der Mäuseerythrozyten ist belanglos. Freischwimmende Modelle sind am besten durch Zerzupfen des Fibrinkoagulum eingebetteter Modelle zu erhalten.

Alle Extraktionslösungen enthielten KCl zur Einstellung der Ionenstärke, 10^{-2} *M* Phosphatpuffer und $2 \cdot 10^{-3}$ *M* Na_3H-Äthylendiaminotetraacetat in 50 vol%iger Glycerinlösung. Die Ionenstärke betrug einheitlich 0.15 μ, das Verhältnis prim/sec Phosphat 35/65 oder 40/60. Extrahiert wurde 24 Stunden bei 0° bis —5° C, danach wurden die Präparate in den Extraktionslösungen bei —18° C, Spermienmodelle gelegentlich auch bei 0° C aufbewahrt. Für die Zusammensetzung der Versuchslösungen, die Extraktionsdauer, die Extraktionstemperatur und ihren Einfluss auf die Verfestigung der Präparate gilt das früher gesagte[17].

Alle Versuchslösungen enthielten KCl zur Einstellung der Ionenstärke, 10^{-2} *M* Phosphatpuffer, 5 bis $10 \cdot 10^{-2}$ *M* $MgCl_2$ und $2 \cdot 10^{-3}$ *M* Cystein. In den Versuchen mit Ca^{++} wurde der Phosphatpuffer durch einen KH_2PO_4-Na_2Glycerinophosphatpuffer ersetzt. Spermienmodelle reagieren gleichmässiger, wenn sie vor Versuchsbeginn 30 min bei 0° C mit ATPhaltigen Lösungen (etwa 10^{-3} *M* ATP) vorbehandelt werden. Die Modelle bleiben über Stunden funktionsfähig, wenn extreme Bedingungen vermieden werden. *Trypanosomen*modelle sind empfindlicher und sollen bald nach der Rückführung in rein wässrige Lösungen in den Versuch genommen werden.

Die Schlagfrequenz wurde im Phasenkontrastmikroskop durch Auszählen bestimmt, die Bewegungsgrösse durch Ausmessen der Fibrillenunschärfe auf langfristig belichteten Mikrophotos und Abzug des Durchmessers der ruhenden Fibrille von dem gefundenen Wert. Alle Versuche fanden bei Zimmertemperatur statt.

Na_4ATP verdanken wir der Firma Homburg (Frankfurt), Salyrgan den Farbwerken Hoechst. Germanin wurde von den Farbenfabriken Bayer (Elberfeld), Heparin-Na (als Liquemin) und Liquoid Roche von der Firma Hoffmann-La Roche, Protaminsulfat von der Firma Schuchardt (München) bezogen.

Herrn Prof. H. H. WEBER danke ich für zahlreiche, anregende Diskussionen, der Deutschen Forschungsgemeinschaft für grosszügige Sachbeihilfen.

ZUSAMMENFASSUNG

Glycerin-wasserextrahierte Geisseln von Spermatozoen und *Trypanosomen* (Geisselmodelle) schlängeln sich unter ATP. In allen ihren Abhängigkeiten entspricht diese Bewegung der Kontraktion von Fibroblasten- und Muskelmodellen, doch ist es eine Besonderheit des kontraktilen Apparats der Geisseln, auch unter konstanten Aussenbedingungen zwischen Kontraktion und Erschlaffung zu wechseln. Diese Spontaneität muss dem kontraktilen Apparat selbst zugeschrieben werden, weil sie in abgetrennten Teilen der Geissel ebenfalls auftritt und weil die Membranen der Zellen und ihre selektive Permeabilität bei der Herstellung der Modelle zerstört werden.

ATP hat für die Geisselbewegungen doppelte Bedeutung. Es ist spezifischer Betriebsstoff und wirkt unspezifisch als Weichmacher. Da die Weichheit der Modelle ihre Bewegungsgeschwindigkeit bestimmt, regelt die ATP-Konzentration die Schlagfrequenz. Germanin ist für die Bewegung von *Trypanosomen*modellen ein äusserst wirksamer Inhibitor.

SUMMARY

Flagella of spermatozoa and *trypanosomes* extracted in glycerine-water (flagellum models), undulate in the presence of ATP. These movements correspond in all respects to the contraction of fibroblast- and muscle-models, but it is a peculiarity of the contractile system of the flagella to

Literatur S. 154.

alternate between contraction and relaxation under constant external conditions. This spontaneity must be attributed to the contractile apparatus itself, because it occurs even in separated parts of the flagellum and because the cell membranes and their selective permeability are destroyed in the preparation of the models.

ATP has a double function in flagellar movement. It works specifically to cause contraction and unspecifically as a plasticiser. Since the plasticity of the models determines the speed of their movement, the ATP concentration controls the frequency of the beat. Germanin is an extremely effective inhibitor of the movement of *trypanosome* models.

RÉSUMÉ

Des flagelles de spermatozoïdes et de *trypanosomes* extraits à l'eau glycérinée (flagelles modèles) sont animés de mouvements ondulatoires en présence d'ATP. Ces mouvements correspondent à tous égards à la contraction des modèles de fibroblastes et de muscles; cependant, le système contractile des flagelles présente la particularité de passer de l'état contracté à l'état décontracté dans des conditions de milieu extérieur constantes. Cette spontanéité est une propriété du système contractile lui-même, puisqu'elle se manifeste en même temps dans des régions séparées du flagelle et puisque les membranes cellulaires et leur perméabilité sélective sont supprimées au cours de la préparation des modèles.

L'ATP intervient de deux façons dans le mouvement des flagelles: il provoque spécifiquement la contraction et il contrôle non specifiquement la plasticité. Puisque la plasticité du modèle détermine la vitesse de ses mouvements, c'est la concentration en ATP qui règle la fréquence des ondulations. La germanine est un inhibiteur extrêmement efficace du mouvement des flagelles modèles de *trypanosome*.

LITERATUR

[1] Zus. fassg. s. bei H. H. WEBER, H. PORTZEHL, *Progr. Biophysics*, 4 (1954) 60.
[2] A. SZENT-GYÖRGYI, *Chemistry of muscular contraction*, New York 1951.
[3] H. HOFFMANN-BERLING, *Biochim. Biophys. Acta*, 10 (1953) 628.
[4] H. HOFFMANN-BERLING, *Biochim. Biophys. Acta*, 15 (1954) 332.
[5] H. HOFFMANN-BERLING, *Biochim. Biophys. Acta*, 14 (1954) 182.
[6] V. ENGELHARDT, *Bull. Acad. Sci. USSR, Ser. biol.*, (1954) 182. zit. nach L. NELSON[12].
[7] E. DE ROBERTIS, G. M. FRANCHI, *J. Appl. Phys.*, 23 (1952) 161.
[8] T. MANN, *Biochem. J.*, 39 (1945) 451.
[9] E. VORHAUS, I. DEYRUP, *Science*, 118 (1953) 553.
[10] W. HASSELBACH, H. HOFSCHNEIDER, E. KASPER, R. LUTZ, *Naturforsch.*, 8b (1953) 204.
[11] W. HASSELBACH, *Naturforsch.*, 7b (1952) 338.
[12] L. NELSON, *Biochim. Biophys. Acta*, 14 (1954) 312.
[13] E. BOZLER, *Am. Journ. Physiol.*, 167 (1951) 267.
[14] H. PORTZEHL, *Biochim. Biophys. Acta*, 14 (1954) 195.
[15] D. DOERR, H. PORTZEHL, *Naturforsch.*, 1954 (im Druck).
[16] J. BENDALL, *Nature*, 172 (1953) 586.
[17] H. HOFFMANN-BERLING, *Biochim. Biophys. Acta*, 15 (1954) 226.
[18] ROEHL, *Arch. exp. Pathol.*, Beih. 26, (1927), zit. nach TH. WAGNER-JAUREGG, *Allg. Therapie der Infektionskrankheiten*, Berlin 1948.
[19] Zus. fassg. s. bei J. RUNNSTRÖM, *Adv. Enzymol.*, 9 (1949) 241.

Eingegangen am 14. September 1954

Short Communications and Preliminary Notes

Sur les relations entre l'ocytocine et la vasopressine d'une part et la protéine de Van Dyke d'autre part

On sait que les deux hormones de la posthypophyse, l'ocytocine et la vasopressine, ont été récemment obtenues sous forme de peptides purs dont la constitution est maintenant bien connue[1,2,3,4] et dont la synthèse a même été réalisée[5,6]. Il nous a paru intéressant de rechercher la nature des relations existant entre ces peptides et une protéine, douée à la fois des propriétés physiologiques de l'ocytocine et de celles de la vasopressine, qui a été isolée à l'état apparemment homogène par VAN DYKE *et al.*[7]

Nous avons préparé cette protéine selon ces auteurs[7]: 100 g de poudre acétonique de lobes postérieurs d'hypophyse de boeuf ont fourni 900 mg de protéine possédant les activités (U.I.) ocytocique, vasopressique et antidiurétique dans le rapport où elles existent dans la glande (1:1:1) et renfermant 14% de l'activité initiale. L'activité par mg d'azote, les constantes de diffusion ($D_{22°} = 8.5 \cdot 10^{-7}$) et de sédimentation ($s_{22°} = 2.7 \cdot 10^{-13}$) sont les mêmes que celles indiquées par les auteurs américains; le poids moléculaire calculé d'après ces dernières est de 30,000 environ. L'activité ocytocique ou vasopressique est d'environ 550 U.I. par micromolécule de protéine; c'est approximativement l'activité d'une micromolécule d'ocytocine[8] ou de vasopressine pures[9].

Les expériences suivantes tendent à montrer que la protéine de VAN DYKE est constituée par une association molécule à molécule entre trois constituants: une protéine, le peptide ocytocine et le peptide vasopressine; elles indiquent d'autre part que cette association entre les trois constituants peut être facilement rompue.

1. *Dissociation par électrodialyse.* Lorsque la protéine, purifiée par précipitations répétées en solution saline[7], est finalement dialysée contre l'eau pour être débarassée des sels avant lyophilisation, toute l'activité ocytocique et vasopressique ainsi que la totalité de l'azote restent à l'intérieur du sac. Les activités ne sont donc pas dissociables par simple dialyse contre l'eau. Par contre lorsque cette protéine (15 mg de poudre dissous dans 35 ml d'eau), placée dans le compartiment central d'un appareil à ionophorèse à trois compartiments, est soumise à l'électrodialyse (tension de 120 volts/cm, 5 heures, 25°), on recueille à la cathode 67% de l'activité vasopressique, 10% de l'activité ocytocique et 9% de l'azote. L'électrodialyse permet donc de dissocier les deux activités et d'obtenir à la cathode un produit dont l'activité par mg d'azote (830 U.I.) s'est rapprochée de celle du peptide vasopressine (2,000–2,500 U.I.). En utilisant un procédé ionophorétique de ce genre, HASELBACH ET PIGUET[10] ont réussi à obtenir à partir d'un extrait brut de lobes postérieurs d'hypophyse un produit dont l'activité ocytocique est assez d'autre part en accord avec ceux d'IRVING ET DU VIGNEAUD[11] qui ont observé la séparation des deux activités au cours d'une électrophorèse effectuée sur un jus de presse de posthypophyse.

2. *Dissociation par précipitation.* La protéine (50 mg) en solution à 1% dans l'acide acétique 0.01 *N* est précipitée par l'acide trichloracétique à 5%. On constate que 8% de l'azote, de l'activité ocytocique et 70% de l'activité vasopressique demeurent en solution. Cette solution diluée est placée dans le compartiment central de l'appareil à ionophorèse; après passage du courant (40 volts/cm, 20 heures, 20°), on recueille le liquide cathodique qui renferme les substances actives sans acide trichloracétique. Dans ce liquide deux polypeptides peuvent être mis en évidence par ionophorèse sur papier; leurs cheminements sont respectivement parallèles à ceux de l'ocytocine et de la vasopressine pures (révélation sur des bandes témoins par le bleu de bromophénol)[12]. Lorsque le papier est découpé en bandes de 2 cm de large et qu'après élution par l'eau, on dose les activités se trouvant dans chacune d'elles, on ne trouve pratiquement d'activité ocytocique qu'au niveau de l'ocytocine pure, et d'activité vasopressique qu'au niveau de la vasopressine. D'autre part les substances correspondantes ont respectivement les mêmes compositions en acides aminés que les peptides témoins. La précipitation de la protéine par l'acide trichloracétique à 5% libère donc de l'ocytocine et de la vasopressine.

3. *Dissociation au cours de la distribution par contre-courant.* 20 mg de poudre sont traités par contre-courant dans le système butanol secondaire-acide trichloracétique à 0.5%, chaque phase étant de 5 ml. Après 24 transferts, chaque tube est homogénéisé par addition d'eau, et on effectue les dosages d'activités et d'azote. La Fig. 1 indique les résultats obtenus. On récupère environ 80% de l'activité ocytocique dans les tubes de 11 à 14 et 35% de l'activité vasopressique dans les tubes de 7 à 9. Les contenus de ces tubes sont rassemblés en une fraction ocytocique et une fraction vasopressique qui sont soumises à l'électrodialyse pour être débarrassées de l'acide trichloracétique et du butanol. Par chromatographie sur papier on constate que les produits actifs ainsi purifiés ont respectivement les mêmes comportements que les peptides vasopressine et ocytocine purs. D'autre part la

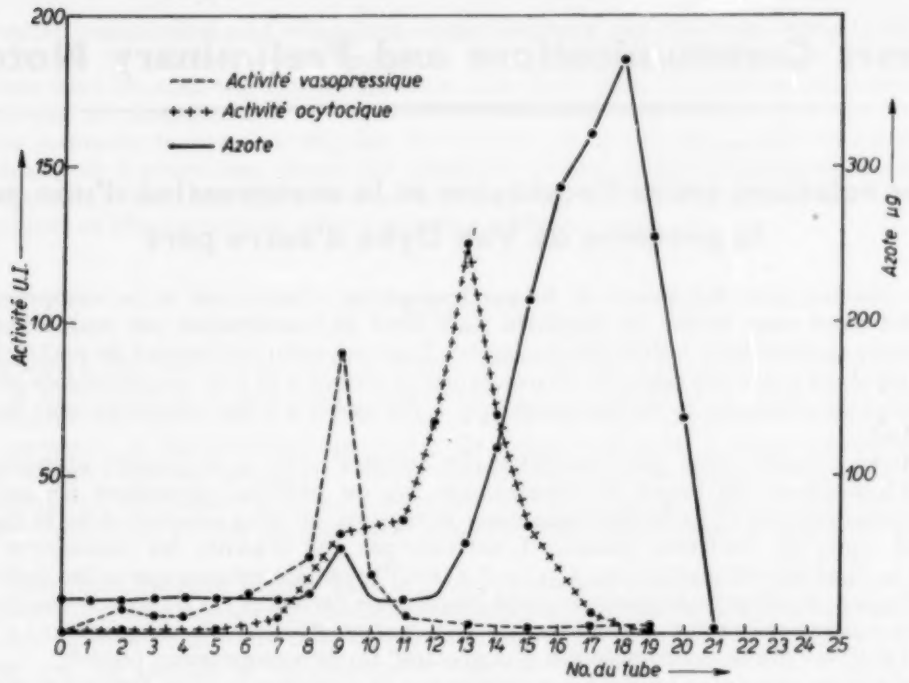

Fig. 1. Distribution par contre-courant de la protéine de VAN DYKE (20 mg de poudre soumis à la distribution das le système butanol secondaire – acide trichloracétique 0.5%, le volume de chaque phase étant de 5 ml)

vasopressine et l'ocytocine, soumises à la distribution par contre-courant dans le système décrit, possèdent les mêmes coefficients de partage que les principes actifs obtenus par ce procédé à partir de la protéine de VAN DYKE.

De l'ensemble de ces expériences il semble que l'on puisse conclure que l'activité de cette protéine correspond bien à la fixation des peptides ocytocine et vasopressine qui sont seuls responsables des activités hormonales de l'association. Une objection à cette conception eût résidé dans le fait que la réduction par la cystéine n'inactiverait ni l'ocytocine, ni la vasopressine[13] alors qu'elle inactiverait la protéine[7]. En fait nous avons répété les expériences de réduction de la protéine par la cystéine, dans les conditions décrites par VAN DYKE *et al.*[7] sans pouvoir constater aucune inactivation.

Il apparaît ainsi qu'il existe une association entre une protéine que nous proposons d'appeler *neurophysine*, et les deux peptides *ocytocine* et *vasopressine*. Il est encore impossible de définir le mode d'union en jeu ainsi que de décider s'il s'agit d'un artefact, ou au contraire d'une association présentant une signification biologique profonde.

ROGER ACHER
GEORGES MANOUSSOS
GHISLAINE OLIVRY

Laboratoire de Chimie biologique
de la Faculté des Sciences,
Paris (France)

[1] H. TUPPY ET H. MICHL, *Monatsh.*, 84 (1953) 1011.
[2] V. DU VIGNEAUD, C. RESSLER ET S. TRIPPETT, *J. Biol. Chem.*, 205 (1953) 949.
[3] V. DU VIGNEAUD, H. C. LAWLER ET E. A. POPENOE, *J. Am. Chem. Soc.*, 75 (1953) 4880.
[4] R. ACHER ET J. CHAUVET, *Biochim. Biophys. Acta*, 14 (1954) 421.
[5] V. DU VIGNEAUD, C. RESSLER, J. M. SWAN, C. W. ROBERTS ET P. G. KATSOYANNIS, *J. Am. Chem. Soc.*, 76 (1954) 3115.
[6] V. DU VIGNEAUD, D. T. GISH ET P. G. KATSOYANNIS, *J. Am. Chem. Soc.*, 76 (1954) 4751.
[7] H. B. VAN DYKE, B. F. CHOW, R. O. GREEP ET A. ROTHEN, *J. Pharmacol. Exp. Therap.*, 74 (1942) 190.
[8] J. G. PIERCE, S. GORDON ET V. DU VIGNEAUD, *J. Biol. Chem.*, 199 (1952) 929.
[9] P. FROMAGEOT, R. ACHER, H. CLAUSER ET H. MAIER-HUSER, *Biochim. Biophys. Acta*, 12 (1953) 424.
[10] C. H. HASELBACH ET A. R. PIGUET, *Helv. Chim. Acta*, 35 (1952) 2131.
[11] G. W. IRVING ET V. DU VIGNEAUD, *J. Biol. Chem.*, 123 (1938) 485.
[12] H. G. KUNKEL, S. P. TAYLOR ET V. DU VIGNEAUD, *J. Biol. Chem.*, 200 (1953) 559.
[13] R. R. SEALOCK ET V. DU VIGNEAUD, *J. Pharmacol. Exp. Therap.*, 54 (1935) 433.

Reçu le 4 novembre 1954

Purification of thrombin by chromatography

In a previous paper[1] it was shown that testicular hyaluronidase may be successfully chromatographed on a column of Amberlite IRC-50. Although the isoelectric range of purified bovine thrombin preparations has been found to be about pH 4.1–4.7[2], thrombin is adsorbed on glass[3] as is hyaluronidase[4]. For this reason, chromatography of thrombin on the cation exchanger Amberlite IRC-50 was also attempted.

The thrombin used was a bovine, freeze-dried preparation from Leo Pharmaceutical Products. Thrombin activity was measured at 38° C as follows: To 1.0 ml of prewarmed 0.1% fibrinogen in 0.1 *M* sodium phosphate buffer at pH 6.8 was added from 0.095 to zero ml of the same phosphate buffer plus from 0.005 to 0.1 ml thrombin solution to give a final volume of 1.1 ml. The tube was shaken and immediately replaced in the water bath; it was then rotated quickly by hand and the time in seconds noted until fibrin thread formation occurred. A standard curve with known amounts of thrombin, 10–150 γ, as abscissa and the corresponding coagulation times in seconds as ordinate was prepared each day determinations took place.

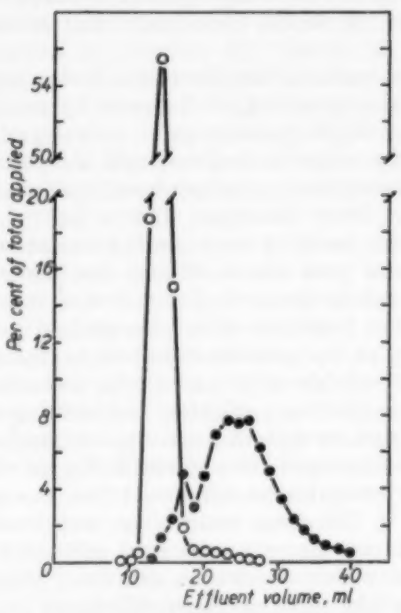

Fig. 1. Chromatography of 30 mg thrombin preparation on a 0.9 × 38 cm column of IRC-50. Eluant: 0.3 *M* sodium phosphate buffer, pH 7.42. Volume of fractions 1.5 ml. ○-protein content of fractions in % of total applied. ●-thrombin content in % of total activity.

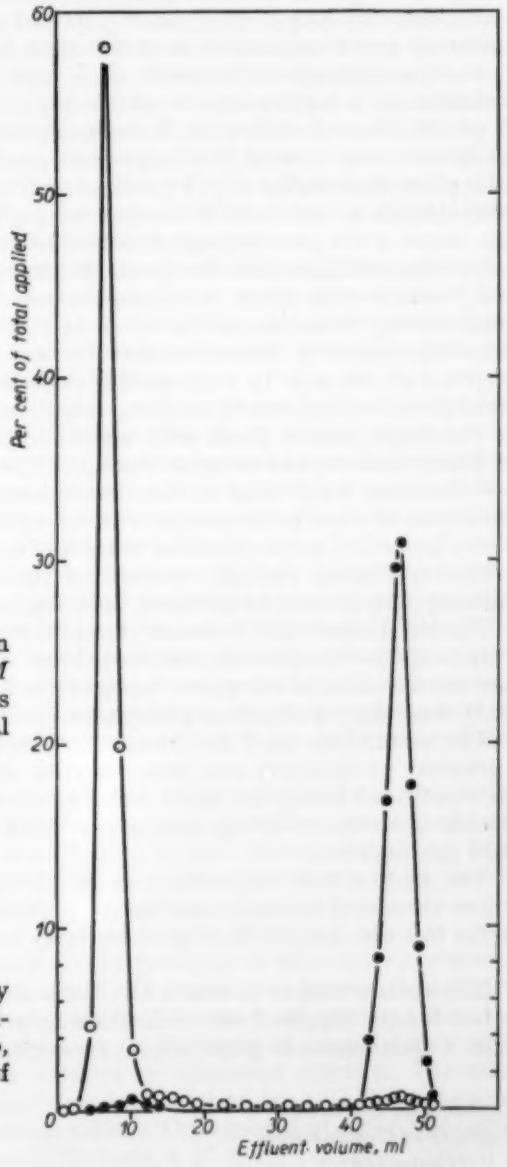

Fig. 2. Purification of thrombin (100 mg applied) by adsorption on a 0.9 × 15 cm column of IRC-50 conditioned with 0.05 *M* sodium phosphate buffer of pH 7.0, and elution with 0.3 *M* sodium phosphate buffer of pH 8. ○-protein; ●-thrombin.

Amberlite IRC-50 of about 250 mesh was treated successively with 2 *N* HCl, water, 2 *N* NaOH, water, and thereafter with primary sodium phosphate of the same molarity as that for the experiment until the pH of the supernatant was at the desired value. The resin was then treated with the appropriate buffer.

Fig. 1 shows an experiment with a 0.9 × 38 cm column at room temperature and under circumstances (0.3 *M* sodium phosphate buffer, pH 7.42) where the adsorption of thrombin was found

reversible. 30 mg of the thrombin preparation was dissolved in *ca.* 0.5 ml of the buffer and applied on the column. Buffer was run through at a flow rate of 3 ml per hour and fractions were collected in 1.5 ml increments. The protein levels were measured by absorption in the ultraviolet at 280 mμ. Both the protein content and the thrombin activity of each fraction in Fig. 1 is given in per cent of total amount applied.

It is seen from Fig. 1 that most of the protein passes directly through the column in a narrow band at about 14 ml of effluent. The thrombin activity eluted more slowly, attaining its peak at about the 25th ml. The activity per fraction in the peak region was 7.8% of the total whereas the protein was only about 0.2% of the total thus giving a 40-fold purification. Although the thrombin peak is not very sharp, most of the eluted activity was found between the 15th and 35th ml of effluent. Only 68% of the activity and 94% of the protein applied could be accounted for in the effluent. It was found, however, that purified thrombin is adsorbed on glass at this buffer concentration and pH. Elution from glass could be effected by 1 *M* secondary potassium phosphate. The yield of only 68% in this case is probably to some extent a result of adsorption on the glass tubes.

Other experiments may be summarized as follows: With sodium phosphate buffers 0.1 *M* pH 6.0, 0.2 *M* pH 6.8, 0.2 *M* pH 7.25 and 0.2 *M* pH 7.5 no thrombin activity escaped from the columns. At 0.25 *M* pH 7.55 and 0.3 *M* pH 7.2 elution of thrombin took place, but so slowly that the activity curve was much more flat than in Fig. 1.

For purification of thrombin on a more preparative scale, adsorption at a low ionic strength and elution at a higher one is useful. Fig. 2 illustrates this possibility. A 0.9 × 15 cm column of IRC-50 conditioned with 0.05 *M* sodium phosphate buffer of pH 7.0 was used. 100 mg of thrombin preparation in *ca.* 2 ml of this buffer was applied. When the solution had run into the column 0.3 *M* sodium phosphate buffer of pH 8.0 was run through at a flow rate of 7.2 ml per hour. Later at 40–50 ml effluent the flow rate had decreased to 4.4 ml per hour. Four fractions were collected per hour. Again, most of the protein passed immediately through the column; a very small amount of thrombin activity was contained in this peak. Between the 41st and 51st ml of effluent the main thrombin activity was eluted; these fractions showed very little protein present. The pH was found here to increase slowly from the initial value of 7. The most active fractions showed a 50-fold purification. Yield with respect to thrombin activity was 120%; 95% of the protein could be accounted for by absorption at 280 mμ. In very similar experiments activity yields of 97 and 115% have been found. A yield of more than 100% activity might be due to removal of an inhibitor, but mixing of samples from the large protein peak with purified thrombin did not inhibit the activity of the latter. It is more likely that a yield of more than 100% is due to experimental error. Only 0.005 ml of the most active fractions were used in the determination and the coagulation time was but 11–12 seconds. A difference of 1 sec in this range corresponds to about 12% difference in activity; duplicate determinations, however, gave identical results. The very small volume was preferred instead of a larger one from a diluted sample, because of the activity loss which occurs on dilution. Dilution with stabilizing agents such as glycerol, carbohydrates and the like have not been tried.

During dialysis and freeze drying of the purified fractions, containing less than 0.5 mg of protein per ml, much of the activity was lost. Most of the loss is probably due to adsorption upon the cellophane membrane and the glass. Some of the lost activity could be eluted from the dialysis membrane by 1 *M* secondary potassium phosphate.

The conditions used in the adsorption–elution experiment of Fig. 2 have up to now given the greatest purification and concentration of the thrombin. When adsorption took place at pH 6, other conditions being the same, more of the inert protein was adsorbed which then eluted with the thrombin activity, yielding only about a 15-fold purification. Adsorption at pH 6.6 resulted in a 30-fold purification.

The finding that thrombin can be chromatographed on Amberlite IRC-50 poses the question whether thrombin is really an "acid" protein. If this is so, then not only some basic and neutral proteins but also certain acid proteins may be chromatographed on IRC-50.

The author wishes to thank Dr. TAGE ASTRUP, Biological Institute of the Carlsberg Foundation, who has kindly supplied me with fibrinogen. A gift of thrombin preparation from Løvens Kemiske Fabrik, Copenhagen, is gratefully acknowledged.

P. STRØIER RASMUSSEN

Biochemical Institute,
University of Copenhagen
(Denmark)

[1] P. STRØIER RASMUSSEN, *Biochim. Biophys. Acta*, 14 (1954) 567.
[2] W. H. SEEGERS, R. I. MCCLAUGHRY AND E. B. ANDREWS, *Proc. Soc. Exp. Biol. Med.*, 75 (1950) 714.
[3] D. F. WAUGH AND B. J. LIVINGSTONE, *J. Phys. and Colloid Chem.*, 55 (1951) 1206.
[4] P. STRØIER RASMUSSEN, *Acta Chem. Scand.*, 8 (1954) 633.

Received November 6th, 1954

Infrared studies on initiation of the autoxidation of some fatty acid esters with and without light-sensitized chlorophyll, ultraviolet light and lipoxidase*

The studies by application of tracer techniques involving particularly deutero-oleate have indicated that the induction period is not basically due to trace impurities, but rather to the role played by the double bonds together with the alpha methylene groups during the transition states of activation in the initial stages of autoxidation reactions. The removal of the trace impurities[1,2] has added further support to the same concept. The recent investigations employing the infrared spectra[3–6] have also brought forth more conclusive experimental evidence for the initiation processes in autoxidation of methyl oleate, linoleate and linolenate. The purpose of the present preliminary report is to show by means of the infrared absorption analysis that in the above initiation step, isomerization and molecular rearrangement of the substances used occurs at the intermediate transition states of their reactions with oxygen.

Methyl oleate was prepared from olive oil methyl esters by a combination of low-temperature crystallization and fractional distillation at reduced pressure[7]. The product was subjected to mild hydrogenation to remove the traces of polyethenoid impurities and finally to low-temperature crystallization[8]. Methyl oleate (Iodine number = I.N., 85.6) showed no absorption at 10.36 μ characteristic of *trans* olefines. Linoleic acid was first prepared by bromination and debromination procedure and then recrystallized twelve times for petroleum ether at —65° to —60° C according to the method of MATHEWS *et al.*[8] *cis, cis*-methyl linoleate (I.N., 172.2 and free of *trans* double bond) was prepared by first esterifying such linoleic acid and then distilling under reduced pressure. Methyl linolenate (I.N., 259.4) prepared by the usual bromination and debromination procedure showed some absorption characteristic of *trans* double bond in the infrared region.

Methyl oleate and linoleate were autoxidized to 10% peroxide content and methyl linolenate o 5%. Oxygen-free nitrogen was bubbled through all the samples as a precaution against further oxidation. The solvents, ether, alcohol, petroleum ether (b.p., 30°–60°), heptane were purified by the usual methods. All analytical determinations in this report were carried out on the substances isolated from solutions as the necessity arose due to experimental conditions.

Of four different samples (each, 25–30 g) of methyl oleate (a–d), two samples (a, b) were autoxidized in darkness at room temperature (25–30°) and the other two (c, d) under irradiation with ultraviolet at 35°. However, the degree of agitation in some of these samples was varied by employing a and c as a layer in a shallow dish in the still atmosphere of air and by agitating b and d contained in narrow cylindrical tubes (each, 1″ × 10″) by oxygen bubbled through a gas dispenser (Corning fritted glass). The peroxides formed were isolated by counter-current extraction[9]. The solvent pair used was, 87% alcohol and petroleum ether saturated with the same alcohol. Infrared analyses on (i) Peroxide concentrates (5540–5780 m.equiv./kg), (ii) recovered unoxidized materials revealed that the former contained all the *trans*-isomer absorbing at 10.36 μ and the latter none. The peroxide concentrates from the four autoxidized samples, a–d, contained respectively, 61–66%, 74–76%, 65–68% and 87–90% of *trans*-form. These estimates are based on comparisons with the absorption of methyl elaidate, assuming a constant molecular extinction coefficient for an isolated *trans* double bond. These variations in isomerization indicate the primary role played by oxygen itself during autoxidation under different environmental conditions.

In our initial experiments[10], the photo-chlorophyll oxidation of methyl linoleate was found to form linoleate hydroperoxide with an isolated *trans* double bond. Since certain percentage of the original linoleate also had an isolated *trans* double bond[10], it was not known definitely whether this gave rise to the peroxide with an isolated *trans* double bond in spite of much experimental evidence. In the present work, photo-chlorophyll oxidation of pure *cis, cis*-linoleate (25–30 g at a time) as a 30% solution in heptane below o° C yielded decisive results. Methyl linolenate (25–30 g at a time) has also been oxidized using the same technique in the presence of chlorophyll with similar results. Due to the instability of the peroxides, modifications in the procedures for isolation had to be introduced. The peroxides were concentrated by counter-current extraction[9] without letting the temperature rise above 10°. The peroxide concentrates (5980 m.equiv./kg in the case of linoleate and 5560 m.equiv./kg in that of linolenate products) were reduced by stannous chloride. The reduced products were extracted by cold ether. The ether extract was first washed by 3% HCl solution and then thoroughly by water and dried over anhydrous sodium sulfate. On removal of ether, the products were dissolved in precooled petroleum ether and passed through a 3″ × 12″ column packed with 1″ charcoal over 2″ dry sugar (dried in vacuum at 90° for 1 h) to remove any chlorophyll products and finally eluted by 1% ether in petroleum ether. The temperature was kept below 20° for linoleate and below 10° for linolenate.

---

* Most of the experimental work was completed through the courtesy of the different laboratories in U.S.A.

Chemical and physical analyses including infrared indicated that the products were monohydroxy linoleate and linolenate. Both types of products consisted of the similar types of isomers, absorbing moderately at 10.55 μ (*cis, trans* conjugated), strongly at 10.12 μ (*trans, trans* conjugated) and moderately at 10.36 μ (isolated *trans*).

The formation of the peroxides with the isolated *trans* double bond by the *cis, cis*-linoleate should indicate the formation of 11-hydroperoxide. Similarly, the isolated *trans* double bond in the case of linolenate peroxides should mean the formation of either 11-, or 14-hydroperoxide that has not been reported before. These observations establish one missing link in the field of autoxidation of methyl linoleate and linolenate. In no other autoxidation reactions for linoleate[10] and linolenate except this photo-chlorophyll oxidation, was such peroxide obtained. Peroxides, from autoxidation of linolenate[5], from catalyzed autoxidation by ultraviolet irradiation (3% oxidation being accomplished below 0° C), and from lipoxidase catalyzed oxidation carried out according to the previous methods[4,11,12] below zero degree (5% oxidation) in the case of linolenate soap, or in that of emulsion of methyl linolenate (by means of gum gutty) in the present investigation, did show small amounts of *cis,trans* and majority of *trans, trans* conjugated products by infrared absorption analyses. Great pains were taken in controlling factors, such as, temperature, pH, duration and extent of oxidation which have a profound influence on the final products[9].

It is, thus, evident that the hydroperoxide with the isolated *trans* double bond, once formed, is stable, undergoes no rearrangements and can be easily detected. It seems, therefore, probable that the rearrangement of the non-conjugated linoleate and linolenate almost entirely to conjugated products by autoxidation reactions in general should have occurred during the intermediate transition states involved in the reactions with oxygen. The changes in the geometric configurations of the different peroxidic products indicate isomerization under the same circumstances. These concepts are also borne out by the fact that the extent of isomerization during the autoxidation reactions varied under different environmental conditions for the different fatty acid esters, especially methyl oleate in the present work. Hence, the doubt expressed by SEPHTON AND SUTTON[6] regarding the presence of 11-hydroperoxide in the autoxidized methyl linoleate is confirmed by our experimental results. Similarly, the 11-, or 14-hydroperoxide has been proved to be absent in the autoxidized methyl linolenate. Anomalous results in literature on autoxidation of methyl linolenate obtained by various workers may be attributed to the extreme difficulties in isolating the highly unstable primary hydroperoxides.

The foregoing data on the initial stages of autoxidation reactions offer experimental evidence for, (a) the isomerization and other molecular changes occurring only in the autoxidized products of methyl oleate, linoleate and linolenate and none in their unoxidized fractions; (b) the occurrence of such isomerization (geometrical) during the intermediate activated stage involving energy transfer and leading to the formation of monomeric monohydroperoxides; (c) the activity of alpha methylenic groups (especially, that in 11-C in linoleate and 11-C, or 14-C in linolenate) in all autoxidation reactions in close proximity with the double bonds; and (d) the absence of hydroperoxides at Carbon, 11 in autoxidized linoleate, as well as the absence of those at Carbon, 11 or 14 in the autoxidized linolenate products. These findings may demand some modifications in the mechanistic concept of the initiation steps of autoxidation reactions.

N. A. KHAN*

[1] N. A. KHAN, *J. Am. Oil Chemist's Soc.*, 30 (1953) 273.
[2] N. A. KHAN, *J. Am. Oil Chemist's Soc.* 30 (1953) 40.
[3] O. S. PRIVETT, W. O. LUNDBERG, N. A. KHAN, W. E. TOLBERG AND D. H. WHEELER, *J. Am. Oil Chemist's Soc.*, 30 (1953) 61.
[4] N. A. KHAN, *Arch. Biochem. Biophys.*, 44 (1953) 247.
[5] N. A. KHAN, *J. Chem. Phys.*, 21 (1953) 952.
[6] H. H. SEPHTON AND D. A. SUTTON, *Chem. and Ind.*, (1953) 667.
[7] H. D. FOREMAN AND J. B. BROWN, *Oil and Soap*, 21 (1944) 183.
[8] N. L. MATHEWS, W. R. BRODE AND J. B. BROWN, *J. Am. Chem. Soc.*, 63 (1941) 1064.
[9] N. A. KHAN, paper in preparation.
[10] N. A. KHAN, W. E. TOLBERG, D. H. WHEELER AND W. O. LUNDBERG, *J. Am. Oil Chemist's Soc.*, (in press).
[11] S. BERGSTROM AND R. T. HOLMAN, *Advances in Enzymology*, 8 (1948) 449.
[12] A. L. TAPPEL, P. D. BOYER AND W. O. LUNDBERG, *J. Biol. Chem.*, 199 (1952) 267.

Received November 16th, 1954

* Present Address: Department of Physiology, University of Minnesota, Minneapolis, Minnesota, U.S.A.

On the organisation of collagen fibrils in bone

An alternative structure for the Haversian Systems in bone is suggested by observations of decalcified sections of bone under the polarising microscope, a typical section being shown in Figs. 1 and 2.

The appearance of sections of compact bone cut perpendicular to the length of the Haversian Systems closely resembles that of spherulites formed by certain artificial polymers. The extinction patterns of these spherulites can be explained[1] if the direction of the maximum refractive index winds in a helix with its axis directed radially from the centre of the spherulite. Spherulites with helical angles from 0 degrees to 90 degrees have been obtained; those with small helical angles show concentric birefringent and isotropic rings and a dark extinction cross between crossed nicols.

The birefringence in sections of decalcified bone is mainly positive form birefringence and not intrinsic birefringence of the collagen. This is due to the presence of submicroscopic rodlet-shaped spaces previously occupied by the inorganic hydroxyapatite crystals, which have been shown by FINEAN AND ENGSTROM[2] to have their long axes parallel to the 640 A spacing of the collagen molecules. The direction of the maximum refractive index is consequently parallel to the collagen molecules and also to the fibrils. In view of the resemblance between spherulites and Haversian Systems between crossed nicols it is suggested that the direction of the collagen fibrils winds in a helix of small helical angle with its axis directed radially from the central canal. This structure explains further observations (Fig. 3) of the extinction pattern such as the uniform change in birefringence across the birefringent rings, and also the change in direction of the birefringence in the plane of the section. This latter can be obtained from the direction of the dark lines which cross the birefringent rings to form the extinction cross. The generally accepted concept of the fibrils forming helices concentric with the central canal, where each birefringent and isotropic ring corresponds to a separate helix[3], does not account for the

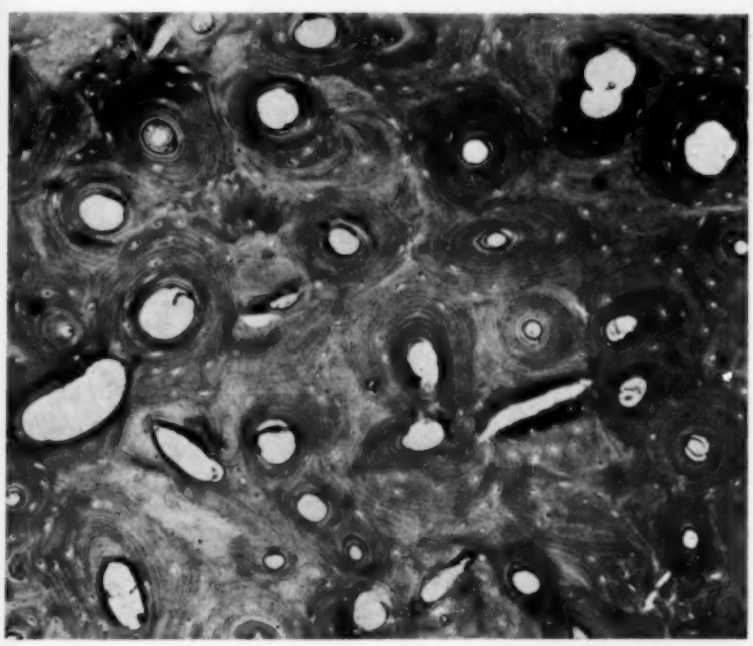

Fig. 1. A typical field in a section of decalcified bone cut perpendicular to the length of the Haversian Systems, Magnification × 60. Stained with Haematoxilin, Phloxine and Tartrazine

Fig. 2. Same field as Fig. 1 but with Polars crossed

observations. In order to do so it is necessary to postulate a very large number of helices with the helical angle increasing continuously in successive helices. There is, however, no further evidence for such a structure.

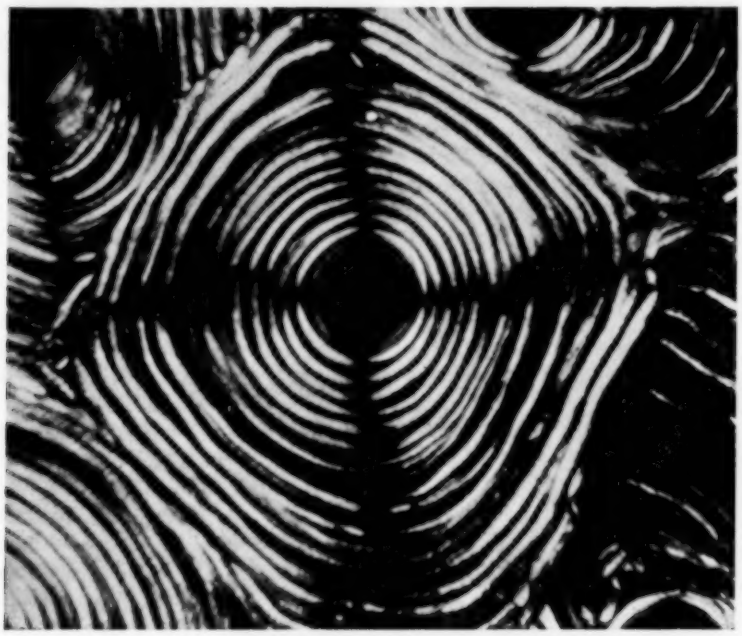

Fig. 3. Single Haversian System in unstained section with Polars crossed showing birefringent and isotropic rings and the dark extinction cross

In Haversian Systems the variation in direction of the fibrils suggested by the structure of pherulites is supported by the similarity in chemical structure of collagen and the artificial polymers. They are all long chain molecles, while nylon, one of the polymers studied by KELLER, and collagen are polypeptides. Furthermore, the formation of Haversian Systems takes place slowly in the primary bone which has been previously laid down and in this respect resembles[1] the formation of spherulites which are obtained when the polymer is kept at a temperature a few degrees below its softening point. Moreover, spherulites of inorganic salts such as barium carbonate are only obtained if the rate of crystallisation is slow, as for instance by allowing a solution of barium chloride to diffuse into a gel containing dissolved sodium carbonate.

This structure offers a straightforward explanation for the existence of Haversian Systems in bone as being a form of crystallisation of collagen analogous to the formation of spherulites from artificial polymers.

Pathology Research Laboratory,
University of Bristol,
Bristol (England)

N. M. BLACKETT

[1] A. KELLER, *Nature*, 169 (1952) 913.
[2] J. B. FINEAN AND A. ENGSTROM, *Biochim. Biophys. Acta*, 11 (1953) 178.
[3] A. A. MAXIMOW AND W. BLOOM, *A Textbook of Histology*, Philadelphia 1952.

Received November 26th, 1954

On the phosphamidase activity of human seminal ~~phosphate~~ Phosphatase

The idea that the phosphamidases form a group of enzymes distinct from the phosphatases[1,2] seems no longer valid. There do exist perhaps specific phosphamidases that do not attack the P–N compounds and specific phosphamidases that do not attack the P–O compounds analogous to their own substrates, but so far in all cases where the so-called unspecific phospho-mono-esterases have been investigated carefully, they have also displayed phosphamidase activity.

Preparations of alkaline phosphatases, more or less purified, have been shown to catalyze the hydrolysis of P–N compounds[3,4,5,6,7] and also to catalyze the transfer of phosphate from a P–N donor to certain acceptors[4,5,7].

As for the acid phosphatases PERLMANN has demonstrated the P–N splitting abilities of potato and intestinal phosphatase. Transferase and hydrolytic activity of crude seminal plasma using creatinephosphate as substrate has been demonstrated by GREEN AND MEYERHOF[5] and confirmed by MORTON[7] with partially purified human prostatic phosphatase. In contradistinction to these results on acid phosphatases stand the findings of PERLMANN[6]. Using a purified preparation of prostate phosphatase she found no hydrolysis of N- (*p*-chlorophenyl) amido phosphate and only a slight splitting of N-phosphoryl-DL-phenylalanine methyl ester. Likewise, ANAGNOSTOPOULOS *et al.*[8] found practically no splitting of anilidophosphate.

Since prostate phosphatase has been used to characterize the nature of the phosphate linkage in proteins[8,9,10,11,12] it seems desirable to investigate the ambiguity in the demonstration of its phosphamidase activity. Therefore, the following observations on purified human seminal phosphatase with amido-phosphate* ($NaHPO_3NH_2$) as substrate are presented.

The enzyme was prepared and kindly given by Dr. FRANK LUNDQUIST**. It consists of the dialyzed precipitate formed between 40 and 70% saturation with ammonium sulfate, at 0° C in human seminal plasma acetate buffered at pH 5. The phosphatase activity of such preparations is about 5400 Gutman units per ml; in spite of the purification they still display slight proteolytic activity[13].

The cleavage of amidophosphate which is acid consuming was followed by means of a pH-stat[14], in a medium containing 0.5 *M* KCl, 25° C. The substrate ($pK_3 = 7.95$; 25° C, 0.5 *M* KCl (15)) shows a rather high *autohydrolysis*, the first order kinetic constant being 0.0236 h^{-1}. (log_{10}), 0.5 KCl, 25° C (ROSENBERG's[15] more accurate determination gives 0.0234 h^{-1}), in the pH interval 4 to 6.5. Below pH 4 acid catalysis sets in[15], while from pH 6.5 the rate falls off along an S-shaped curve reaching zero at pH 9.5.

The enzyme-catalyzed reaction, 0.5 *M* KCl, 25° C, $1.6 \cdot 10^{-2}$ *M* amidophosphate, followed almost the first order kinetic scheme with a pH-optimum at 6.7.

In order to prevent difficulties with CO_2 and enzyme inactivation[16], most of the experiments have been carried out at pH 4.6. Under these conditions an almost linear relationship between enzyme concentration and activity was found.

The Michaelis-Menten constant was found to be $1 \cdot 10^{-3}$ *M* amidophosphate (initial rate, Lineweaver-Burk plot). This is notable since the corresponding values for monophenyl phosphate have been found by LUNDQUIST[17] to be $0.892 \cdot 10^{-3}$ *M*, 25° C, pH 6.0, $\mu = 0.15$ and by SCHØNHEYDER[18] to be $0.906 \cdot 10^{-3}$ *M*, 22° C, pH 5.6, $\mu = 0.3$ (2% NaCl).

The activity at pH 4.6 is not significantly inhibited by one of the reaction products, NH_4^+ (0.1 *M*), but measurably so by the other product, phosphate.

On the (not proven) assumption that this inhibition is competitive, the dissociation constant for the enzyme-phosphate complex can be calculated to be $2 \cdot 10^{-3}$ *M*. This is somewhat higher than found by SCHØNHEYDER[18], $1.4 \cdot 10^{-3}$ *M*, 22° C, pH 5.6, $\mu = 0.3$ (2% NaCl). Strong inhibition of the reaction with KF, 10^{-3} *M*, pH 4.6 was observed but found not to be instantaneous. At pH 8.6 the inhibition seemed to be much smaller. The following substances had no significant action on the phosphamidase activity at pH 4.6: $BeSO_4$ ($5 \cdot 10^{-4}$ *M*), $CoCl_2$ ($5 \cdot 10^{-4}$ *M*), Versene ($1.4 \cdot 10^{-2}$ *M*), ascorbate ($2.8 \cdot 10^{-3}$ *M*).

A comparison of the activity (expressed in millimols substrate split per minute) of this enzyme measured as a phosphatase *ad modum* LUNDQUIST[19], ($4.55 \cdot 10^{-3}$ *M* monophenylphosphate, but at pH 5.2 and corrected to pH-optimum and 25° C), with the activity measured as a phosphamidase (corrected to pH-optimum and $4.55 \cdot 10^{-3}$ *M* amidophosphate) gives P–N-ase/P–O-nase = 1.3. This result is only to be taken as an order of magnitude, because a comparison is not strictly permissible due to *e.g.* differences in enzyme dilution procedure, presence of citrate in one case only, and so on.

Free and paper electrophoresis of two different enzyme preparations gave three main peaks, the greater part of the activity being accumulated in the middle peak, named B. At 0.5° C, phosphate buffer $\mu = 0.1$, pH 6.5, the mobility of peak B in free electrophoresis was about $-3 \cdot 10^{-5}$ cm^2, $volt^{-1}$, sec^{-1} (ascending limb). This is somewhat different from the value $-1 \cdot 10^{-5}$ cm^2, $volt^{-1}$, sec^{-1} (descending limb), pH 6.5, $\mu = 0.05$ found by DEROW AND DAVISON[20] and from KUTSCHER AND PANY's[21] value $-10 \cdot 10^{-5}$ cm^2, $volt^{-1}$, sec^{-1} in 10^{-3} *M* citrate buffer. As seen in Tables I and II the ratio P–N-ase/P–O-ase is practically constant in the electrophoretic fractions and the untreated enzymes.

The enzyme was found to act as a transferase with amidophosphate as donor and glycerol as an acceptor, pH 4.6, 25° C.

As already mentioned the enzyme preparation shows proteolytic activity. HOLTER AND LI[22] have found phosphamidase activity in pepsin, trypsin and rennin, pH-optimum 4.6, 37° C, with *p*-chloro-anilidophosphate as substrate; therefore rennin (BERRIDGE[23] cryst.), pH 4.6, pepsin (porcine, cryst. Armour), pH 4.6 and subtilisin (cryst. GÜNTELBERG AND OTTESEN[24]) pH 4.6 and 8.6, were tested for phosphamidase activity with amidophosphate as substrate, but with negative result.

---

* A gift from Dr. THOMAS ROSENBERG, Nordisk Insulin Laboratorium, Gentofte, Denmark.

** Institute of Forensic Medicine, University of Copenhagen.

The main results of the present study make it highly probable that seminal phosphomonoesterase and phosphamidase are identical, a finding well in accordance with KOSHLAND's[25] theoretical considerations.

TABLE I

FREE ELECTROPHORESIS OF 9.588 ml DIALYZED ENZYME PREP. 3a

Fraction	*Phosphamidase act. per ml arbitrary units*	*Phosphatase act. per ml arbitrary units*	*Ratio Phosphamidase / Phosphatase*	*Total Phosphatase act.*
(1) ascending limb	0.42	0.055	7.6	0.20
(2) ascending limb	61.1	9.0	6.8	32.0
(3) bottom	82.5	12.3	6.7	30.5
(4) descending limb	84.0	12.8	6.6	45.6
(5) descending limb	25.9	3.8	6.8	13.2
				sum: 121.5
Preparation (3a) dialyzed 9.588 ml	86.3	13.2	6.5	126.6

TABLE II

Exp. No.	*Buffer*	*pH*	*Volt per cm*	*Time min*	*B-peak*				*Phosphatase activity recovered*			
					Total phosphamidase activity	*Total phosphatase activity*	*Ratio phosphamidase / phosphatase*	*Ratio for untreated (3a) prep.*	*Distribution per cent*			*Per cent of initial act.*
									peak A	*peak B*	*peak C*	*peak A + B + C*
IV	phosphate	7.08	9.16	248	1.26	0.1943	6.5	6.5	1	97	2.8	71%
VIII	veronal acetate sulfate	7.06	3.97	740	0.400	0.0665	6.0		1	98	1.7	24%*

* Bad recovery in this case probably due partly to nature of buffer, partly to exclusion of the paper areas corresponding to the zones of overlapping fractions. In spite of this enzyme loss the activity distribution is the same as in the other experiment.

Further investigations are in progress. A more detailed publication will appear in *Compt. rend. trav. lab. Carlsberg.*

To Dr. FRANK LUNDQUIST and Dr. THOMAS ROSENBERG I am indebted for many helpful suggestions.

I also want to thank Dr. H. HOLTER and Professor K. U. LINDERSTRØM-LANG for suggesting the problem and especially for very valuable advice and discussions.

K. MAX MØLLER

Carlsberg Laboratory, Copenhagen (Denmark)

[1] A. SCHÄFFNER, *Die Methoden der Fermentforschung*, II, (E. BAMANN UND K. MYRBÄCK, editors), George Thieme Verlag, Leipzig (1941) p. 1976.
[2] H. HOLTER AND SI-OH LI, *Compt. rend. trav. lab. Carlsberg, Sér. chim.*, 27 (1951) 393.
[3] T. WINNICK AND E. M. SCOTT, *Arch. Biochem.*, 12 (1947) 201 and 209.
[4] O. MEYERHOF AND H. GREEN, *J. Biol. Chem.*, 178 (1949) 655, and 183 (1950) 377.
[5] H. GREEN AND O. MEYERHOF, *J. Biol. Chem.*, 197 (1952) 347.
[6] G. E. PERLMANN, *Phosphorus Metabolism*, II, (W. D. MCELROY AND B. GLASS, editors), The Johns Hopkins Press, Baltimore (1952) p. 167.
[7] R. K. MORTON, *Nature*, 172 (1953) 65.
[8] C. ANAGNOSTOPOULOS, M. PACHT, E. BOURLAND AND P. GRABAR, *Bull. soc. chim. biol.*, 33 (1951), 699–704.

[9] G. E. PERLMANN, *J. Gen. Physiol.*, 35 (1952) 711.
[10] G. E. PERLMANN, *J. Amer. Chem. Soc.*, 74 (1952) 6308.
[11] G. E. PERLMANN, *Biochim. Biophys. Acta*, 13 (1954) 452.
[12] G. E. PERLMANN, *Nature*, 174 (1954) 273.
[13] F. LUNDQUIST, unpublished results.
[14] C. F. JACOBSEN AND J. LÉONIS, *Compt. rend. trav. lab. Carlsberg, Sér. chim.*, 27 (1951), 333–39.
[15] T. ROSENBERG, unpublished results.
[16] W. KUTSCHER AND A. WÖRNER, *Z. physiol. Chemie*, 239 (1936) 109.
[17] F. LUNDQUIST, *Acta Physiol. Scand.*, 14 (1947) 263.
[18] F. SCHØNHEYDER, *Biochem. J.*, 50 (1951) 378. The results have been recalculated by the author of the present paper.
[19] F. LUNDQUIST, *Acta Physiol. Scand.*, 19, Suppl. 66 (1949) 39.
[20] M. A. DEROW AND M. M. DAVISON, *Science*, 118 (1953) 247.
[21] W. KUTSCHER AND J. PANY, *Z. physiol. Chemie*, 255 (1938) 169.
[22] H. HOLTER AND SI-OH LI, *Acta Chem. Scand.*, 4 (1950) 1321.
[23] N. Y. BERRIDGE, *Biochem. J.*, 39 (1945) 179.
[24] A. V. GÜNTELBERG AND M. OTTESEN, *Compt. rend. trav. lab. Carlsberg, Sér. chim.*, 29 (1954) 36.
[25] D. E. KOSHLAND, *The Mechanism of Enzyme Action* (W. D. MCELROY AND BENTLEY GLASS, editors) The Johns Hopkins Press, Baltimore (1954), p. 608.

Received November 10th, 1954

A new cofactor in the conversion of serine to glycine

Cell-free extracts of an unidentified *Clostridium*, strain HF[1], catalyze the net production of glycine from serine. The fate of the β-carbon of serine has not yet been determined. Upon extensive dialysis of the extracts, glycine production shows a clear dependence on DPN, Mn^{++} and pyridoxal phosphate (see Experiment I). Following treatment with Dowex 1 HCl and subsequent overnight dialysis, the system can no longer be reactivated by these three cofactors. A fourth factor obtained from boiled extracts of *Clostridium cylindrosporum* is required in addition; it shall be referred to as Co C. Experiment II demonstrates that Co C is essential, and that its presence does not abolish the requirements for DPN, Mn^{++} and pyridoxal phosphate.

Co C is not identical with any of the folic acid derivatives found active in the systems of SAKAMI[2] and BLAKLEY[3]. Experiment II demonstrates that in this system folic acid and anhydroleucoverin are inert, but that citrovorum factor (C F) and tetrahydrofolic acid (*thf*) have an effect. In contrast to Co C, which is active at catalytic levels*, good activity is obtained with C F and *thf* only at substrate concentrations. Furthermore, DPN is not required when these compounds are used, (inhibition by DPN is usually observed) whereas DPN is required for activity with Co C. Another basis for distinguishing Co C from C F and *thf* is that saturation curves reveal that C F can never give as good activity as Co C, and that *thf* can at substrate concentrations give better activity (perhaps as a stoichiometric acceptor for the one carbon piece). Co C is not attacked by potato nucleotide pyrophosphatase. It is absorbed at low pH on Norite, and can be removed by ammoniacal ETOH; it is stable to boiling in dilute alkali (0 05 *N*) and is destroyed under similar conditions in dilute acid. Co C can be distinguished chromatographically from folic acid, C F, anhydroleucoverin, and *thf*; it has repeatedly been recovered from a fluorescent spot on paper chromatograms in various solvent systems.

Experiment I

The assay mixture contains the following substances in a total volume of 0.6 ml: 20.0 μM DL-serine**, 0.02 μM DPN, 2.0 μM $MnSO_4$, 0.02 μM pyridoxal phosphate, 0.04 ml *M* K-phosphate buffer pH 6.5, and 0.2 ml of an enzyme preparation (20 mg protein/ml) which was dialyzed 43 hours against 0.01 *M* phosphate buffer pH 7.2. The samples were incubated 2 hours at 28° C. The control value in the absence of serine (= 0.046 μM) is subtracted from each experimental value given.

Sample	*Omitted from assay mix*	*μM glycine formed†*
1	—	0.314
2	DPN	0.078
3	Mn^{++}	0.108
4	pyridoxal phosphate	0.134

* The most highly purified preparation of Co C obtained thus far by charcoal and paper chromatography has an absorption peak at 275–280 mμ. Assuming that the molecular extinction coefficient is the same as that for the folic acid derivatives ($\varepsilon_{280(max)}$ = 18,000–26,000) UV absorption at 280 mμ indicates that Co C is active at less than 0.01 the concentration of the glycine formed.

Experiment II

The assay mixture contains the following substances in a total volume of 0.4 ml: 6.0 μM DL-serine**, 0.02 μM DPN, 2.0 μM $MnSO_4$, 0.02 μM pyridoxal phosphate, 0.04 ml M K-phosphate buffer pH 6.5, and 6 units of enzyme. One enzyme unit yields 0.1 μM glycine at saturation levels of Co C after two hours' incubation at 38° C. A unit of Co C is an amount ($<$ 0.001 μM)[2] yielding 0.1 μM glycine in the presence of one unit enzyme. The control value in the absence of serine (= 0.012 μM) is subtracted from each experimental value given.

Sample	*Omitted from assay mix*	*Special addition*	*μM glycine formed*†
1	—	—	0.016
2	—	*ca.* 6.0 units Co C	0.600
3	DPN	*ca.* 6.0 units Co C	0.202
4	Mn^{++}	*ca.* 6.0 units Co C	0.268††
5	pyridoxal phosphate	*ca.* 6.0 units Co C	0.409
6	—	0.02 μM folic	0.032
7	—	0.05 μM anhydroleucoverin	0.004
8	—	0.006 μM C F	0.080
9	—	0.02 μM C F	0.180
10	—	0.10 μM C F	0.280
11	DPN	0.10 μM C F	0.324
12	Mn^{++}	0.10 μM C F	0.088
13	pyridoxal phosphate	0.10 μM C F	0.312
14	—	0.006 μM *thf*	0.068
15	—	0.06 μM *thf*	0.120
16	—	0.60 μM *thf*	0.350
17	DPN	0.60 μM *thf*	0.412
18	Mn^{++}	0.60 μM *thf*	0.066
19	pyridoxal phosphate	0.60 μM *thf*	0.288

** For dialyzed preparations, the optimum serine concentration is 20.0 μM, as opposed to 6.0 μM for Dowex-treated enzyme. This difference is probably due to fewer side reactions involving serine in the presence of Dowex-treated enzyme.

† The glycine is assayed by chemical methods[4].

†† Some Mg^{++} was added with the Co C due to the method of purification. Since Mg^{++} can replace the Mn^{++} requirement to some extent, this value is unusually high.

Acknowledgments. I wish to thank Dr. T. C. STADTMAN for giving me space in her laboratory as well as stimulating discussions which aided in these investigations. I am also indebted to Dr. T. MILES for synthesizing *thf*[5]; to Dr. J. RABINOWITZ for encouraging the use of *Cl. cylindrosporum* as a possible source of cofactor; to Dr. M. SILVERMAN for citrovorum factor, to Dr. H. BROQUIST of Lederle Laboratories for a sample of anhydroleucoverin, and to Dr. A. KORNBERG for a sample of purified potato nucleotide pyrophosphatase.

BARBARA E. WRIGHT

Laboratory of Cellular Physiology, National Heart Institute, National Institutes of Health, Public Health Service, Department of Health, Education, and Welfare, Bethesda, Maryland (U.S.A.)

[1] T. C. STADTMAN, *J. Bact.*, 67 (1954) 314.
[2] R. L. KISLIUK AND W. SAKAMI, *J. Am. Chem. Soc.*, 76 (1954) 1456.
[3] R. L. BLAKLEY, *Nature*, 173 (1954) 729.
[4] B. ALEXANDER, G. LANDWEHR AND A. M. SELIGMAN, *J. Biol. Chem.*, 160 (1945) 51.
[5] H. P. BROQUIST, M. J. FAHRENBACH, J. A. BROCKMAN Jr., E. L. R. STOKSTAD AND T. H. JUKES, *J. Am. Chem. Soc.*, 73 (1951) 3535.

Received November 1st, 1954

Fluorescent globulin of the lens*

In the study of the optical properties of structural proteins the lens, as a material, deserves special attention since, in contrast to other organs, it contains no colouring matter (such as cytochromes) which would interfere with observation.

If a lens, freshly isolated from a bullock's eye, is illuminated with near UV light it shows a brilliant blue fluorescence. If the incident light is polarised, the fluorescent emission has a high degree of polarisation indicating that the emitting molecules have no free mobility. The fluorescent material can be extracted and shows the reactions of an euglobulin. It is possible that fluorescence is not a specific property of this lentoglobulin but is a general property of its group and is not observable in other organs because of optical heterogeneity. Such a possibility is supported by the fact that another optically homogeneous tissue, the corneal epithelium, also shows a vivid fluorescence. The fluorescence of nails or the skin epithelium may be connected with their anhydrous solid state.

The isolated lentoglobulin shows a strong absorption maximum at 2800 A; consequently one may expect that most of the fluorescent light is emitted in the UV and escapes visual observation. It seems to involve the protein molecule as a whole since it is readily lost on heat denaturation. The lentoglobulin is easily denatured and becomes hereby increasingly opalescent or turbid. It seems possible that some such change is involved in the genesis of cataracts.

Experimental. 86 g of bullock's lenses were kept at —20° C for a month, and then placed in a 500 ml jar. The jar was filled with water and the material, after thawing, blended for two minutes in the Servall Omnimixer. After storing the liquid for two hours in the refrigerator, undissolved particles were eliminated in the Sharples centrifuge, using its closed bowl. About one tenth of the supernatant was set aside, while the rest, 360 ml, was mixed with 210 ml saturated ammonium sulphate which brought the saturation to 40%. Twenty minutes later the precipitate was separated in the Sharples, then dissolved in 150 ml water and freed from undissolved material in the same centrifuge. To the supernatant was added 100 ml saturated ammonium sulphate solution, then the precipitate was separated by centrifugation and dissolved in a small volume of water and dialysed overnight against 0° distilled water. The salt-free solution was diluted with 50 ml water to a volume of 150 ml. 1% acetic acid was added till a granular precipitate was formed at pH 6. The precipitate was dissolved in water, $NaHCO_3$ being added to bring the pH to 7.5. The 80 ml final solution contained 10 g protein. It was opalescent and showed a strong fluorescence in the UV.

The solution of the globulin could be lyophylised. Ammonium sulpahte caused gradual denaturation which rendered the protein insoluble. Ammonium sulphate precipitates the lentoglobulin at a fairly sharp limit: at 0.33 saturation there is no precipitation while at 0.37 saturation the precipitation is almost complete. Acetic acid precipitates the protein only in absence of salts. The extinction of a 1 cm layer of a solution containing 0.02% lentoglobulin was 0.3.

The lens also contains a considerable amount of albumin which is left in solution at 0.4 saturation with ammonium sulphate or on acidification. This dissolved albumin showed only a weak fluorescence which might have been due to an admixture of globulin.

At neutral reaction and in absence of salts the solution of the lentoglobulin can be boiled without any apparent change in dispersity, but its fluorescence is lost. The fluorescence cannot be detached from the protein by hot alcohol. The lability of the globulin makes it necessary to carry out its preparation as quickly as possible and at low temperature. The final product showed in the ultracentrifuge, in addition to the main fraction, a more rapidly settling component, which was probably denatured globulin.

ALBERT SZENT-GYÖRGYI

Institute for Muscle Research,
Marine Biological Laboratory,
Woods Hole, Mass. (U.S.A.)

* This research was supported by grants from Armour and Co., Chicago, the American Heart Association, the Muscular Dystrophy Associations, and the Association for the Aid of Crippled Children.

Received November 12th, 1954

The kinetics of the deuterium exchange of insulin with D_2O. An amendment

In continuation of previously reported experiments[1] it has been found that P_2O_5 is unfit for drying deuterium-loaded insulin. However fast P_2O_5 is transferred from bottle to desiccator, it will have time to absorb sufficient water from the air to enable it to replace a considerable quantity of deuterium atoms in the frozen-dried protein by ordinary hydrogen atoms during the subsequent drying process (5 days). The amorphous character of the solid insulin in combination with its extremely light and spongy structure is favorable for the exchange process. The problem of the deuterium exchange of insulin in aqueous solution has therefore been reinvestigated using the improved drying technique indicated below. It was consistently found (16 estimations) that almost all exchangeable hydrogen atoms, *viz.*, 89 $\pm$ 1 out of 91 per mole pork insulin (Mw 5777), exchanged in the course of 12–20 hours at 38°. Special control experiments combining determinations of the nitrogen content and weight of the dry protein have secured that the higher value obtained does not originate in insufficient drying of the samples.

In view of these findings our previous exchange-curve must be re-interpreted, *i.e.*, it does not represent the number of hydrogen atoms which dissolved insulin will exchange with deuterium atoms from D_2O, but rather the number of deuterium atoms in the *dry* protein which will *not* exchange back with H_2O from P_2O_5. Since the figure 46 atoms per mole is quite reproducible ($\pm$ 2 atoms) if the drying is performed with P_2O_5 as described, our previous experiments do reveal something about the stability of the 48 hydrogen atoms in the backbone of solid, amorphous insulin, and show the extreme reactivity of the hydrogen atoms in the side chains even when water is virtually absent.

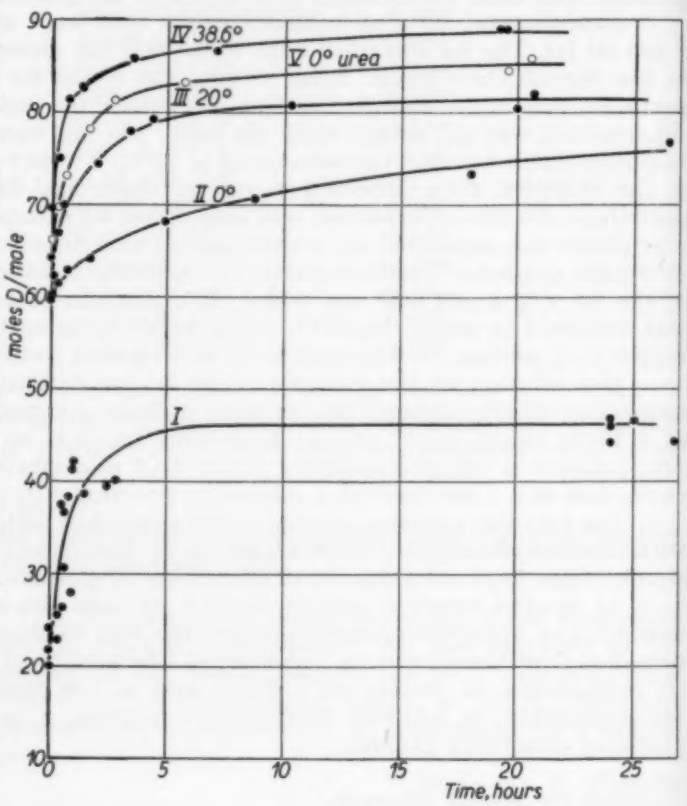

Fig. 1

The question of the true rate of exchange of dissolved insulin was approached in the following way: 200 μl of a 2 % insulin solution, pH 3, were lyophilized and dried over P_2O_5. Next 200 μl 99.7 % D_2O were added to the dry protein and allowed to react with it for 20 hours at 38°, after which time D_2O was distilled off *in vacuo* at low temperature (cryodistilled) using a cold trap (—60° to —80°). When the protein was almost dry it was heated to 60° for 2 to 4 hours to drive the residual water over into the trap. Finally the protein was dissolved as fast as possible in 200 μl H_2O (or urea solution), and samples of 15 μl were taken out at suitable times, frozen to —60°, and cryodistilled. The density of the water in the trap was determined in the gradient tube[2]. Fig. 1, curves II–IV, shows the rate of this back-exchange at different temperatures. It is apparent that about 59 hydrogen atoms exchange at a rate which is too high to be measured. The remaining 32 however are characterized by much a smaller reactivity, especially at 0°, and fall in different groups with greatly differing rate constants. It is too early to discuss the significance if this observation in detail, but we venture to maintain that these slowly exchanging hydrogen atoms are situated in the peptide groups and are hydrogen-bonded in the secondary structure of the protein. Curve V which represents experiments at 0°, pH 3, 5.2 molar urea, strengthens this view in that it shows the activating influence of a denaturing agent upon the hydrogen exchange. It will be observed that curve I[1], will roughly coincide with curve IV if it is displaced upwards a distance corresponding to the 45 odd hydrogen atoms lost in the drying over P_2O_5. Therefore the rate measured in the first, indeterminate part of curve I is probably that of the slow exchange of hydrogen atoms in the backbone of dissolved insulin. The possibility that the curves in Fig. 1 represent rates of dissolution of insulin and of some "ageing" processes in the solution (dissociation of higher complexes in which hydrogen atoms are "masked") may be excluded for several reasons. The following small experiment is interesting in this respect: 100 μl aged insulin solution were cooled to 0° and mixed with 100 μl D_2O at 0°. After 1 min and 60 min 50 μl samples of the mixture were frozen and

lyophilized, and the protein dried at 60° for 2.5 hours as described above. Then 25 μl H_2O were added and after 2 hours back-reaction at 38° the solutions were cryodistilled and the density of the water determined. Exchange values of 60 and 62 respectively were found, in good agreement with curve II.

Our wish to correct our previous errors as quickly as possible had led us to omit a discussion of the behavior of SANGER'S A-chain on which experiments are in progress. It should, however, be noted that renewed experiments with the tetrapeptide leucyltriglycine, using the improved technique, have shown that all 6 labile hydrogen atoms exchange instantaneously if the peptide is lyophilized prior to dissolution, so that it is brought into rapid contact with the solvent. The exchange with H_2O during the drying over P_2O_5 is considerably slower than in the case of insulin, which may be due to the fact that the lyophilized peptide is crystalline. A similar assumption may explain why the A-chain does not seem to exchange with P_2O_5[1].

The method and results will be described more fully elsewhere.

Carlsberg Laboratorium, Copenhagen (Denmark)

AASE HVIDT
K. LINDERSTRØM-LANG

[1] AASE HVIDT AND K. LINDERSTRØM-LANG, *Biochim. Biophys. Acta*, 14 (1954) 574.
[2] AASE HVIDT, GORDON JOHANSEN, K. LINDERSTRØM-LANG AND FRED VASLOW, *Compt. rend. trav. lab. Carlsberg, Sér. chim.*, 29 (1954) 9.

Received December 2nd, 1954

Influence of methionine on protein and nucleic acid synthesis in *Pseudomonas hydrophila* *

The recent findings of SCHMIDT *et al.* showed an increase in the biosynthesis of acid-insoluble and acid-soluble adenine and guanine fractions in yeast cells grown in a synthetic medium supplemented with methionine. The present investigation deals with the influence of DL-methionine on nucleic acid and protein synthesis in *Pseudomonas hydrophila*.

Pseudomonas hydrophila NRC 492 was grown at three concentrations of DL-methionine in a synthetic medium[2] for 24 hours with constant shaking. The cells, harvested in a centrifuge, were washed four times with ice cold water, frozen and dried.

The following estimations were made on the freeze-dried material.

a. *Protein:* 20 mg of the freeze-dried material was incubated with 2 ml of 5% trichloroacetic acid (TCA) at 0° C for 2 hours and centrifuged at 4° C. The residue, washed twice at 4° C with 5% TCA, was taken up in 3% NaOH and the protein in a 4 ml aliquot was estimated by the colorimetric biuret method of HILLER *et al.*[3] Intensity of color was measured in a Beckman spectrophotometer at 550 mμ.

b. *Total nucleic acid phosphorus* (TNA-P): 30 mg of the freeze-dried material was incubated with 4 ml of 5% TCA at 0° C for 2 hours and centrifuged at 4° C. The residue was washed four times at 4° C with 5% TCA, once with ethanol, three times with a mixture of ethanol: ether (3:1) at room temperature. The washed residue was extracted three times with 2 ml aliquots of 5% TCA at 90° C for 10 min. The TCA extracts were made up to 10 ml and phosphorus was estimated in an aliquot according to the method of KING[4].

c. *Desoxyribonucleic acid* (DNA-P): 80 mg of the freeze-dried material was incubated with 5 ml of 5% TCA at 0° C for 2 hours and centrifuged at 4° C. The residue was washed with TCA and lipid solvents as described above. The washed residue was taken up in 2 ml *N* KOH and the mixture was kept for 18 hours at 37° C. It was then chilled in an ice bath and DNA and protein were precipitated with 0.4 ml 6*N* HCl and 2 ml 5% TCA. The mixture was held at 0° C for 15 min and centrifuged at 4° C. The residue was washed at 4° C with 5% TCA. The washed residue was extracted three times with 1 ml aliquots of 5% TCA at 90° C for 10 min and the phosphorus in the extracts estimated according to the procedure of KING[4].

d. *Ribonucleic acid phosphorus* (RNA-P): RNA-P was obtained by substracting DNA-P from TNA-P.

The turnover of ribonucleic acid phosphorus as effected by DL-methionine was studied by using ^{32}P. *P. hydrophila* was grown in a synthetic medium[2] with or without added 0.02 *M* DL-methionine. Labeled phosphorus (1.5 μc/ml of medium) was supplied as $H_3{}^{32}PO_4$. Twenty-four hour cultures were centrifuged and the cells were washed six times with ice cold water. The washed cells were suspended in 7% TCA (2.5 ml TCA per g of wet cells) and held at 0° C for two hours. The suspension was then centrifuged at 4° C and the residue was washed six times with 5% TCA at 4° C and with

* Issued as N.R.C. No. 3480.

lipid solvents as described above. The residue was extracted three times for 1 hour each at 100° C with 10% NaCl. To the pooled extracts two volumes of ethanol were added. The precipitate of Na-nucleate was washed with ethanol and ether and dried. The Na-nucleate was hydrolysed with 0.3 *N* KOH at 37° C for 18 hours and the RNA nucleotides were separated by paper ionophoresis and their activities determined according to procedure of DAVIDSON AND SMELLIE[5].

TABLE I

INFLUENCE OF DL-METHIONINE ON THE NUCLEIC ACID AND PROTEIN SYNTHESIS IN *Pseudomonas hydrophila*

DL-methionine concentration in the medium	Dry weight of cells, mg (400 ml culture)	In 100 mg dry cells		
		mg protein	μg DNA-P	μg RNA-P
1.	475	53.23	37.8	707.5
2. 0.01 *M*	540	66.10	36.1	745.2
3. 0.02 *M*	546	71.43	36.2	782.0
4. 1.05 *M*	570	73.32	37.4	843.1

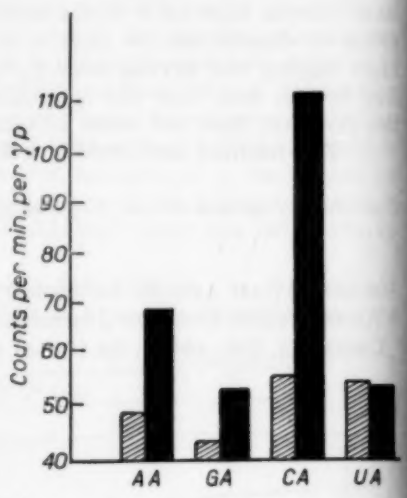

Fig. 1. Effect of DL-methionine on incorporation of ^{32}P into ribonucleotides of *P. hydrophila*. AA = adenylic acid; GA = guanylic acid; CA = cytidylic acid; UA = uridylic acid. Black: with 0.02 *M* DL-methionine. Shaded: control.

In *P. hydrophila*, DL-methionine caused an increase in growth and in the synthesis of protein and ribonucleic acid, but had no apparent effect on DNA content of the cells (Table I). In addition, presence of methionine in growing cultures of *P. hydrophila* brought about an increase in the turnover of RNA phosphorus (Fig. 1). CALDWELL AND HINSHELWOOD[6] reported that the amount of DNA per cell of *Bacterium lactis aerogenes* remained approximately constant even if the organisms were grown under a wide range of conditions. The ribosenucleic acid content on the other hand showed considerable variation. SPIEGELMAN AND KAMEN[7] showed that turnover of RNA phosphorus in yeast cells was several times higher when the cell was producing protein and that several factors inhibiting the protein synthesis also inhibited the replacement of RNA phosphorus. In *P. hydrophila*, methionine brought about higher production of protein and higher turnover of RNA phosphorus. Thus there was a positive correlation between protein and RNA synthesis. This evidence lends further support to the accumulated data showing that RNA is involved in protein synthesis[9–11].

The author wishes to thank Dr. R. W. WATSON for his interest and encouragement during the course of this investigation.

K. K. REDDI*

Division of Applied Biology
National Research Council
Ottawa (Canada)

1 G. SCHMIDT, K. SERAYDARIAN, L. M. GREENBAUM AND S. J. TANNHAUSER, *Federation Proc.*, 13 (1954) 291.
2 R. M. HOCHSTER AND R. W. WATSON, *Nature*, 170 (1952) 357.
3 A. HILLER, J. R. MCINTOSH AND D. D. VAN SLIJKE, *J. Clin. Invest.*, 4 (1927) 235.
4 E. J. KING, *Biochem. J.*, 26 (1932) 292.
5 J. N. DAVIDSON AND R. M. S. SMELLIE, *Biochem. J.*, 52 (1952) 599.
6 P. C. CALDWELL AND C. HINSHELWOOD, *J. Chem. Soc.*, (1950) 1415.
7 S. SPIEGELMAN AND M. D. KAMEN, *Cold Spring Harbour Symposia*, 12 (1947) 211.
8 J. BRACHET, *Arch. Biologie*, 53 (1941) 207.
9 J. BRACHET, *Symp. Soc. exp. Biol.*, 1, (1947) 207.
10 T. CASPERSSON, H. LANDSTRÖM-HYDEN AND L. AQUILONIUS, *Chromosoma*, 2 (1941) 111.
11 E. F. GALE AND J. P. FOLKES, *Nature*, 173 (1954) 1223.

Received November 23rd, 1954

* National Research Council of Canada Postdoctorate Fellow, 1953–54.

BIOCHIMICA ET BIOPHYSICA ACTA

Vol. 16 No. 1 Januari 1955

CONTENTS

An investigation of the structure of silk fibroin
by R. E. Marsh, R. B. Corey and L. Pauling (Pasadena, Calif.) 1
Some sensitive and recording volumeters
by B. Kok (Stanford, Calif. and Wageningen) 35
Étude autoradiographique de l'incorporation dans le foie de souris de précurseurs des acides nucléiques et des protéines
par A. Ficq et M. Errera (Bruxelles) 45
Some properties of the manganese and copper catalyzed oxidation of catechol and some other *ortho*-dihydroxybenzene derivatives
by J. R. Gillette, D. Watland and G. Kalnitsky (Iowa City) 51
The acetate-activating enzyme of *Rhodospirillum rubrum*
by M. A. Eisenberg (New York) 58
The structure of cilia
by B. P. Potts and S. G. Tomlin (Adelaide) 66
Thiamine pyrophosphatase, acid and alkaline phosphatase activity in the chicken brain in vitamin B_1 deficiency
by D. Naidoo and O. E. Pratt (London) 75
Further observations on the electron microscope changes following induction of *E. coli* K12
by R. H. Gorrill and C. E. Challice (London) 82
The transfer of potassium between mammalian muscle and the surrounding medium
by H. McLennan (Montreal) 87
The biosynthesis of radioactive estradiol. I. Synthesis by surviving tissue slices and cell-free homogenates of dog ovary
by J. L. Rabinowitz and R. M. Dowben (Philadelphia) 96
Studies on the induced synthesis of β-galactosidase in *E. coli*. The kinetics and mechanism of sulfur incorporation
by D. S. Hogness, M. Cohn and J. Monod (Paris) 99
Observations on nucleic acid and polyphosphate in *Torulopsis utilis*
by R. Chayen, S. Chayen and E. R. Roberts (London) 117
The relationship between tobacco mosaic virus and an accompanying abnormal protein
by C. C. Delwiche, P. Newmark, W. N. Takahashi and M. J. Ng (Berkeley, Calif.) 127
The interaction of polymyxin E with bacterial and other lipids
by A. V. Few (Cambridge) 137
Geisselmodelle und Adenosintriphosphat
von H. Hoffmann-Berling (Heidelberg) 146

Short Communications and Preliminary Notes

Sur les relations entre l'ocytocine et la vasopressine d'une part et la protéine de Van Dyke d'autre part
par R. Acher, G. Manoussos et G. Olivry (Paris) 155
Purification of thrombin by chromatography
by P. Strøier Rasmussen (Copenhagen) 157
Infrared studies on initiation of the autoxidation of some fatty acid esters with and without light-sensitized chlorophyll, ultraviolet light and lipoxidase
by N. A. Khan [Minneapolis] 159
On the organisation of collagen fibrils in bone
by N. M. Blackett (Bristol) 161
On the phosphamidase activity of human seminal ~~phosphate~~ phosphatase
by K. Max Møller (Copenhagen) 162
A new cofactor in the conversion of serine to glycine
by B. E. Wright (Bethesda, Md.) 165
Fluorescent globulin of the lens
by A. Szent-Györgyi (Woods Hole, Mass.) 167
The kinetics of the deuterium exchange of insulin with D_2O. An amendment
by A. Hvidt and K. Linderstrøm-Lang (Copenhagen) 168
Influence of methionine on protein and nucleic acid synthesis in *Pseudomonas hydrophila*
by K. K. Reddi (Ottawa) 169

CONTENTS

Viscosity behavior of non-fibrous desoxyribonucleohistone in media of different ionic strengths
by R. S. Welsh (Stanford, Calif.) 171
Inactivation, par les rayons X, d'un facteur transformant du pneumocoque
par H. Ephrussi-Taylor et R. Latarjet (Paris) 183
Action des rayons U.V. sur l'acide adénosinetriphosphorique des spermatozoïdes de grenouille
par D. Kanazir et M. Errera (Bruxelles) 198
Ultracentrifuge studies on soya bean protein
by W. E. F. Naismith (Dumfries) 203
Influence of the protein moiety on the viscosimetric behavior of deoxyribonucleoprotein
by H. H. Henstell, R. I. Freedman and I. Cooper (Los Angeles) 211
The disappearance of pyruvic decarboxylase and α-ketoglutaric decarboxylase from pigeon muscles on thiamine-deficient diets
by C. H. Monfoort (Utrecht) 219
Effects of acetylcholine on phosphate turnover in phospholipides of brain cortex *in vitro*
by L. E. Hokin and M. R. Hokin (Montreal) 229
Dissimilation of 6-phosphogluconate by *Azotobacter vinelandii*
by L. E. Mortenson, P. B. Hamilton and P. W. Wilson (Madison, Wis.) 238
Chromatography of prostatic phosphatase
by H. G. Boman (Uppsala) 245
Observations upon the behaviour of some phosphate esters in brain at the start of convulsions induced by fluorocitrate and fluoroacetate
by R. M. C. Dawson and R. A. Peters (Oxford) 254
The oxidation of reduced xanthine dehydrogenase in chicken liver
by D. B. Morell (Sydney) 258
The effect of urea on the inhibition of trypsin by soybean trypsin inhibitor
by K. Jacobsson (Lund) 264
Electrical activity in electric tissue. I. The difference between tertiary and quaternary nitrogen compounds in relation to their chemical and electrical activities
by M. Altamirano, W. L. Schleyer, C. W. Coates and D. Nachmansohn (New York) 268

Short Communications and Preliminary Notes

Phenyl thiohydantoins in amino acid analysis
by J. Sjöquist (Lund) 283
Effect of 2:4-dinitrophenol and phenylmercuric acetate on enzymic activity of myosin
by G. D. Greville and D. M. Needham (Cambridge) 284
The stimulation of the adenosinetriphosphatase activities of myofibrils and L-myosin by 2:4-dinitrophenol
by J. B. Chappell and S. V. Perry (Cambridge) 285
An enzymic mechanism for amino acid activation in animal tissues
by M. B. Hoagland (Boston, Mass.) 288
Remarks on preparations of ribonuclease from different manufacturing sources
by L. Ledoux and J. Brachet (London and Brussels) 289
Purification of tetanus toxin by multi-membrane electrodecantation
by J. F. Largier (Cape Town) 291
Conversion of D-xylose to D-xylulose phosphate by extracts of *Pseudomonas hydrophila* 291
by R. M. Hochster (Ottawa) 293
Some properties of the casein of mouse milk (RIII)
by V. Ross and D. H. Moore (New York) 295
Bemerkung zur Spiralstruktur von Eiweiss und Nukleinsäuren
von H. Linser (Wien) 297
Degradation of ribonuclease by subtilisin
by S. M. Kalman, K. Linderstrøm-Lang, M. Ottesen and F. M. Richards (Copenhagen) 299
The nature of the reaction between diisopropylfluorophosphate and chymotrypsin
by R. A. Oosterbaan, P. Kunst and J. A. Cohen (Rijswijk) 300
Purification of cholinesterase from ox red cells
by M. G. P. J. Warringa and J. A. Cohen (Rijswijk) 301
The contraction of muscle fiber and myosin B thread in KI and KSCN solutions
by K. Laki and W. J. Bowen (Bethesda, Md.) 302
The action of carboxypeptidase on ribonuclease
by G. Kalnitsky and E. E. Anderson (Iowa City) 304
The biosynthesis of mucopolysaccharides in the skin of alloxan-diabetic rats
by S. Schiller and A. Dorfman (Chicago) 305
The intracellular distribution of enzymes in *Serratia marcescens*
by A. W. Linnane and J. L. Still (Sydney) 305